STUDIES OF IONIC LIQUIDS AND NANOPARTICLES BASED HYBRID NANO-ADDITIVES FOR ENHANCEMENT OF TRIBOLOGICAL PERFORMANCE OF LUBRICANTS

A Thesis Submitted in partial fulfilment of the requirements for the award of the Degree of

DOCTOR OF PHILOSOPHY

in

MECHANICAL ENGINEERING

by

Maurya Upendra Kanta
(Roll No.: 717125)

Supervisor

Prof. V. Vasu
(Professor)

DEPARTEMENT OF MECHANICAL ENGINEERING
NATIONAL INSTITUTE OF TECHNOLOGY,
WARANGAL (TS), INDIA 506004
November 2022

NATIONAL INSTITUTE OF TECHNOLOGY
WARANGAL (T.S) INDIA 506 004

CERTIFICATE

This is to certify that the dissertation work entitled **STUDIES OF IONIC LIQUIDS AND NANOPARTICLES BASED HYBRID NANO-ADDITIVES FOR ENHANCEMENT OF TRIBOLOGICAL PERFORMANCE OF LUBRICANTS,** which is being submitted by **Mr. Maurya Upendra Kanta** (Roll No. 717125), is a bonafide work submitted to the Department of Mechanical Engineering, National Institute of Technology, Warangal in partial fulfillment of the requirement for the award of the degree of **Doctor of Philosophy in Mechanical Engineering.**

To the best of our knowledge, the work incorporated in this thesis has not been submitted elsewhere for the award of any degree.

Prof. V. Vasu
Supervisor
Department of Mechanical Engineering
National Institute of Technology
Warangal-506004

Prof. V Suresh Babu
Head
Department of Mechanical Engineering
National Institute of Technology
Warangal-506004

Dedicated

to

- **My beloved parents & All my family members**

- **All my Teachers and Professors who taught and encouraged me with positive thoughts.**

THESIS APPROVAL FOR Ph.D

This Thesis entitled "**STUDIES OF IONIC LIQUIDS AND NANOPARTICLES BASED HYBRID NANO-ADDITIVES FOR ENHANCEMENT OF TRIBOLOGICAL PERFORMANCE OF LUBRICANTS"** by **Maurya Upendra Kanta** is approved for the Degree of Doctor of Philosophy.

Examiners

_____

_____

_____

Supervisor(s)

Prof. V. Vasu
(Supervisor)
Professor, Mechanical Engineering Department, NIT Warangal

Chairman

Prof. V Suresh Babu
Head, Mechanical Engineering Department, NIT Warangal

NATIONAL INSTITUTE OF TECHNOLOGY

WARANGAL (T.S) INDIA 506 004

DECLARATION

This is to certify that the work presented in the thesis entitled **"STUDIES OF IONIC LIQUIDS AND NANOPARTICLES BASED HYBRID NANO-ADDITIVES FOR ENHANCEMENT OF TRIBOLOGICAL PERFORMANCE OF LUBRICANTS"** is a bonafide work done by me under the supervision of **Prof. V. Vasu** and was not submitted elsewhere for the award of any degree. I declare that this written submission represents my ideas in my own words and where other's ideas or words have been included, I adequately cited and referenced the original sources. I also declare that I have adhered to all principles of academic honesty and integrity and have not misrepresented or fabricated or falsified any idea/data/fact/source in my submission. I understand that any violation of the above will be a cause for disciplinary action by the Institute and can also evoke penal action from the sources which have thus not been properly cited or from whom proper permission has not been taken when needed.

Date: 22/10/2022
Place: Warangal

(Maurya Upendra Kanta)
Research Scholar,
Roll No.717125

ACKNOWLEDGEMENTS

I would like to express my sincere gratitude and it gives me an immense pleasure to acknowledge the people who were the part of this research work in plenty ways. It would not have been possible without close association with many people. I take this opportunity to extend my sincere gratitude and appreciation to all those who made this research work possible. First and foremost, I would like to express my sincere gratitude to my research supervisor Prof. V. Vasu for his continuous guidance, advice, inspiration, encouragement, for facilitating all the requirements and continuous support, throughout my research work. His enthusiasm, integral view on research and mission for providing high-quality work, has made a deep impression on me. I indebted to him for his persistence in moulding me as a researcher with his methodical supervision that enabled me to complete the research work in the present form. I will never forget his association and encouragement and whole hearted support during my entire tenure of research. During our course of interaction, I have learnt many things, like how to explore new possibilities and how to approach a problem by systematic thinking. I owe him with lots of gratitude for showing me this way of research.

I am grateful to Prof. N.V. Ramana Rao, Director-NIT Warangal who has been a constant source of inspiration for me. I thank Prof. V Suresh Babu, Head of the Department of Mechanical Engineering for providing the necessary facilities to carry out the research. I would like to express my sincere thanks to Prof. Srinadh K V S, Dr. Syed Ismail, Dr. Bonta Srinivasa Rao (Metallurgical and Materials Engineering Department), learned members of my Doctoral Scrutiny Committee for being helpful and generous during the entire course of this work.

This work was not possible without inspiration of my M. Tech. Supervisors Prof. G. Harmain (Mechanical Engineering Dept., NIT Srinagar, Jammu and Kashmir, India). He inspired me during my post-graduation studies and accelerated my passion of pursuing higher studies with greater impact. He is my constant source of the inspiration throughout my life.

I am always grateful to my institute NITW, where I learn many things along with the research. I express my heart-felt gratitude to Dr. Syed Ismail, associate professor Mechanical Engineering Department and other faculty members of the institute during the stay. They are very kind enough to extend their help at various phases of this research, whenever I approached them, and I do hereby acknowledge all of them.

I am also thankful to all the supporting and technical staff of Department of Mechanical Engineering who has directly or indirectly helped during the course of my work. I am very thankful to all production lab technical staff and section head.

My heartfelt thanks to fellow-scholars for their consistent help, moral support and encouragement. My special thanks to Dr. Arun Manohar, Dr. Sandeep M, Dr. Nikhil Thopil, Mr. Jyotish Pandi, Mr. Anuj Kumar, Mr. Naresh, Mrs. Sripada, Dr. Siva Prasad, Mr. Mahesh, Mr. Rakesh, Mr. shatish, Mr. Nitin, Mr. Kranti, Dr. Manoj Dundi, Dr. Pritam Das, Dr. Raj Pittala, Dr. Lokesh, and many others for always standing by my side and sharing a great relationship as compassionate friends. I will always cherish the warmth shown by them.

I am very much thankful to all my special Marathi Mandal and fellow research scholars specially, to Dr. Uday Bagle, Dr. Prashant Suryawanshi, Dr. Abhay Lingayat, Dr. Vinay Rangari, Dr. Harshal Patil, Dr. Gajanan Suryawanshi, Dr. Roshan Bodile, Dr. Ganesh Gawale, Mr. Kishor Ingle, Dr. Avinash Borgaonkar, Dr. Swapnil Adsul, Mr. Vikas Hakke, Mr. Sandip Khobragale, Ms. Vividha Landge, Ms. Sneha Korpe, Ms. Shital Potdar, Ms. Diksha Pandey, Dr. Sarita Prasad, Ms. Sana. I am very much thankful to all my M. Tech friends Dhananjay Singh, Sanbhit, and Himalaya.

In this auspicious moment, I owe my deepest regards to my family members and well-wishers for their eternal support and understanding of my goals and aspirations. My heartfelt regards go to my parents, Sri Kanta Maurya and Smt. Rita Maurya and my brother Pankaj Maurya and my dear wife Smt. Pratibha Maurya. My special regards to my all brother and sister-in laws and for their patience and understanding during the entire period of the research work. I also must thank all my hostel mates for making my stay at NIT Warangal become more memorable.

As always it is impossible to mention everybody who had an impact on this work, however, there are those whose spiritual support is even more important. I feel a deep sense of gratitude to each and every one who directly or indirectly extended their support to fulfill my research. Finally, I am thankful to library staff and administrative staff of NITW for their cooperation.

NIT Warangal (**Maurya Upendra Kanta**)

November 2022

ABSTRACT

Enhancement in the performance of lubricants and energy efficiency of the system continues to be a major challenge to the transportation and lubricant industries. The reduction of carbon emissions is key to meeting sustainable development goals, especially for the transportation and industrial sectors. Lubricants play a vital role in efficiently keeping the crucial machine/equipment parts healthy and running. However, the drive towards employing lower viscosity oils with low SAPS (Sulphated Ash, Phosphorous, and Sulphur) to enhance the fuel economy impacts the wear and durability of critical tribo-pairs operating under the boundary lubrication (BL) regime. Thus, to comply with stringent norms, novel lubricants, particularly composed of new age additives nano oils (oils with nanoparticles) and ionic liquids, are currently the focus of research attention. In the past decade, nanoparticles (NPs) of several solid lubricants of various categories (polymeric, metallic, inorganic, and carbonaceous) have been explored as additives in oils and greases. While oil miscible ionic liquids were first explored as lubricant additives in 2012 and considering the vastness of unique ionic liquids, very few ionic liquids have been explored in lubricants, possessing great untapped potential for further research. Based on an extensive literature survey in this thesis work, research gaps were identified, which led to the objectives of the work.

This thesis attempts to explore the synergy between phosphonium ionic liquid and various categories of nanoparticles as hybrid lubricant additives for the potential enhancement of tribological performance. The study also aims to replace/minimize SAPS compounds prevalent in modern lubricants. For this, we conducted a feasibility study by formulating hybrid nano-oils composed of phosphonium phosphate ionic liquids and three oxide nanoparticles (CuO, Al_2O_3, SiO_2). Best performing hybrid nano-oil (composed of IL and CuO) gave nearly 36% wear reduction compared to the base oil. The formulated nano-oil showed poor dispersion stability (1-2 days) which severely limited its real application.

Further role of cation and anion in lubricants is not well understood. For this three ionic liquids (ILs) (1) trihexyltetradecylphosphonium bis(2,4,4-trimethylpentyl) phosphinate, (2) trihexyltetradecylphosphonium bis(2-ethylhexyl)phosphate, and (3) trihexyltetradecylphosphonium dibutyl phosphate were synthesized and added with nanoparticles in a synthetic base oil to obtain hybrid nanolubricants (PAO+ILs+NPs). Tribological and extreme pressure performances of the lubricants were tested using a four-ball tribometer. Hybrid nanolubricants showed excellent synergy in friction (23-30%) and wear (41-57%) reduction which was significantly higher (1.5-2 times) than the performance of

commercial ZDDP (20 and 25% friction and wear reduction respectively). Further hybrid nanolubricants enhanced extreme pressure properties of the base oil by up to 75% while ZDDP improved by 40%. Despite showing superior tribological performance compared to ZDDP, the hybrid nano-oil gave poor dispersion stability (4 days to 1 week) which again limits its application.

The performance of any additive not only depends on its chemistry but also on compatibility with other additives in that formulation hence studying their synergistic and antagonistic behavior becomes a pre-requisite for availing the potential of additives. We studied complex three-way interactions among oil miscible phosphonium phosphate ILs, metal oxide NPs (ZnO), and common commercial dispersant (PIBSA, used in engine oil to disperse insoluble compounds) in synthetic base oil (PAO6) for steel-steel tribopair under boundary lubrication. This study provides not only physicochemical compatibility among these additives but also their mutual synergistic/antagonistic interaction with rubbing surfaces. Based on antifriction, antiwear performance, and surface characterization we observe that the PIBSA dispersant did not negatively affect the performance of base oil or any additive combination. No precipitation or cloudiness was observed, inferring plausibly no chemical reaction among IL, NP, and dispersant PIBSA during sample preparation or storage.

In pursuit of long term stable dispersion of hybrid nano-oil, we have further explored novel nanoparticles (Boehmite and Zinctitanate) for better dispersion stability and their synergistic effect with the best-performing phosphonium ionic liquid. We observed wear reduction in the range of 49 and 53 % for Zinctitanate and Boehmite hybrid nano-oil respectively. Further, we have conducted extensive surface characterization of worn surfaces and observed active elements (P, and residues of nanoparticles) on the respective worn surface, confirming the tribochemical reaction and tribosintering process as the dominant mechanism of tribofilm formation for ILs and NPs, respectively. All the hybrid nanolubricants outperformed ZDDP indicating that compatibility between ILs and NPs can help in decreasing overdependence on ZDDP provided the long-term dispersion stability of NPs is addressed. Based on the performance of different formulated lubricants we recommend Zinctitanate hybrid nano-oil with 49% wear reduction and over 100 days of stability.

Content

List of Figures

List of Tables

Nomenclature

Abbreviation	
AFA	Anti-Friction Additive
API	American Petroleum Institute
AWA	Anti-wear Additive
BTMPP	bis(2,4,4-trimethylpentyl) phosphinate
DEHP	bis(2 ethylhexyl)phosphate
DBP	dibutyl phosphate
DLS	Dynamic Light Scattering
EDS	Energy Dispersive X-ray Spectroscopy
EPA	Extreme Pressure Additive
FESEM	Field Emission Scanning Electron Microscopy
HRTEM	High Resolution Transmission Electron Microscopy
ILs	Ionic Liquids
IL1	trihexyltetradecylphosphonium bis(2,4,4-trimethylpentyl) phosphinate
IL2	trihexyltetradecylphosphonium bis(2 ethylhexyl)phosphate
IL3	trihexyltetradecylphosphonium dibutyl phosphate
MRS	Micro-Raman Spectroscopy
MoDTC	Molybdenum Dialkyldithiocarbamate
MO	Mineral Oil
NLs	Nanolubricants
NPs	Nanoparticles
PAO	Poly Alpha Olefines
PWL	Pre-weld Load
P66614	Trihexyltetradecylphosphonium chloride
SL	Solid Lubricants
SAPS	Sulphated ash, Phosphorous, and Sulfur
WL	Weld-Load
WSD	Wear Scar Diameter
XRD	X-ray Diffraction
XPS	X-ray Photoelectron Spectroscopy
ZDDP	Zinc dialkyldithiophosphates

PIBSA	Polyisobutylene Succinic Anhydride

Chapter - 1

Introduction

1.1. General

Tribology is an interdisciplinary approach to studying friction, wear, and lubrication of interacting surfaces under relative motion. The word “Tribology” was first coined by British Mechanical engineer, Peter Jost in his famous report “popularly known as Jost report” published in 1966. He surveyed British industries and estimated a potential loss of 515 million pounds (roughly 1.1-1.4% of GDP) attributed to friction, wear, and corrosion[1–3]. This made the word “Tribology” popular, which is derived from the Greek word “tribos” meaning ‘rubbing or sliding’ and can be loosely translated as “the science of rubbing”. But the field of tribology is not new, it existed in its traditional form since the beginning of recorded human history. It is well documented that early human civilizations used natural lubricants (oils, animal fats) and developed methods such as bearings and other low friction surfaces to reduce friction and wear[1]. The scientific study of tribology can be traced back as far as the 15th century to Leonardo da Vinci’s unpublished note, where he observed proportionality between limiting frictional force and normal reaction. The quest to control friction and wear continued for the next few centuries and a seminal understanding of basic underline mechanisms were made such as fundamental laws of friction (Guillaume Amontons in 1699, Charles-Augustin de Coulomb in 1785), hydrodynamic lubrication (Osborne Reynolds in 1886), Archard equations of wear based on the theory of asperity contact (John Frederick Archard in 1953)[1].

Wear not only reduces mechanical performance but also expedites material wastage and any reduction in wear can significantly boost overall efficiency and productivity. Wear is primarily caused by friction between interacting surfaces which further leads to energy dissipation. According to Holmberg et.al 28% of the fuel energy is wasted in overcoming friction losses in an automotive car, while 21.5% is actually available for moving the vehicle[4]. As per estimates, one third of currently used energy is being wasted in overcoming friction in one form or another [5]. Proper lubrication and material selection are the most effective methods to mitigate wear, reduce friction, and enhance productivity.

The worldwide energy demand is projected to increase by 50% by 2050. To fulfill future energy requirements and reduce over dependency on conventional sources researchers are exploring renewable energy alternates such as (solar, biofuels, wind, etc.). This has prioritized research in the generation and storage of cleaner energy and improving existing technologies of production and storage with the overall aim to reduce energy losses. The demand for extremely efficient equipment having low fuel consumption characteristics is ever

increasing. Formulating new lubricants consisting of advanced lubricant additives may significantly reduce emissions, improve fuel economy and increase the useful life of machines. This has been a strong motivation for exploring new lubricants, methods, and related technologies.

1.2. Lubricants

Almost all mechanical equipment under relative motion (sliding/rubbing) requires lubricants in some form or other. Lubricant provides a protective film between interacting surfaces (due to lesser direct metal to metal contact) under relative motion and reduces asperity contacts and subsequently reduces friction and wear. Friction and wear are system properties and are highly influenced by the nature of operation or equipment design. Lubricants may provide diverse functionalities; a few are listed below[6].

(a). Lubrication: Lubricant film decreases metal to metal contact between rubbing surfaces resulting in decreased friction, wear, and energy to move one surface over another.

(b). Cooling: Lubricants may take away heat from critical components of equipment such as gears, and automotive engines.

(c). Clean operation: Lubricant suspends harmful products such as wear debris, dust, sludge, and carbon resulting in cleaner operations.

(d). Protection: Lubricants may consist of additives such as AW, EP, antioxidants, rust, and corrosion inhibitor which reduces their exposure to water, oxygen, acids, etc. resulting in prevention from oxidation, corrosion, and wear.

(e). Transfer power: In some applications (hydraulic systems) lubricants may be used for power transmission in addition to surface protection. Circulating systems, transmissions, fork lifts, and earth movers are a few examples of hydraulic systems.

Lubricants are generally liquid but depending on specific service requirements, they may be applied in different forms i.e. solid, semi-solid, and liquids. Molybdenum disulfide (MoS_2) and graphite are the most common used solid lubricants. Greases are categorized as semi-solid lubricants and are generally preferred where maintenance intervals are large. Greases not only provide lubrication but also protects components from dirt and water (external

impurities) by staying in contact. Liquid lubricants are the most popular and commonly found application in gear, engine, hydraulic, and various industrial components. Liquid lubricants can enter in the contact zone and provides lubricity due to excellent wettability. Depending on the viscosity, applied load, and service condition liquid lubricants may provide protective film ranging from monolayer to several nanometres thick, which controls the overall tribo-performance.

Depending on the applications and service conditions lubricants are formulated using base oil and performance additives. The base oil may be mineral or synthetic or a combination of both, and controls the bulk of the lubricant properties. For instance, if base oil is fire-resistant and biodegradable, then formulated lubricant is most likely to be fire-resistant and biodegradable. While the additives are chemical compounds, which are added to impart particular desirable properties or improve existing ones in a dosage ranging from 0.1 to 30% of the overall oil composition. Selecting a lubricant for a specific task is based on Common lubricant selection criteria which are listed below (figure 1.1)[6].

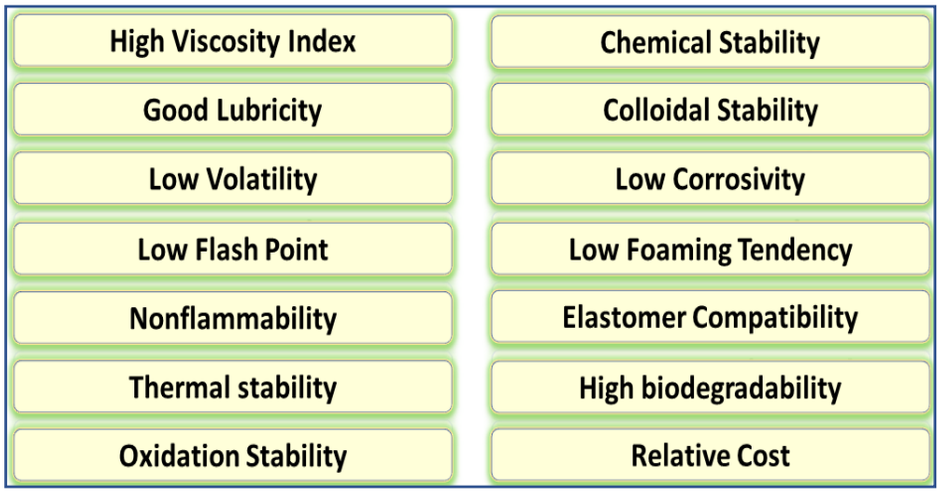

Figure 1.1 common lubricant selection criteria.

1.2.1. Base oils

Since its inception, human civilization was dependent on vegetable oil till the drilling of the first oil well (the year 1859 at Titusville, Pennsylvania, USA) in the second half of the 19th century. Due to superior stability and cost-effectiveness, Mineral oils rapidly replaced vegetable oil, which facilitated rapid industrialization in the 20th century. Currently, the majority of the lubricants market share is comprised of mineral-based oils. Crude oil is

composed of organic compounds (primarily hydrocarbons) and some residuum (contaminant of metal and metal salts) and their composition varies greatly attributed to changes in density, wax content, Sulphur content, and geographical location[6]. The organic parts can further be categorized as hydrocarbons (paraffinic, naphthenic, aromatic), asphaltenes, aromatics, hetero-organic compounds, and resins, along with atomic nitrogen, sulphur, and oxygen in their structures. These complexities make it extremely difficult to know the exact chemical structure of mineral oil and hence are generally categorized based on viscosity, sulphur content, and degree of refining (API group 1,2,3).

Table 1.1 Mineral oil groups based on API categorization

Category of base oil	Sulphur content (%)	Viscosity Index	Saturates (%)
Group I (Mineral)	> 0.03	80 to 120	And or < 90
Group II (Mineral)	≤ 0.03	80 to 120	And ≥ 90
Group III (Mineral)	≤ 0.03	> 120	And ≥ 90
Group IV (Synthetic)	All polyalphaolefins (PAO)		
Group V (Others)	All others not included in the above 4 groups		

Contrary to mineral oil synthetic oils have known molecular structures and give predictable behaviour. While mineral oil due to complexities, residuum, and unknown molecular structure may not give predictable behaviour. Synthetic processes enable molecules to be built in a laboratory using chemistry (polymerization, esterification, alkylation) from simpler substances to give the precise or desired oil properties. In this chapter synthetic word is exclusively used to refer to man-made compounds used for lubrication. Even though mineral oil is economical and abundant, they have several disadvantages compared to synthetic oils such as relatively poor oxidation stability, shear-thinning, lower flash and fire point, higher pour point, etc. It is well known that MWFs derived from synthetic base oil inherit better thermos-oxidation and chemical stability than mineral oil. Synthetic oils can be classified into 7 categories based on chemical compounds used for formulation[6]. (1) Synthetic Hydrocarbon Polymers (Polybutenes, Alkylated Aromatics, Polyalphaolefins), (2) Phosphate Esters, (3) Carboxylate Esters (Polyol Esters, Aliphatic Esters), (4) Silicon Compounds (Silicate Esters, Silicones), (5) Poly-alkylene glycols, (6) Halogenated Hydrocarbons, (7) Poly-phenyl ethers.

Based on chemical structure these synthetic oil groups possess distinct physicochemical properties and cost. MWFs formulated from a synthetic hydrocarbon can be economically as close to mineral oil and may give superior performance to that of mineral oil. In addition, synthetic oils have low-temperature fluidity, stable at extreme temperatures and pressure but are economically restrictive and in limited supply.

1.2.2. Lubricant additives:

Neat base oil is generally not adequate for dynamic operating conditions and may require performance-enhancing compounds called additives (up to 30%) to be blended into the base oil. Additives may be in liquid or particulate (including nanoparticles) form and are generally categorized as chemically inert or chemically active. Generally, additives either enhance desirable properties or suppresses undesirable properties of the base oil and are generally expected to fulfill three functions[6, 7].

- Additives must fulfill the primary function for their addition in base oil
- Preferably additives should be miscible in oil (except particle additives).
- Ideally, additives should not hamper the performance of other additives in the base oil.

Lubricant additives are generally categorized based on their function as shown in figure 2[6].

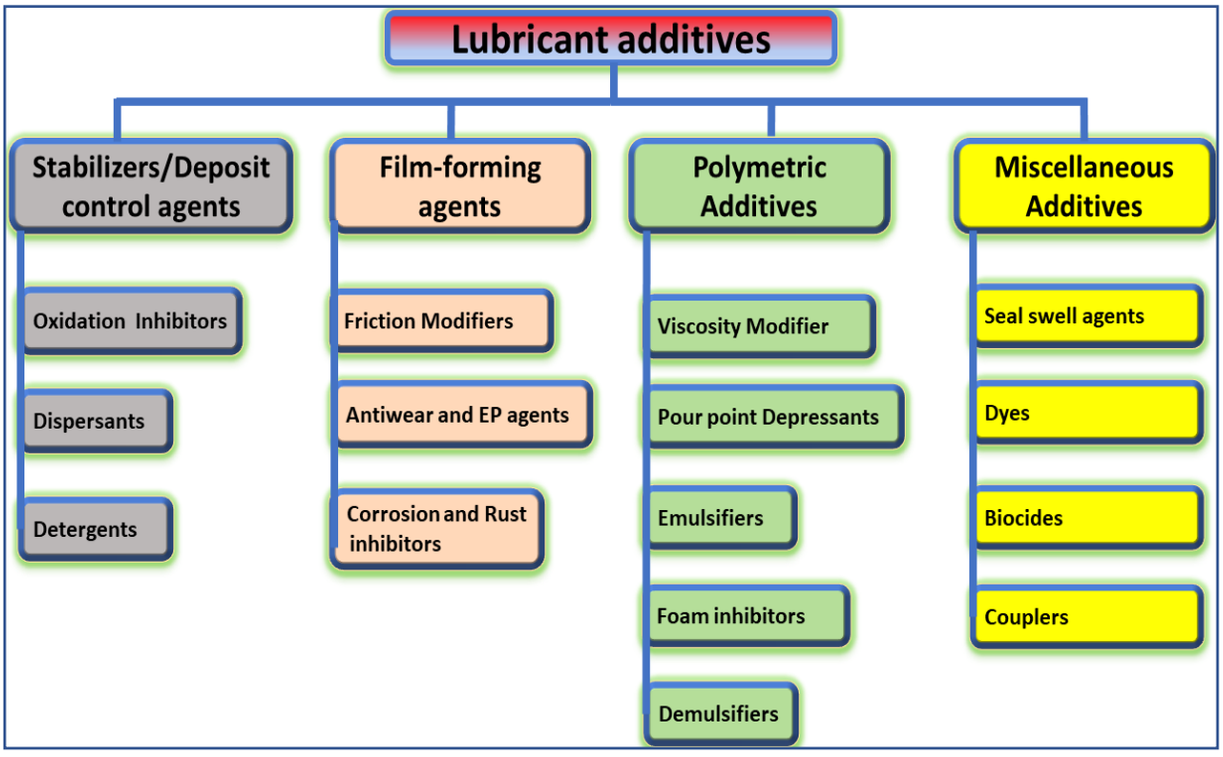

Figure 1.2 Categorization of lubricant additives based on their functions

- **Oxidation inhibitors**- control the decomposition of lubricants due to oxidation.
- **Dispersants**- Enhances colloidal stability of insoluble components of lubricants including nano-additives
- **Detergents**- Protects metal surfaces from acid attacks from combustion by-products (primarily acidic nature) by suspending and neutralizing them.
- **Film-forming agents**- forms chemical films or increase the durability of the film on counter surfaces.
- **Friction modifiers**- usually decrease the friction coefficient, resulting in improved fuel economy.
- **Antiwear and EP additives**- generally disintegrate under tribostress and chemically react to the rubbing surfaces forming regenerative surface-bound protective tribofilm and reducing subsequent surface wear.
- **Rust and corrosion inhibitor**- prevents rust and corrosion of metallic surfaces in contact with lubricants.
- **Viscosity modifiers**- decrease the effect of temperature increase on viscosity change.
- **Pour point depressants**- enhances lubricants ability to flow at a lower temperature.
- **Emulsifiers**- generally used in metal working lubricants and hydraulic fluids for mixing water and oil.
- **Demulsifiers**- separate water contaminants from the oil.
- **Foam inhibitors**- decreases persistent foam formation ability of lubricants.
- **Seal swell agents**- it maintains seal integrity.
- **Dyes**- generally used to colour coding lubricants.
- **Biocides**- prevent lubrication degradation due to microbial attack.
- **Couplers**- stabilizes the water and organic microemulsions.

The additives such as detergents, dispersants, extreme pressure (EP), antiwear (AW), corrosion and rust inhibitor, and oxidation inhibitors are chemically active and react with metallic surfaces or oxidative by-products. While additives such as demulsifiers, emulsifiers, foam inhibitors, and pour point depressants, VI improvers are chemically inert and enhance the physical properties of the lubricants. The following section discusses the additives which primarily enhance the tribological performance of the base oil.

1.3. Tribological additives in lubricants

Antifriction (AFA), antiwear (AWA) and extreme pressure (EPA) additives are additives that improve the tribo-performance of the base oil.

1.3.1. Antiwear additives (AWA)

AWA generally disintegrate under tribostress and chemically react to the rubbing surfaces forming regenerative surface-bound protective tribofilm and reducing subsequent surface wear. Zinc-alkyldithiophosphates (ZDDPs) are the most popular antiwear additive class used in a wide range of lubricant formulations due to their excellent solubility, low cost, and ability to form tribofilm rich in S, P, and Zn on underline metallic surfaces. The AW additives are suitable only for mild and moderate pressure conditions and reduce wear, friction, scoring, and scuffing under boundary lubrication conditions. AW additives are generally polar materials such as esters, acids, and fatty oils composed of Phosphorus, Sulphur, and various Chlorine compounds[8].

1.3.2. Antifriction additives (AFA)

AFA control friction coefficient hence also known as friction modifiers. These additives generally form residual films on the rubbing surfaces having extremely low shear resistance resulting in overall friction reduction. AF additives are generally categorized into two broad groups, one is organic friction modifiers while the other is organomolybdenum (OM). The OM additives may further be categorized into three types based on phosphorus and sulphur compositions i.e. molybdenum dialkyldithiophosphate, molybdenum dithiocarbamates, molybdate ester[9].

1.3.3. Extreme Pressure additives (EPA)

Usually, EPA remain dormant in lubricants and get activated at extreme pressure conditions (specific temperature and pressure) during sliding. They may chemically interact with rubbing metallic surfaces and form hard tribofilm, having lower shear resistance than the underline metallic surface. EP additives also control wear, reduce friction and decrease the severity of surface damage. This particular class of boundary lubricants are also called anti-scuffing additives. The kinetics of the tribo-chemical reaction is highly influenced by an increase in localized heat due to initiation and breakage of short-lived micro weld junctions

between rubbing surfaces. Modern EP additives are generally composed of phosphorus, sulphur, borate, and chlorine compounds.

1.4. Need for energy efficient oils

The new stringent regulations to control automotive emissions have limited the use of sulphur (0.5%) and phosphorus (0.08% or 800 ppm) for engine lubricants. The new regulations have forced lubricant manufacturers and researchers to develop a new class of environment benign additives composed of lower SAPS (Sulphated ash, Phosphorous, and Sulfur) compounds. As per reports, fuel economy in the automotive industry can be improved by up to 5.5% by using less viscous engine oil. But these lower viscosity engine oils may shift the lubrication regime from hydrodynamic towards mixed and boundary lubrication, which may result in higher asperity contacts and subsequently elevated friction and wear. While advanced lubricant additives may facilitate employing relatively lower viscosity base oil for formulating less viscous lubricants which may meet and excel existing service requirements along with a potential for multifold benefits such as fuel economy, reduced cooling, and exhaust losses.

Moreover, modern lubrication systems are being pushed to severe operating conditions (higher temperature, sliding speed, loads, and torque transfer) in many industrial components such as heavy duty engines, and wind turbines (>10 MW). Increasing lubrication system efficiency with decreased surface distress mandates continuous innovation in lubricants and surface engineering (texturing, coating).

1.5. Organization of this Thesis

Chapter 1: Briefly explains research preliminaries and the conceptual background of the research area particularly key aspects of tribology, and lubrication, with an emphasis to base oil lubrication, additives, and their functions. This chapter also includes the need for developing energy efficient lubricants.

Chapter 2: A Systematic Literature Review has been conducted to find the literature related to oil miscible ionic liquids, nanoparticles, and their synergy. The literature review attempts to give detailed evolution of ionic liquids, the effect of their physicochemical properties on miscibility, and the tribological performance of lubricants. Nano lubricants, especially based

on NPs of solid lubricants, (SLs) is discussed. Further, this chapter covers the synergistic effect between ionic liquids, nanoparticles, and their underline mechanism. Finally, it identifies the research gaps, objectives, and execution strategy.

Chapter 3: Reveals the particulars of selected materials chosen for the investigations. Various techniques employed for the characterization, development of nano-oils, and performance evaluation and instruments/apparatus utilized are discussed.

Chapters 4, 5, 6, and 7 comprise the experimental investigations on formulated hybrid oils.

Chapter 4: Reveals the outcome of the study investigating the compatibility between phosphonium ionic liquid and three oxide nanoparticles (CuO, Al_2O_3, SiO_2) for their tribo-performance in API Group 1 mineral oil. A different set of lubricants were formulated composed of ionic liquid, nanoparticles, and hybrid additive to assess their tribological performances and potential compatibility. Excellent synergy has been observed for CuO and Al_2O_3 hybrid nanolubricants with friction and wear reduction up to 24 and 36% respectively while no conclusive evidence of synergy was observed for SiO_2 hybrid nanolubricant.

Chapter 5: Investigates the synergistic effects between three common cation based phosphonium ionic liquids and nanoparticles as a hybrid oil additive and their comparative study with commercial ZDDP. Even though all ILs share the same cation and phosphorus concentration but they performed distinctively, inferring that trio chemistry of both cation and anion are equally important for tribofilm formation. Further, all the hybrid nanolubricants outperformed ZDDP indicating that compatibility between ILs and NPs can help in decreasing overdependence on ZDDP.

Chapter 6: Investigates the Three-way compatibility study among Nanoparticles, Ionic Liquid, and Dispersants for potential in lubricant formulation. Formulated commercial lubricants consist of base oil and more than half a dozen of performance additives and their overall performance does not only depend on their chemistry but also on compatibility with other additives in that formulation. Based on antifriction, antiwear performance, and surface characterization we observed that PIBSA dispersant did not negatively affect the performance of ionic liquid or any additive combination.

Chapter 7: Explores the potential of novel Boehmite and Zinctitanate NPs study as lubricant additives along with their synergistic effect with ionic liquid. Visual inspection and DLS analysis show excellent dispersion stability (negligible sedimentation for the first 30 days) of

Boehmite NPs due to their ability to slow agglomeration. Zinctitanate nanoparticles also showed excellent dispersion stability (majority dispersed even after 225 days) in the synthetic base oil, and the DLS study confirms very limited agglomeration of colloidal nanoparticles over time. Based on the performance of formulated lubricants we recommend 0.5 and 1 wt% as optimum concentrations for Boehmite and Zinctitanate nanoparticles for excellent wear reduction. Further synergistic studies of these nanoparticles were studied with the best-performing phosphonium phosphate ionic liquid.

Chapter 8: Summarizes the salient conclusions of the research work in the thesis and recommends future work to be taken forward. Based on the study it is evident that ionic liquids and nanoparticles both contribute to the protective tribofilm formation. All hybrid nanolubricants outperformed commercial antiwear additives indicating the potential of replacing harmful existing antiwear additives with hybrid nanolubricants provided the long-term dispersion stability of NPs is addressed.

Chapter - 2

Literature Review

2.1. Lubricant additive development timeline

The first patent to enhance lubricity using organic fatty acids was filed in 1918. Since then dozens of distinct additive groups have been developed over the years. Among these additives, nanoparticles and ionic liquids are fairly recent and have the potential to replace/minimize SAPS compounds used in commercial additives. Figure 2.1 details additive development over the years and highlights recent additives (IL, NPs).

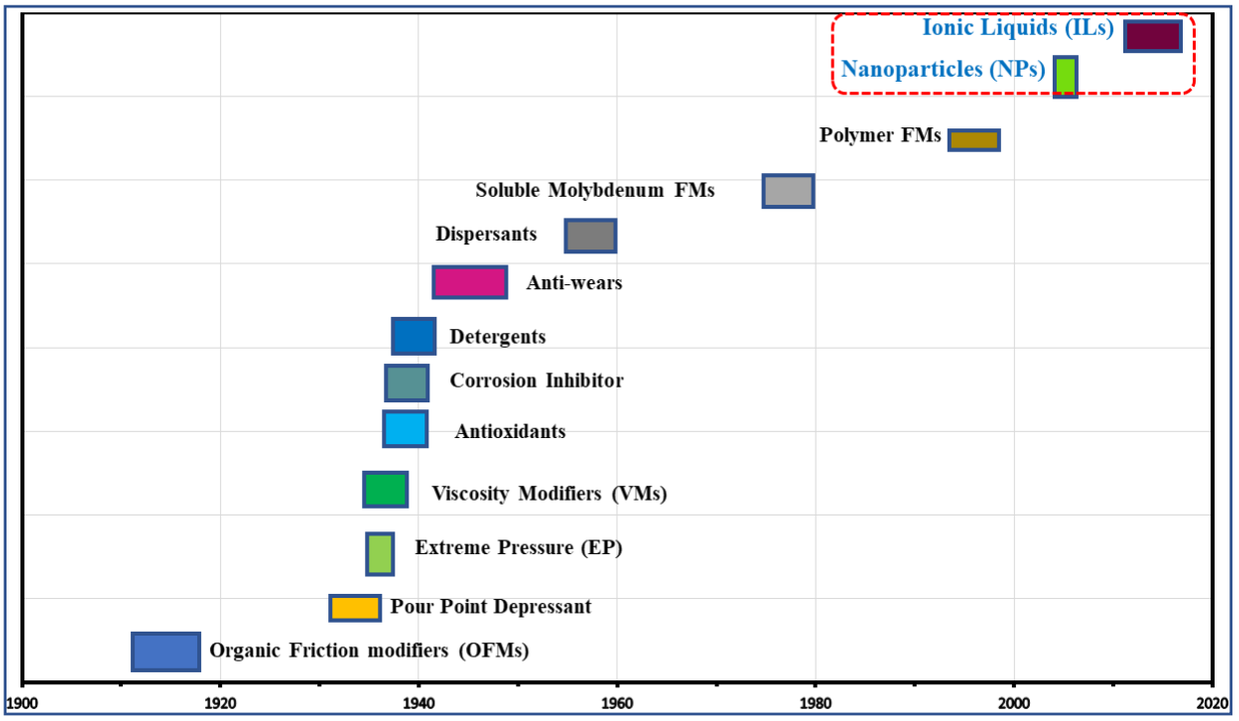

Figure 2.1 Additive groups developed over the years

2.2. Ionic liquids

Ionic liquids (ILs) are innovative compounds with tuneable physical, chemical, biological and thermal properties. These inherent properties have promising potential to revolutionize many disciplines of science and engineering research such as solvents, catalysts, machining, electrolytes, cell biology, and many more at both laboratory and commercial scales [10–12]. Ionic liquids are entirely made up of ions (cation and anion). Technically molten table salt can be categorized as an ionic liquid having a melting temperature of 801°C but at standard temperature and pressure, it remains in the solid crystalline phase. Nowadays in scientific literature and general use the term "ionic liquids" refers to the ionic compounds that are in a liquid phase below 100°C while the ionic compounds having a melting temperature above

100°C is loosely termed “molten salt”[11, 13, 14]. “Room-temperature ionic liquids” (RTIL) are another term used for these ionic liquids; generally, consisting of organic cations and organic or inorganic anions.

Ionic liquids are also called “designer solvents”, for the possibility of obtaining desired physicochemical properties by altering cations and anions (hence tuneability). For instance, by altering cations and anions or both, viscosity, water miscibility, corrosive resistance, and polarity can be tuned for task-specific applications[13]. Ionic liquids inherit several desirable properties such as negligible vapour pressure or nonvolatility at ambient conditions, noncorrosive, nonflammable, excellent thermal stability, tunable polarity, solubility, basicity, acidity, etc[10, 11]. Compared to hazardous volatile organic compounds (VOCs) ionic liquids are often considered green solvents since it has extremely low vapour pressure.

2.2.1. A brief evolution of ionic liquids.

Paul Walden in the year 1914 synthesized the first-ever room temperature ionic liquid (ethyl ammonium nitride) by metathesis reaction between hydrochloride salt and lipophilic counterions[15]. The compound was water-like with a melting temperature of 12°C. Following decades several other first-generation ionic liquids were synthesized using derivatives of imidazolium and pyridinium cations with metal halide anions[16]. Chloroaluminate and other metal halide anions of first-generation ionic liquids attributed toxicity, non-biodegradability, water reactivity, and air sensitivity, making it difficult to handle other than in an inert atmosphere[17–19].

The limitations of first generational ILs prompted the exploration of water and air stable, second-generation ILs. This was achieved by replacing water and air sensitive metal halide anions with halides (Cl^-, Br^-, I^-) and other sets of anions such as tetrafluoroborate (BF_4^-), hexafluorophosphate (PF_6^-), etc[17, 20]. While two more cation groups i.e., Ammonium and Phosphonium derivatives were also introduced along with earlier imidazolium and pyridinium-based cations. These second-generation ILs pioneered novel applications in various disciplines of scientific and engineering research due to their excellent physicochemical properties. These ILs were still economically restrictive due to higher initial material costs (particularly fluorinated anions) and costly final product purification methods[18]. One of the major limitations of these ILs was their toxicity and corrosive nature which could be attributed to

halides. To eliminate toxicity and for excellent biodegradability third-generation, ILs were synthesized from biodegradable cations and anions replacing harmful halide anions. Environment benign and stable anions such as fatty acids, amino acids, sulphates, phosphates, etc. are being explored in the third generation ILs providing several advantages such as excellent biodegradability, lower cost, lower toxicity, no purification requirement, etc. Generally, ILs are categorized by their cation group and alkyl-imidazolium, alkyl-ammonium, alkyl-pyridinium, and alkyl-phosphonium are the most widely studied ILs. In particular, functionalized alkyl imidazolium has been widely reported in the literature due to its higher thermal stability and lower melting points. Figure 2.2 shows the molecular structures of the most common cations and anions used in the ILs research for friction reduction.

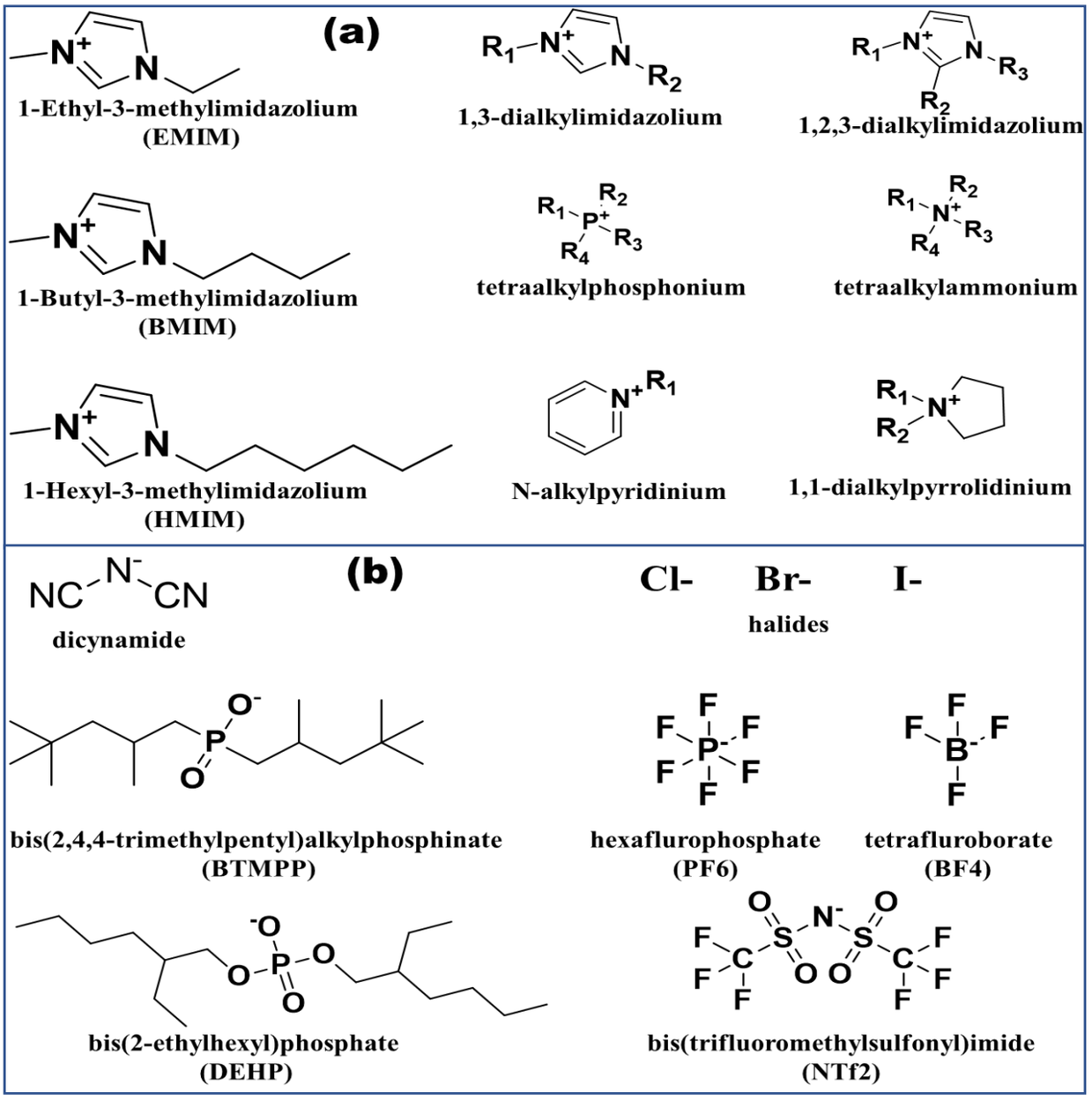

Figure 2.2. Most common (a) cation and (b) anion groups in the IL research.

2.2.2. Physicochemical properties of ionic liquids

Physical properties of ILs such as melting point, miscibility, viscosity, density, hydrophobicity, and thermal stability have shown a strong correlation with cation and anion structure. That means depending on the service condition ILs properties can be tuned by altering the molecular structure of the cation and anion[21, 22]. By attaching functionalized groups on both the ions of ILs the specific properties can be induced in the ILs. For instance, tribo-active elements and groups such as phosphates, sulphate, etc. can be added in ILs by replacing imidazolium and pyridinium-containing cations with phosphonium and ammonium groups to enhance the protective film formation capability of the lubricants[21, 23–26].

Researchers have reported that the melting point of ILs highly depends on the composition, symmetry, and chain length of both the ions of ILs[27–30]. It was observed that with the same anion group melting temperature of IL was decreased by replacing shorter cations with larger cation groups. In general, published literature has reported that bulky unsymmetric cations reduce the melting point of the ILs[28, 30]. Zheng et.al. varied symmetry and chain length of imidazolium ILs and reported that symmetric ILs with shorter chain length (N=4, 6) normally crystallized while asymmetric ILs with longer chain lengths gave comparatively lower melting temperatures [30]. Holbrey et.al. classified ILs in three categories based on their thermal behavior and also observed similar results of an increase in chain length decreased the melting point due to decreased lattice energy, disordered crystal packing, and prolongation of molecular structure[27]. Similarly, anion's molecular structure also influences the melting point of the ILs. Fredlake et.al explored 13 imidazolium-based ILs having different anions and observed increased melting points with anion order Br> Cl> BF_4> PF_6> Tf_2N[31]. In addition, they observed a decrease in density with an increase in cation chain length while an increase in density with an increase in the molecular weight of anions.

A direct correlation between ILs structure and viscosity can be established. It was reported that an increase in chain length, symmetry, and branching of cation or anion increased the viscosity of ILs[32–34]. Xue and coworkers studied the effect of alkyl chain branching on the physicochemical properties of ILs and reported that for the same Carbon number the branched structure registered higher viscosity than the linear structure[32]. They attributed this to relatively higher stable packing between both the ions (cation and anion) due to symmetry. An increase in alkyl chain length increased the viscosity due to stronger van der Walls interaction between ions reported by Zeng et. al[33]. Viscosity also influences the fluid film

formation during machining and generally higher viscosity may provide a better surface finish. The tunable properties of ILs may be used to obtain desirable viscosity by altering the molecular structure of cations and using higher molecular weight for anions.

The inherent properties, such as excellent thermal stability and lower vapor pressure are some of the biggest advantages of using ILs in lubricants. ILs may have broader fluidity, ranging from -100 to 450^{o}C suitable for application in many disciplines particularly for high temperature applications[35]. As per published literature for cation with symmetric structure, ILs thermal stability was relatively enhanced while on the other hand increased chain length decreased thermal degradation temperature[28, 36]. Tao et.al. explored imidazolium cation by altering it with varying functional groups such as n-alkyl, cyclo-alkyl, aromatic, and aliphatic[37]. Further, they reported that ILs composed of the n-alkyl group are most stable among the functionalized groups with a degradation temperature of 436^{o}C. Shirota et.al. reported that Di-cationic imidazolium-based ILs showed higher decomposition temperatures than mono-cationic ILs with anions such as NTf2, BF4, NPf2, and NO3[38]. Several studies have also reported the effect of anions structure on the stability of ILs having the same cation[31, 35, 39–42].

2.2.3. Ionic liquid in lubricants before 2012

IL was first studied as a lubricant in 2001 by Ye et al[43]. They evaluated 1-methyl-3-hexylimidazolium tetrafluoroborate and 1-ethyl-3-hexylimidazolium tetrafluoroborate's tribological properties using optical SRV ball on disc configuration. Following the lead of Ye's group, several other researchers explored various ILs as neat lubricants[44–47]. Despite their excellent tribological properties, ILs as base oils are economically restrictive due to their high cost. Iglesias et al. attempted to blend 1 wt% crystal [N12,H,H,H] [Cl] in a neutral base oil, which was way over the solubility limit of the base oil nevertheless, they reported improved tribological properties for aluminium-steel tribopair[48]. Several other researchers attempted to use ILs as an additive in base oils, but limited success was achieved since earlier ILs were immiscible in base oils due to their relatively shorter anion chain length[7, 49–51]. From year 2001 to 2011 most of the ILs were imidazolium and pyrrolidinium cation based along with small inorganic anions such as PF_6, Sulphate, BF_4, Cl and hence were immiscible in nonpolar oils.

2.2.4. Ionic liquids as lubricants additives

The breakthrough was made in 2012 by Qu's group with the synthesis of phosphonium based oil miscible IL. They reported two ILs i.e. trihexyltetradecylphosphonium bis(2-ethylhexyl) phosphate ([P6,6,6,14][DEHP]) and trihexylltetradecylphosphonium bis(2,4,4-trimethylpentyl) alkylphosphinate ([P6,6,6,14][BTMPP]) which were soluble with all the common nonpolar base oils[52, 53]. Since 2012 several other oil miscible ILs such as phosphonium, ammonium, pyrolidium, and imididazolim based have been studied[7]. Phosphonium and ammonium based IL have been the focus of study for their better affinity towards metallic surfaces when added as a lubricant additive. Table 2.1 gives important studies exploring the performance of phosphonium and ammonium based ILs compared to different groups of the base oil.

Table 2.1 Important Ionic Liquids studies as lubricant additives and their observations

SN.	Ionic liquids	Base oil	comments	References
1	$[P_{66614}][DEHP]$	PAO, 5W-30	• IL was fully miscible up to 5%. • IL showed a 60% reduction in friction • IL blend decreased wear by three times compared to the base oil. • IL was stable up to 347^0C	[54]
2	$[P_{66614}][DEHP]$, $[P_{26614}][DEHP]$	PAO, 10W, 10W30	• Both the ILs were fully miscible up to 5% blend and stable up to around 350^0C • Both ILs decreased friction significantly and wear twice less than the base oil	[53]
3	$([P_{4444}]$-$[DEHP]$, $[P_{66614}][DEHP]$, $[P_{66614}][i\text{-}C_7H_{15}COO]$, $[P_{66614}][n\text{-}C_7H_{15}COO]$, $[P_{66614}][i\text{-}C_9H_{19}COO]$, $[P_{66614}][n\text{-}C_9H_{19}COO]$, $[P_{66614}][nC_{17}H_{35}COO]$, $[P_{66614}][RSO_3]$	PAO	• For eight ILs temperature stability was up to 250,310, 347,348, 308, 330, 327, 308, 431 ^{0}C respectively • Sulfonate IL was the most oxidation-stable and carboxylate was the least stable. • For eight ILs solubility was found to be between 1% to 10%. • It was found that IL with shorter alkyl chain lengths were having less solubility. • All the IL showed excellent antiwear properties • The antiwear ranking observed was. Phosphonium phosphate> phosphonium carboxylate > phosphonium sulfonate	[24]
4	**5 aprotic ILs** i.e $([N_{2222}][DEHP])$, $([N_{4444}][DEHP])$ $([N_{6666}][DEHP])$ $([N_{8888}$-$][DEHP])$ $([N_{8881}][DEHP])$ **4 protic ILs** i.e. $([N_{222\text{-}H}][DEHP])$ $([N_{444H}][DEHP])$ $([N_{666H}][DEHP])$ $([N_{888H}][DEHP])$	Engine oil without AW additives	• $[N_{8888}][DEHP]$, $[N_{8881}][DEHP]$ and $[N_{888\text{-}H}][DEHP]$ was blended with base oil in concentration of 2.04, 1.78 and 1.74 wt%, respectively. • ILs were also compared with ZDDP. • $[N_{888H}][DEHP]$ and $[N_{8881}][DEHP]$ both showed superior wear protection properties than ZDDP. • Protic $[N_{888H}][DEHP]$ generated the least amount of wear.	[55]
5	Five ILs different cations but same anions.$([P_{8888}][DEHP])$ $[P_{66614}][DEHP]$,	GTL 4 base oil	• It was observed that each alkyl chain should be of at least 6 carbons atoms long for oil solubility.	[56]

	([P_{44414}][DEHP]) ([P_{4448}][DEHP]), ([P_{4444}][DEHP])		• [P_{8888}][DEHP] and [P_{66614}][DEHP] enhanced wear protection of the base oil	
6	[$P_{4,4,4,2}$][$C_2C_2PO_4$], [$P_{6,6,6,14}$][$(C_2F_5)_3PF_3$]	Three easter oil and one Vegetable oil	• Both ILs show improved antifriction and antiwear properties at1% ILs blended in the base oil. • Due to very low melting points, both lubricants can be used at very low temperatures. • Pure [$P_{4,4,4,2}$][$C_2C_2PO_4$] shows low coefficient of friction but inferior anti-wear properties and bad temperature stability than [$P_{6,6,6,14}$][$(C_2F_5)_3PF_3$].	[57]
7	N_DEHP, N_DBDTP, P_TMPP, P_TFSI, P_DMP, P_DEDTP compared with ZDDP	Blend of SN 150 and bright stock 90	• N_DEHP showed the lowest coefficient of friction. • N_DEHP and P_TFSI outperformed ZDDP, but N_DBDTP, P_TMPP, P_DMP, and P_DEDTP performed inferior to ZDDP for wear reduction.	[25]
8	[P_{66614}][$(iC_8)_2PO_2$], [P_{66614}][BEHP] compared with ZDDP	YUBASE	• Both the ILs enhanced the antifriction properties of the base oil. • Is was observed that [P_{66614}][BEHP] blended with base oil performed better than[P_{66614}][$(iC_8)_2PO_2$]. • [P_{66614}][BEHP] showed superior wear reduction than [P_{66614}][$(iC_8)_2PO_2$]. • The ZDDP showed less friction than both ionic liquids.	[58]
9	P[6,6,6,14]DPP, P[6,6,6,14]BEHP, P[1,4,4,4]DPP, C_3mpyrNTf_2, P[6,6,6,14]NTf_2, P[6,6,6,14](iC_8)$_2PO_2$.	VO, TMP, PE MO and PAO.	• All the blended IL showed reduced friction and wear properties over the base oil. • The research shows that the majority of the properties of the blended lubricant depend on the unique performances of the base oils, e.g. If base oil shows high friction and wear then, IL blend in the base oil did not improve the base oil performances.	[59]
10	Two oil-miscible quaternary ammonium phosphites ILs(POPA and PTPA) compared with ZDDP.	PAO 10	• Both the ILs outperformed the ZDDP in friction and wear reduction. • Both the ILs have better extreme pressure properties than ZDDP.	[60]

2.3. Nano-oils/Nano-lubricants

Due to very tiny size, dispersibility, large surface area, insolubility, durability, nonvolatility, and nonreactivity with other additives, researchers quickly understood the potential of nanoparticles (NPs) in lubricants, opening a new exciting stream of nanolubricants. Choi et al. first coined the term "Nanofluids" referring to colloidal nanoparticles in base fluid[61]. The advantages of NPs are their nanometer size and higher aspect ratio, since they may interact with asperities of rubbing surfaces and may reduce friction and wear by mechanisms such as ball bearing, mending, polishing, and film formation. The other significant benefit of NPs over Sulphur and Phosphorus-based commercial antiwear additives is that NPs need not rely on tribochemical reactions which are system sensitive[5]. As per characteristic chemical compositions, Gulzar et.al has categorized these nanoparticles into 7 major classes[62].

1. Metals (Cu, Ti, Fe, Al, Pb, etc.)
2. Metal oxide or sulphides (CuO, Fe_2O_3, TiO_2, ZnO, etc.)
3. Carbon based (graphene, graphite, etc.)
4. Chalcogenides (MoS_2, WS_2, etc.)
5. Nanocomposites (Al_2O_3/SiO_2, SiO_2/ZrO_2, etc.)
6. Ceramics (hBN, Al_2O_3, SiO_2, etc.)
7. Others (PTFE, etc)

2.3.1. Mechanism of nanoparticles in lubricants

Well-dispersed NPs get attracted toward rubbing metallic surfaces due to two important factors. The first is undulation due to increased temperature at the rubbing junctions propagating NPs towards the rubbing surface. While the other is a stronger electric field due to the generation of exo-electron on the rubbing surface which may lead to the migration of NPs[63]. Based on surface characterization reported in the literature there are four known mechanisms for enhanced wear protection provided by nanoparticles[64, 65]. Two of these mechanisms could be accredited to the direct action of NPs (film formation, and ball bearing) while others are due to secondary surface-enhancement (polishing and mending effects).

(a) Mending (self-repairing) effect- This occurs if nanoparticles occupy the scars and grooves of the counter surfaces, compensating for the loss of material (NPs fill the groves and scars), which may result in reduced wear[64].

(b) Polishing effect- the average roughness of rubbing surfaces is minimized due to the abrasive action of the nanoparticles. Owing to lower surface roughness this polishing or "artificial smoothing" effect results in improved tribological performance[64].

(c) Ball bearing or rolling effect- this is the result of a direct action of nanoparticles, which occurs when quasi-spherical or spherical nanoparticles roll between counter surfaces, converting sliding friction into a combination of rolling and sliding friction[64].

(d) Protective film- Film formation results in a coherent, smooth and sacrificial thin film on top of the rubbing surface attributed to tribosintering/chemical reaction between substrate and nano-additives under tribostress. Due to very low shear resistance, this film may reduce wear and friction significantly. For effective protection of substrate,

the tribofilm formation rate should be higher than the progressive material removal rate due to wear.

Though, in various studies, the classification of active mechanisms is still a subject of discussion[9, 64, 65].

2.3.2. Dispersion of nanoparticles

Colloidal NPs tend to sediment over time predominantly due to agglomeration caused by Brownian motion and gravity (since NPs are denser than base oil)[66]. For stable dispersion, the nanoparticles should be small, preferably less than 100nm. Due to no affinity towards oil, significant proportions of the nanoparticles are difficult to disperse in the base fluid. It is extremely difficult to obtain stable dispersion without dispersants/surfactants. The colloidal stability of these NPs may be improved by:

- Using polymer groups to functionalize nanoparticles, reduces agglomeration due to steric repulsion.
- Using ionic dispersant and surfactants, which provides electrostatic repulsion resulting in reduced agglomeration
- Using high polarity base oil

Ultrasonic based methods (bath and probe sonication) is the most popular method employed for dispersing NPs in lubricants. Probe sonication is the most effective method which generates successive sequences of high pressure (around 500 bar attributed to cavitation effect) for an extremely short duration (microseconds) due to the passing of high frequency ultrasonic waves in lubricants. Dispersants are employed to enhance the colloidal stability of nonmiscible constituents of lubricants (dirt and impurities) and has become an integral part of commercial lubricants. Numerous research has proved the effectiveness of dispersants in enhancing the colloidal stability of NPs.

2.4. Synergy between ionic liquids and nanoparticles

Several researchers have contributed to the exploration of IL as a base oil and performance additive in mineral, synthetic as well as in biolubricants as discussed in section 2.2.4. [67]. ILs and NPs can fulfill the expectations of modern lubricants and appear promising as hybrid lubricant additives. But very few researchers have concentrated their efforts on exploring the synergy between IL and other additives moreover the tribofilm formation for synergy is still not well understood[68–73]. Xiaoqiang Fan et.al. produced modified graphene oxide (MGO) using graphene oxide (GO) and three alkyl imidazolium ILs i.e. LB104, LP105, LF106 by epoxide ring opening reaction[72]. The MGO and GO were added in multialkylated cyclopentanes (MACs) as an additive in 0.1 wt% concentration. The study reported that hybrid additive in MACs provided effective separation of tribo-surfaces which was instrumental in excellent friction and wear reduction properties i.e. 27% and 74% respectively compared with neat MACs. Raman spectra of the worn surface showed two weak D and G bands, confirming the presence of modified Graphene (MG) on the surface, which may have adsorbed on the rough surfaces due to relative sliding motion and made a physical protective film. XPS spectra confirmed the formation of wear resistant components such as FeF_2 and B_2O_3 due to the tribo-chemical reaction of ILs. The study claimed that there was a synergy between hybrid additives. Their proposed theory for tribomechanism was physical adsorption film for modified graphene and tribo-chemical reaction film formation for IL. Jose Sanes et.al. also explored the synergy between imidazolium based IL (1-octyl-3-methylimidazolium tetrafloroborate) and graphene hybrid additive in paraffinic mineral oil and fully formulated engine oil[70]. The hybrid lubricant showed 33% friction reduction and lowest (almost negligible) material loss compared to paraffinic mineral oil. EDS analysis showed a similar atomic concentration of Carbon and Oxygen outside and inside of the wear track which was in accordance with a negligible material loss for hybrid lubricant. On the other hand for fully formulated engine oil (FFO) the highest wear reduction was observed with FFO+IL blend and not with FFO+IL+G, inferring that no synergy was observed between IL and graphene in fully formulated oil which could be attributed to no continuous physical protective layer of graphene on the steel surface. Moreover when 0.005 wt.% graphene was added exclusively in FFO Surprisingly 73% reduction in friction coefficient was observed.

Yi Li et.al. explored the synergy between ILs and Mo NPs in PEG base oil[69]. Their group developed two new series of 2-mercaptobenzothiazole (N12 & EM) based ILs and added

in base oil along with Mo NPs in 0-1wt% concentration and tested on a ball on a disc tribometer. It was interesting to note that there was no clear trend observed for the friction coefficient of the single and hybrid additives, but all the single and hybrid additives managed to decrease wear significantly at lower and elevated temperatures. The highest wear reduction was observed for PEG+N12+Mo hybrid additive which was almost 2% (98% wear reduction) of base oil at elevated temperature. Although the wear reduction was excellent at elevated temperature ~~but~~ a similar trend was observed at a lower temperature ~~also~~. The superior tribological performance was credited to the formation of tribochemical product i.e. MoS_2, MoO_2, MoO_3, and Fe_2O_3 on the worn surface confirmed by EDS and XPS spectroscopy. Raman spectra of worn surface also confirmed the formation of MoS_2 (Mo from NPs and S from MBT anion) tribofilm at elevated temperature. Raman spectra showed the presence of MoS_2 tribofilm only on the surfaces lubricated with a hybrid additive and not with any single additive. Yi Li's group claimed that MoS_2 concentration is directly proportional to sliding time and at the end of the test 50-90 nm thickness of tribofilm was found on the worn surface. Rashi Gusain et al. synthesized graphene-ionic liquid hybrid nanomaterial by covalently grafting imidazolium ring and using three distinct anions, bis(salicylate)borate (BScB), Oleate (OL), and hexafluorophosphate (PF_6)[71]. Graphene-IL hybrid nanomaterials were blended in PEG-200 in a concentration ranging from 0-0.05mg/mL. Their group observed that Gr-BScB hybrid nanomaterial recorded the lowest friction (28%) at an optimum concentration of 0.02 mg/mL. Gr-OL showed good wear protection but Gr-PF_6 blend showed the highest friction coefficient, even higher than base oil due to the tribo-corrosive effect from the decomposition of Gr-PF_6 under high load. When Gr-IL blend was directly compared with the IL blend, wear reduction was 55-78% and 7-39% respectively at a concentration of 0.02 mg/mL. The superior friction and wear reduction was attributed to tribo-chemical thin film formation by Gr-IL along with good mechanical strength of graphene nanosheets.

Jun Qu et.al. focused their efforts in exploring the synergy between IL and ZDDP, a common antiwear additive in GTL base oil[68]. For this they selected three phosphonium ([P_{8888}][DEHP], [P_{66614}][DEHP], [P_{66614}][BTMPP] and one ammonium [([N_{888H}][DEHP])] based IL in different proportions such that maximum phosphorus limit do not cross regulatory limit for engine oil of 0.08 wt%. The study concluded that ([P_{8888}][DEHP] and [P_{66614}][DEHP] showed synergy while [P_{66614}][BTMPP] and [([N_{888H}][DEHP] had no such synergy with ZDDP even though these two ILs share same cation or anion with [P_{66614}][DEHP] indicating that both cation and anion are critical and play an important role for synergy. The study credited a very

high concentration of active agents such as Oxygen, Zinc, Sulphur, and phosphorus on the worn surface for synergy between some of ILs and ZDDP. Whereas Zinpeng Li et al. explored the synergy between alkylphosphate-ammonium IL (DOPD) and alkylphenylborate IL (DBDB) in rapeseed oil and tested in a different concentrations ranging from 0.25 to 1% by using four-ball tribotester[73]. It was observed that DOPD and DBDB showed different friction and wear reduction properties. DBDB showed very slight friction reduction properties at high loads (392N and 490N) except 1wt.% . While DOPD firstly decreased friction up to 196N and then showed an increasing trend of friction coefficient at higher load. Moreover, the combination of the DOPD and DBDB showed synergy and a declining trend of friction coefficient with the increase of applied load. While wear performance slightly varies from the friction reduction trend, for instance, DOPD performed remarkably superior to DBDB in wear reduction, this implies that it resists shearing force effectively at higher load. When both the ILs were blended in base oil synergy was observed for wear reduction and at lower load the wear reduction of the combined ILs were similar to DOPD but at higher load the combined ILs performs superior to DOPD alone due to formation of more compact surface protection film which was confirmed by the SEM and XPS spectra. Nasser et al. explored three phosphonium-based ILs with hBN nanoparticles in highly viscous synthetic gear oil for wind turbine application and observed synergy with friction (17–28%) and wear (65–92%) reduction over the base oil[74]. Seymour et al. explored polymer brush grafted silica NPs with phosphonium ILs in synthetic base oil and observed synergy with 20–35% friction reduction compared to single additives. Based on tribofilm characterization they further reported that both additives underwent tribochemical reaction and possible formation of covalent bond (Si, P, O) between anion of IL and silica NPs[75].

2.5. Inadequately researched, literature review of key papers.

2.5.1. Inadequately researched Trihexyltetradecyl phosphonium [P66614] cation based Ionic Liquids-

ILs reported till 2011 in lubrication posed several concerns such as thermal oxidation, corrosion, cost, toxicity, and miscibility[7]. Qu et.al first synthesized Trihexyltetradecyl phosphonium cation-based oil miscible ionic liquids ([P66614][DEHP], ([P66614][BTMPP])) in 2012[54]. The cation and anion of both these ILs are composed of quaternary molecular

structure which could be attributed to excellent miscibility in most of the mineral and synthetic non-polar base oil. With the introduction of oil miscible ionic liquid in 2012, the mainstream approach has been shifted from employing ILs as a base (neat) lubricant to using them as lubricant additives. Since then, dozens of thermally stable, noncorrosive, and oil miscible ionic liquids have been synthesized which has addressed above mentioned technical barriers[21]. Zhou et.al explored [P_{66614}] with various carboxylate anions ([i-$C_7H_{15}COO$], [n-$C_{17}H_{35}COO$] and [i-$C_9H_{19}COO$],) having different alkyl chain lengths to understand the effect of chain length on miscibility and tribological performances[24]. They reported varying miscibility range (2-10%) attributed to distinct long alkyl chains and branched structures of those ILs. Various studies have confirmed in laboratory scale and engine dynamometer test that the addition of ILs even in relatively low concentration can significantly improve the tribological performance of the lubricants, suggesting affordability and feasibility for real industrial usage[7]. Several studies have confirmed that surfaces lubricated with phosphonium ILs generally show a strong phosphorus signal on the worn surface indicating the formation of phosphorus containing tribofilm. While the exact mechanism is still not known but based on the surface characterization results a hypothesis is proposed. First, an initial layer of the protective film is formed due to a tribochemical reaction between rubbing metallic surface and anion of ILs and its decomposed product with oxygen. This initial layer acts as a foundation for new tribofilm growth but it may also hamper further reaction between the metal substrate and ILs. For continuous tribofilm growth and self-healing, there are two primary sources of metal cations to react with ILs. (a) exposer of a fresh nascent surface due to wear, (b) deposition of nucleated tribochemical product on the surface.

Most of the studies have used base oil to blend ILs without using any additive packages. Except for a couple of studies exploring the compatibility of ILs with commercial antiwear additives (ZDDP), little is known about IL interaction with other surface adsorbing additives such as dispersants, detergents, and friction modifiers. This may be an important area of research for formulating ILs in an additive package for the potential commercial application. Long term stability of ILs in formulated lubricants are still to be explored particularly interaction with the lubricant byproducts such as acids, soot, water, fuels, and wear particles. Considering the vastness of the unique ILs very few have been explored so far and need further studies by altering different cation and anion groups.

2.5.2. Inadequately researched nanoparticles

Since the last decade several researchers have dispersed metal (Cu, Ni, Mo, W)[76–78], metal oxides (CuO, ZnO, TiO_2)[78–80], ceramic (Al_2O_3, SiO_2)[81, 82], composites (Ag/MWCNT, TiO2/SiO2)[83, 84], polymer (PTFE)[85], chalcogenides (MoS2, WS2)[86, 87], nitride (hBN)[88] and Carbon-based (Graphite, Graphene, Diamond)[89, 90] NPs in diverse base oils (synthetic, mineral, biolubricants). These studies have revealed the potential of NPs in reducing surface wear, friction coefficient, and enhancing EP performance. Most of the above mentioned nanoparticles have been studied for their shapes, sizes, and concentrations in a different base oil. Generally, colloidal NPs perform superior to micro sized particles due to higher surface area to volume ratios resulting in increased interaction with metallic surface and oil molecules. Reported studies confirm that nanolubricants performance is influenced by various factors such as morphology, size, concentration, and chemical composition of NPs[64, 65]. Antiwear properties generally depend on the nature of the tribofilm formation on the counter surface under boundary lubrication which is highly influenced by the chemical composition of the NPs[65]. This has been a strong motivation for exploring various NPs groups (metal, metal oxide, composites, etc.) having different Physico-chemical properties for their antiwear, antifriction, and EP performances[65].

Oxide and ceramic nanoparticles used in this study such as CuO, Al_2O_3, SiO_2, hBN, and ZnO are already explored as nanolubricants but their synergy with ionic liquids is not known. In this study despite showing excellent synergy with ILs, these NPs showed poor dispersion stability. In pursuit of better colloidal stability novel study of nanoparticles (boehmite and Zinctitanate) were undertaken. Boehmite comes under unique categories of NPs called hydroxide minerals such as Talc, and Serpentine. The natural and synthetic Serpentine minerals also known as Magnesium Silicate Hydroxide ($Mg_3Si_2O_5(OH)_4$) have been explored as a lubricant additive by several researchers[91–97]. A couple of studies have explored Talc as a lubricant additive and claimed excellent friction and wear reduction properties due to the formation of SiOx and MgO compounds on the worn surface[98, 99].

On the other hand, Boehmite (γ-AlOOH) which checks many desirable brackets i.e., green, biocompatible, and eco-friendly mineral has not been explored for its tribological properties. Boehmite also called Aluminium oxide hydroxide mineral, one of the common constituents of Aluminium ore bauxite is stable and if heated above $450^{O}C$ leads to dehydration of its crystals ($2AlOOH \Longrightarrow Al_2O_3+H_2O$) and formation of Aluminium oxide (Al_2O_3)[100, 101].

It has a lamellar (orthorhombic) structure and in every layer, the O atom has closed (cubic) packing while OH groups are on the surface making the overall structure loosely packed[102]. Due to its extremely low toxicity, biocompatibility, eco-friendliness, and low cost, Boehmite has found application in various fields such as photocatalysis, antimicrobial activity, determination of toxic metals, flame retardation, etc[101, 103–106]. Boehmite material has some inherent advantages such as lower molecular weight (59.988 g/mole), lower density ($3g/cm^3$), and lower Mohs scale hardness (3.5), making it a promising candidate for lubricant additive. Lei Zhang et al. covalently synthesized hybrid material consisting of Graphene oxide, Boehmite, and 3-glycidoxypropyl-trimethoxysilane (GO-GPTS-AlOOH) to enhance the dispersion stability of Graphene oxide in lubricating oil[107]. they claimed that the improved friction and wear reduction was due to the excellent strength of the lamellar Graphene sheet, while no detail was given regarding the role of Boehmite grafted particles in friction and wear reduction.

On the other hand, Zinctitanate ($ZnTiO_3$) has been investigated in various disciplines such as microwave dielectric, antibacterial, nanofiber, catalyst, gas sensor, white pigment, corrosion inhibitor, and luminescent material due to its outstanding properties, but its potential tribological properties have not been explored[108]. Further agglomeration of colloidal NPs in nonpolar base oil accelerates the sedimentation rate and is the single biggest hurdle for commercializing NPs in lubricants. This ternary oxide material inherits a larger specific surface area which could be instrumental in enhancing colloidal stability.

2.5.3. Inadequately researched synergistic effects

Sane et al. observed the synergy between imidazoliumbased IL and graphene NPs in paraffinic mineral oil, while no synergy was observed in fully formulated engine oil [109]. Gusain et al. synthesized three graphene–IL hybrid nanomaterials and dispersed 0.02% in PEG-200 base oil [26]. Their group reported synergy for Gr-BScB and Gr-OL, but Gr-PF6 recorded higher friction than the base oil. Qu et al. explored the synergy between four ILs and ZDDP, a common friction modifier additive [110]. Their group reported that no synergy was observed for [P66614] [BTMPP] and [N888H][DEHP] with ZDDP even though they share either the same cation or anion with the other two ILs which showed synergy with ZDDP. The above results express that multiple factors affect the synergy between ILs and other performance

additives, and a more focused study exploring the synergy of ILs with other additive packages is required.

2.6. Research gap, motivation and problem formulation.

Based on the extensive literature survey, following research gaps were identified.

- Considering the vastness of unique ionic liquids, very few ionic liquids have been explored in lubricants, possessing great untapped potential for the introduction of novel IL.
- The role of the cations and anions of the ionic liquids on the tribo-performance (EP, AW, AF) is not well understood and calls for further research.
- Antiwear properties generally depend on the nature of the tribofilm formation on the counter surface under boundary lubrication which is highly influenced by the chemical composition of the nanoparticles and colloidal stability, this is a strong motivation for exploring various NPs groups (metal, metal oxide, composites, etc.) having different Physico-chemical properties and higher dispersion stability for antiwear, antifriction, and EP performances.
- The effect of ionic liquids and NPs in combination can lead to synergism. However, little is reported on this aspect in the literature. It would be interesting to investigate the combo-effect of ionic liquids and NPs of varying categories and morphology.

The above research gap has been the motivation for undertaking this study and based on research gap objectives have been formulated.

2.7. Objectives

- To investigate compatibility between phosphonium ionic liquid and three oxide nanoparticles (CuO, Al_2O_3, SiO_2) for their tribo-performance in mineral base oil (SN 500).
- To explore synergism between three common cation based phosphonium ionic liquids and nanoparticles as a hybrid oil additive and their comparative study with commercial ZDDP.
- Three-way compatibility study among Nanoparticles, Ionic Liquid, and Dispersant for potential in lubricant formulation.

- To explore the potential of Boehmite and Zinctitanate NPs as lubricant additive and their synergistic effect with Ionic Liquids.

2.8. Work methodology

As per the above-defined objectives, the following strategy was implemented step-wise for the completion of the study.

Step 1: Selection of base oil, ionic liquids, nanoparticles

a. Selection of base oil (mineral or synthetic)
b. Selection/synthesis of ionic liquids
c. Selection of nanoparticles

Step 2: Characterization of Ionic liquids and nanoparticles

Step 3: Preparation of hybrid nano-oils by optimizing various factors i.e. nanoparticles and ionic liquid concentrations, sonication time and method, dispersant type etc.

Step 4: Physical characteristics of hybrid nanolubricants i.e. viscosity, density, stability etc.

Step 5: Assessing the tribological properties of the formulated lubricants.

Step 6: Worn surface characterization after tribo-tests.

The following figure 2.3 details a graphical representation of the work methodology implemented for the completion of the study.

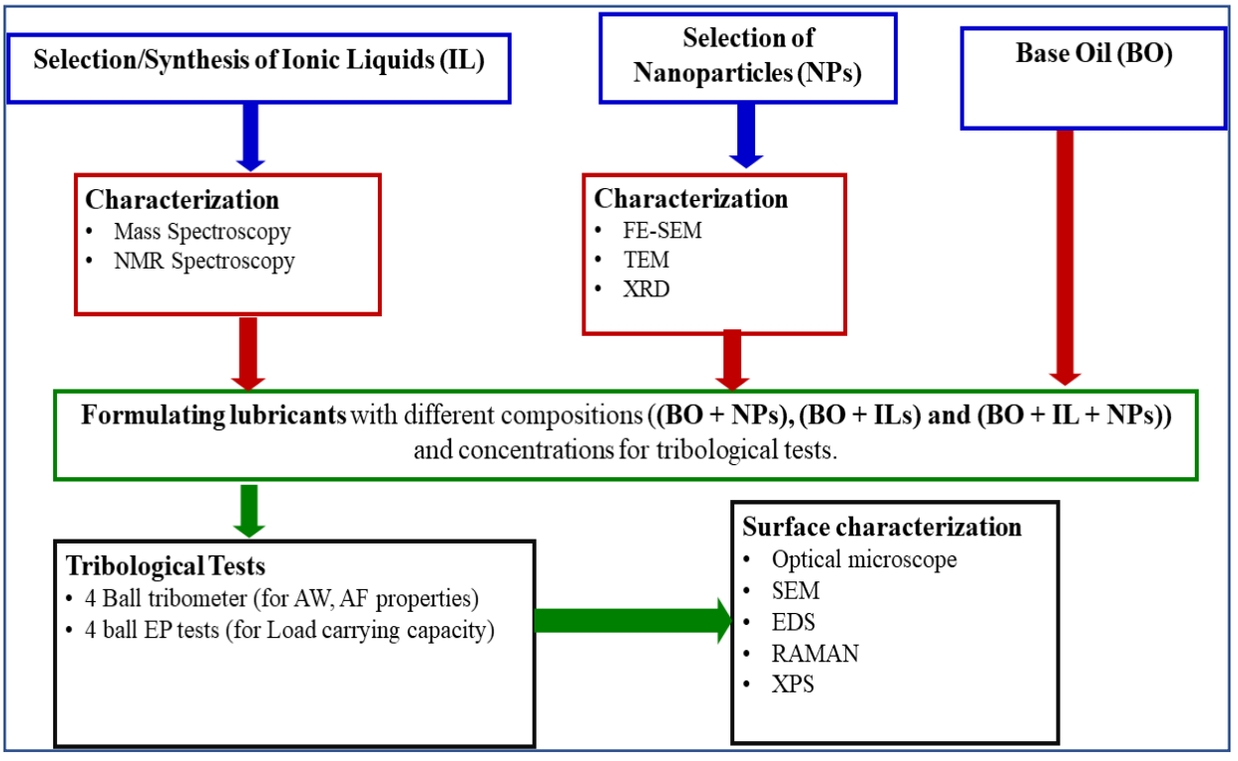

Figure 2.3 Schematic depicting implementation methodology.

Chapter - 3

Instrumentation and Experimental Methods

3.1. Selected material details

3.1.1. Base oil

Primarily API (American Petroleum Institute) group IV base oil, PAO was employed for the formulation of multiple series of lubricants with ILs, and NPs. The PAO is synthetic base oil and is generally named based on the value of its kinematic viscosity at 100 ^{o}C (e.g., PAO-6). PAO was selected due to its high viscosity index (VI), oxidation stability, low volatility, low temperature flowability, non-toxicity, and compatibility with mineral oil. PAO-6 was obtained from Synthomaxx India and was used as received. Table 3.1 details the data provided by the supplier.

Table 3.1 Details of the base oil (PAO6) as provided by the supplier.

Base Oil	**Physical Properties**		**Values**
Polyalphaolefins 6 (PAO-6)	Kinematic Viscosity	@40^{o}C	30.92 (mm^2/s)
		@100^{o}C	5.916 (mm^2/s)
	Viscosity Index		139
	Density	@ 29.5^{o}C	0.8187 (g/cm^3)
	Pour Point		-68^{o}C
	Flash Point		238 ^{o}C
	Fire Point		271 ^{o}C

3.1.2. Selected dispersant

To enhance the colloidal stability of NPs in base oil a commercial dispersant PIBSA (product code: UNOL P 1057) from Univenture Industries Pvt. Ltd was used. PIBSA (Polyisobutylene Succinic Anhydride) is derived from different grades of polyisobutylene by reacting it with maleic anhydride which helps in dispersing immiscible constituents of the lubricants. PIBSA dispersant was blended at a fixed concentration of 1 wt% in selected lubricants to minimise its possible intervention with other additives[88, 111]. Table 3.2 gives a few of the physicochemical properties of PIBSA.

Table 3.2 Important details of dispersant PIBSA.

Product name	Appearance	Specific Gravity	Viscosity @ 100°C	Flash Point ^{0}C
UNOL P 1057	Thick Amber	0.92-0.99	600-950	180-200

3.1.3. Selected nanoparticles details

Studies confirm that nanolubricants performance is influenced by various factors such as morphology, size, concentration, and chemical composition of NPs[64, 65]. Antiwear properties generally depend on the nature of the tribofilm formation on the counter surface under boundary lubrication which is highly influenced by the chemical composition of the NPs[65]. This has been a strong motivation for exploring various NPs groups (metal, metal oxide, composites, etc.) having different Physico-chemical properties for their antiwear, antifriction, and EP performances

In search of better dispersion stability and tribological performance different categories of NPs i.e. metal oxides (CuO, ZnO), ceramic (Al_2O_3, SiO_2), nitride (hBN), hydroxide (AlOOH) and hybrid ($ZnTiO_3$) were added with ILs to study their synergistic effect in a base oil. The following table summarizes important information about nanoparticles.

Table 3.3 Gives important details of selected nanoparticles.

Sr No	Nanoparticle	Supplier	APS (nm)	Density (g/cm^3)	Colour	Molecular Weight (g/mol)
1	CuO	SRL Pvt.Ltd	40	6.31	Black	79.54
2	SiO_2	Alpha Aesar	30-50	2.64	White	60.08
3	Al_2O_3	Nano Research Lab	30-50	3.98	White	101.96
4	ZnO	SRL Pvt.Ltd	30	5.6	White	81.38
5	hBN	SRL Pvt.Ltd	70	2.1	White	24.82
6	AlOOH	SRL Pvt.Ltd	20	3	White	59.99
7	$ZnTiO_3$	Sigma Aldrich	<100	5.18	White	161.26

3.1.4. Ionic liquids.

Three phosphonium phosphate ILs were used in this study composed of common cation trihexyltetradecylphosphonium ([P66614]).

1. trihexyltetradecylphosphonium bis(2,4,4-trimethylpentyl) phosphinate i.e. ([P66614] [BTMPP]),
2. trihexyltetradecylphosphonium bis(2 ethylhexyl)phosphate i.e. ([P66614] [DEHP])
3. trihexyltetradecylphosphonium dibutyl phosphate i.e. ([P66614] [DBP])

Among these ([P66614] [BTMPP]) was obtained from Sigma-Aldrich (>95%, CAS number- 465527-59-7, Molecular weight 773.27 g/mol) and was used as received. While the other two ILs ([P66614] [DEHP]) and ([P66614] [DBP]) were synthesized in the organic chemistry lab of NIT Warangal. Common cation, trihexyltetradecylphosphonium chloride (≥ 95%, CAS number- 258864-54-9, Molecular weight-519.31 g/mol) was obtained from Sigma-Aldrich. Both anions bis(2-ethyl hexyl) phosphate(≥97%, CAS number- 298-07-7, Molecular weight 322.42 g/mol), and Dibutyl phosphate(≥ 97%, CAS number-107-66-4, Molecular weight- 210.21 g/mol) were obtained from Sigma Aldrich.

Table 3.4 Gives important details of selected Ionic Liquids.

Ionic Liquids	Cation	Anion	Supplier	CAS No	Code
trihexyltetradecylphosphonium bis(2,4,4-trimethylpentyl) phosphinate	$[P_{66614}]$	[BTMPP]	Sigma Aldrich	465527-59-7	IL1
trihexyltetradecylphosphonium bis(2-ethylhexyl)phosphate	$[P_{66614}]$	[DEHP]	Synthesized		IL2
trihexyltetradecylphosphonium dibutyl phosphate	$[P_{66614}]$	[DBP]	Synthesized		IL3

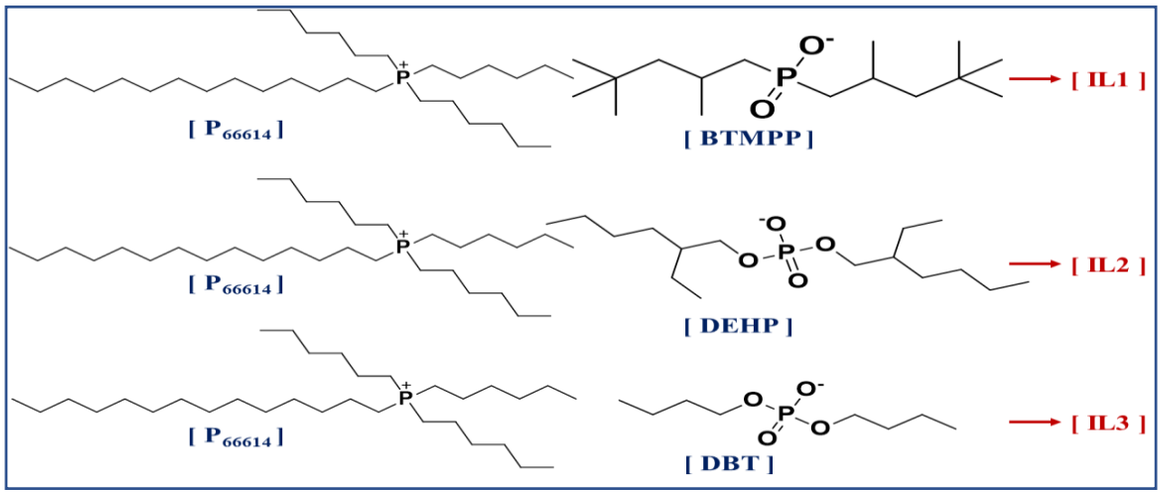

Figure 3.1 Molecular structure of the Cations and Anions of the three ILs

3.1.4.1. Synthesis of ionic liquids

ILs were synthesized by following the process reported by J.sun. et.al [112]. The typical procedure is as follows: equal moles of cation feedstock (4g of trihexyltetradecylphosphonium chloride) were mixed in anion feedstock (2.48g of bis 2-ethyl hexyl phosphate or 1.61g of dibutyl phosphate) in 10g of hexane. A solution was made using an equal mole of KOH (0.43g) with 10g distilled water and was added into the reaction system dropwise, followed by stirring the mixture at room temperature for over 4 hours. The organic compound was separated and washed with distilled water three times to remove KCl; the solvent was removed by rotary evaporation, and the compound was dried in a vacuum. The synthesis of ILs were confirmed by mass spectroscopy. IL2 mass spectroscopy m/z ES^+ 483.5 ($[C_6H_{13}]_3C_{14}H_{29}P^+$), ES^- 321.2 ($[C_8H_{17}O]_2OPO^-$), IL3 Mass spectroscopy m/z ES^+ 483.5 ($[C_6H_{13}]_3C_{14}H_{29}P^+$), ES^- 209.1 ($[C_4H_9O]_2OPO^-$). The synthesis yielded 6g of ([P66614] [DEHP]) and 5.25g of ([P66614] [DBP]), which was approximately 92 and 93 yield %, respectively. Figure 3.2 shows the scheme of reaction for IL2 and IL3, while figure 3.3 highlights the process for the synthesis of ILs.

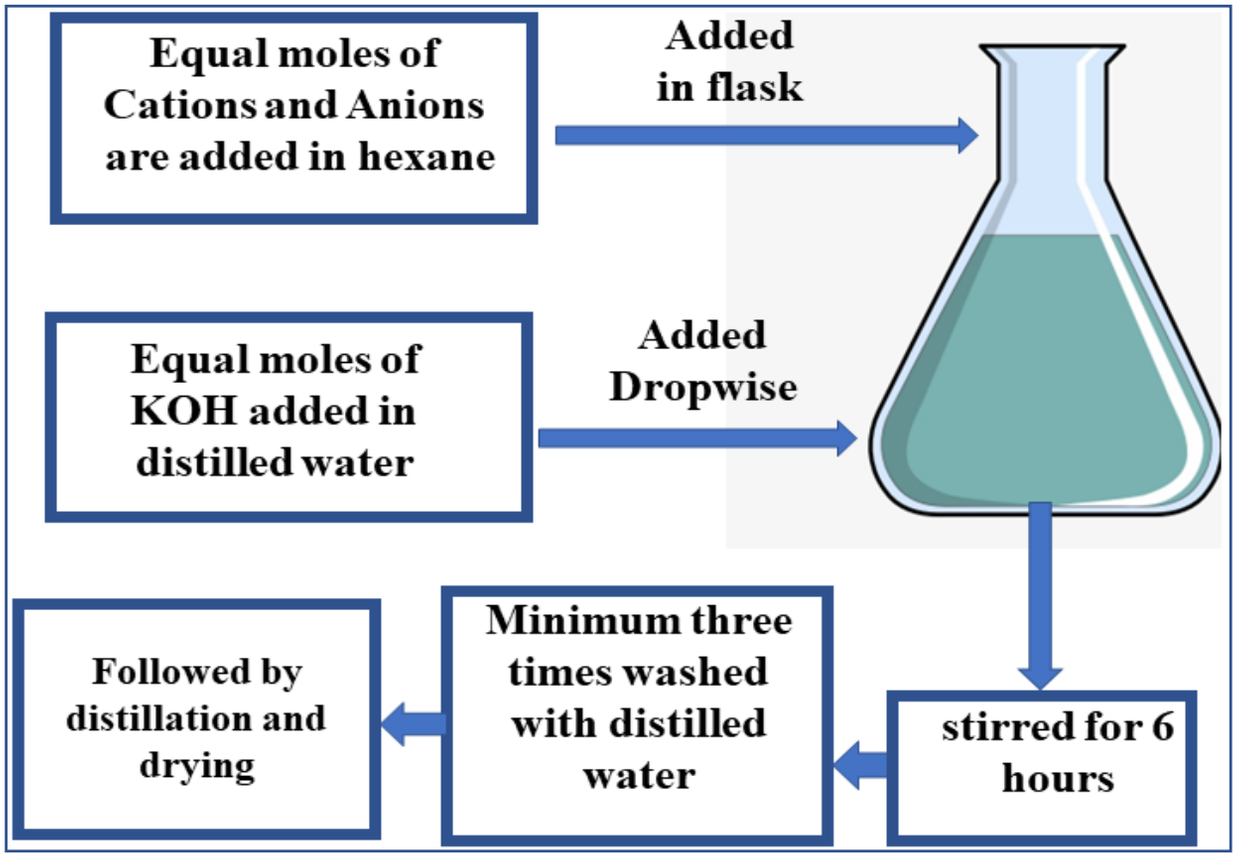

Figure 3.2 Graphical representation of the reaction scheme

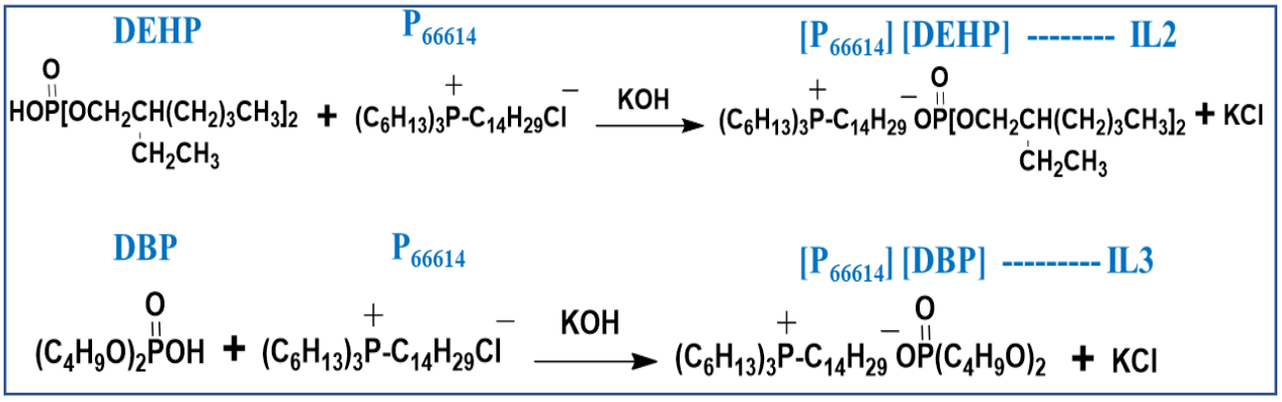

Figure 3.3: Reaction scheme for synthesis of (IL2) i.e., ([P66614] [DEHP]) and IL3 i.e., ([P66614] [DBP]).

3.1.5. Zinc dithiophoshate (ZDDP)

ZDDP is the primary commercial antiwear additive used in the formulation of most hydraulic oils, motor oils, and greases[6]. Other than better tribological properties ZDDP is also known to provide secondary enhancement of lubricants properties and acts as an antioxidant and corrosion inhibitor. They are generally added in the range of 600-2000 ppm of phosphorus in modern lubricants[6]. In this study, ZDDP was used for a comparative study with hybrid nanolubricants composed of ILs and NPs. The ZDDP was obtained from United Petrofer Limited India (product code: ADDIV SPG 4575) consisting of active elements i.e. Phosphorus (9.9%), Zinc (10%), Sulphur (19%). Figure 3.4 gives the molecular structure of ZDDP.

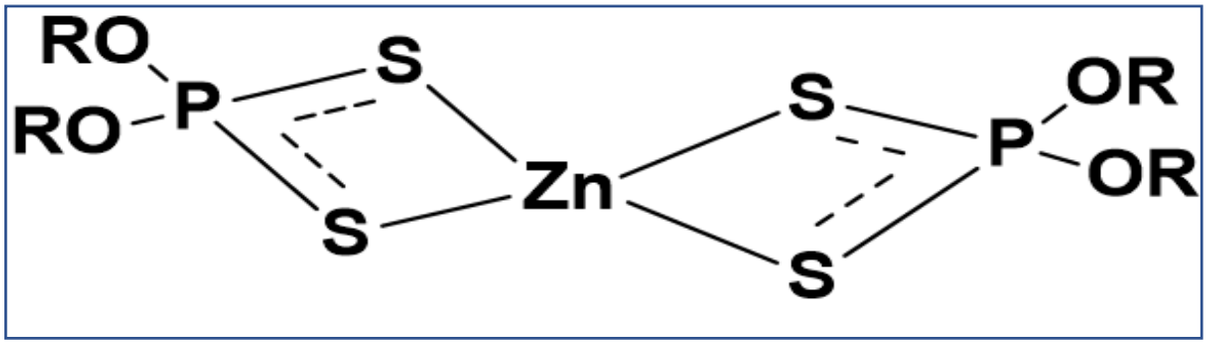

Figure 3.4 Molecular structure of ZDDP.

3.2. Characterization of nanoparticles

3.2.1. X-Ray Diffraction

X-Ray Diffraction (XRD) is a very powerful technique used for identifying the phase and unit cell dimension of crystalline material. It works on the principle of X Ray's constructive interference and crystalline sample. XRD technique (make Bruker D8 Advance) with monochromatic Cu Kα (λ = 1.5406 Å) radiation was used to analyze the crystal size and phase structure of the NPs. Average crystal size was calculated using Scherrer's equation (D β cosø=k λ, where D is crystalline size, k is Scherrer's constant, β is FWHM, λ is X-ray wavelength).

3.2.2. Field Emission Scanning Electron Microscope

A Field Emission Scanning Electron Microscope (FE-SEM) (model JSM-7800F, JEOL, Japan) coupled with energy-dispersive X-ray spectroscopy (EDS) of oxford instruments was used to understand the morphology of the nanoparticles. the instrument has a spatial resolution of up to 0.5 nm.

3.2.3. High Resolution Transmission Electron Microscope.

High Resolution Transmission Electron Microscope (HRTEM, make FEI Tecnai TF20) was employed to characterize the morphology and size of selected nanoparticles. it has 200 kV field emission gun, capable enough to produce high resolution micrographs.

3.3. Sample preparation

Two step methods have been employed for mixing additives in a base oil. At first, the additives were added in base oil being stirred (magnetic stirrer) at 1000 rpm for rapid mixing followed by 45 min ultrasonic probe sonication (make Dakshin Ultrasound, 190 W power, 20 kHz frequency, operated in a pulsed mode of 2 s on and 1 s off). Probe sonication is the most effective method which generates successive sequences of high pressure (around 500 bar attributed to the cavitation effect) for an extremely short duration (microseconds) due to the passing of high frequency ultrasonic waves in lubricants.

3.4. Dispersion stability studies.

The colloidal stability of NPs depends on various factors such as the physicochemical characteristics of NPs, base oil, and dispersion method. Colloidal NPs tend to sediment over time predominantly due to agglomeration caused by Brownian motion and gravity (since NPs are denser than base oil). For formulating commercial nano-oils, dispersion stability becomes a prerequisite and should be studied. Visual inspection and Dynamic Light Scattering (DLS) methods were used to study NPs stability in the base oil.

3.4.1. Visual inspection

Visual inspection is a simple and popular method used to study the dispersion stability of the NPs in the PAO base oil. Well dispersed nano-oil is kept in a transparent container and stored for an extended period of time, with regular observation. Photographs were taken at regular intervals without any disturbance to the sample while in storage.

3.4.2. Colloidal particle size analysis using Dynamic Light Scattering-

Dynamic Light Scattering (DLS) is a technique used to find the average hydrodynamic dimeter (d_h) of suspended particles in the base oil. It uses the following Stokes-Einstine equation to estimate the hydrodynamic dimeter of colloidal particles.

$d_h = \frac{k_\beta T}{3\pi\eta_o D}$ where T is the absolute temperature, k_β is Boltzmann's constant, D is diffusion coefficient, η_o is medium viscosity.

To study the agglomeration of NPs over time, dynamic light scattering (Zetasizer nano 590 Malvern Instruments UK) was employed. Formulated nanolubricant is generally too thick to be directly used for DLS analysis hence it was diluted with petroleum ether/base oil in a particular weight ratio. For dilution, prepared nanolubricants were stored without any disturbance in separate containers, and just before the DLS study, a sample was taken out on a stipulated day from the top of the container. Extreme care was taken to not disturb the settled NPs of the container while taking out samples for the DLS study.

3.5. Tribological testing

The tribological performances of the lubricants were evaluated under a mixed and boundary lubrication regime, using a four-ball tribometer (DuCom Instruments, India). The tribometer

uses tetrahedral geometry in which the top steel ball is rotated at desired rpm against three stationary balls submerged in lubricant as shown in figure 3.5. The tetrahedral contact of balls is loaded with a lever mechanism, and frictional torque is recorded continuously on the computer. For the wear analysis, the wear scar diameter (WSD) of the bottom three balls are measured using an optical microscope at the end of the test. For reliability and repeatability, all the tests were conducted three times, and average, WSD, and COF were considered with the provision for standard deviation in data representation. Bearing balls of diameter 12.7mm, average roughness (Sa) 35nm, AISI 52100 steel balls with chemical composition of C, 0.98-1.10%; Si, 0.15-0.35%; Mn, 0.25-0.45%; P, < 0.025%; S, < 0.025%; Cu, 0.30<; Cr, 1.3-1.6%; Ni,0.30< having hardness of 63-66 HRC (as provided by supplier) were used for both the wear and extreme pressure (EP) tests. The tribological tests were performed according to ASTM 4172B test standards, which include 1200 rpm, 40kg applied load, 75^0C temperature, and 60 minutes of test duration. The EP tests were performed according to the energy institute's standard IP 239, which is similar to ASTM 2783 test standards. The typical test parameters include the speed of 1450 rpm, room temperature, 60 seconds of test duration, and progressive loading till the seizure occurs. According to IP 239 for each test, the load is increased in steps from 10kg to 100kg and if the seizure doesn't occur the load is increased by 25kg stepwise beyond 100 kg till the seizure occurs. Once the seizure occurred at any particular point, the load is reduced by 10 kg stepwise to obtain maximum non-seizure load. All the loads below the weld load are considered the maximum non-seizure load or pass load for the lubricants.

Table 3.5 Tribological testing parameters

Test parameter	**ASTM 4172**	**EP tests IP 239**
Equipment	4-ball tribometer	4-ball tribometer
Load, N	392	Increasing load in the step of 25kg till seizure or welding occurs followed by 10kg stepwise reduction for maximum non-seizure load
Speed, RPM	1200	1450
Temperature, ^{0}C	75	Room temperature
Test duration,	60 min	60 Sec

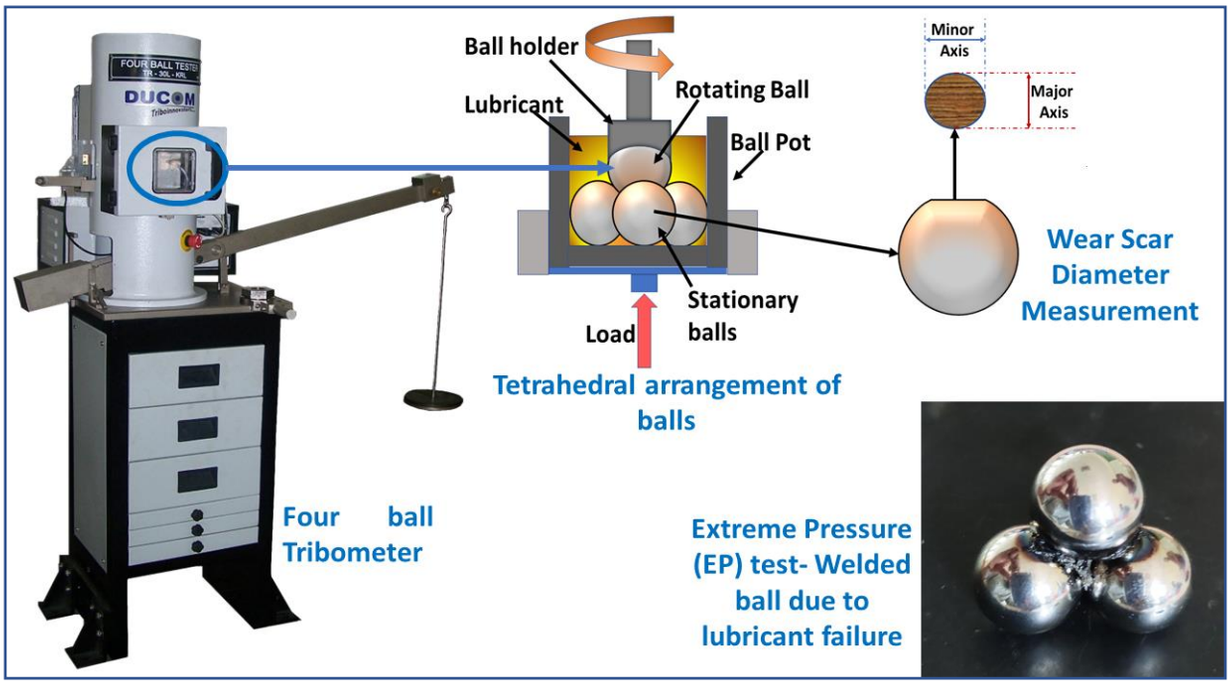

Figure 3.5 Camera image of four ball tribometer along with a tetrahedral arrangement of balls and concept of wear scar diameter (WSD) and Seizure load measurement. The tribometer is used to assess the lubricants performance with respect to friction, wear reduction and load bearing capacity.

3.6. Density, Viscosity measurement of formulated lubricants

Stabinger viscometer (SVM 3000) following ASTM D7042 standards was used to measure the kinematic viscosity and density of the lubricants. The viscometer works on the Couette principle, and the measurement of kinematic viscosity and density is based on torque and speed measurement. The other important parameter for lubricant is the viscosity index (VI), which is a unitless number indicating the temperature dependence of the lubricant's kinematic viscosity. The viscosity index was calculated according to ASTM D-2270 in which the viscosity of the prepared sample at 40^{O}C and 100^{O}C is compared with standard reference oil having 0 (naphthenic base oil) and 100 (paraffinic base oil) viscosity index[6]. The higher the viscosity index, the more stable the oil is with respect to changes in temperature.

3.7. Worn surface characterization techniques employed

3.7.1. Field Emission Scanning Electron Microscope (FESEM) or Scanning Electron Microscope (SEM).

Based on the availability FESEM or SEM was employed for characterizing the morphology of worn surfaces lubricated under different oils. The FESEM details have already been discussed in section 3.2.2. The scanning electron microscope (SEM) (model Tescan VEGA-3 LMU) was used with an accelerating voltage of 20 kV to study the morphology of the worn surface. An energy-dispersive X-ray spectroscopy (EDS) of oxford instruments coupled with SEM was used to study the elemental composition of worn surfaces. To remove any weakly absorbed contaminants (lubricant residues) tribo-tested balls were sonicated in Hexane for 5 minutes prior to any surface characterization.

3.7.2. Raman spectroscopy

To understand the nature of the tribofilm and the role of additives in tribofilm formation, for selected lubricants, Raman spectroscopy was employed (Renishaw InVia Raman with 10 mW laser powered and 532 nm excitation wavelength). The instrument is coupled with Leica microscope to observe the surface being scanned.

3.7.3. X-Ray Photoelectron Spectroscopy

X-ray photoelectron spectroscopy (XPS) is a widely employed technique for exploring the chemical state of tribofilm. XPS (make K ALPHA+, Thermo Fisher Scientific Instruments, UK) with Al Kα monochromatic radiation (1486.7 eV, beam current 6 mA) and 150 eV pass energy over a spot size of 200 μm was employed to understand the chemical state of tribofilm. Further core level spectra of triboactive elements were acquired using pass energy of 30 eV. The binding energy of C 1s (284.8 eV) was used for the calibration of other elements. XPS analysis chamber pressure was maintained below 10^{-8} mbar. For depth profiling, several rounds of Ar-ion sputtered were conducted to obtain near surface zone (100 nm deep) for selected worn surfaces. The peak fitting feature of Origin software was used for baseline correction and deconvolution.

Chapter - 4

Compatibility between phosphonium ionic liquid and three oxide nanoparticles as hybrid lubricant additive in mineral base oil

4.1. General

Modern-day lubricants are a mixture of base oil and few performance additives, hence compatibility becomes one of the important factors for the application of any additive in commercial lubricants. Since IL as a lubricant additive is the newest dimension in lubricant science and due to economic constraints it is not feasible to use IL as a neat lubricant, hence it becomes of great interest to explore the synergy, mechanism of tribofilm formation and compatibility of IL with other commercial additives. On the other hand metal oxide and ceramic NPs have been the center of attraction since the last decade[113–115]. This study is an attempt to explore the synergy between IL and the three distinct NPs along with the mechanism of tribofilm formation. Way over 80% of currently used lubricant is still dominated by mineral base oils. Moreover, most of the synergy study is conducted in synthetic lubricants hence group 1 mineral base oil is selected for this study.

4.2. Materials and methods.

4.2.1. Ionic liquid and nanoparticles

ILs and NPs used in this study were procured and used without any further processing. The IL trihexyltetradecylphosphonium bis(2,4,4-trimethylpentyl)phosphinate ([P_{66614}][BTMPP]),was purchased from Sigma Aldrich. The CuO NPs of average particle size (APS) 40 nm were purchased from SRL laboratories Ltd., Al_2O_3 NPs were purchased from Alpha Aesar with APS of 30 to 50 nm while SiO_2 NPs with 30-50 nm were obtained from Nano Research Lab. More details about ILs and NPs are provided in chapter 3. Group 1 mineral oil SN500 was obtained from Hindustan Petroleum Corporation Limited. Table 4.1 gives the physicochemical properties of the base oil used in this study. Table 4.2 shows the cation and anion of the ([P_{66614}][BTMPP]).

Table 4.1 physical properties of Base oil SN 500.

Physical Properties	Results	Test Standards
Colour	L 2.0 – 2.5	ASTM D 1500
Density @ 29.5^{O} C	0.886	ASTN D 1298
Kinetic viscosity @ 40^{O} C	110	ASTM D 445
Kinetic viscosity @ 100^{O} C	11.82	ASTM D 445
Viscosity Index	90.7	ASTM D 2270
Flash Point ^{O}C	234	ASTM D 92
Pour Point ^{O}C	-3	ASTM D 97

Table 4.2 Physical properties of IL.

Cation and Anion of ([P_{66614}][BTMPP])	Molecular weight	Density g/ml @ 20°C
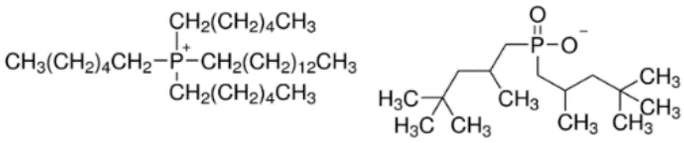	773.27	0.895

4.2.2. Sample preparation

([P_{66614}][BTMPP]) has very good solubility in mineral oil but the international lubricants standardization and approval committee (ILSAC GF-5) has set the limit for phosphorus concentration at 800 ppm in engine oil to avoid the poisoning effect of exhaust gases. During this study, we blended 0.2, 0.5, and 0.8 wt % IL in the mineral base oil. Even though all the blends improved the tribological properties but there was very little difference between the 0.5 and 0.8% blend's friction and wear reduction performances, however, the phosphorus concentration was significantly high in 0.8% compared to the 0.5% IL blend. Moreover, our objective was to study the synergy between IL and NPs as a hybrid lubricant additive, hence we chose 0.5 wt% (Phosphorus content <500 ppm) of IL to explore the synergy with NPs while limiting the phosphorus content well within 800 PPM, as the limit set by ILSAC-GF6 for lubricants. For NPs different concentrations (0.05, 0.1, 0.15, 0.2 wt. %) were added to the base oil without any dispersant to obtain the same effective concentration for all three NPs. Among NPs, SiO_2 showed improvement up to 0.05% (0.2% for CuO and Al_2O_3) and at 0.1% the tribological performances deteriorated, the reason for poor tribological performances may be caused by the abrasive effect due to a higher concentration of SiO_2 on steel tribopair. Due to poor performance at higher concentrations of SiO_2 the optimum concentration was fixed at 0.05 wt. % for all NPs as a single additive. For the hybrid additives, NPs concentration was kept the same (0.05%) while IL concentration was reduced to 0.45% so the maximum additive concentration remains at 0.5%. Two step method has been used for a homogenous distribution of additives in the base oil. In the first step lubricant containing additive was stirred for 6 minutes, followed by ultrasonically dispersing for 10 minutes. The same two steps method is used for the hybrid (BO+IL+NPs) lubricant sample preparation as well. After dispersing NPs with the help of ultrasonication in the base oil, due to very small particle size (30-50nm), the nanoparticles were dispersed in the base oil well over two days

before any visual sign of settling down and all the tests were performed within 6 hours of the sample preparation. Moreover, using additives other than IL and NPs (any dispersant) may influence the tribological performances of the lubricant blend and it would have been very difficult to draw any conclusion with respect to IL and NPs performance exclusively in hybrid lubricant. Hence no dispersant was used for this study. Figure 4.1 shows the photos of the hybrid nanolubricant and figure 4.2 shows the FE-SEM images of nanoparticles used in this study. The FE-SEM images confirm that all the NPs have spherical morphology.

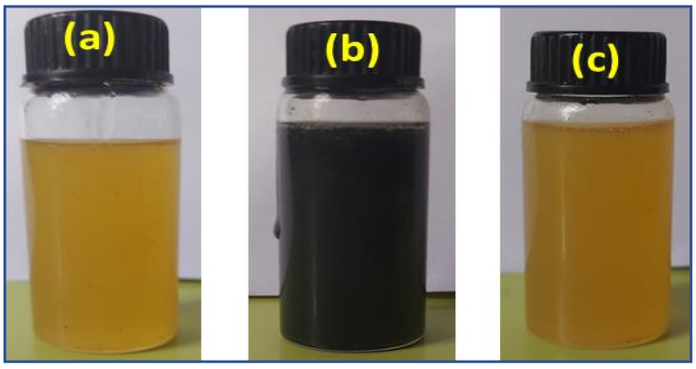

Figure 4.1 Camera Image of formulated hybrid nano-lubricant (a) Mo+IL1+Al_2O_3 (b) Mo+IL1+CuO (c) Mo+IL1+SiO_2

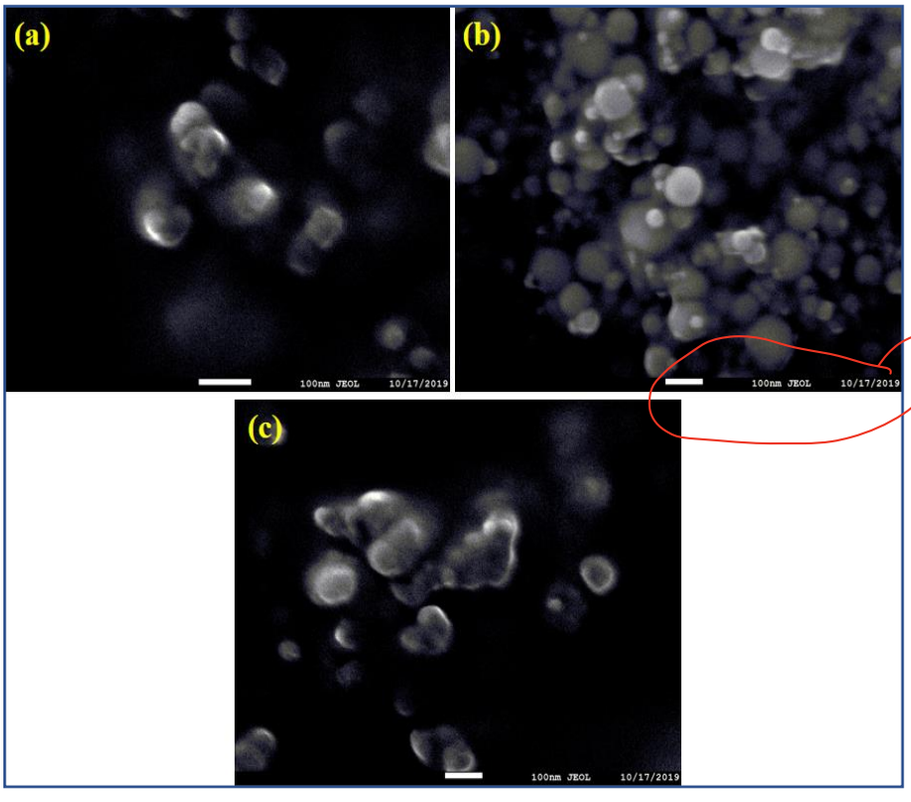

you should redraw these scale bars so they are legible.

Figure 4.2 FE-SEM image of (a) Al_2O_3 (b) CuO and (c) SiO_2 shows nearly spherical morphology

4.2.3. Tribological testing

DuCom's four ball tribometer was used for the tribological testing and its technical details are given in chapter 3. Repeatability is a very important factor for reliability, hence all the tests were repeated at least three times. The friction and wear assessment tests were conducted following ASTM 4172B standards while the EP properties of the lubricants were tested according to ASTM D2783 using four ball tribometer, which involves stepwise progressive loading until the welding of the balls occurs. The test duration is for 10 seconds at a constant speed of 1760 RPM. The load at which the welding occurred is termed the failure load and the last un-welded load is considered the pass load or maximum non-seizure load. Since in ASTM D2783, the loading gap between successive loadings are wide eg. 63-80-126-160-200-250kg hence intermediate loads of 5kg in progression have been taken into consideration for pinpointing the closest non-seizure load. Table 4.3 gives characteristic values for standard test, and EP tests.

Table 4.3 Characteristic values for the tests

Test parameter	Tribological tests	EP test
	ASTM D: 4172B	**ASTM D:2783**
Load, N	392	Up to seizure
Speed, RPM	1200	1760
Lubricant temperature, ^{0}C	75 ± 5	Room temperature
Test duration,	60 min	10 Sec

4.2.4. Surface characterization of worn surfaces

The morphology of the worn surface was studied using Tescan VEGA-3 LMU Scanning Electron Microscope and an electron-accelerating voltage of 15KV was employed. For WSD comparison HUVITZ LUSIS HC-30MU optical microscope was used. An oxford instrument's energy dispersive X-ray spectrometer (EDS) coupled with SEM was used to probe the elemental composition of the WSD surface. To further investigate tribofilm formation on the worn surface, Renishaw InVia Raman spectra with an excitation wavelength of 532 nm and laser power of 10 mW was used. Before surface characterization, the steel balls were cleaned ultrasonically using hexane for 6 minutes to remove lubricant residues.

4.3. Results and Discussion

4.3.1. Friction and wear reduction performances

Figure 4.3 gives the frictional torque variation, wear scar diameter, and friction coefficient performance tested following ASTM 4172B standard for base oil and all the single and hybrid nanolubricants. It is evident from figure 4.3(a) that the frictional torque of base oil fluctuates continuously till 1800 seconds and then becomes stable but remains highest and lubricates the surface poorly. When 0.5 wt% ionic liquid was blended in base oil the friction coefficient reduced significantly with an overall friction reduction of 11.86% as shown in figure 4.3(c). It was interesting to note that the ionic liquid blend showed the lowest starting frictional torque up to the first 230 seconds which can be attributed to the adsorption of IL on steel surfaces due to its affinity towards rubbing surfaces. On the other hand, the addition of NPs in the base oil, other than SiO_2 both CuO and Al_2O_3 show similar and significant friction reduction which was around 12% than the neat base oil. CuO hybrid nanolubricant performed better than Al_2O_3 hybrid nanolubricant and their friction reduction was 24, and 19% respectively. SiO_2 hybrid nanolubricant showed 5.8% overall friction reduction which was less than the performance of the IL blend indicating no synergy. While Al_2O_3 and CuO hybrid nanolubricant showed lower friction coefficients inferring synergy between NPs and IL.

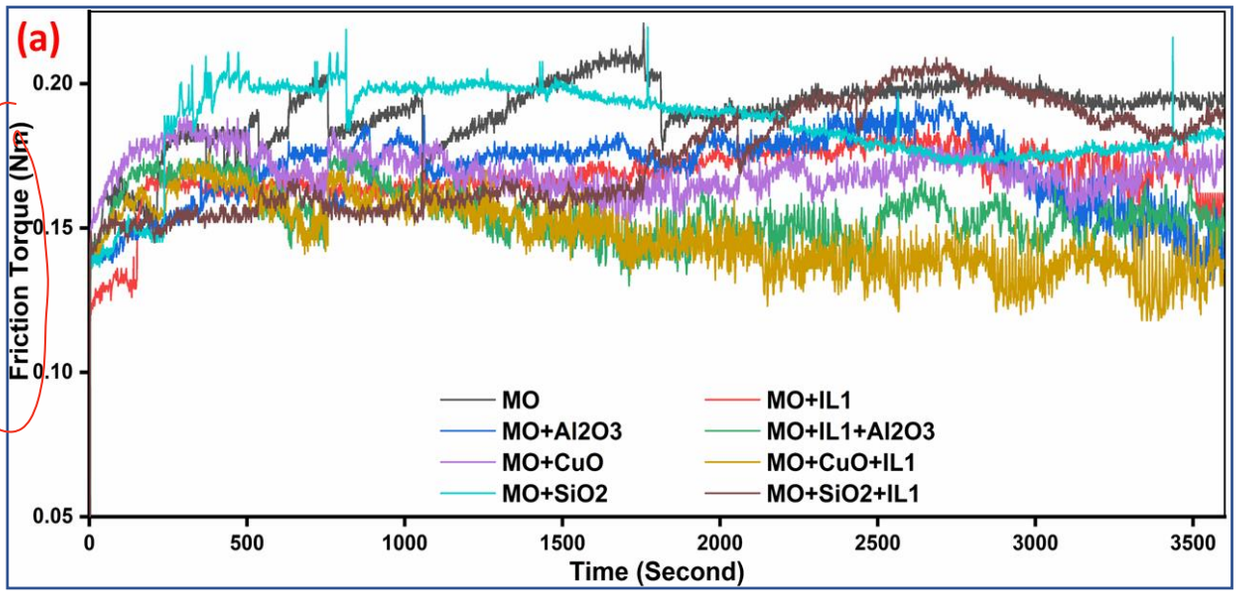

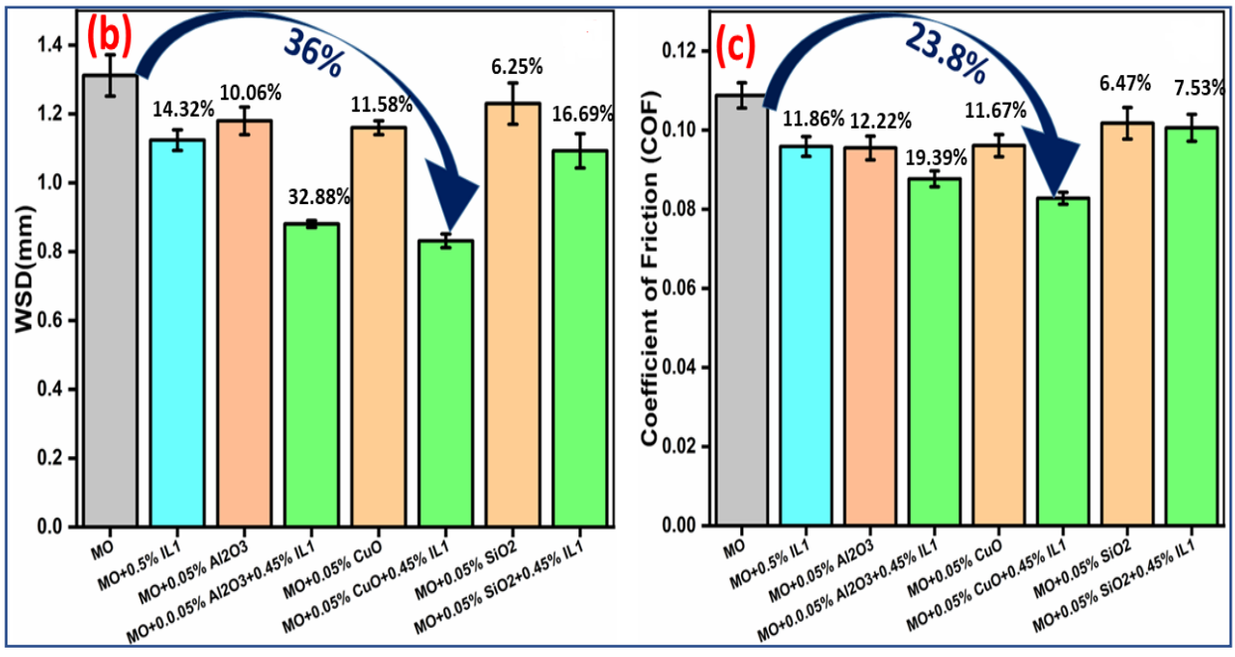

Figure 4.3 (a) Frictional torque variation Vs time (b.) average wear scar diameter (c.) average friction coefficient tested following ASTM: D 4172B test conditions,

Figure 4.3 shows the average wear scar diameter (WSD) and the friction coefficient of lubricant samples tested at ASTM 4172B test conditions. The highest WSD was observed for base oil as shown in figure 4.3(b). By blending 0.5% IL the reduction in WSD was 14.32% compared to the neat base oil. The addition of CuO, Al_2O_3, and SiO_2 NPs in base oil also decreased WSD by 10.06, 11.58, and 6.25% respectively. Even though all the NPs have APS around 50 nm but still they showed quite distinct tribological properties. All the hybrid nanolubricant performed superior to the single additive. The CuO hybrid nanolubricant showed the lowest wear of 36.64%, followed by Al_2O_3 hybrid nanolubricant which reduced wear by 32.88 % compared to the neat base oil. The most surprising change was observed in SiO_2 hybrid nanolubricant with an overall wear reduction of 16.69% which is slightly better than the Ionic liquid blend.

It is also sometimes nice to include atypical image of the wear scar (to scale) as calculated in the methods section. Also in results chapter to show the actual quality of the measurements.

4.3.2. Extreme pressure performances

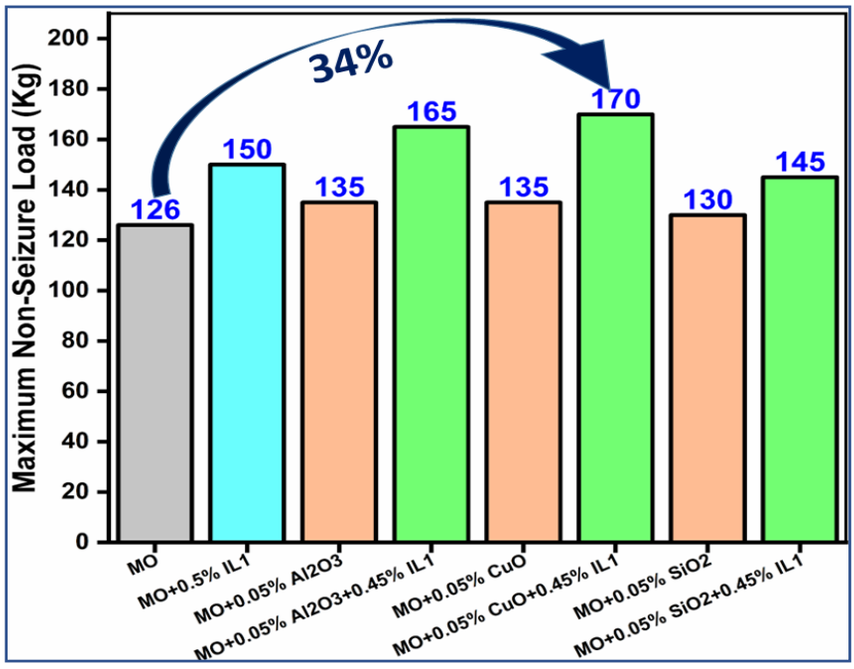

Figure 4.4 Extreme Pressure performance of lubricants.

Figure 4.4 gives the comparative load carrying capacity of single and hybrid nanolubricant tested according to ASTM D 2783 test parameters. Even though the test duration is 10 seconds, in this short duration lubricant undergoes extremely severe pressure and tribostress due to which the top surface is worn out rapidly and fresh surfaces are exposed continuously. It is interesting to note that IL blend in the base oil has the highest non-seizure load among the single additives (19.04%) compared to BO, the reason may be the formation of adsorption film due to inherent polarity of cation and anion of the IL, which is evident from lowest friction coefficient registered for the first 250 seconds observed in figure 3. The NPs improved EP performance of the lubricant slightly due to tribo-sintering but the best EP performance was observed for hybrid nanolubricant of Al_2O_3 and CuO, which increased load-bearing capacity by 30.95 and 34.92% respectively clearly indicating synergy between IL and NPs. Even though SiO_2 hybrid lubricant enhanced load carrying capabilities by 15% but synergistic behavior between IL and SiO_2 wasn't observed since IL as a single additive performs better than SiO_2 hybrid nanolubricant.

Figure 4.5 showed the photograph of steel balls undergone the EP test at 130 kg. Due to the high load and speed of rotation excessive heat is generated on non-conformal ball contact which leads to deformation or welding of the steel balls. Figure 4.5(a) shows the welded steel balls lubricated with neat BO. It can be inferred from the figure that at 130 kg load, base oil

couldn't separate the rubbing surface and high contact pressure lead to the generation of excessive heat resulting welding of steel balls within 10 seconds. Ball (b) and (e) lubricated with IL blend and SiO_2 hybrid nanolubricant respectively, withstand the test at 130kg but shows some sign of plastically deformed steel due to excessive heat generation caused by high friction. The plastically deformed surface appears to be black in colour around the circumference of WSD. Figure 4.5 (c),(d) shows very low or no black texture which reflects that Al_2O_3 and CuO hybrid nanolubricant managed to separate rubbing surfaces more effectively.

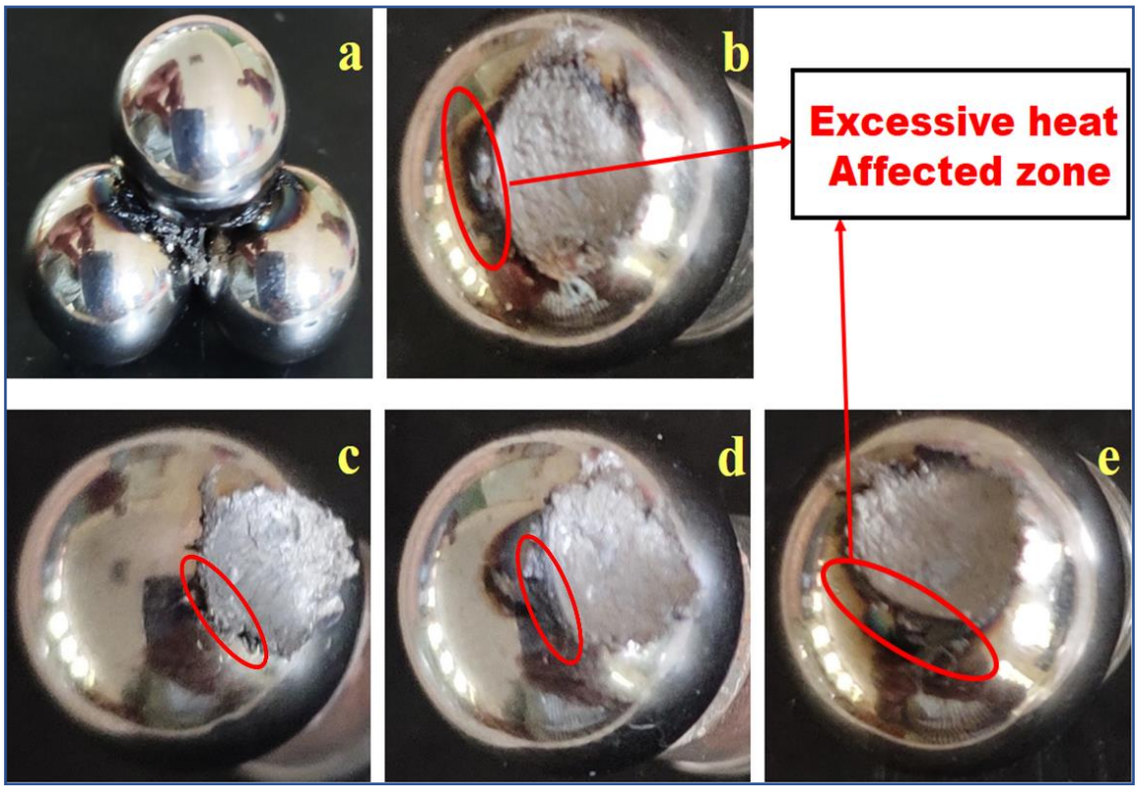

Figure 4.5, steel Balls after EP test at 130 kg (a) BO, (b) BO+0.5% IL, (c) BO+0.45% IL+0.05% Al_2O_3 (d) BO+0.45% IL+0.05% CuO, (e) BO+0.45% IL+0.05% SiO_2

4.3.3. Surface Characterization

4.3.3.1. Morphology of worn surface using SEM

Four ball tribometer and EP test results of this study have demonstrated the synergistic effect between IL and NPs. In order to understand the principle and mechanism of synergies several surface characterization techniques such as SEM, EDS, and Raman spectra have been

employed. Figure 4.6 shows the SEM analysis of the worn surface lubricated with the base oil and all three hybrid nanolubricants at ASTM D 4172B test conditions. The suffixes 1,2 are being used to annotate the same wear scar for 200 and 20µm scale respectively. Deep and rough furrows are present throughout the WSD of the steel ball lubricated with the base oil, indicating excessive wear during the rubbing process as shown in figure 4.6(a). Although the WSD of the SiO_2 hybrid nanolubricant was slightly less if compared with the base oil but it also shows deep and rough furrows and no sign of SiO_2 adsorbed on the worn surface due to tribosintering. Tribosintering occurs when the oxide nanoparticles come into contact with rubbing surfaces and due to high load, temperature, and tribostress NPs get sintered on the surface[116–118]. The tribosinterd particles form a protective film called tribofilm which decreases direct metal to metal contact between tribopair resulting in decreased wear. Figure 4.6 (a) and (d) are the SEM image of the worn surface for BO and SiO_2 hybrid nanolubricant. Both have severe wear throughout the WSD, indicating the phenomenon of intense metallic adhesive wear. CuO and Al_2O_3 hybrid nanolubricant have almost similar shapes to the WSD which has some deep furrows at the center and very shallow scratches at the top and bottom of WSD nevertheless smallest WSD if compared with the base oil figure 4.6 (b),(c). the worn surfaces appear relatively smooth, indicating Al_2O_3 and CuO NPs firmly sintered on the rubbing surfaces respectively and forming strong tribofilm resulting decreased in metal to metal contact[117].

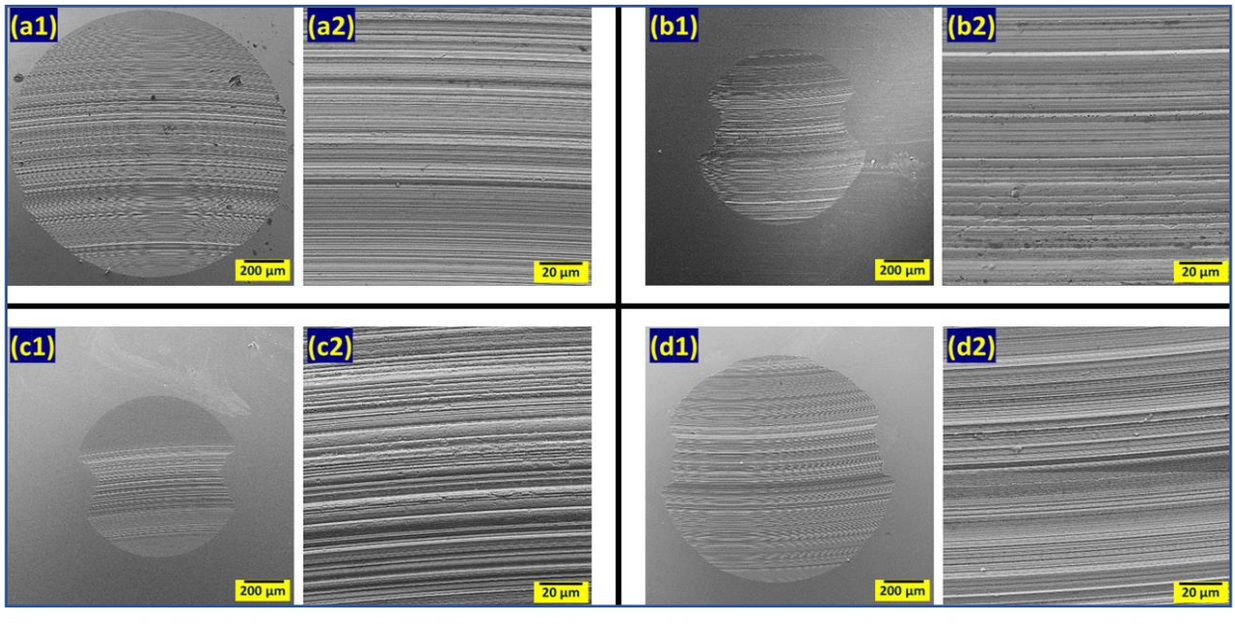

Figure 4.6 SEM images of WSD at 200 and 20 µm respectively for ($a_{1,2}$). BO ($b_{1,2}$). BO+0.45%IL+0.05%Al_2O_3 ($c_{1,2}$). BO+0.45%IL+0.05%CuO ($d_{1,2}$). BO+0.45%IL+0.05%SiO_2

4.3.3.2. Elemental composition of worn surface using EDS analysis

Table 4.4 gives the elemental concentration of the worn surface obtained by EDS while figure 4.7 shows the EDS spectra of the worn surface lubricated with IL blend and all three hybrid nanolubricant. EDS spectroscopy is not a quantitative technique but it can be used for a comparative study of the same material worn surface lubricated with different additives. Table 4.4 shows the atomic concentrations of worn steel surface which was lubricated with base oil contains 5.66% oxygen concentration highest among all the tested samples. The high oxygen present on the worn surface indicates that BO was not able to separate the rubbing surface effectively and due to high wear fresh surface was exposed to oxidation. IL blend showed good oxidation-reduction properties since the reduction in oxygen presence on the worn surface was approximately five times compared to the base oil figure 4.7(a). IL blend showed a very high amount of carbon (24%) presence on the worn surface with a reduction of iron when compared to the base oil. Jun Qu et.al. explored tribofilm formation by $[P_{66614}][BTMPP]$ in GTL for Steel and gray cast iron tribopair[68]. On XPS spectra of worn surface, their group claimed that tribofilm was formed on the worn surface due to tribochemical reaction of IL. The product of tribochemical reaction primarily oxide phosphate (20.7%) was found on the worn surface. These oxide phosphates showed a more intense O-P bond and having a binding energy of 531.5eV resulting in a pretty stiff tribofilm. In this study also the EDS spectra of worn surface lubricated with IL blend showed an elevated level of phosphorus (0.91%). These high concentration of phosphorus must be in the phosphate phase, inferring the formation of phosphate rich tribofilm on the worn surface figure 4.7(b).

The EDS spectra of Al_2O_3 and CuO hybrid nanolubricant show 0.85 and 0.81% phosphorus on the worn surface, reflecting almost no change in the formation of phosphate rich tribofilm, even with tribosintering of Al_2O_3 and CuO NPs. On the other hand, SiO_2 NPs in hybrid lubricant decreased phosphorus concentration on the worn surface to 0.39% which is nearly half the amount if compared with IL. Due to the abrasive nature of SiO_2, the tribochemical product (phosphate) adsorbed on the worn surface must have been abraded due to relatively high wear.

EDS spectra of worn surface lubricated with Al_2O_3 and CuO hybrid nanolubricant shows a strong presence of Al (0.51%) and Cu (0.69%) on the worn surface figure 4.7 (b),(c). On the other hand, almost negligible trace of Si has been observed for worn surfaces lubricated with

SiO_2 hybrid lubricant indicating SiO_2 is not able to sinter on the rubbing surface in these operating conditions figure 4.7(e).

Table 4.4 EDS Atomic percentages of WSD after the test at ASTM conditions

Lubricants	Atomic percentages of the WSD, after the test at ASTM conditions							
	C	Fe	O	Cr	P	Al	Cu	Si
BO	3.61	89.2	5.66	1.52	--	--	--	--
BO+0.5% IL	24.59	72.03	1.03	1.44	0.91	--	--	--
BO+0.05% Al_2O_3+0.45% IL	12.6	83.67	0.82	1.55	0.85	0.51	--	--
BO+0.05% CuO+0.45% IL	11.39	84.95	0.47	1.69	0.81	--	0.69	--
BO+0.05% SiO_2+0.45% IL	6.91	87.25	3.53	1.83	0.39	--	--	0.09

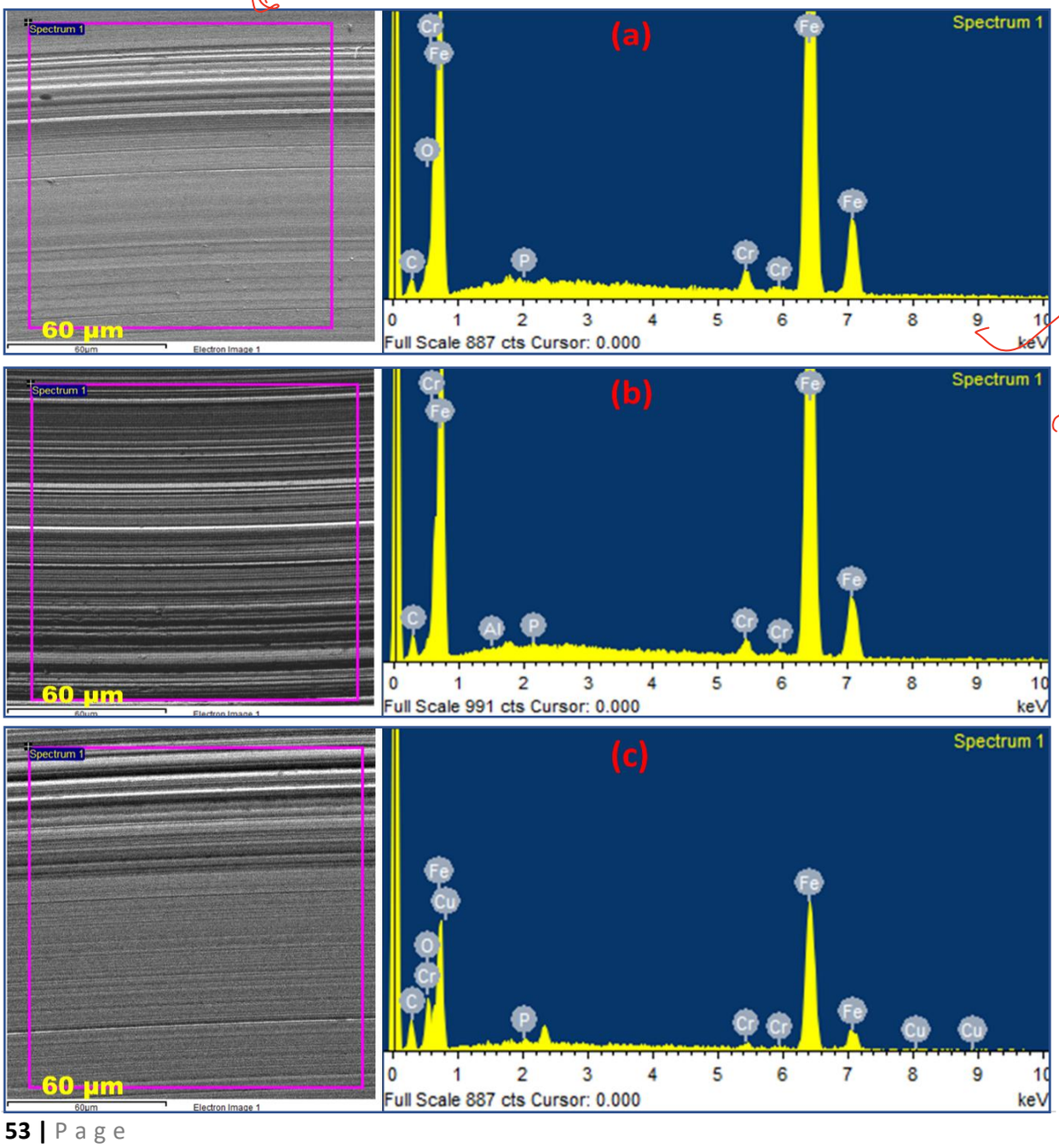

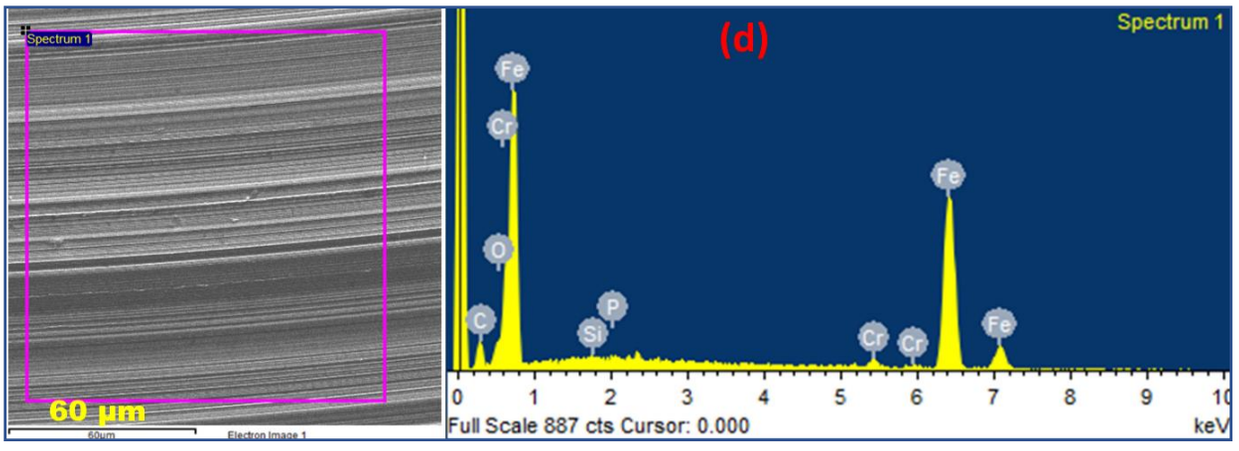

Figure 4.7 EDS analysis of worn surface at ASTM test conditions lubricated with (a). BO+0.5%IL (b). BO+0.45%IL+0.05%Al_2O_3 (c). BO+0.45%IL+0.05% CuO (d)BO+0.45%IL+0.05%SiO_2

4.3.3.3. Raman spectroscopy of worn surfaces

Figure 4.8 gives the Raman spectra of worn surface lubricated with BO, Al_2O_3, and CuO hybrid nanolubricant. Tribological properties are the surface phenomenon, especially the top few nanometers of surface depth control the friction and wear behavior of any tribopair. The results of the four ball test and SEM analysis show the synergistic behavior between IL and NPs and a significant reduction in friction and wear. To further investigate the protective film formation of the worn surface lubricated with BO, Al_2O_3, and CuO hybrid nanolubricant, micro Raman spectra were performed using Renishaw InVia Raman spectra with an excitation wavelength of 532nm and laser power of 10 mW as shown in figure 4.8. The Raman spectra of worn surface lubricated with CuO hybrid nanolubricant shows three peaks at 291, 341, and 628 cm^{-1}. Due to the very less concentration of CuO on the worn surface, the Raman peaks are small, and also the peak at 341 cm^{-1} has a very weak Raman intensity but the other two peaks are easily distinguishable. CuO has only two molecules per unit cell and belongs to the C^6_{2h} space group and has 9 zone-centered optical phonon modes but only three modes are Raman active i.e. A_g+2B_g. out of the observed Raman spectra for the CuO, peak 291 cm^{-1} can be assigned to A_g, and peaks 341 and 628 cm^{-1} can be assigned to B_g modes[119]. Xu J et.al. and Gulzar et.al have obtained similar Raman spectra for rubbing surfaces lubricated with CuO nanolubricant[116, 119]. The similarity confirms the formation of tribofilm due to the tribosintering of CuO.

For Al_2O_3 there is 7 allowed vibration and raman band ranging from 375 to 751 cm^{-1} but in our study lubricated surface with Al_2O_3 hybrid nanolubricant shows no distinguishable raman peak[120]. Raman spectroscopy is a weak phenomenon and multiple factors affect the spectra such as low concentration, strong fluorescent background and detector noise generated. These factors may be responsible for the ~~not~~ distinguishable Raman peak in the spectra even though EDS spectra have shown a significant presence of Al on the worn surface.

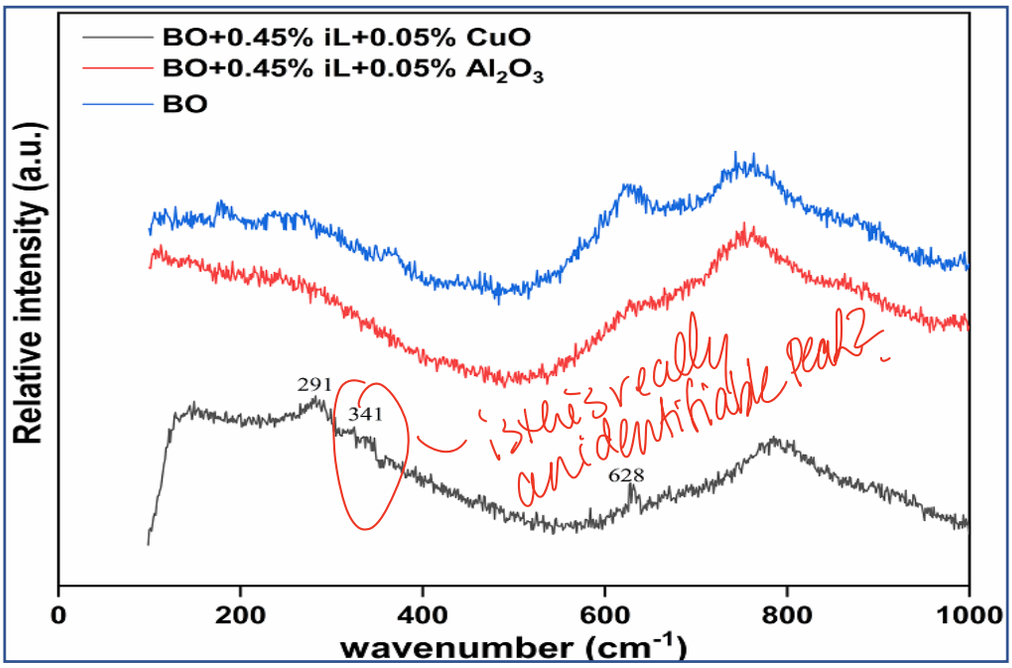

Figure 4.8. Raman spectra of worn surface

4.4. Mechanism of the tribofilm formation

The surface characterization of the worn surface lubricated with hybrid nanolubricant (CuO and Al_2O_3 hybrid lubricant) confirms that there are two predominant mechanisms associated with tribofilm formation in hybrid nanolubricants; first is tribochemical reaction for ILs, and second is tribosintering for oxide nanoparticles. Phosphonium based ILs have a good affinity towards metallic surfaces. During operation initially, the IL ~~gets~~ adsorbed on the rubbing surfaces, and when the load is applied at elevated temperature, IL undergoes a tribochemical reaction and forms a tribofilm rich in phosphate (O-P with binding energy 531.5eV). This phosphate rich tribofilm along with weak adsorbed IL film provides very good protection for rubbing surfaces. These tribochemical reactions are a continuous process and the abraded film is replaced continuously throughout the operation. On the other hand, the oxide NPs provide a bearing effect due to rolling action and get accumulated in the asperities, decreasing surface

roughness. Under the application of load due to high stress, these NPs undergo the tribosintering process and form a strong protective film on the worn surface as confirmed by SEM, EDS, and Raman Spectra.

The mechanism of tribochemical reaction and tribosintering are responsible for excellent synergy observed for CuO and Al_2O_3 hybrid lubricants. The EDS spectra show an increased concentration of Cu (0.69%) and Al (0.51%) along with phosphorus and carbon, on the worn surface lubricated with CuO and Al_2O_3 respectively, confirming that both the additives contribute in enhancing tribological performance. For instance, as shown in figure 4.4 at ASTM 4172B test conditions 0.5 wt% IL blend decreased wear by 14.32% while 0.05% CuO and Al_2O_3 NPs decreased wear by 10.06 and 11.58% respectively. In contrast, CuO and Al_2O_3 hybrid nanolubricant decreased wear by 36.64 and 32.88% respectively, which is more than double of either single additive. These results indicate compatibility between IL and NPs in friction and wear reduction as a hybrid lubricant additive. On the other hand, due to the abrasive nature, there was no synergy observed between IL and SiO_2 hybrid lubricant. EDS spectra of worn surface lubricated with SiO_2 hybrid lubricant shows negligible tribosintering of SiO_2 NPs (0.09% Si) and decreased phosphorus concentration (0.39 %) on the worn surface, which is less than half of the phosphorus (0.91%) concentration for the surface lubricated with IL blend. The decreased phosphorus concentration infers that SiO_2 NPs increased the rate of abrasion resulting in poor sustainability and a low concentration of phosphorus rich tribofilm.

4.5. Important observation

The study explored the synergy between phosphonium based IL and three NPs, i.e. CuO, Al_2O_3, SiO_2, as hybrid nanolubricant added in group 1 mineral oil. Based on the tribological tests and surface characterization techniques following conclusions are drawn.

- 0.5 wt% IL1 blend in base oil has the lowest friction coefficient for the first 230 seconds and managed to decrease friction by around 12% and wear nearly 16% compared to the base oil.
- Excellent synergy has been observed for CuO and Al_2O_3 hybrid nanolubricant and 0.5 wt% of these hybrid nanolubricants decreased the friction coefficient by nearly 24 and 19% respectively, while wear reduction was 36 and 32% respectively.

- SiO_2 hybrid nanolubricant decreased wear by 16.69%, while at the same test conditions IL blend decreased wear by 16%, hence no conclusive evidence of synergy was observed for SiO_2 hybrid nanolubricant.
- IL blend improved the extreme pressure property by 19%, indicating IL has the very good load-bearing capability and certain synergy has been observed for CuO and Al_2O_3 hybrid nanolubricant which registered 34 and 30% increases in non-seizure load respectively. On the other hand, no synergy has been observed for SiO_2 hybrid nanolubricant since its load-carrying capacity was less than the IL blend.
- There are two predominant mechanisms associated with tribofilm formation and responsible for excellent tribological properties associated with NPs and IL1. IL1 ($[P_{66614}][BTMPP]$) undergoes tribo-chemical reaction and generates tribofilm of a strong phosphate layer on the worn surface, confirmed by XPS and EDS spectra. Whereas deposition of NPs on the worn surface takes place due to the tribosintering process which is confirmed by SEM, EDS, and Raman analysis.

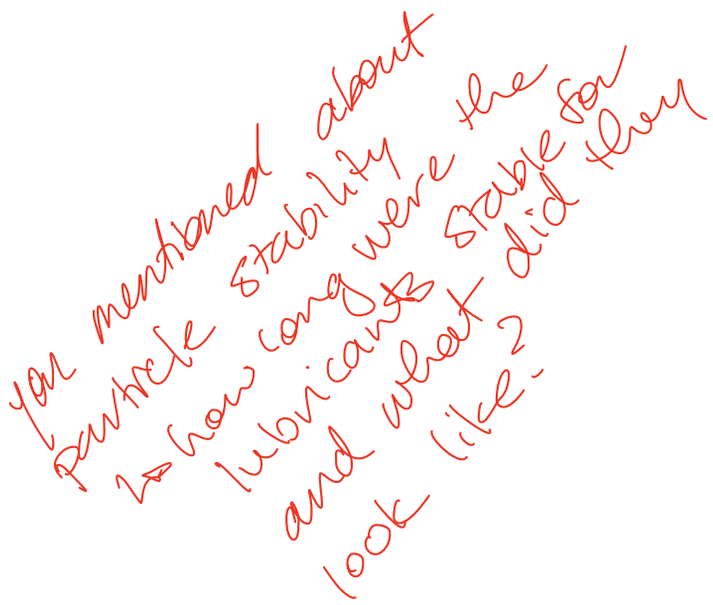

Chapter - 5

Ionic liquid-nanoparticle based hybrid-nanolubricant additives for potential enhancement of tribological properties of lubricants and their comparative study with ZDDP

5.1. General

Most of the currently used friction and wear modifier additives were invented over a half-century ago and contain a Sulphur based additive such as Zinc dithiophosphate (ZDDP). ZDDP has biocompatibility issues and poisons the catalytic converter of automotive vehicles[121, 122]. These performance limitations and environmental impact can be reduced by developing new additives such as Ionic liquids (ILs) and Nanoparticles (NPs). ILs and NPs can fulfill the expectations of modern lubricants and appear promising as hybrid lubricant additives. There are few studies exploring the synergy between ILs and NPs as discussed in chapter 2.

Can ZDDP (a common antiwear additive) be replaced/minimized with ionic liquids (ILs) and nanoparticle (NPs) based hybrid nanolubricant additives? To answer this question, three ionic liquids (ILs) **(1)** trihexyltetradecylphosphonium bis(2,4,4-trimethylpentyl) phosphinate i.e.([P66614] [BTMPP]), **(2)** trihexyltetradecylphosphonium bis(2-ethylhexyl)phosphate i.e. ([P66614] [DEHP]) and **(3)** trihexyltetradecylphosphonium dibutyl phosphate i.e. ([P66614] [DBP]) were added with nanoparticles (hBN and ZnO) in synthetic base oil (PAO) to obtain hybrid nanolubricants (PAO+ILs+NPs). To the best of our knowledge, this is the first study exploring trihexyltetradecylphosphonium dibutyl phosphate ([P_{66614}] [DBP]) as a lubricant additive while few studies have reported the performance of ([P_{66614}][BTMPP]) and ([P_{66614}] [DEHP]) as lubricant additive[24, 123–125]. Further, there is no published report dealing comparative performance of ILs and NPs based hybrid lubricant additives with commercial antiwear additives (ZDDP). In this chapter complex interaction between three common cations based ILs and two NPs (hBN, ZnO) with respect to their dispersibility, viscosity index, tribological, and EP properties have been explored under boundary lubrication. Further, this study reports a comparative study between hybrid nanolubricants with ZDDP additives aiming to assess the feasibility of reducing our overdependence on harmful ZDDP. The study also attempts to understand the mechanism of tribofilm formation for hybrid nanolubricants and the role of cations and anions in it.

5.2. Materials and Methods

5.2.1. Materials

IL1, trihexyltetradecylphosphonium bis(2,4,4-trimethylpentyl) phosphinate ([P_{66614}][BTMPP]) (≥95 % sigma-aldrich) were used as received. While IL2, trihexyltetradecylphosphonium bis(2-ethylhexyl)phosphate ([P_{66614}] [DEHP]) and IL3, trihexyltetradecylphosphonium dibutyl phosphate ([P_{66614}] [DBP]) were synthesized using, common cation trihexyltetradecylphosphonium chloride (≥95 % sigma-aldrich), and two distinct anions i.e. bis(2-ethyl hexyl) phosphate(≥97 % sigma-aldrich) and Dibutyl phosphate(≥97 % sigma-aldrich) respectively. Two distinct crystal structured NPs are used in this study, one is Zinc Oxide Nanoparticles (APS 30 nm) and the other hexagonal Boron Nitride (APS 70 nm), known for 2D-planner structure. The ZDDP was obtained from United Petrofer Limited India (product code: ADDIV SPG 4575) consisting of active elements i.e. Phosphorus (9.9%), Zinc (10%), Sulphur (19%). For base oil, Polyalphaolefins (PAO-6 Synthomax India) was used as received. The material characteristics of PAO, ILs, and NPs are given in table 5.1.

5.2.2. Ionic liquid and nanoparticles

Out of a total of 3, two ionic liquids ([P_{66614}] [DEHP]) and ([P_{66614}] [DBP]) reported in this study were synthesized in our Synthesis lab following the process reported by j.sun.et al. [112]. The detailed synthesis process is reported in chapter 3. Figure 5.1 (a), (b) gives the FE-SEM (make JOEL 7800F) image of hBN and ZnO nanoparticles, respectively. Both of these NPs shows nearly spherical morphology.

Table 5.1 Material characteristics of base oil, ionic liquids, and nanoparticles used in this study as provided by supplier.

Material	**Properties**			
Nanoparticles	**Size (APS)**	**Density (g/cm^3)**	**Supplier**	**CAS No**
hBN	70	2.1	SRL Pvt.Ltd	10043-11-5
ZnO	30	5.6	SRL Pvt.Ltd	1314-12-2

Ionic Liquids	Cation	Anion	Supplier	CAS No
trihexyltetradecylphosphonium bis(2,4,4-trimethylpentyl) phosphinate	$[P_{66614}]$	[BTMPP]	Sigma Aldrich	465527-59-7
trihexyltetradecylphosphonium bis(2-ethylhexyl)phosphate	$[P_{66614}]$	[DEHP]	Synthesized	
trihexyltetradecylphosphonium dibutyl phosphate	$[P_{66614}]$	[DBP]	Synthesized	

Base Oil	Physical Properties		Values
Polyalphaolefins 6 (PAO-6)	Kinematic Viscosity	@40°C	30.92 (mm^2/s)
	Viscosity	@100°C	5.916 (mm^2/s)
	Viscosity Index		139
	Density	@ 29.5°C	0.8187 (g/cm^3)
	Pour Point		-68
	Flash Point		238
	Fire Point		271

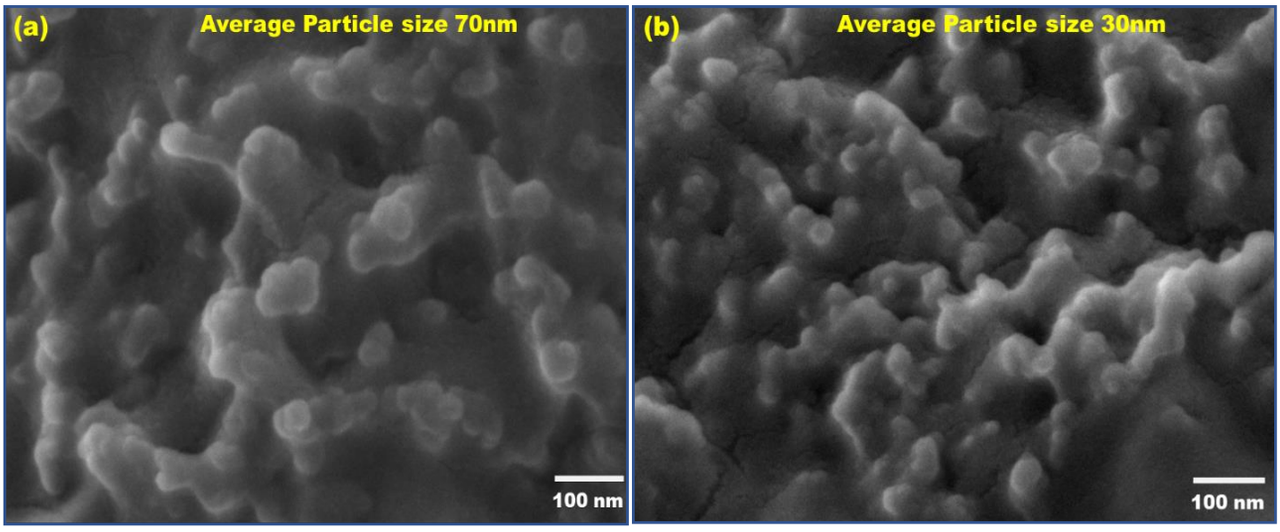

Figure 5.1 : FE-SEM image of (a) hBN nanoparticles and (b) ZnO nanoparticles.

5.2.3. Sample preparation

ILSAC (International Lubricants Standardization and Approval Committee) has set 0.08 wt%, or 800 ppm the upper limit of phosphorous concentration for engine oil, hence IL and ZDDP blends in base oil were prepared in such a way that maximum phosphorus concentration was limited to 800 ppm as single additives. The optimum concentration for ZnO and hBN NPs

reported in the literature varied between 0.4-1.2 wt%[64, 80, 107, 126] and 0.1-1wt%[88, 127–129] respectively. To obtain the optimum NPs concentration for this study, NPs were dispersed in varying concentration ZnO (0.25,0.5,0.75,1wt%) and hBN (0.4,0.7,1wt %) and was tested using a four-ball tribometer. ZnO nanolubricant improved wear up to 0.5 wt% beyond that performance deteriorated, while hBN showed improvement up to 1 wt% concentration. Hence 0.5 and 1 wt% concentrations of NPs were used for ZnO and hBN respectively when used as a single additive in the base oil. The study compares hybrid nanolubricants (IL+NPs) tribological performance with single additives i.e. IL, NPs and ZDDP hence while formulating hybrid nanolubricant, the concentration was reduced to half of their single additive concentration, i.e., 400 ppm phosphorus concentration for ILs and 0.25 and 0.5 wt % for ZnO and hBN NPs respectively for fair comparison. A two-step method was used for the sample preparation, first stirring (magnetic stirrer 1000 r/min) for 2 hours followed by 45 minutes ultrasonic probe sonication (make Dakshin Ultrasound, 190 W power, 20 kHz frequency, operated in a pulsed mode of 2 seconds on and 1 second off).

5.2.4. Worn surface analysis

A scanning electron microscope (SEM) (model Tescan VEGA-3 LMU) was used with an accelerating voltage of 20kV to study the morphology of the worn surface. An energy-dispersive X-ray spectroscopy (EDS) of oxford instruments coupled with SEM was used to study the elemental composition of worn surfaces. X-ray photoelectron spectroscopy (XPS) (make K ALPHA+, Thermo Fisher Scientific Instruments, UK) with Al Kα monochromatic radiation (1486.7 eV, beam current 6 mA) and 150 eV pass energy over a spot size of 200 µm was employed to understand the chemical state of tribofilm. Further core level spectra of O 1s, P 2p, B 1s, N1s, and Zn 2p were acquired using pass energy of 30 eV. The binding energy of C 1s (284.8 eV) was used for the calibration of other elements. XPS analysis chamber pressure was maintained below 10^{-8} mbar. Tested balls were ultrasonically washed in hexane for a minimum of 10 minutes to eliminate any adsorbed lubricant residues.

5.2.5. Tribological experiments

The tribological performances of the lubricants were evaluated under boundary lubrication regime, using a four-ball tribometer (DuCom Instruments, India). The detailed experimental setup is discussed in chapter 3. The tribological tests were performed according to ASTM 4172B test standards, which include 1200 rpm, 40kg applied load, 75^0C temperature, and 60 minutes of test duration. The EP tests were performed according to the energy institute's standard IP 239, which is similar to ASTM 2783 test standards. The typical test parameters include the speed of 1450 rpm, room temperature, 60 seconds of test duration, and progressive loading till the seizure occurs. All the loads below the weld load are considered the maximum non-seizure load or pass load for the lubricants.

5.3. Results and Discussion

5.3.1. Stability analysis

PAO base oil is a transparent liquid; hence visual inspection method was used for stability analysis for prepared lubricant samples. ([P_{66614}][BTMPP]) and ([P_{66614}] [DEHP]) ILs have shown good miscibility in different base oil as reported in the literature [24, 123–125]. For ([P_{66614}] [DBP]), miscibility was studied following Otero et.al, in which 5 wt% IL was blended in base oil and centrifuged for 10 minutes at 1400 rpm[57]. No separate phase was observed indicating, excellent miscibility of all three ILs (minimum of 5 wt% concentration) in PAO base oil, which could be attributed to the longer molecular chain length of both cation and anion. To study the influence of ILs on dispersion stability of NPs, photographs of prepared samples of hybrid nanolubricants were taken every 8 hours interval. Figure 5.2 shows no sedimentation for both the NPs and hybrid nanolubricants for the first 24 hours. After 48 hours, the ZnO nanolubricant showed significant sedimentation of NPs at the bottom of the container while very few sedimentations were observed for the hBN nanolubricant. This may be due to the lower density of hBN (2.1g/cm^3) compared with ZnO (5.6 g/cm^3) NPs. On the other hand, hBN hybrid nanolubricants (PAO+ILs+hBN) did not show any sedimentation, while ZnO hybrid nanolubricant (PAO+ILs+ZnO) showed some sign of sedimentation; nevertheless, the majority of NPs were dispersed even after 48 hours. After 72 hours, some degrees of sedimentation were observed in all the samples, but it was interesting to note that all the hybrid

nanolubricant had more dispersed NPs than their single additive counterparts. hBN nanolubricants showed significant settlement at the bottom of the container, while its hybrid nanolubricants showed very little settlement. Similarly, almost all the ZnO NPs settled after 72 hours in the single additive sample, while in the ZnO hybrid additive, sample significant proportion of NPs were still dispersed. After 96 hours, ZnO hybrid nanolubricants showed the settlement of almost all the NPs while the hBN nanolubricant appeared clear by visual inspection only after a week.

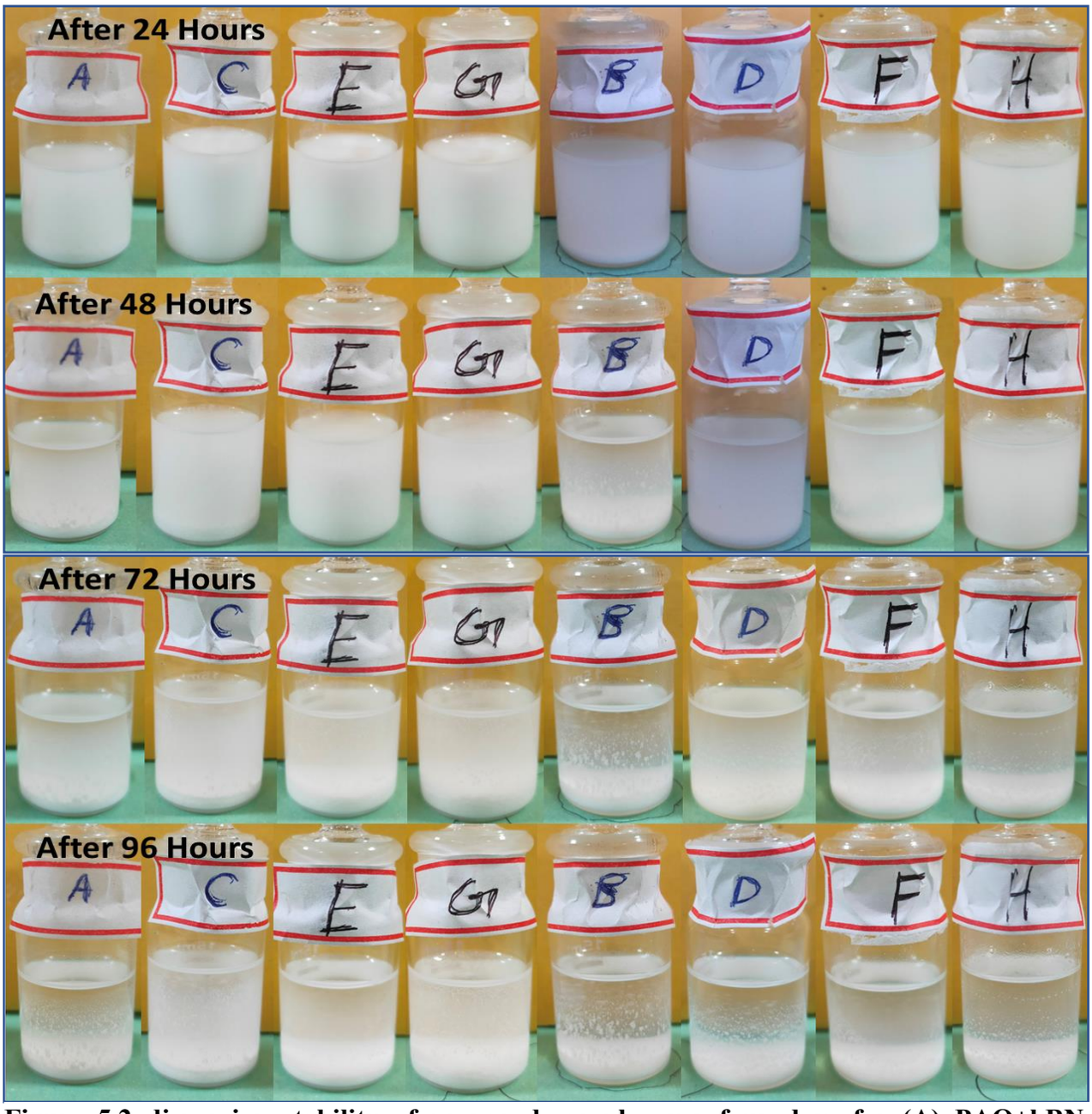

Figure 5.2 dispersion stability of prepared sample over four days for (A) PAO+hBN, (C) PAO+IL1+hBN, (E) PAO+IL2+hBN, (G) PAO+IL3+hBN, (B) PAO+ZnO, (D) PAO+IL1+ZnO, (F) PAO+IL2+ZnO, (H) PAO+IL3+ZnO. ILs have shown marginal improvement (2 days to one week) of NPs dispersion inferring that ILs on its own may not provide long term dispersion stability in lower viscosity oils.

Nasser et al. have reported that 1 wt% phosphonium phosphate ILs enhanced the dispersion stability of hBN NPs at least by 60 days[74]. Other than blended ILs this could be attributed to the higher viscosity of the base oil. They used highly viscous (PAO-32 base oil, generally used as transmission oil, kinematic viscosity 32 cSt at 373.15 K) base oil which gave over two months dispersion stability on its own. While in the present study the dispersion stability was enhanced marginally i.e., almost a week and 2 days for hBN and ZnO NPs respectively due to relatively lower viscosity of base oil. Based on the above results an inference can be drawn that phosphonium phosphate ILs perform relatively better in dispersion stability for highly viscous oil while ILs on their own may not provide adequate long term dispersion stability in low viscosity base oil. Other methods such as surface modifications (e.g. hairy nanoparticles) and dispersants for enhancing colloidal NPs stability in low viscous base oils may be prerequisite for availing benefits of hybrid nanolubricants [66, 75].

5.3.2. Effect on Viscosity and Density

Table 5.2 Viscosity, Viscosity Index and Density change with additive addition in base oil

Lubricants	Kinematic Viscosity (mm^2/s)				Viscosity Index (VI)	% VI Change	Density (g/cm^3) @ 29.5°C	% Density Change
	@ 40°C	% Change @ 40°C	@ 100°C	% Change @ 100°C				
PAO	30.92	----	5.92	----	139.20	----	0.8187	----
PAO+hBN	32.39	4.76	6.26	5.94	146.71	5.40	0.8268	0.99
PAO+ZnO	31.98	3.43	6.15	4.13	143.87	3.35	0.8263	0.93
PAO+IL1	31.16	0.78	6.01	1.69	142.34	2.26	0.8198	0.13
PAO+IL1+hBN	32.04	3.62	6.19	4.74	145.55	4.56	0.8257	0.86
PAO+IL1+ZnO	31.71	2.55	6.10	3.21	143.17	2.85	0.8241	0.66
PAO+IL2	31.20	0.91	5.98	1.18	140.41	0.87	0.8194	0.09
PAO+IL2+hBN	31.94	3.30	6.20	4.91	146.81	5.47	0.8259	0.88
PAO+IL2+ZnO	31.67	2.43	6.11	3.38	144.01	3.46	0.8246	0.72
PAO+IL3	31.02	0.32	5.95	0.68	140.11	0.65	0.8192	0.06
PAO+IL3+hBN	32.03	3.59	6.14	3.89	142.98	2.71	0.8251	0.78
PAO+IL3+ZnO	31.56	2.07	6.08	2.88	143.20	2.87	0.8239	0.64

Table 5.2 shows the kinematic viscosity, and density values obtained from Stabinger viscometer (SVM 3000), which works on the Couette principle and measures viscosity

according to ASTM D7042. IL1 and IL2 improved the viscosity marginally (0.78 and 0.91% respectively) at 40^{o}C, while IL3 improved 0.32% as a single additive. This could be due to the shorter chain length of IL3 compared with the other two ILs. hBN NPs performed better than ZnO as a single additive, this could be due to the higher concentration of hBN NPs (1 and 0.5 wt % for hBN and ZnO respectively). Interestingly, at elevated temperature(100^{o}C), hBN and ZnO nanolubricants improved viscosity by 5.94 and 4.13% respectively, which was significantly higher than their respective viscosity at 40^{o}C. Similarly, at elevated temperature, ILs also performed significantly better and enhanced viscosity by 1.69, 1.18, and 0.68% for IL1, IL2, and IL3 respectively. This could be due to the thinning effect of base oil at an elevated temperature and comparatively negligible thinning for ILs while NPs remained indifferent. For hybrid nanolubricant, the viscosity was highly influenced by their NPs constituents, and improvement is lesser than their respective individual nanolubricants performance since hybrid nanolubricants consist of only half of the NPs concentration. IL1 and IL2 improved viscosity index (VI) by 2.26 and 0.87% respectively, while marginal improvement (0.65%) by IL3 as a single additive. Nanolubricants showed a similar trend as that of their viscosity performance and improved VI by 5.40 and 3.35 % for hBN and ZnO nanolubricants respectively. No significant improvement in density was observed by the addition of ILs (≈0.1%), while marginal improvement was observed with NPs (≈0.9%) due to the higher relative density of NPs.

5.3.3. Tribological performances

Figure 5.3 (a)(b) shows the average wear and friction performance of lubricants tested at ASTM 4172 standard. The PAO base oil registered the highest average friction and wear and lubricated the surface poorly. As expected ZnO and hBN nanolubricants showed excellent antiwear properties with 23 and 27 % reduction of WSD respectively, while the friction reduction was recorded 9 and 11% respectively compared to neat PAO. It is evident from these tribological performances that both the NPs managed to separate the rubbing surface effectively due to the formation of tribofilm on the rubbing surface, by a combination of mechanisms such as Bearing effect, mending effect, polishing effect, and film formation, resulting in reduced friction and wear[64, 122, 130]. The average wear reduction for IL1,2,3 was 8, 30, and 21%, and friction was reduced by 10, 25, and 19 % respectively. Due to the ionic nature and inherent polarity, ILs adsorb on metallic surfaces forming weak adsorbed protective

layers on the rubbing surfaces. Under high temperature and tribostress, these adsorbed layered ILs form tribofilm on the rubbing surfaces due to tribochemical reaction. These weak adsorption layers with the phosphate-film are self-repairing and responsible for improved tribological properties[7]. The performance of ILs depends on its chemistry and test results have shown IL2 and IL3 performed relatively better compared to IL1 even though all the ILs have common cation and similar phosphorus concentrations. The poor performance of IL1 may be due to the inability to form sustainable tribofilm at elevated temperature and high tribostress indicating both cation and anion play important role in tribofilm formation. It is interesting to note that even though nanolubricants showed excellent wear reduction but their friction reduction was not as impressive as IL2 and IL3, indicating that these ILs may provide better friction reduction properties compared to NPs.

When it comes to synergistic behavior, IL1 blended hybrid nanolubricants (PAO+IL1+hBN, PAO+IL1+ZnO) showed synergy and decreased friction by 18 and 22% respectively, which is significantly higher than that of both the NPs and IL1 as a single additive. While marginal improvement was observed for antiwear properties since average wear reduction was 32 and 29% respectively, which is slightly higher than respective nano lubricant's performance as single additives. IL2 hybrid nanolubricants (PAO+IL2+hBN, PAO+IL2+ZnO,) decreased friction by 30 and 29%, while wear reduction was 57 and 50% respectively. IL3 hybrid nanolubricants (PAO+IL3+hBN, PAO+IL3+hBN) reduced friction by 26 and 23 %, while wear reduction was 41 and 43% respectively. The tribological properties for IL2 and IL3 blended hybrid nanolubricants showed excellent synergy in reducing friction and wear, indicating that both mechanisms of tribofilm formation for NPs and ILs complemented each other.

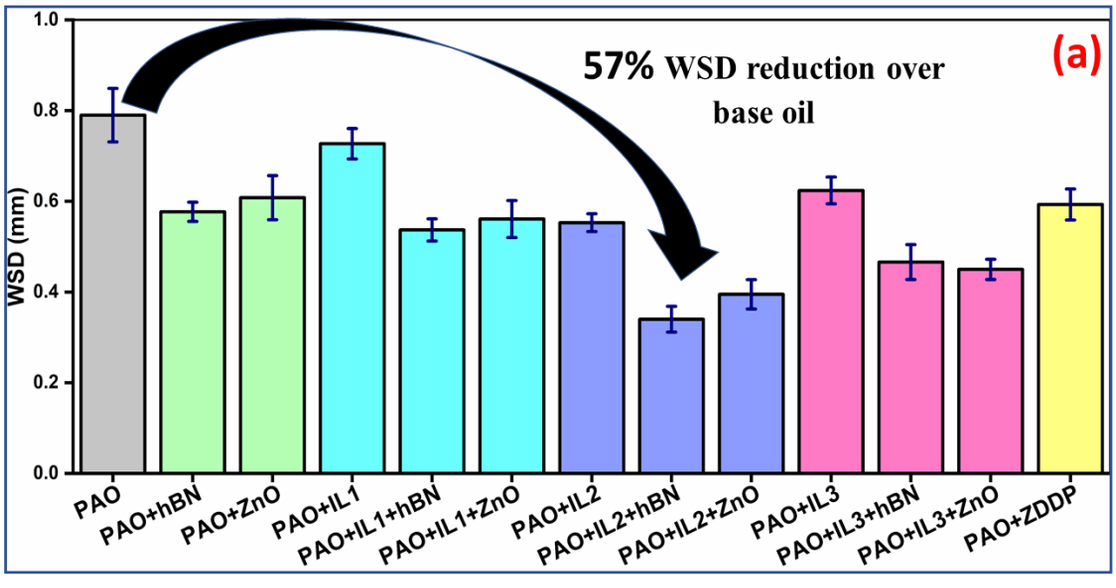

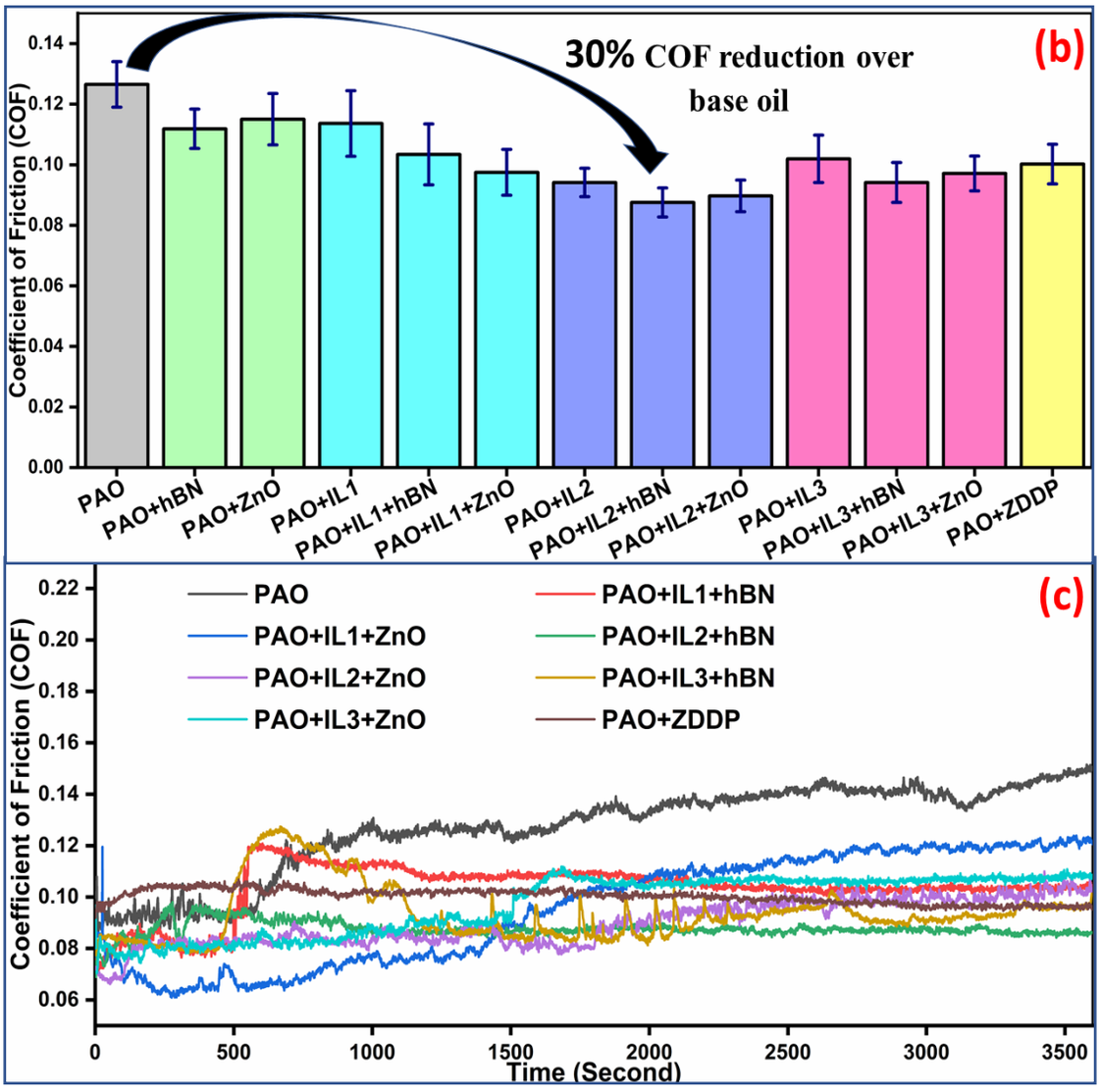

Figure 5.3 lubricant performance tested according to ASTM 4172 standards i.e. 40kg load, 1200 rpm, 75°C temperature for 3600 seconds (a) Wear performance of lubricants (b) Friction performance of lubricants (c) Friction coefficient vs time performance of lubricants. ILs and NPs based hybrid nanolubricants shows synergy and outperforms commercial ZDDP antiwear additives.

Further ZDDP had a similar phosphorus concentration as that of ILs and showed good friction (20%) and wear (25%) reduction over the base oil. The performance of ZDDP was slightly better than IL3 as a single additive while IL2 showed better friction and wear reduction compared to ZDDP. On the other hand, IL1, IL2, and IL3 hybrid nanolubricants showed synergy and outperformed ZDDP significantly even though they were composed of half of the phosphorus concentrations and no Sulphur as that of ZDDP. Figure 5.3(c) gives the average COF performance over the entire test duration (3600 seconds) for hybrid. All the hybrid nanolubricants show lower starting friction compared to base oil due to effective synergy

between ILs and NPs. It is interesting to note that COF value of base oil keeps ascending throughout the test duration due to lack of protective additives.

5.3.4. Extreme Pressure performances

The EP performance of lubricants was tested according to IP 239 test standard and results are shown in figure 5.4. The test duration is for 60 seconds, and due to high tribostress top surface layers get removed several times, and new tribofilm is replaced continuously. The inability to provide protective film by the lubricants at these extreme working conditions leads to excessive heat generation due to direct metal-to-metal contact and ultimately seizure of these rubbing surfaces. The PAO was capable of separating tribopair up to 100 kg, and at 115kg, seizure occurred. IL1, IL2, and IL3 improved non-seizure load by 15, 40, and 25% respectively. ZnO (50%) nanolubricants slightly outperformed hBN (40%) nanolubricants despite higher concentration of hBN (1 wt%) NPs compared to ZnO (0.5 wt%). Other than the morphology and physico-chemical properties of NPs this could be plausible due to the smaller average particle size of ZnO (30 APS) compared to hBN (70 APS) NPs. IL1 hybrid nanolubricants showed the same performance as that of its single hBN and ZnO NPs respectively while IL2 hybrid nanolubricant showed excellent synergy with both the NPs and improved non-seizure load by 65 and 75% with hBN and ZnO NPs respectively. IL3 hybrid nanolubricant also showed synergy with both the NPs, and improvement was 65% with both the NPs. On the other hand, ZDDP showed better performance than IL1 and IL3 and similar performance as of IL2 as a single additive but IL2 and IL3 hybrid nanolubricants significantly outperformed ZDDP.

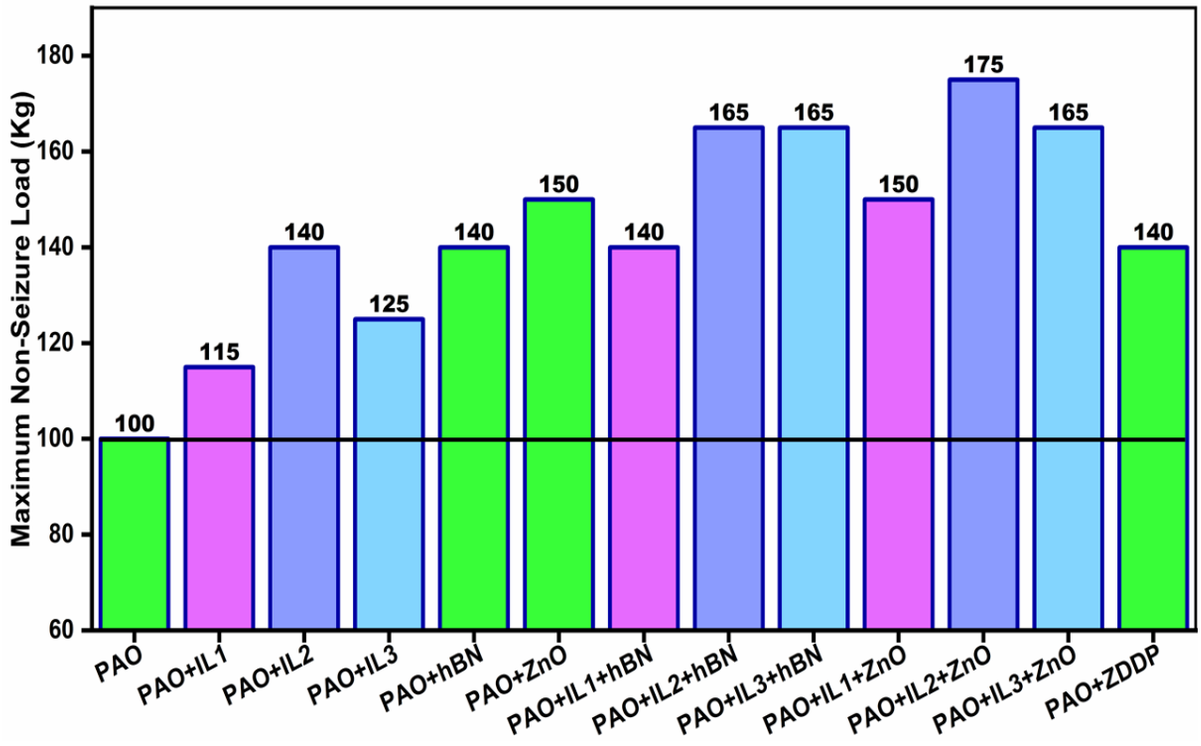

Figure 5.4 Extreme Pressure (EP) performance of formulated lubricants tested following IP 239 standard i.e. step wise progressive loading till seizure, room temperature, 1450 rpm and 60 seconds of test duration. Hybrid nanolubricants outperform all the single additives having similar additive concentrations.

5.3.5. Surface characterization

5.3.5.1. SEM-EDS analysis of worn surfaces

To understand the worn surface morphology and possible tribofilm formation on lubricated surfaces, SEM and EDS spectroscopy were employed. Base oil protects the surface poorly, which is evident from the morphology of the worn surface, as shown in figure 5.5 (a). The surface shows deep long grooves and pits throughout the worn surface, which may have been caused due to abrasive and adhesive wear (plastic deformation) respectively. Under high load and tribostress, lubricant fails to separate the asperities of rubbing surfaces resulting in wear of the tribopair. In abrasive wear, the asperities of rubbing surfaces dig into the other and may produce long and deep grooves, while in adhesive wear localized bonding takes place in which a chunk of material adheres to the opposite surfaces and get removed or plastically deformed during subsequent sliding[122]. The addition of additives still showed abrasive and adhesive wear but the severity of the wear and WSD was relatively lesser compared to the base oil. On the other hand, Both the NPs showed a combination of minor abrasive and adhesive wear as

shown in figure 5.5 (b, c). Similar wear morphology was also observed for ILs except for IL1 (figure 5.5 d) which showed few deeper pits and just 8% WSD reduction indicating poor surface protection. Hybrid nanolubricants showed minor pits and grooves (little surface damage) throughout the worn surface nevertheless gave relatively smoother surface. Surface lubricated with ZDDP lubricant showed negligible adhesive wear while moderate abrasive wear concentrated in small patches. In general, the worn surface morphology is in good agreement with the wear and friction behavior discussed above.

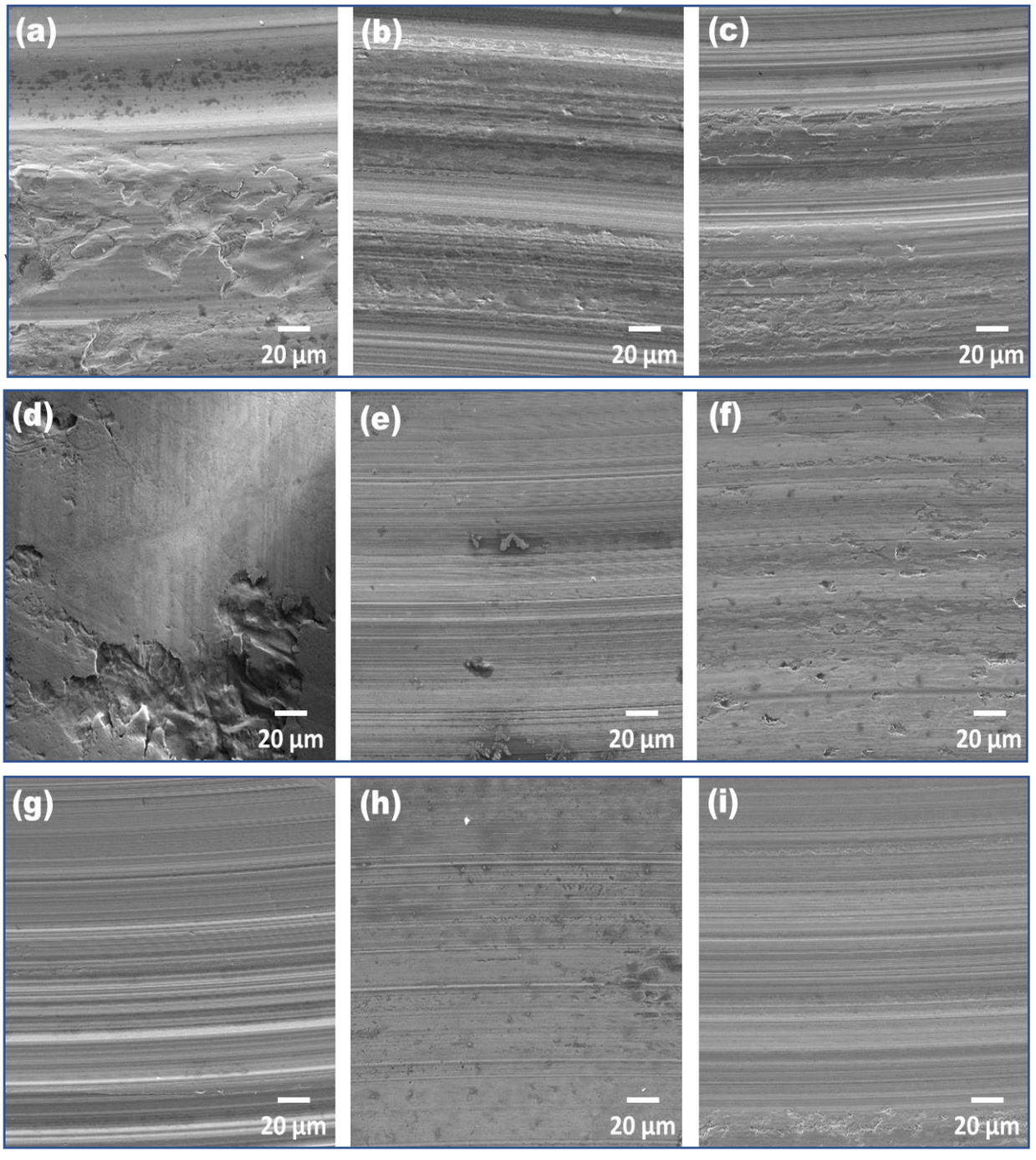

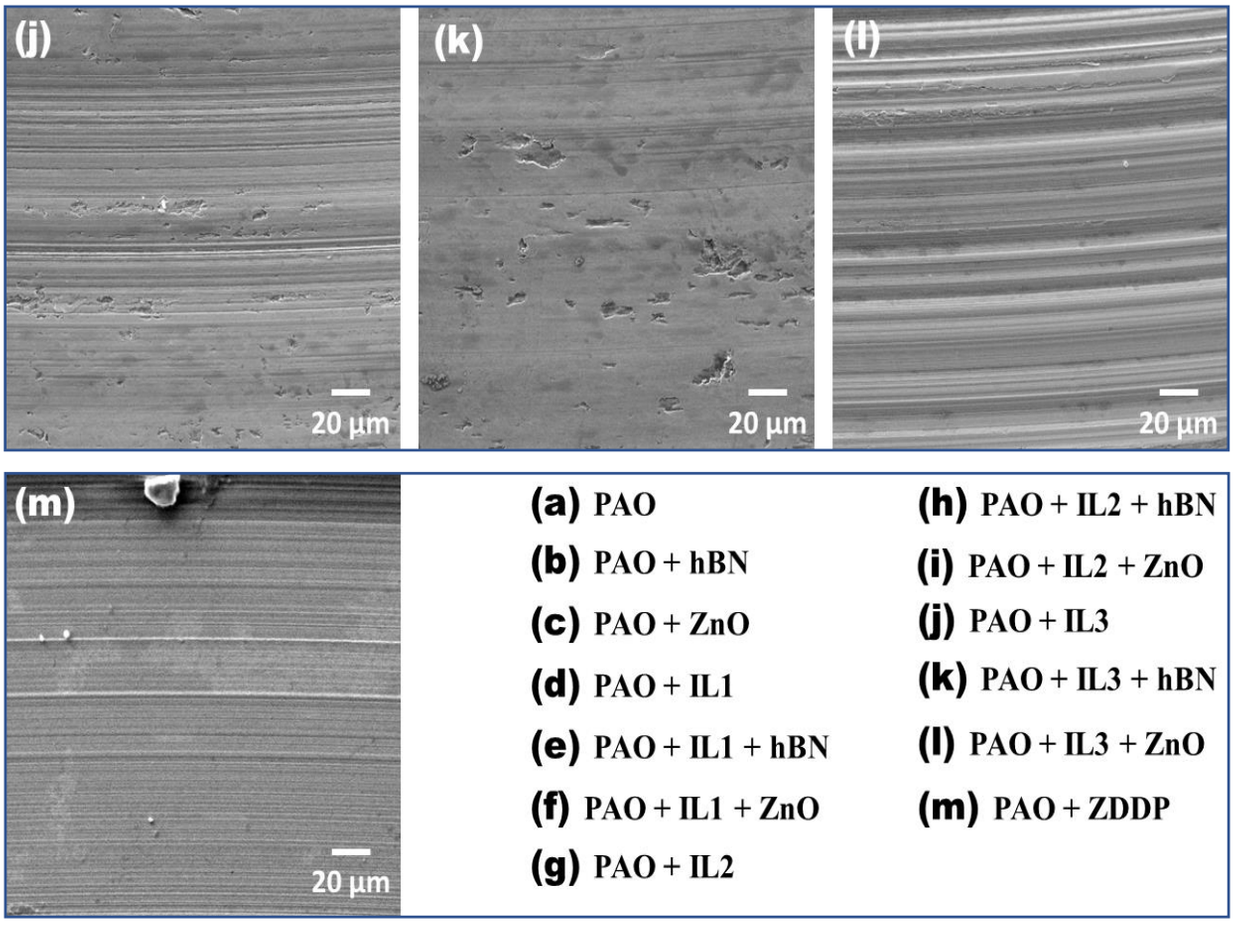

Figure 5.5 SEM micrograph of worn ball surfaces lubricated with different formulation listed at bottom right. Base oil lacks effective surface protection and shows dominant adhesive wear (plastic deformation). As expected, addition of additives improved surface morphology and reduced overall WSD. Hybrid nanolubricants showed synergy and provided effective surface protection as evident from smoother surface with little surface

Table 5.3 Elemental composition of worn surface lubricated with different formulations.

Lubricants	Atomic % of the worn surface								
	O	P	S	Zn	B	N	C	Fe	Cr
PAO	6.10	0	0	0	0	0	4.58	87.79	1.53
PAO+hBN	4.01	0	0	0	2.09	1.37	3.28	88.04	1.21
PAO+ZnO	9.57	0	0	1.92	0	0	5.34	81.75	1.42
PAO+IL1	3.24	0.58	0	0	0	0	4.38	90.64	1.16
PAO+IL1+hBN	3.25	0.34	0	0	1.45	0.67	11.18	81.67	1.44
PAO+IL1+ZnO	7.33	0.25	0	0.78	0	0	7.86	82.42	1.36
PAO+IL2	9.26	1.92	0	0	0	0	7.61	79.82	1.39
PAO+IL2+hBN	3.61	1.69	0	0	1.53	0.84	5.86	85.16	1.31
PAO+IL2+ZnO	5.32	1.22	0	1.83	0	0	12.67	77.52	1.44
PAO+IL3	6.81	1.67	0	0	0	0	6.31	83.7	1.51
PAO+IL3+hBN	5.23	0.91	0	0	1.72	0.95	3.52	86.41	1.26
PAO+IL3+ZnO	5.54	1.10	0	1.2	0	0	4.92	85.86	1.38
PAO+ZDDP	8.26	1.27	0.91	0.83	0	0	9.13	78.14	1.46

EDS is a semi-quantitative technique that gives the elemental composition of the surfaces and can be very effective in a comparative study of the worn surface. Table 5.3 gives the elemental composition of worn surfaces lubricated with different formulations. In general, Nascent steel surfaces exposed during rubbing get oxidized and form ferrous oxide compounds (primarily FeO, Fe_2O_3)[85, 110]. Few studies have linked higher oxygen concentration in the tribofilm to poor surface protection and higher wear[131, 132]. In our study too, surfaces lubricated with best performing (IL2 and IL3) hybrid nanolubricants gave relatively lower Oxygen concentrations (3-5%). But few additives (Table 5.3) despite giving lower WSD registered higher Oxygen concentration compared to the base oil. Hence in these working conditions higher oxygen concentration to base oil may not correlate to poor surface protection. But at the same time, a direct correlation between the phosphorus concentration of the tribofilm and tribological performance of the lubricants can be drawn. IL2 hybrid nanolubricant showed 1.69 and 1.23% P concentration with hBN and ZnO NPs respectively, which is higher (1.1 and 0.9%) than that of IL3 hybrid nanolubricant. Higher P concentration in the tribofilm could

mean thicker tribofilm (plausibly composed of $FePO_4$) and be the plausible explanation for the better performance of IL2 over IL3[110, 133]. On the other hand, IL1 hybrid nanolubricant showed a very low concentration of phosphorus (0.34,0.25 %) in the tribofilm, which was around 4-5 and 3-4 times lesser compared to IL2 and IL3 hybrid nanolubricants respectively. The poor performance of IL1 blended lubricants could be attributed to the inability of IL1 in defusing higher active P concentration in the tribofilm despite having the same cation and concentration of phosphorus as that of IL2 and IL3[110]. In boundary lubrication under high load lubricant films between rubbing surfaces become thinner, NPs (if in sufficient concentration) may support the proportion of the loads and reduce adhesive wear. At the nanoscale level, metallic surfaces generally are not smooth and consist of uneven asperities and valleys. Further, these NPs transferred between rubbing surface and under tribostress formed self laminating protective film primarily due to polishing, mending effects and film formation[107, 130]. hBN hybrid nanolubricant showed an almost similar concentration of B and N on the worn surface, irrespective of the ILs combination. While Zn concentration in IL1 hybrid nanolubricant is significantly less than compared with IL2 and IL3 hybrid nanolubricant. Worn surfaces of hybrid nanolubricants gave relatively lesser triboactive element composition compared to their respective single additive formulation due to reduced additive concentration and probable competition between both the additives for adsorption on the rubbing surface[131]. ZDDP is known to disintegrate and self-react with rubbing surfaces under tribostress and form metal phosphates and oxides[110, 134]. ZDDP gave a significant concentration of P on the worn surface while a lower concentration of S indicating tribofilm has predominantly consisted of phosphates and lower concentrations of sulfides.

5.3.5.2. XPS analysis

To understand the nature and chemical state of the tribofilm, XPS spectroscopy was employed. XPS is a powerful technique, scans a few atomic layers (1 to 5 nm) depth of the surface and can help in profiling integration of additives in the tribofilm[135]. IL1 and IL2 have been reported undergoing tribochemical reactions and forming phosphate tribofilm in literature while newly synthesized IL3 is not explored [136, 137]. Figure 5.6 shows the complete XPS survey spectra of surfaces lubricated with IL3 hybrid nanolubricants along with key core level spectra of individual triboactive elements of the worn surface. The atomic composition obtained from quantitative XPS analysis (Table 5.4) shows elevated additive concentration (2-4 times) compared to EDS elemental composition results tabulated in Table 5.3. This could be

attributed to the different probing depths of EDS (few micrometers) and XPS (few nanometers). Core level XPS spectra of both the surfaces lubricated with PAO+IL3+hBN and PAO+IL3+Zn gave P 2p peaks at ≈133.6 and ≈133.5 eV BE respectively which could be attributed to phosphates (P-O) bond[57, 75]. This suggests that IL3 (just like IL1 and IL2) decomposed due to higher tribostress and react with the rubbing surfaces and subsequently form protective film composed of phosphates. For surface lubricated with PAO+IL3+Zn two distinct O 1s peaks were observed; the peak at ≈531.03 eV BE can be attributed to phosphate (O-P bonding) excluding Fe-O-P bonds and the other peak ≈530.4 eV BE can be associated with Fe-O bonds and Fe-O-P bonds[56, 75, 138]. Similarly, the surface lubricated with PAO+IL3+hBN also shows two peaks; peak at ≈530.7 eV BE can be associated with phosphates while ≈530.1 eV can be attributed to Fe-O and Fe-O-P bonds. Further, the surface lubricated with PAO+IL3+hBN showed peaks of B 1s at ≈190.3 eV BE and ≈191.2 eV BE which are in accordance with the observation made by Kimura Yoshitsugu et al[139]. The peak of 191.2 eV could be attributed to some form of Boron oxides (obviously not stoichiometric Boron oxide generally assigned peak at ≈192.8 eV), inferring hBN NPs undergoing mechano-chemical induced oxidation[139]. While the lower peak of B 1s (≈190.3 eV) could be attributed to Boron nitride. The peak of N 1s at ≈398.5 eV could be attributed to hBN[140]. The surface lubricated with PAO+IL3+Zn showed a single peak of Zn 2p at ≈1023 eV BE corresponding to ZnO NPs.

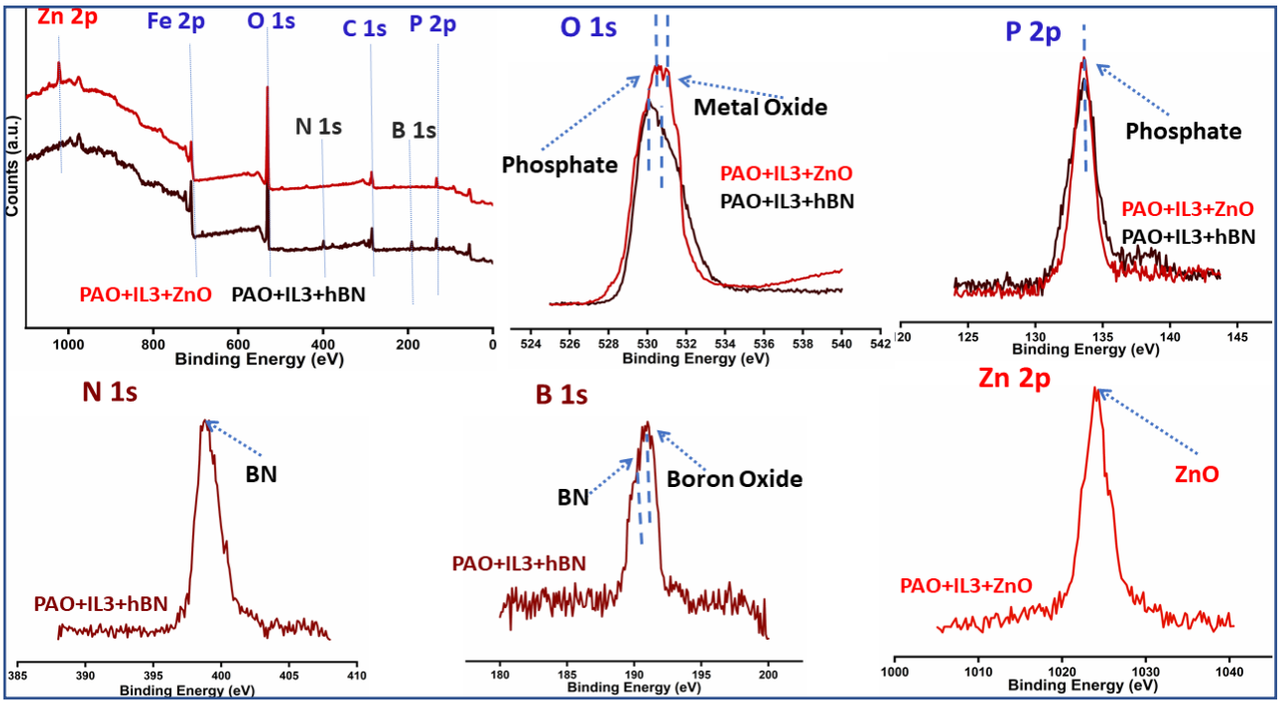

Figure 5.6, from top left clockwise, XPS survey spectra of worn surface (WSD) of balls lubricated with PAO+IL3+hBN and PAO+IL3+Zn hybrid nanolubricants and core level spectra of O 1s, P 2p, Zn 2p, B 1s, N 1s.

Table 5.4 atomic composition of the tribofilm obtained from XPS quantitative analysis

Samples	Elements in tribofilm (at%)						
	Fe	O	C	P	B	N	Zn
PAO+IL3+hBN	12.5	65.4	9.5	5.2	3.5	3.9	0
PAO+IL3+ZnO	10.3	69.3	8.1	5.9	0	0	6.4

5.4. Mechanism of tribofilm formation

does applying a bias to the sample change this?

Based on the tribological, EP performance, and surface characterization techniques we deduce possible mechanism of the tribofilm formation as follows. Dispersed Ionic liquids get adsorbed on steel surfaces due to their affinity towards metallic surfaces (polar nature)[7]. These weakly adsorbed films, under tribostress, may undergo chemical degradation releasing active elements which react with the nascent steel surface and subsequently form complex tribofilm composed of phosphates and ferrous oxides as evident from the above-reported surface characterization results. Simultaneously, NPs provide a protective film on the worn surface due to the tribosintering mechanism[130]. Tribological performance and surface characterization techniques infer compatibility between ILs and NPs with the formation of

regenerative tribofilm composed of residues from both additives. Based on the above results we deduce that the weak adsorbed ILs film, tribochemically reacted phosphate film, and tribosintered NPs reduce/prevent direct surface to surface contact between rubbing surfaces due to the formation of regenerative sacrificial tribofilm. Figure 5.7 (a) depicts the tetrahedral arrangement of lubricated steel balls. Figure 5.7(b) shows ILs and NPs between the asperities of the steel balls. Figure 5.7(c) depicts the formation of regenerative sacrificial tribofilm composed of phosphate and tribosintered NPs on the steel substrate.

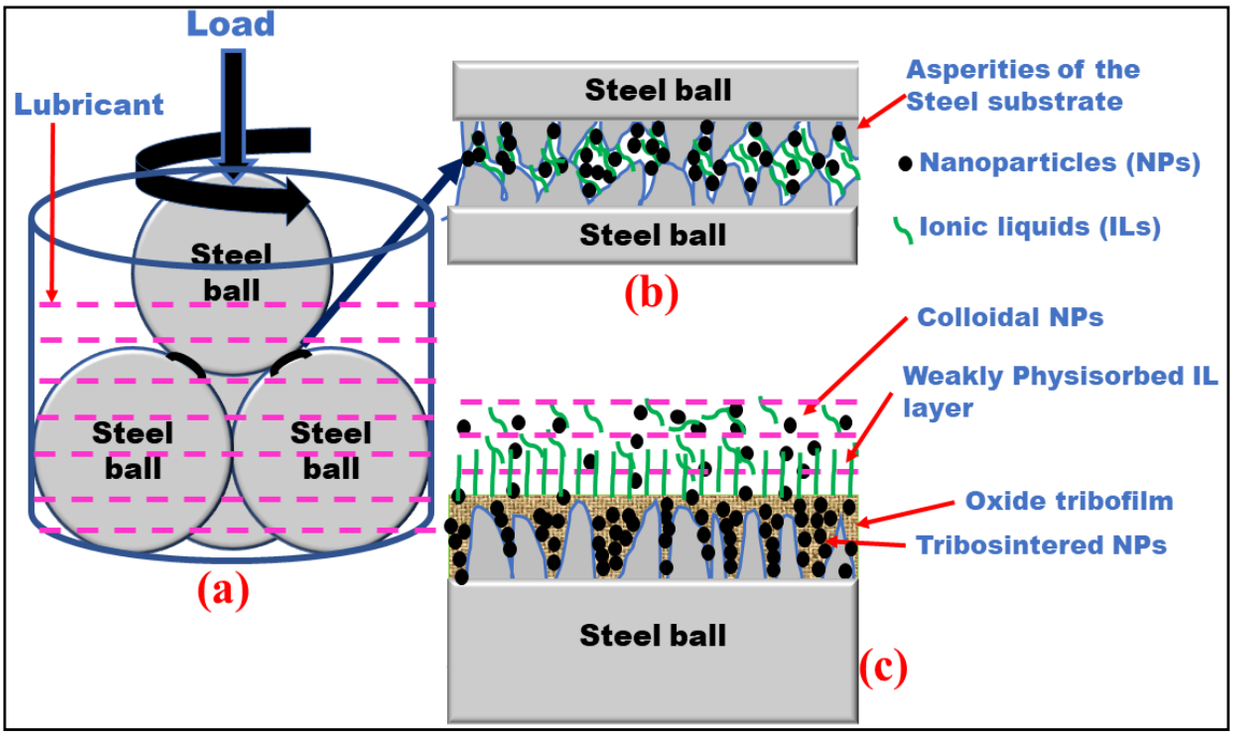

Figure 5.7 Mechanism of tribofilm formation for hybrid nanolubricants (a) Tetrahedral arrangement of the lubricated steel balls (b) ILs and NPs in asperities (peaks and valleys) of rubbing surfaces. (c) tribofilm (brown colour) composed of complex phosphate compounds (Fe-P-O) along with tribosintered NPs. ILs due to polarity also provide weak physisorbed layer top of the rubbing surfaces.

5.5. Important observations

In this study the synergy between ILs (([P66614][BTMPP]), ([P66614] [DEHP]) ([P66614] [DBP])) and NPs (hBN, ZnO) based hybrid nanolubricant additives have been explored for steel-steel contact under boundary lubrication. The performances are also compared with a common commercial antiwear additive i.e., ZDDP. This study also reports phosphonium IL ([P66614] [DBP]) for the first time as a lubricant additive.

Based on tribological performance and surface characterization we would like to conclude that:

- All ILs showed excellent miscibility (at least 5 wt%) in PAO and excellent tribological performance with 21 and 19% of wear and friction reduction respectively.
- IL2 and IL3 hybrid nanolubricants showed excellent synergy in friction, wear reduction. IL2 hybrid nanolubricants (PAO+IL2+hBN and PAO+IL2+ZnO) decreased friction by 30 and 29%, while wear reduction was 57 and 50% respectively. IL3 hybrid nanolubricants (PAO+IL3+hBN and PAO+IL3+ZnO) reduced friction by 25 and 23 %, while wear reduction was 41 and 43% respectively.
- The IL1 hybrid nanolubricants improved wear reduction marginally if compared with the other two ILs, even though it shares the same cation and phosphorus concentration as that of IL2 and IL3, inferring that tribochemistry of both cation and anion are equally important for the tribofilm formation.
- IL2 and IL3 hybrid nanolubricants showed synergy and enhanced extreme pressure (EP) performance of the base oil up to 65 - 75% respectively.
- Ionic liquids (ILs) enhanced the dispersion stability of hBN and ZnO NPs by a week and 2 days respectively. But it was observed that ILs on their own may not provide prolonged stability in lower viscosity oils and further dispersion stability enhancement methods for NPs should be explored.
- All the hybrid nanolubricants outperformed ZDDP indicating that compatibility between ILs and NPs can help in decreasing overdependence on ZDDP provided the long term dispersion stability of NPs is addressed.
- Relative viscosity enhancement of base oil was higher at elevated (100^{o} C) by the addition of ILs (1-2%) and NPs (≈5%) due to their physicochemical properties. While NPs improved the density of base oil marginally (<1%), and negligible changes were recorded for ILs.
- Surface characterization techniques confirmed synergy between ILs and NPs in the formation of regenerative sacrificial tribofilm on the counter surfaces composed of phosphates (Fe-P-O) and tribosintered NPs.

Chapter - 6

Three-way compatibility study among Nanoparticles, Ionic Liquid, and Dispersant for potential in lubricant formulation

6.1. General

According to HOLMBERG et.al, 23% of the world's energy consumption can be traced back to tribological contacts[141]. 20% energy is consumed to overcome friction while 3% is consumed to reproduce the worn components. It is estimated that with the advances in materials and lubricants, the energy losses associated with friction and wear can be reduced up to 40% which is nearly 1.4% of the world's GDP[141]. This has prompted the relentless pursuit of efficient, durable, and relatively greener lubricants but the biggest motivation is still the lowest possible friction and higher efficiency. Further to reduce pumping losses and minimize hydrodynamic shear, attempts are being made to develop lubricants with the lowest possible viscosity, effective enough to decrease friction and wear between rubbing surfaces[65]. Southcombe et.al filed the first lubricant patent in 1918, which used vegetable-derived fatty acid additive in mineral oil and reported improved lubricity[142]. Since then, several different additives have been developed such as antioxidant, antiwear, friction modifiers, dispersants, etc[7, 121, 143].

Among these two of the most promising and newest additive friction modifier groups are nanoparticles (NPs) and Ionic Liquids (ILs). NPs have been a fascination for the last two decades and have seen limited applications in commercial lubricants and greases. NPs may decrease friction and wear due to either of these four mechanisms i.e., bearing, mending, polishing and film formation attributed to tribochemical reaction[65]. While on the other hand, ILs are relatively new, the first oil miscible ILs were synthesized in the year 2012 and gave excellent antifriction (AF), antiwear (AW) performance as lubricant additives[125]. ILs may also contain triboactive elements such as P, N, F, and B which under tribostress may disintegrate and chemically react to nascent surfaces resulting in relatively stronger protective film[21, 125, 144]. The most common cation groups used in lubricants research with excellent tribological properties are phosphonium, ammonium, pyridinium, imidazolium[125].

Formulated commercial lubricants consist of base oil and more than half a dozen of performance additives[122]. There are few studies exploring the compatibility between the newest additive groups i.e. ILs and NPs[74, 82, 109, 145, 146]. Most of these studies have reported excellent synergy between ILs and NPs and possess the potential to limit or replace ecologically harmful SAPS (Sulphated Ash, Phosphorus, Sulphur) compounds from existing commercial lubricants[89]. But generally, colloidal NPs in lubricants have poor stability due to agglomeration and are prone to sedimentation. Generally, two approaches are prevalent for

enhancing the dispersion stability of colloidal NPs[66]. The first method attempts to change lubricant formulation by the addition of dispersant compounds along with NPs. While the other method involves modification of NPs by amphiphilic compounds to achieve stable suspension of NPs[66]. A prolonged colloidal suspension is obtained when Brownian motion overcomes attractive forces (due to interaction between NPs) of colloidal NPs. Inferring for successful exploitation of NPs potential in commercial lubricants dispersion (dispersant compounds, modification of NPs by amphiphilic compounds) methods will be instrumental.

The performance of any additive not only depends on its chemistry but also compatibility with other additives in that formulation hence studying their synergistic and antagonistic behavior becomes a pre-requisite for availing the potential of additives. The only study exploring the interaction among ILs, friction modifier (MoDTC), and dispersant is published by Weimin Li. et.al in 2020[131]. Further, to the best of our knowledge, no study exploring the three-way interaction between IL, NPs, and dispersant (used in engine oil to disperse insoluble compounds) is reported yet. This chapter reports, complex three-way interactions among oil miscible phosphonium phosphate ILs, metal oxide NPs (ZnO), and common commercial dispersant (PIBSA) in synthetic base oil (PAO6) for steel-steel tribopair under boundary lubrication. This study provides not only physicochemical compatibility among these additives but also their mutual synergistic/antagonistic interaction with rubbing surfaces. This study may provide a platform for new lubricant formulation composed of ILs, NPs, and dispersants along with other additives.

6.2. Materials and Methodology

6.2.1. Materials

Poly-alpha-olefin (PAO-6) synthetic base oil was obtained from Synthomaxx India and was used as received. The PAO is generally named (e.g., PAO-6) based on their kinematic viscosity at 100^{o}C. Based on comparative study (chapter 5) best performing phosphonium phosphate IL was used in this study i.e. trihexyltetradecylphosphonium bis(2-ethylhexyl)phosphate ([P66614] [DEHP]). The IL was synthesized in our synthesis lab following the process reported by Sun. J et. al[112]. The information about cation, anion and detailed synthesis process is reported in chapter 3. Zinc Oxide (ZnO) NPs were obtained from SRL Pvt.Ltd (CAS number: 1314-13-2, Molecular weight: 81.38) and were used as received.

While the dispersant Polyisobutylene Succinic Anhydride (PIBSA) was obtained from Univenture Industries Pvt.Ltd (Trade Name: UNOL P 1057).

6.2.2. Sample preparation

International Lubricant Specification Advisory Committee (ILSAC-GF-6) for API Engine Oil has limited the maximum Phosphorus concentration to 800 ppm or 0.08 wt%[147]. The IL used in this study was added in base oil in such a way that the maximum Phosphorus concentration was within 800 ppm concentration. Varying concentrations of ZnO NPs (0.4-1.2 wt%) have been reported in the literature[64]. Further 0.5 wt% ZnO NPs concentration was used in this study after optimum concentration test (detailed in result and discussion section). A constant 1 wt% of PIBSA dispersant was used for all the formulations in this study[99]. For fair comparison among IL, NPs, and their hybrid (IL+NPs) additives, the concentration of ILs and NPs were halves (i.e. 400 PPM phosphorus concentration for ILs and 0.25% wt% for ZnO NPs) for hybrid nanolubricants composed of PAO+ IL+ZnO. Mechanical stirring (2 hours) followed by probe sonication (45 minutes, make Dakshin Ultrasound) was used for dispersing NPs in formulated lubricants, while ILs were dispersed by stirring (1 hour) at room temperature.

6.2.3. Surface characterization

To explore the morphology of the worn surface Scanning Electron Microscopy (SEM) make Tescan VEGA-3 LMU was employed. Elemental composition of worn surface can give a thorough understanding of additives role in tribofilm formation responsible for improved tribological performance. For this Energy-Dispersive X-Ray Spectroscopy (EDS) make oxford instruments coupled with SEM was used in this study. An optical microscope (HUVITZ LUSIS HC-30MU) was used for WSD comparative study. To remove any weakly adsorbed lubricant residues, tribo-tested steel balls were washed in hexane for at least 10 minutes.

6.2.4. Tribological Testing

Antifriction and antiwear performance of formulated lubricants were assessed using DUCOM's four-ball tribometer. It uses a tetrahedral arrangement of four steel balls (AISI E 52100, diameter 12.7mm, average surface roughness 35 nm, hardness 63-66 HRC) and its specifications and methods are discussed in chapter 3. The antifriction and antiwear tests were performed following ASTM 4172 test standards which include 392 N load, 75^{O}C temperature, speed 1200 RPM, and test duration of 1 hour. Figure 6.1(a, b) shows an optical image of

formulated hybrid nanolubricant (PAO+PIBSA+IL+ZnO) and FE-SEM images of ZnO NPs respectively. The ZnO NPs show spherical morphology having APS of 30 nm.

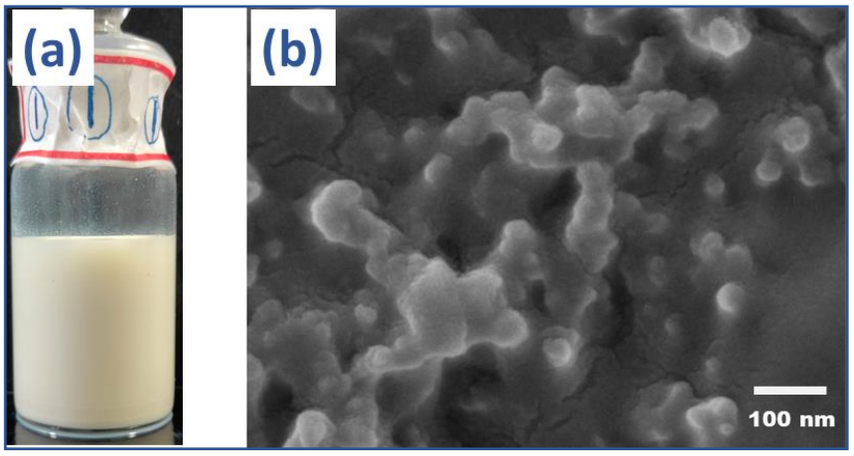

Figure 6.1 (a) optical image of formulated hybrid nanolubricant composed of (PAO+PIBSA+IL2+ZnO) (b) FE-SEM image of ZnO nanolubricants showing near spherical morphology.

6.3. Results and Discussion

6.3.1. Antifriction and antiwear performance.

As discussed in sample preparation, section 6.2.2, the optimization tests were performed to obtain optimum ZnO NPs concentration and test results are shown in figure 6.2(a, b). The highest wear reduction of 23% was observed at 0.5 wt% NPs concentration and beyond that performance did not improve. On contrary at 1 wt % NPs concentration the friction and wear increased. Hence based on the highest wear reduction (least wear scar diameter), 0.5 wt% ZnO NPs were used in this study as a single additive.

Figure 6.3 (a, b) shows average wear and friction reduction respectively tested following ASTM 4172 test standards. Without any additive base oil protects the surface poorly which is evident from the higher wear scar diameter (WSD) and friction coefficient (cof). The addition of dispersant (PIBSA) marginally improved average cof (≈1%) and average wsd (≈2%) but overall performance was similar to that of the base oil. The addition of ZnO NPs significantly improved antiwear performances (23%) and friction reduction (9%) over the base oil. This could be attributed to mechanisms such as ball-bearing effect, mending effect, polishing effect, and film formation[64, 85]. Among these balls bearing effect and film formation are attributed to the direct action of NPs while the mending effect and polishing effect provides secondary

surface enhancement. The ball bearing mechanism proposes that spherical NPs rolls during rubbing of counter surfaces, acting as nano-sized bearing balls, and may further convert sliding friction into a combination of sliding and rolling friction[99, 132]. While in film formation mechanism NPs either chemically react or get tribosintered due to tribostress resulting in protective sacrificial tribofilm formation. Effective prolong surface protection mandate the self replenishment rate of tribofilm to be higher than wear rate[64]. These mechanisms due to the direct action of NPs form a regenerative sacrificial protective film on the counter surfaces[64, 65]. During the mending effect, NPs compensate for the loss of material due to wear and fill the grooves and scars of the rubbing surface resulting in enhanced surface finish[85]. While in polishing effect roughness of the rubbing surfaces is reduced by abrasive treatment of the NPs[85]. The dispersant PIBSA added with ZnO NPs did not hamper ZnO NPs performance and marginally improved the friction (11%) and wear (24%) reduction compared to ZnO nanolubricant performance. Phosphonium phosphate IL ([P_{66614}][DEHP]) used in this study registered excellent friction (26%) and wear (30%) reduction over base oil. This could be attributed to the disintegration of ILs under tribostress and subsequently the formation of protective tribofilm composed of phosphate compound[82, 110, 124, 144, 148]. Further dispersant PIBSA added with IL gave similar friction (26%) and wear (29%) reduction performance as that of IL inferring compatibility between ILs and PIBSA.

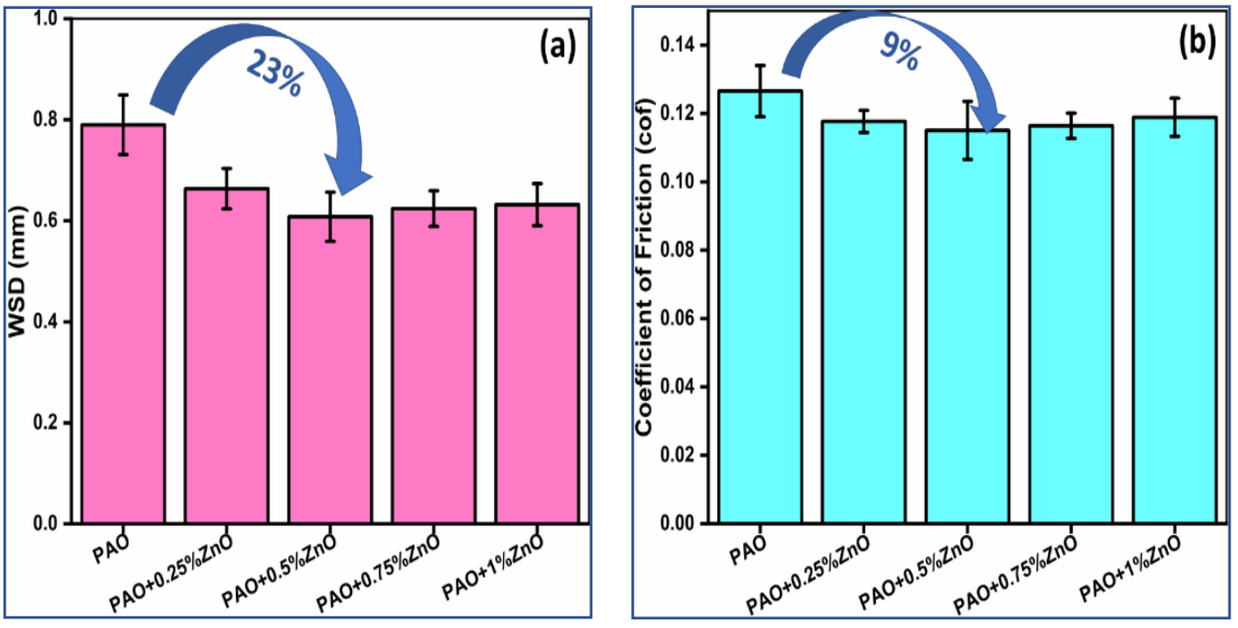

Figure 6.2 Optimization test varying ZnO concentration (a) wear scar diameter (b) friction coefficient. Based on the least wear scar diameter, 0.5 wt% concentration was selected for further study.

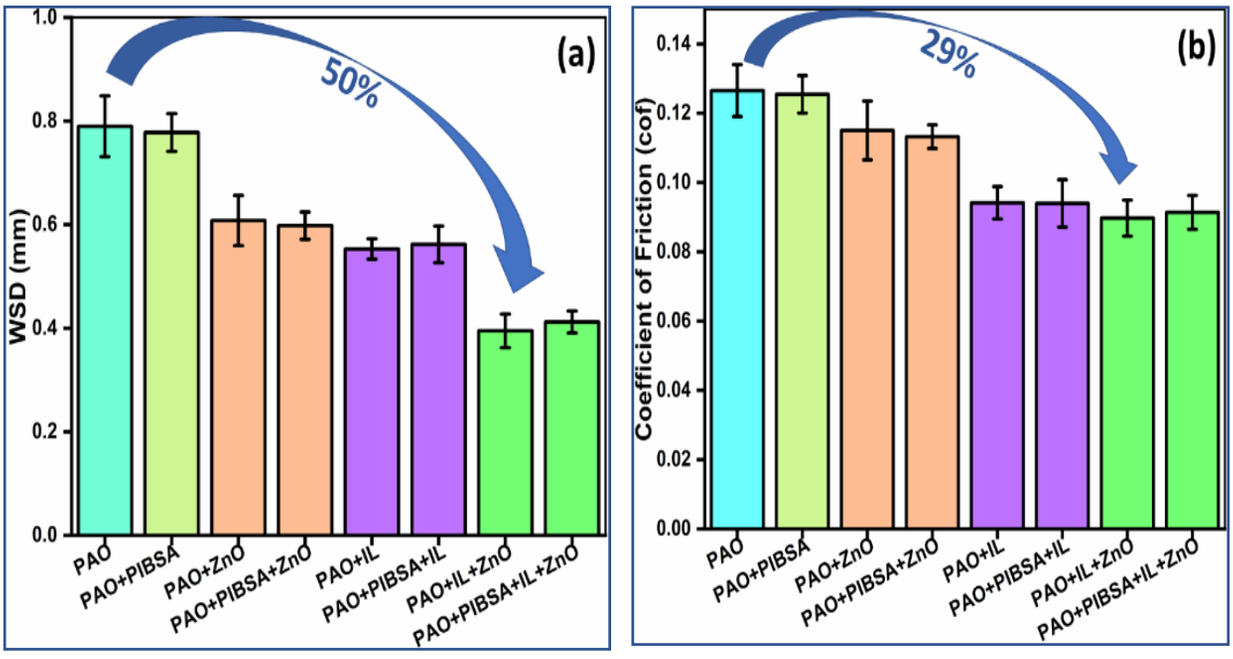

Figure 6.3 tribological performance of formulated lubricants tested following ASTM 4172 standard (a) average wear scar diameter (b) average friction coefficient. Above results shows excellent synergy between IL and NP in reducing friction and wear. Further these results confirm no antagonistic effect due to addition of dispersant PIBSA on the performance of IL and NP as single additive or hybrid nanolubricants.

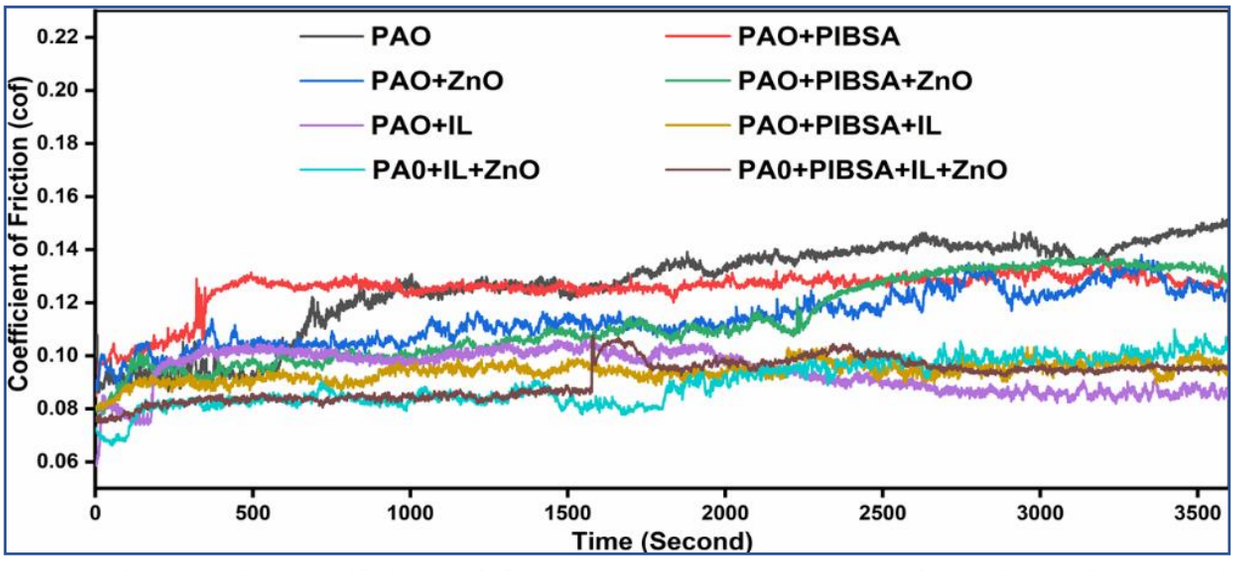

Figure 6.4 Friction coefficient of formulated lubricant tested following ASTM 4172 standard for entire test duration of (60 minutes)

Hybrid nanolubricant composed of IL and NPs additive showed the highest improvement in friction and wear reduction i.e. 29 and 50% respectively. This infers excellent synergy between IL and NPs in protective film formation. The addition of dispersant PIBSA further did not hamper synergy between ILs and NPs, provided similar friction and wear reduction performance. Figure 6.4 gives the comparative cof performance of all the lubricant

formulations along with base oil for the entire test duration of 60 minutes. As discussed earlier base oil shows poor surface protection due to the absence of additives which is evident from ascending friction coefficient throughout the test duration. It was interesting to note that hybrid nanolubricant (PAO+ZnO+IL) with or without dispersant PIBSA registered the lowest starting friction which remained lower throughout the test.

6.3.2. Surface characterization

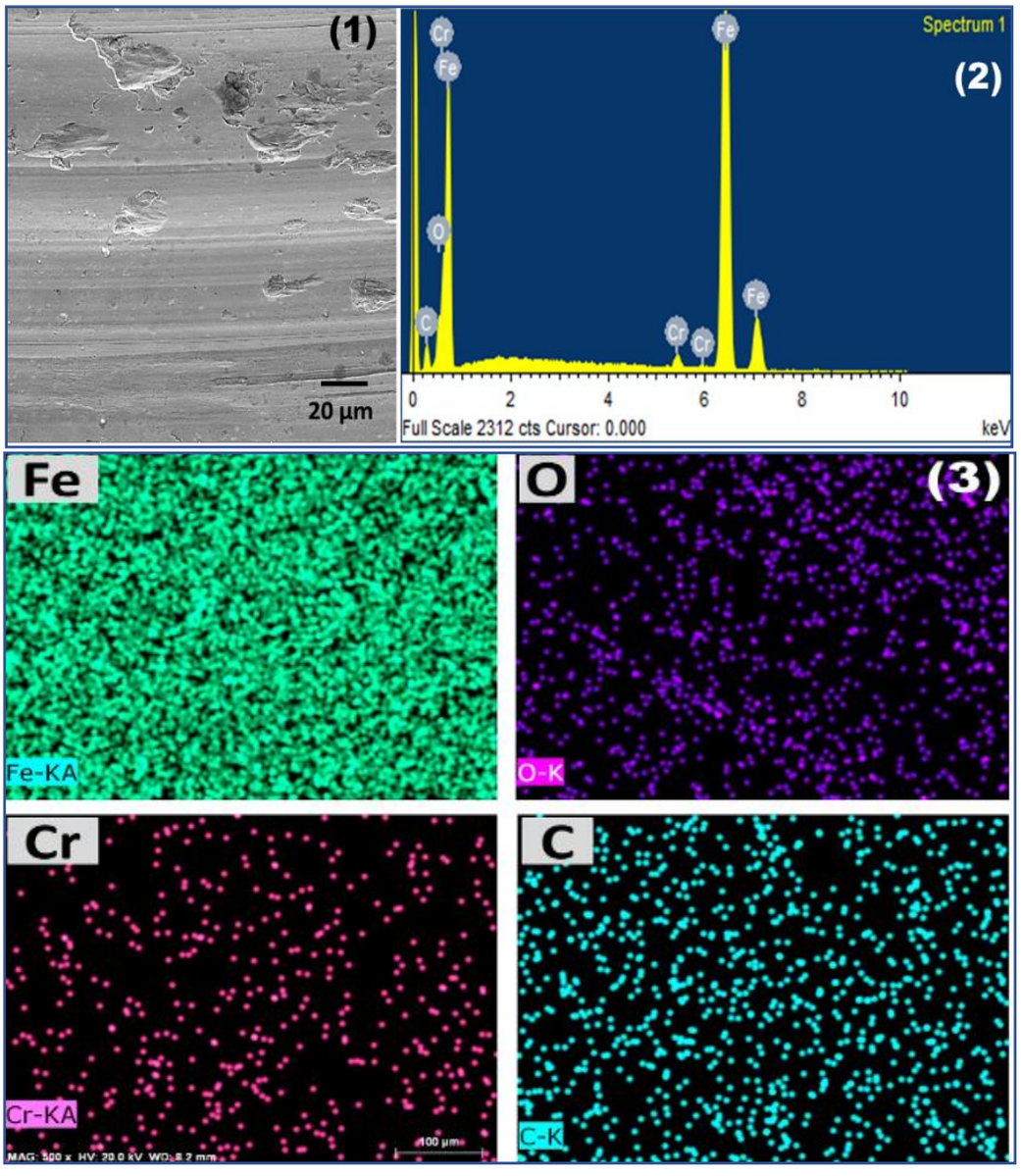

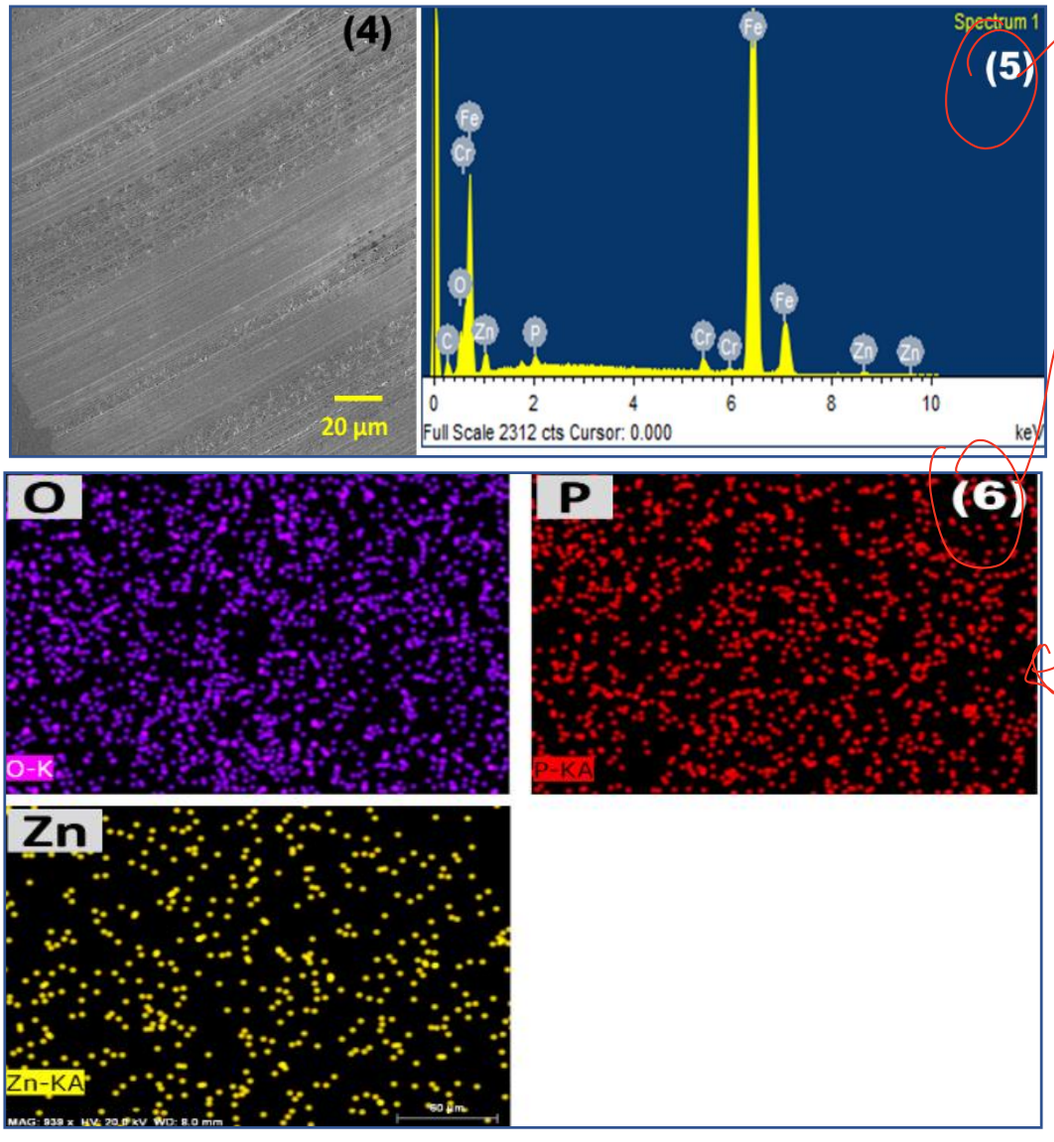

Figure 6.5 (1) SEM image of worn surface (2) EDS spectra (3) elemental mapping of worn surfaces lubricated with PAO base oil. (4) SEM image of worn surface (5) EDS spectra (6) elemental mapping of worn surfaces lubricated with hybrid nanolubricants (PAO+PIBSA+IL+ZnO). SEM images of worn surface lubricated with hybrid nanolubricant shows minor abrasive wear while in absence of any additive base oil shows deep pits inferring adhesive wear. EDS spectra and elemental mapping shows presence of Zn, and P throughout the worn surface inferring contribution of both additives (IL and NP) in tribofilm formation.

The SEM, EDS surface characterization techniques were employed to understand the morphology and elemental composition of worn surfaces. The SEM, EDS results along with elemental mapping of worn surface of base oil (PAO) and hybrid nanolubricant (PAO+PIBSA+IL+ZnO) are shown in figure 6.5. The worn surface lubricated with base oil shows deep grooves and furrows due to adhesive and abrasive wear as shown in Figure 6.5 (1). In boundary lubrication, rubbing surfaces are separated by extremely thin lubricants

(monolayer of lubricant molecules), adsorbed on the counter surfaces[122]. Under tribostress, these thin tribofilms are unable to prevent direct asperity contact resulting in abrasive and adhesive wear (plastic deformation). On the other hand, surface lubricated with hybrid nanolubricant shows minor abrasive wear while negligible adhesive wear. This could be attributed to excellent synergy in protective film formation by additive constituents of the hybrid nanolubricants. Figure 6.6 gives the optical image of worn surface lubricated with different formulations.

To further analyze the role of additives and the nature of the tribofilm EDS Spectroscopy was employed. EDS spectroscopy is a semi-quantitative elemental analytical technique, that scans a few micrometer depths and can give the elemental composition of the tribofilm. Worn surface lubricated with base oil shows Fe, O, C, Cr. Elemental O can be traced to oxidation (various oxides) of nascent steel surface due to progressive wear under boundary lubrication[146]. EDS spectra of worn surface lubricated with hybrid nanolubricant (PAO+PIBSA+IL+ZnO) shows peaks of P and Zn additionally, inferring both the additives contributed in the tribofilm. Since the steel balls after the tribotest were washed in Hexane to remove loosely adsorbed lubricant residues on the worn surface prior to surface characterization, the Zn elements of the worn surface are likely to be tribosintered under tribostress[64, 89, 130]. Tribosintering occurs when tiny NPs get trapped between rubbing surfaces and due to high stress get compacted and tribosintered resulting in protective film formation[64, 85, 130]. While elemental P found on the worn surface could be attributed to phosphate film (plausibly $FePO_4$) formed due to tribochemical reaction under tribostress. Initially due to inherent polarity Phosphonium phosphate ILs get adsorbed on the rubbing metallic surfaces resulting in weak film. Further, progressive wear breaks these weak films and direct asperity contacts lead to high thermomechanical stresses. Exposer to these high thermomechanical stresses propagates decomposition of ionic liquid and subsequent tribochemical reaction with rubbing surfaces resulting in relatively stronger tribofilm. Jun Qu et.al reported 200 nm thick phosphate-rich tribofilm formed on the substrate[148]. Similar phosphate film is also reported in literature for surfaces lubricated with lubricants composed of phosphonium phosphate ionic liquids[125, 144, 149, 150]. Tribological performance and surface analysis confirmed that both additives contributed to the formation of sacrificial protective tribofilm.

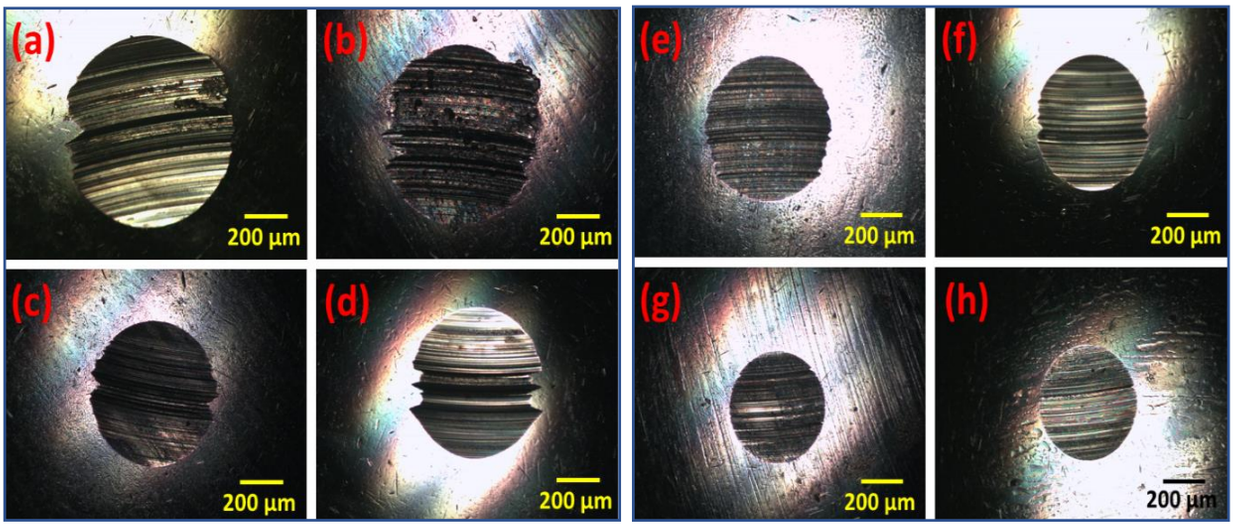

Figure 6.6 Optical images of worn surfaces lubricated with (a) PAO, (b) PAO+PIBSA, (c) PAO+ZnO, (d) PAO+PIBSA+ZnO, (e) PAO+IL, (f) PAO+PIBSA+IL, (g) PAO+IL+ZnO, (h) PAO+PIBSA+IL+ZnO.

The only published study exploring the interaction among IL, dispersant PIBSI, and friction modifier (ZDDP, MoDTC) have reported synergistic and antagonistic behavior[131]. They observed the reaction of PIBSI with aprotic ILs resulting in poor dispersion stability of MoDTC and depletion of ILs ability to form a protective film. While in this study no antagonistic tribological results were observed due to the addition of PIBSA in any of the lubricant formulations. Further, no precipitation or cloudiness was observed with the addition of PIBSA in lubricant formulation. It was interesting to note that the addition of dispersant PIBSA might have marginally improved the antifriction performance of base oil and ZnO nanolubricant apart from enhancing the dispersion stability of the base oil.

6.4. Important observation

Three-way interaction between phosphonium phosphate IL ([P66614][DEHP]), an oxide NP (ZnO), and a commercial dispersant (PIBSA) has been studied. Based on antifriction, antiwear performance, and surface characterization we conclude that PIBSA dispersant did not negatively affect the performance of base oil or any additive combination. No precipitation or cloudiness was observed, inferring plausibly no chemical reaction among IL, NP, and dispersant PIBSA during sample preparation or storage. Further strong synergy between IL and

NP was observed in friction and wear reduction which could be attributed to regenerative protective tribofilm formation composed of residues of both the lubricant additives. The outcome of the present study is not limited to engine oil formulation but any system of lubricant formulations composed of additives such as friction modifiers

Chapter – 7

To explore the potential of Boehmite and Zinctitanate NPs as lubricant additive and their synergistic effect with Ionic Liquids

Part 1: Potential of Boehmite as lubricant additive

7.1 General

It is estimated that lower viscosity lubricants can enhance the fuel economy of automotive vehicles by 5.5% due to the reduction in viscous losses[5]. But lower viscosity will change the lubrication regime towards elastohydrodynamic, mixed, and boundary lubrication, this may further increase direct asperity interactions between rubbing surfaces resulting in accelerated wear and subsequent lubricant failure. One method to achieve the low viscosity effective lubricant is by developing better antiwear (AW) and extreme pressure (EP) additives, compounds that form a protective film on the rubbing surfaces, decrease friction and increase load-carrying capacity. Formulated engine oils are currently dominated by Sulphur and Phosphorus based compounds such as Zinc dithiophosphates (ZDDP), organic phosphates, acid phosphates, organic Sulphur compounds, etc. which have biocompatibility issues and poison the catalytic converters[9]. In particular, ZDDP forms protective film through complex tribochemical reactions, subject to specific operating conditions such as elevated temperature and higher mechanical shear rate[143]. On the other hand, ZDDP may not perform better with non-ferrous tribopairs and coatings which are finding their increasing applications in modern mechanical systems[151]. This has led to the relentless pursuit of new biocompatible, green, and extremely efficient lubricant additives with an overall aim to increase fuel economy and emission reduction. Among various approaches to develop efficient additives, NPs have shown promising potential due to their inherent physicochemical properties.

This is impt. Perhaps include in intro.

The advantages of NPs are their nanometer size since they may interact with asperities of rubbing surfaces and may reduce friction and wear by mechanisms such as ball bearing, mending, polishing, and film formation. The other significant benefit of NPs over Sulphur and Phosphorus-based commercial antiwear additives is that NPs need not rely on tribochemical reactions which are system sensitive[64]. Several studies have revealed the potential of NPs in reducing surface wear, friction coefficient, and enhancing EP performance as discussed in chapter 2.

One of the unique categories of NPs as a lubricant additive could be hydroxide minerals (Talc, Serpentine, and Boehmite). The natural and synthetic Serpentine minerals also known as Magnesium Silicate Hydroxide ($Mg_3Si_2O_5(OH)_4$) have been explored as a lubricant additive by several researchers[91, 92, 94–96, 152, 153]. Chang et al. explored synthetic Serpentine

NPs in PAO base oil and observed excellent wear reduction (≈30-45%)[91, 92]. They also concluded stronger tribofilm rich in Mg, Si, O was formed due to the pressure-dependent decomposition of Serpentine particles. Wang et al. explored Serpentine NPs having different morphology for their tribological properties and observed tubular crystal structure registering the highest antiwear performance among others[94]. Helong Yu et al. dispersed 1 μm sized natural Serpentine particles in the mineral base and claimed the formation of 500-600nm thick porous tribofilm composed of Fe_3O_4, FeSi, AlFe, SiO_2, and Fe_3C compounds. Talc is another silicate mineral consisting of Silicon, Magnesium, Hydrogen, and Oxygen with some metallic impurities. A couple of studies have explored Talc as a lubricant additive and claimed excellent friction and wear reduction properties due to the formation of SiO_x and MgO compounds on the worn surface[98, 99].

On the other hand, Boehmite (γ-AlOOH) which checks many desirable brackets i.e., green, biocompatible, and eco-friendly mineral has not been explored for its tribological properties. Boehmite also called Aluminium oxide hydroxide mineral, one of the common constituents of Aluminium ore bauxite is stable and if heated above $450^{O}C$ leads to dehydration of its crystals ($2AlOOH \Longrightarrow Al_2O_3+H_2O$) and formation of Aluminium oxide (Al_2O_3)[36,37]. It has a lamellar (orthorhombic) structure and in every layer, the O atom has closed (cubic) packing while OH groups are on the surface making the overall structure loosely packed[38]. Due to its extremely low toxicity, biocompatibility, eco-friendliness, and low cost, Boehmite has found application in various fields such as photocatalysis, antimicrobial activity, determination of toxic metals, flame retardation, etc[101, 103–106]. Boehmite material has some inherent advantages such as lower molecular weight (59.988 g/mole), lower density ($3g/cm^3$), and lower Mohs scale hardness (3.5), making it a promising candidate for lubricant additive. Lei Zhang et al. covalently synthesized hybrid material consisting of Graphene oxide, Boehmite, and 3-glycidoxypropyl-trimethoxysilane (GO-GPTS-AlOOH) to enhance the dispersion stability of Graphene oxide in lubricating oil[154]. they claimed that the improved friction and wear reduction was due to the excellent strength of the lamellar Graphene sheet, while no detail was given regarding the role of Boehmite grafted particles in friction and wear reduction. To the best of our knowledge, this is the first study exploring the potential of Boehmite NPs as a lubricant additive. This novel study explores the effect of Boehmite NPs on viscosity index, density, surface wear, friction coefficient, and EP properties of the PAO base oil. This study also explores the colloidal stability and mechanism of tribofilm formation of Boehmite NPs.

7.2. Materials and Methods

7.2.1. Materials and lubricants formulation

The Boehmite (γ-AlOOH) NPs with APS (Average Particle Size) 20 nm were obtained from Sisco Research Laboratories Pvt. Ltd. (Molecular weight 59.99, CAS no 1318-23-6, product code 21772). Polyalphaolefins (PAO-6) base oil having viscosity 6 cst at $100^{O}C$ was obtained from Synthomax India and was used as received. Generally, NPs in the non-polar base oil are known to have poor long-term colloidal stability. To enhance the colloidal stability of NPs in PAO a dispersant PIBSA (Univenture Industries Pvt. Ltd. India) at 1 wt% fixed concentration was added in all the formulated nanolubricants. A two-step method was used to decrease the initial agglomeration of NPs as reported in the literature[89, 99]. In the first step, a measured quantity of NPs was added in Acetone and stirred for 20 minutes (1000 rev/min) followed by sonicating for 30 minutes (make Dakshin Ultrasound, 20 kHz frequency, 190 W power, operating in a pulsed mode of 1 second off and 2 seconds on). In the second step, the sample was added into PAO and was kept on a hot plate for 5 hours, maintained at $65^{o}C$ to evaporate Acetone while continuously stirring the sample. Boehmite NPs were dispersed in 0.25, 0.5, 0.75, and 1wt% concentration in PAO base oil. Table 7.1 gives the concentrations of each constituent in the formulated lubricants and their respective coding.

Table 7.1 Nanolubricants formulation and their coding used in this study

Sr. No	OILs	NPs concentration (wt%)	code
1	PAO (group IV synthetic base oil)	0	**P**
2	PAO+ 1wt% PIBSA (dispersant)	0	**P_d**
3	PAO+ 1wt% PIBSA + NPs	0.25	**$P_{0.25}$**
4		0.5	**$P_{0.5}$**
5		0.75	**$P_{0.75}$**
6		1	**P_1**

7.2.2. Characterization of Boehmite nanoparticles.

The FE-SEM (JSM-7800F, JEOL, Japan) micrograph shows spherical/quasi-spherical morphology of Boehmite NPs as shown in figure 7.1(a). FTIR measures the discrete vibrational frequencies emitted by thermally excited molecules and can help in identifying bonds and individual groups of the molecule. Figure 7.1(b) shows the FTIR spectra (Shimadzu 8400S) of Boehmite NPs with peaks at 3292, 3091, 2095, 1974, 1642, 1384, 1156, 1073, 747, 623, 482 cm^{-1} and are in accordance with earlier reported studies and detailed bond structure can be

found elsewhere[155–157]. Figure 7.1(c) shows the XRD patterns (Bruker D8 Advance) of the Boehmite NPs used in this study. The peaks are in agreement with Joint Committee on Powder Diffraction Standards card number (JCPDS 00-021-1307) and show no other crystalline peak than Boehmite NPs, confirming the purity of Boehmite[155–158]. The FWHM (full width half maximum) value of crystallite 031 diffraction was used in the Scherrer equation to calculate crystallite sizes of Boehmite NPs and the estimated crystallite size was 9nm. XRD peaks confirm the orthorhombic crystal structure of Boehmite NPs as reported in earlier studies.

show fit?

Also scherrer formula?

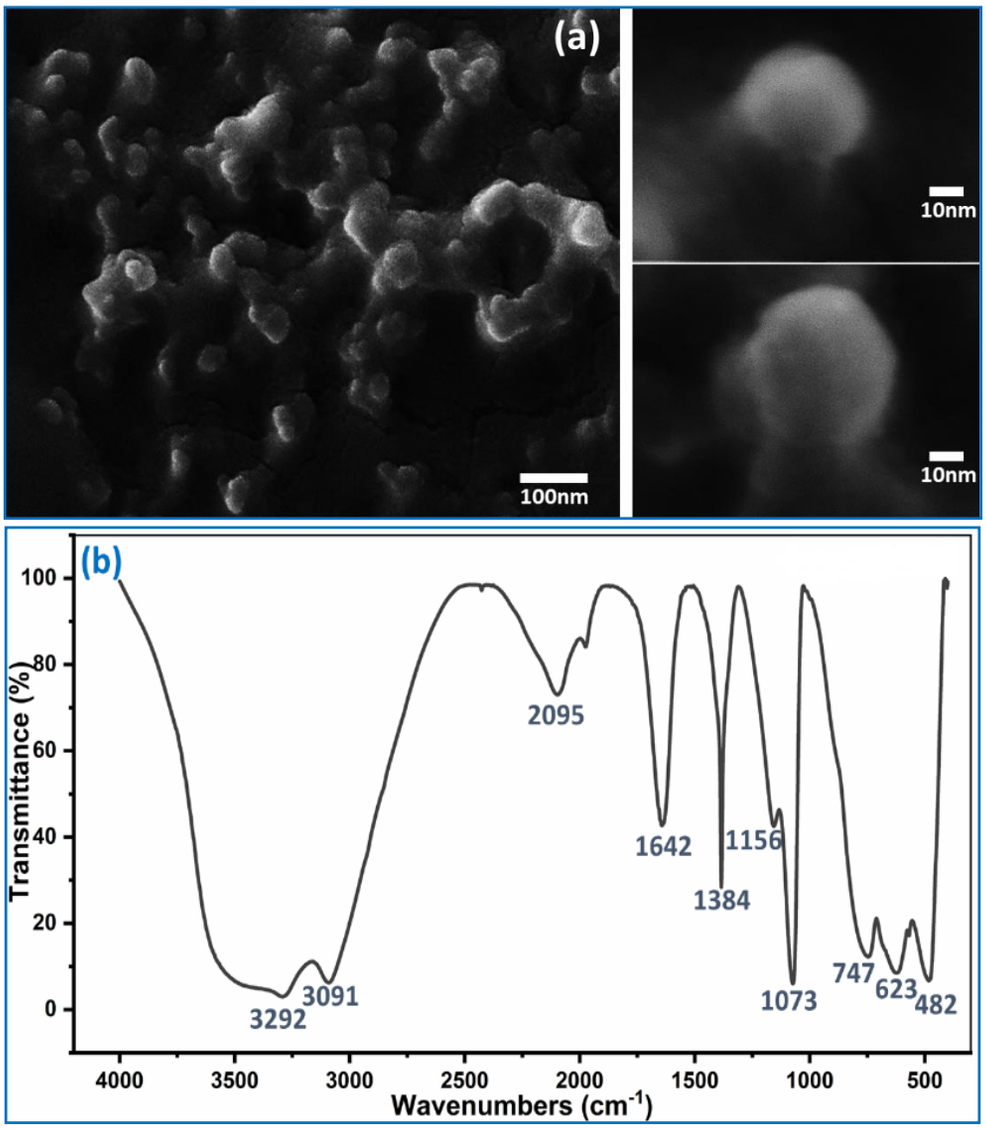

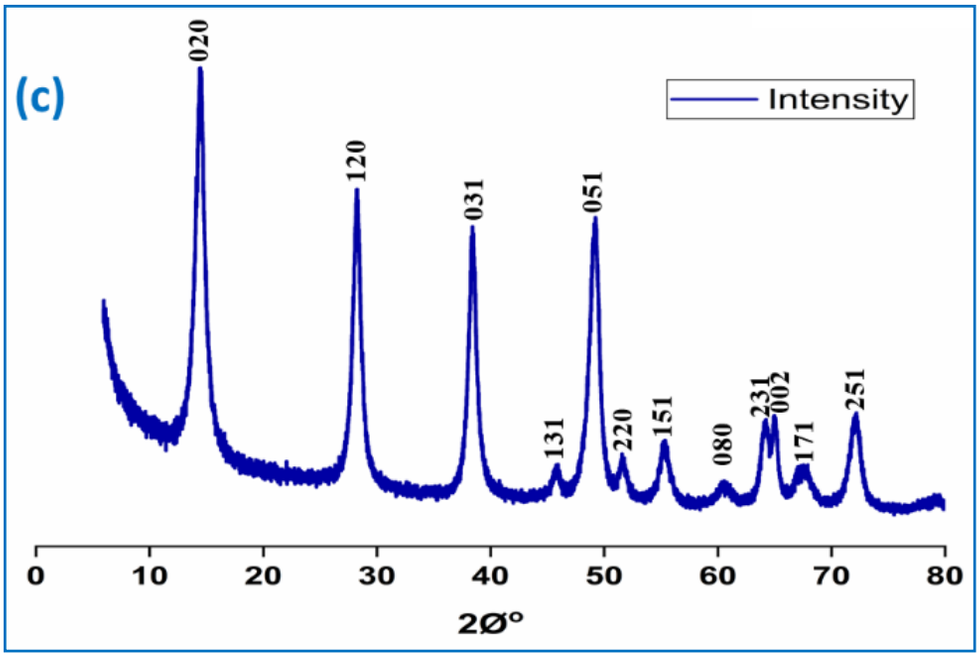

Figure 7.1 (a) FE-SEM micrograph (b) FTIR spectrum (c) XRD spectrum of Boehmite nanoparticles

7.2.3. Tribological and Extreme Pressure (EP) testing

The tribometer (make DuCom Instruments), used in this study consists of four steel balls (material AISI-52100, diameter 12.7mm) arranged in the equilateral tetrahedron configuration. The detailed description of the tribometer is discussed in chapter 3. To enhance reliability average friction and wear of three tests were considered for data representation. The antiwear tests were performed following ASTM 4172 standard which includes 1200 rpm speed, 392 N load, 75^{O}C temperature, and test duration of 60 minutes. The extreme pressure (EP) tests were performed following IP 239 test standards which include 1450 rpm speed, room temperature, test duration of 60 seconds, and progressive loading till seizure.

7.2.4. Surface characterization

An optical microscope (HUVITZ LUSIS HC-30MU) was used for the comparative study of surfaces lubricated with different formulated lubricants. A scanning electron microscope (SEM) (make JEOL, JSM-7800F, Japan) was used to study the wear scar morphology. An EDS (energy-dispersive X-ray spectroscopy) of Bruker corps coupled with SEM was employed to explore the elemental constituents of the protective film formed on the surfaces. To remove any lubricant residues steel balls after tests were washed in hexane prior to surface characterization. Furthermore, to understand the nature of the tribofilm and the role of Boehmite NPs in tribofilm formation, Raman spectroscopy was employed (Renishaw InVia

Raman with 10mW laser powered and 532 nm excitation wavelength). X-ray photoelectron spectroscopy (Thermo Fisher Scientific Instruments, K ALPHA+) with monochromatic radiation of Al Kα (beam current 6 mA, 1486.7 eV) and pass energy of 150 eV on 200 μm spot size was used to analyze the chemical state of the tribofilm. The core-level spectrum of Fe 2p, Al 2p, and O 1s was acquired using 30 eV pass energy.

7.3 Results and Discussions

7.3.1. Dispersion stability

The colloidal stability of NPs depends on various factors such as physicochemical characteristics of NPs, base oil, and dispersion method. Varying degree of NP dispersion stability has been reported in the literature with as low as 2 days to a few months[79, 80, 99]. Visual inspection is one of the methods used to study the dispersion stability of the Boehmite NPs in the PAO base oil. Figure 7.2 shows the dispersion stability of the best performing lubricant sample ($P_{0.5}$) over time. Photographs were taken every day without any disturbance to the sample while in storage. Figure 7.2 shows negligible sedimentation for the Boehmite NPs for the first 30 days. In around 45 days, the nanolubricant showed some sign of sedimentation visible at the top of the container, but a majority of NPs were still dispersed. On the other hand, very few NPs were still dispersed around 60 days while the majority were settled at the bottom of the container. Excellent colloidal stability of Boehmite NPs could be attributed to the lower agglomeration, larger surface area, lower density, and of course dispersant PIBSA. In around 75 days, almost all the NPs were settled.

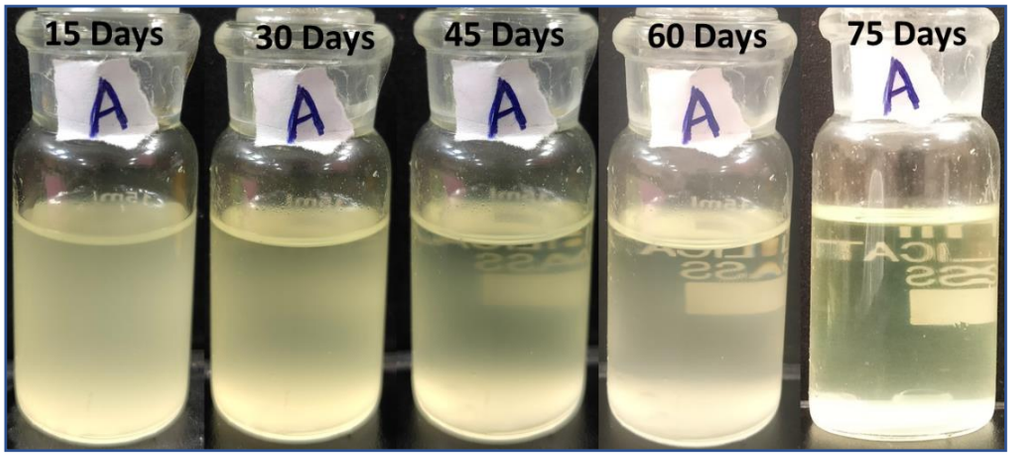

Figure 7.2 Photographs of formulated nanolubricants ($P_{0.5}$) over time

Table 7.2 Average size distribution of Boehmite NPs

Size distribution of NPs over time					
Time (days)	0	20	40	60	75
Avg size (d.nm)	77	87	113	168	Settled

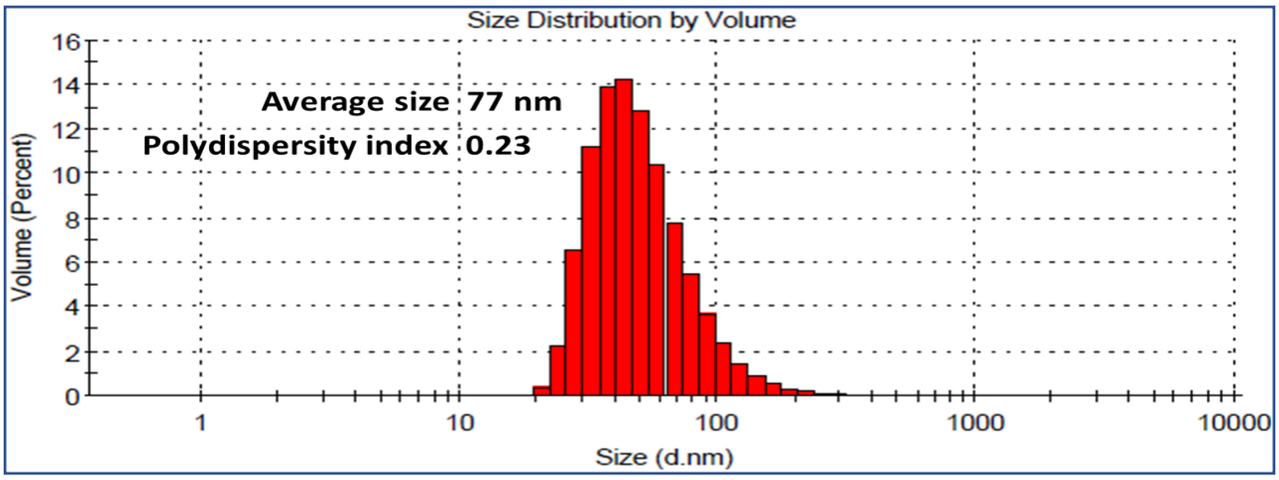

Figure 7.3 Dynamic Light Scattering (DLS), size distribution of nanoparticles (0 days)

Stable dispersion is obtained when Brownian motion due to thermal agitation overcomes the attractive forces among colloidal NPs[66]. Agglomeration of NPs can increase its average particle size which may accelerate the rate of sedimentation several folds. To study the agglomeration of NPs over time, dynamic light scattering (Zetasizer nano 590 Malvern Instruments UK) was employed. Formulated nanolubricant ($P_{0.5}$) was too thick to be directly used for DLS analysis hence it was diluted with petroleum ether in the weight ratio of 6:4. For dilution, prepared nanolubricants were stored without any disturbance in separate containers, and just before the DLS study, a sample was taken out on a stipulated day from the top of the container. Extreme care was taken to not to disturb the settled NPs of the container while taking out samples for the DLS study. DLS analysis gave 77 nm average size of NPs (figure 7.3) just after lubricant formulation inferring some degree (≈4 times) of initial agglomeration since as per supplier, APS of Boehmite NPs was 20nm. DLS analysis cannot give the whole picture for the stability of colloidal NPs on its own, because it only gives the average particle size dispersed after a period without considering settled NPs at the bottom of the container. Hence both methods of visual inspection and DLS analysis should take into perspective while studying the stability of Boehmite NPs. Table 7.2 shows agglomeration started at the time of lubricant preparation and was relatively lower initially. After one month, a clear trend was observed for a rapid increase in the average size of dispersed NPs over time. This could be the reason for

accelerated sedimentation after a month of lubricant formulation as can be seen by visual inspection.

7.3.2.Effect on Viscosity

Stabinger viscometer (SVM 3000) following ASTM D7042 standards was used to measure kinematic viscosity and density of the lubricants. The viscometer works on the Couette principle, and the measurement of kinematic viscosity and density is based on torque and speed measurement. The other important parameter for lubricant is viscosity index (VI), which is a unitless number indicating the temperature dependence of lubricant's kinematic viscosity. The viscosity index was calculated according to ASTM D-2270 in which the viscosity of the prepared sample at 40^{O}C and 100^{O}C is compared with standard reference oil having 0 (naphthenic base oil) and 100 (paraffinic base oil) viscosity index[6]. The higher the viscosity index, the more stable the oil is with respect to changes in temperature.

Table 7.3 shows the kinematic viscosity, and density values obtained from the viscometer. PIBSA dispersant improved the viscosity marginally (0.32 and 0.34%) at 40^{O}C and 100^{O}C. Interestingly, at elevated temperature(100^{O}C), 1wt% Boehmite concentration improved viscosity by 4.56%, which was notably higher than the viscosity increase of 3.75% at 40^{O}C. This could be attributed to the thinning effect of PAO due to an increase in temperature while NPs remained indifferent. A similar trend was also observed for VI improvement and the highest improvement of 4.35% was observed for 1% Boehmite concentration (P_1). The density of the nanolubricants increased gradually with the addition of NPs which can be attributed to the higher density of Boehmite mineral.

Table 7.3 Effect of Boehmite NPs concentration on viscosity and density

Sr. No	Viscosity (cSt) and changes at 40 and 100^0C				Viscosity Index (VI)	Density at 29.5^0C (g/cm^3)
	Kinematic viscosity @40^0C	% change	Kinematic viscosity @ 100^0C	%change		
P	30.92	----	5.92	----	139.20	0.8187
P_d	31.02	0.32	5.94	0.34	139.56	0.8192
$P_{0.25}$	31.22	0.97	6.02	1.69	142.45	0.8225
$P_{0.5}$	31.51	1.91	6.09	2.89	144.11	0.8241
$P_{0.75}$	31.76	2.72	6.14	3.74	144.95	0.8249
P_1	32.08	3.75	6.19	4.56	145.25	0.8261

7.3.3. Tribological performance of lubricants

In four-ball tribometer balls are arranged in a tetrahedral geometry, resulting in three-point contacts between the top rotating ball and bottom 3 fixed balls. These non-conformal point contacts under applied load exert high stress on rubbing surfaces, which results in severe wear or seizure in case of lubricant failure. Figure 7.4(a) shows the average WSD performance for samples tested at ASTM 4172 test standards. Base oil has managed to separate the direct contact between rubbing surfaces but performed poorly with the highest WSD. All the concentrations of Boehmite NPs tested in this study improved the friction and wear performances over the base oil. $P_{0.25}$ nanolubricant showed significant enhancement in wear reduction (19%) and the highest wear reduction was observed for $P_{0.5}$ (24%) over the base oil. On the other hand, no improvement was observed on further increase in NPs concentration as $P_{0.75}$ showed a 16% reduction. In contrast, a 1 wt% concentration of NPs degraded the base oil performance and gave wear reduction of just 11%. Figure 7.4(b) shows the friction coefficient of the nanolubricants and $P_{0.25}$ and $P_{0.5}$ showed the highest improvement of ≈15% while the least improvement of 7% was observed for P_1. The optimum concentration for friction and wear reduction was observed to be in the range of 0.25 – 0.5 wt % concentration beyond that performance did not improve. Surprisingly base oil, similar to that of $P_{0.25}$ gave low initial friction as shown in figure 7.4(c). But after around 500 seconds of initial operation friction coefficient started ascending due to the inability of base oil to provide effective surface protection resulting in increased asperity contacts. While Boehmite nanolubricants provided better surface protection, reduced asperity contacts resulted in a lower friction coefficient. Optical images of worn surface lubricated with formulated lubricants are shown in Figure 7.5.

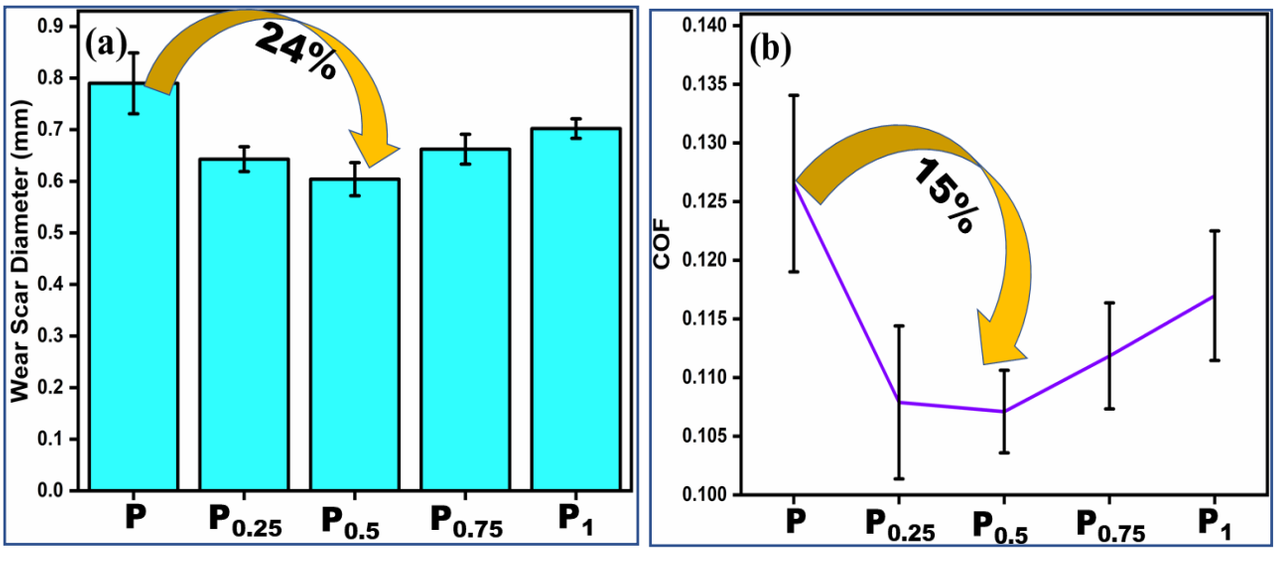

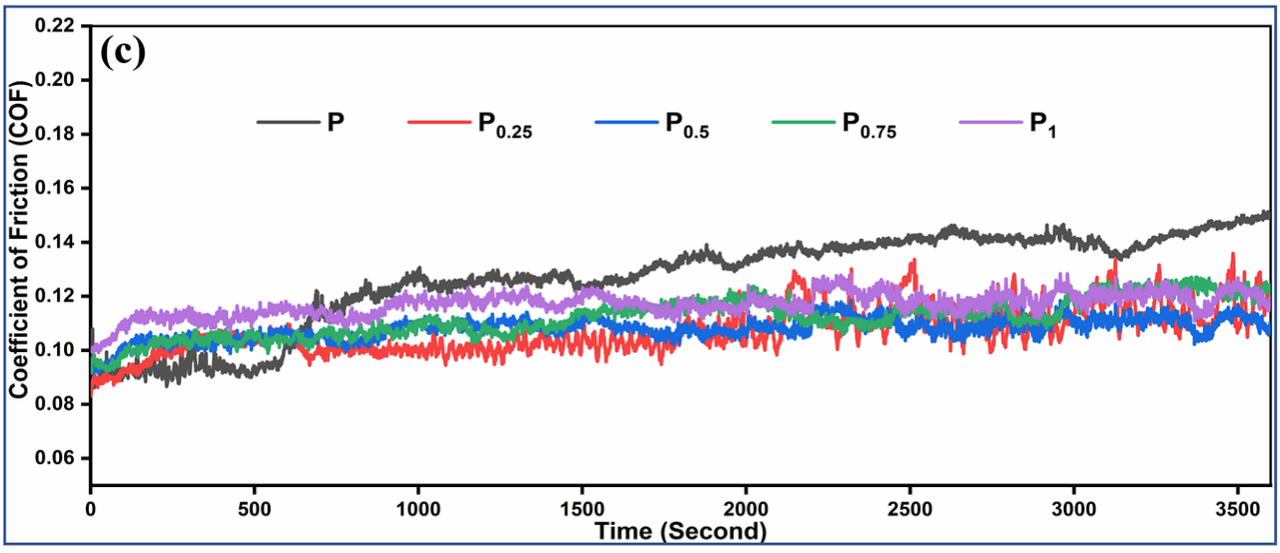

Figure 7.4 Performance of nanolubricants tested following ASTM 4172 standards (a) Average WSD (b) Average COF (c) Friction coefficient over test duration (60 minutes). Boehmite nanolubricant provided better surface protection, reduced asperity contacts as evident from reduced friction and wear.

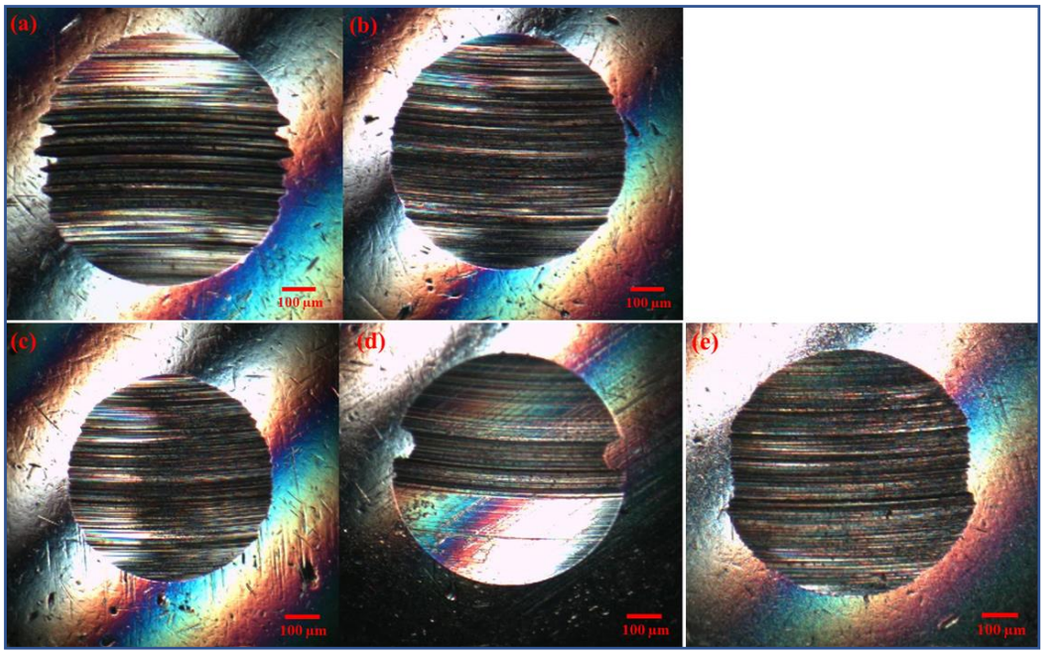

Figure 7.5 WSD of the surfaces lubricated with (a) P (b) $P_{0.25}$ (c) $P_{0.5}$ (d) $P_{0.75}$ (e) P_1

Figure 7.6 shows the SEM (Scanning Electron Microscope) micrographs of worn surfaces. Worn surface lubricated with PAO base oil i.e. figure 7.6(a) shows tiny pits, and deep long grooves, which could be attributed to adhesive and abrasive wear respectively. Abrasive wear occurs when harder asperity digs into the opposite surface and may produce grooves (micro-cutting/plowing) while direct asperity contact under tribostress causes localized bonding which removes a chunk of materials due to subsequent sliding resulting adhesive wear.

For worn surface lubricated with Boehmite nanolubricants i.e. figure 7.6(c) shows narrow groves and negligible pits, this could be attributed to minor abrasive wear and negligible adhesive wear due to reduced asperity contacts and better surface protection provided by Boehmite NPs.

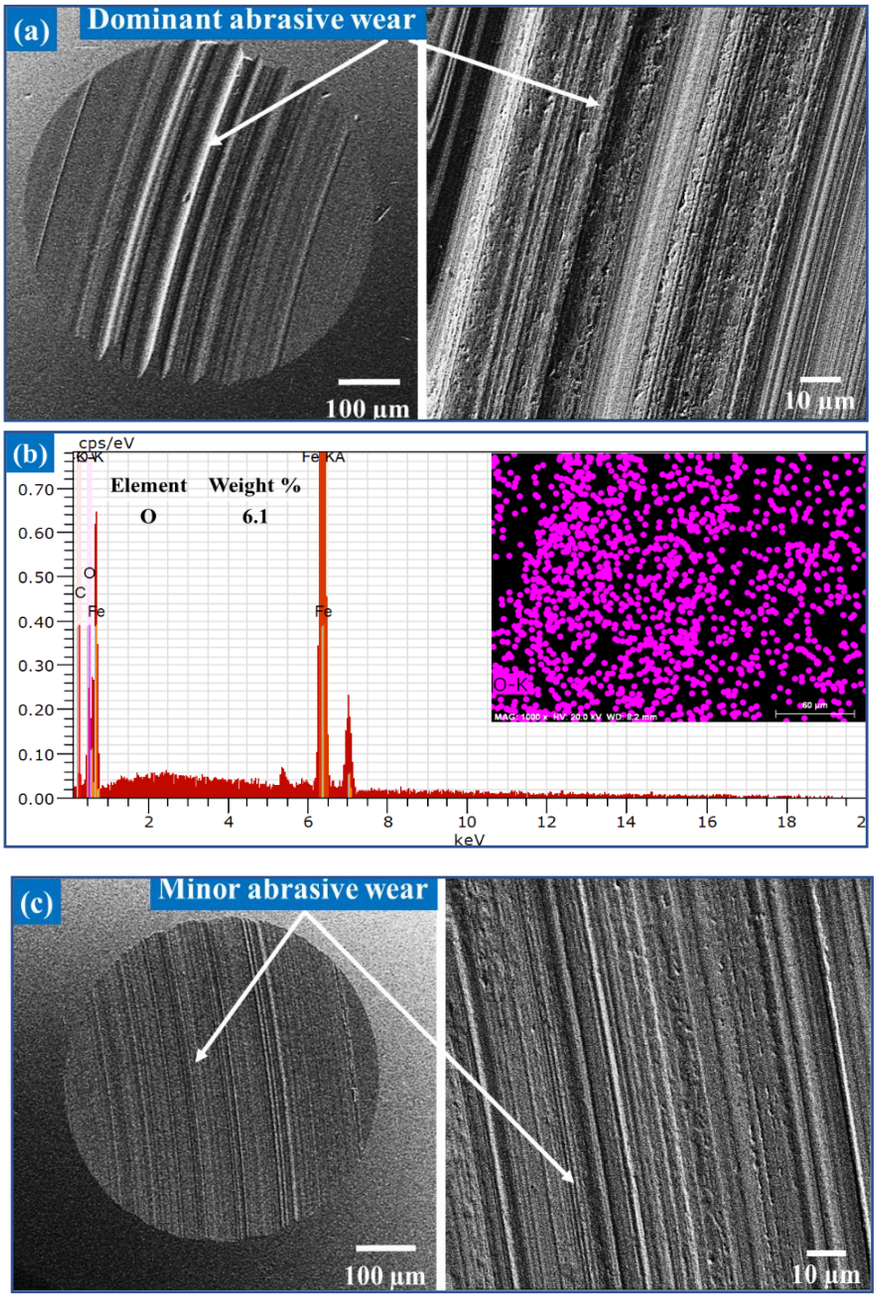

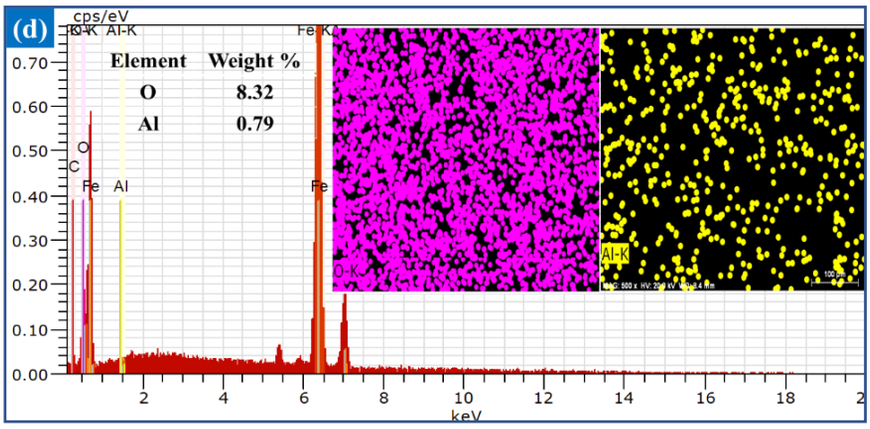

Figure 7.6 (a) WSD of surface lubricated with P (b) EDS analysis of surface lubricated with P (c) WSD of surface lubricated with $P_{0.5}$ (d) EDS analysis of surface lubricated with $P_{0.5}$. Reduced grooves and pits of worn surface lubricated with Boehmite nanolubricants could be attributed to reduced asperity contact and enhanced surface protection due to tribosintered NPs.

To explore the nature of tribofilm EDS Spectroscopy was employed. EDS is a semi-quantitative technique and elemental composition obtained from EDS can be used effectively for comparative worn surface analysis. Figure 7.6(b) shows the full EDS spectrum of the worn surface lubricated with PAO base oil with atomic weight concentration of Fe, O, Cr, C and elemental mapping of O. The spectrum shows the presence of oxygen (6.1%) on the worn surface which may have been induced due to oxidation of nascent steel surface formed during rubbing even in lubricated condition. It is well established that Oxygen forms porous hard tribofilm consisting of various Iron oxides (FeO, Fe_2O_3) on the worn surface via chemical reaction ($2Fe+O_2 \Longrightarrow FeO$ and $4Fe+3O_2 \Longrightarrow Fe_2O_3$)[33,50]. Figure 7.6(d) gives the EDS spectrum of worn surface lubricated with $P_{0.5}$ along with concentration and mapping of elemental Oxygen and Aluminium. Ideally, lower wear exposes less nascent steel surface to oxidation but despite having lower wear, EDS shows a higher concentration of elemental Oxygen on the worn surface lubricated with Boehmite nanolubricants. One plausible explanation could be the dehydration of Boehmite NPs under tribostress, a similar phenomenon was reported for other hydroxide NPs (Serpentine and Talc)[91, 97–99].

Four mechanisms i.e. ball bearing, mending, polishing, and tribofilm formation have been reported in the literature for enhancing tribological properties. Among these two are due to direct action of NPs (ball bearing and tribofilm formation) while mending and polishing effects are due to secondary surface enhancement[64]. However, the occurrence of these mechanisms is subject to discussion in various studies. Quasi-spherical and spherical NPs generally acts as nano-sized ball bearing, rolls between rubbing surface, and may convert

sliding contact friction to sliding-rolling friction. While the protective film is formed due to tribochemical reaction or tribosintering of NP additives on the rubbing surfaces under tribostress. For excellent surface protection, the self-replenishment rate (tribofilm formation) should be higher than the wear rate of rubbing surfaces under boundary lubrication. In the mending effect, NPs occupy cracks and grooves of worn surfaces resulting in a smoother surface and overall reduced friction and wear. In the polishing effect, harder NPs under stress deforms the asperities of the rubbing surfaces resulting in a smoother surface. The elemental Al (0.79%) of the worn surface could plausibly be attributed to predominantly tribosintered NPs since bearing, polishing, and mending effects provide weaker tribofilm and may not have left any residues since balls were washed in hexane before surface characterization.

7.3.4.Extreme Pressure (EP) properties.

EP tests were conducted following the IP 239 test standards and nanolubricants performance is shown in figure 7.7(a). Base oil failed at 125 kg and the reduced load of 115kg as well, making 100 kg the maximum non-seizure load. Due to nonconformal point contact and higher load, the top layer of the balls is removed several times before complete failure of the lubricant i.e. seizure, within 60 seconds of test duration. The $P_{0.25}$ showed significant improvement (25%) in EP performance over the base oil but further concentration increase (0.5 wt%) showed no increase in load-carrying capacity. It is interesting to note that at ASTM D 4172 wear test condition beyond 0.5% concentration performance of friction and wear deteriorated while in EP tests the increased concentration to 1 wt% ($P_{0.75}$ and P_1) has increased load carrying capacity by 40%. This may be due to a shorter test span and relatively higher load index in EP tests and higher NPs concentration may increase the availability of NPs between asperities for tribofilm repair. Moreover, the high concentration of Boehmite NPs can also occupy intermediate space between asperities and directly support the load.

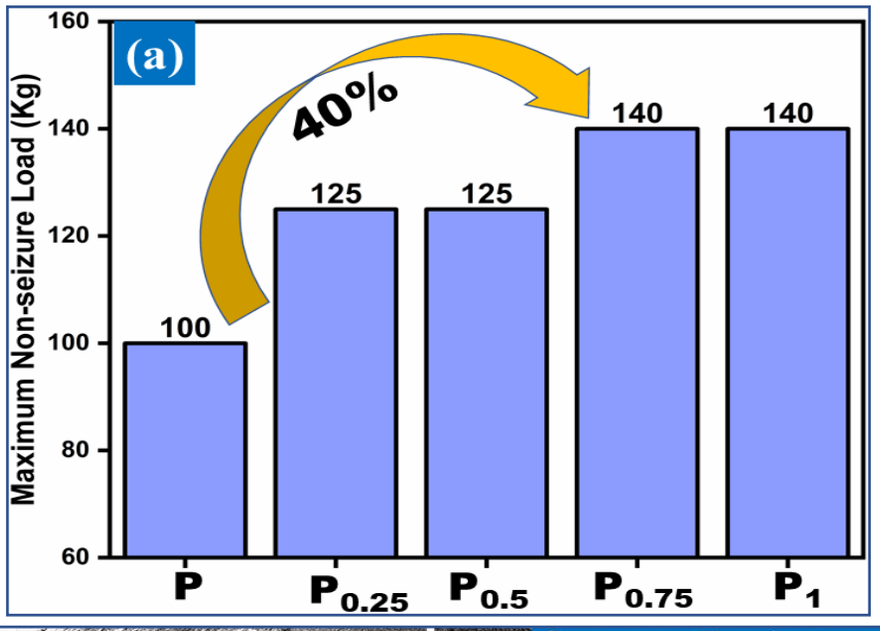
(a)
Maximum Non-seizure Load (Kg)
160
140
120
100
80
60
40%
100
125
125
140
140
P
P0.25
P0.5
P0.75
P1

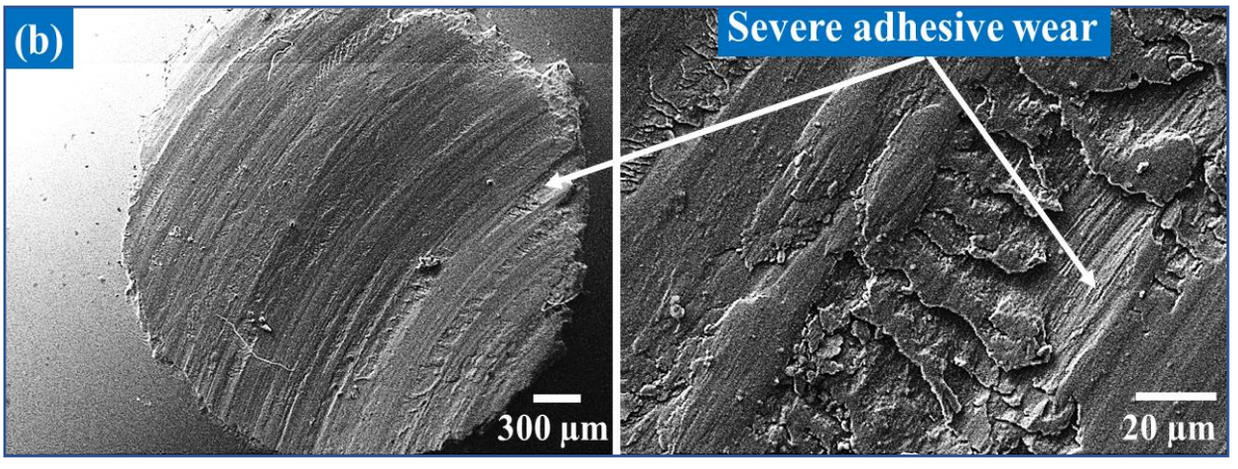
(b)
Severe adhesive wear
300 µm
20 µm

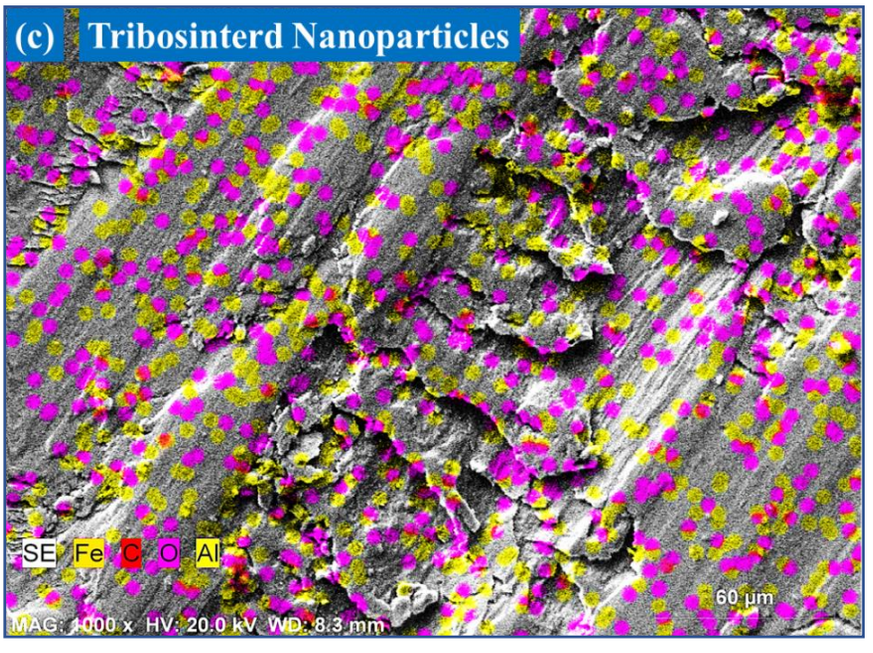
(c)
Tribosinterd Nanoparticles
SE Fe C O Al
60 µm
MAG: 1000 x HV: 20.0 kV WD: 8.3 mm

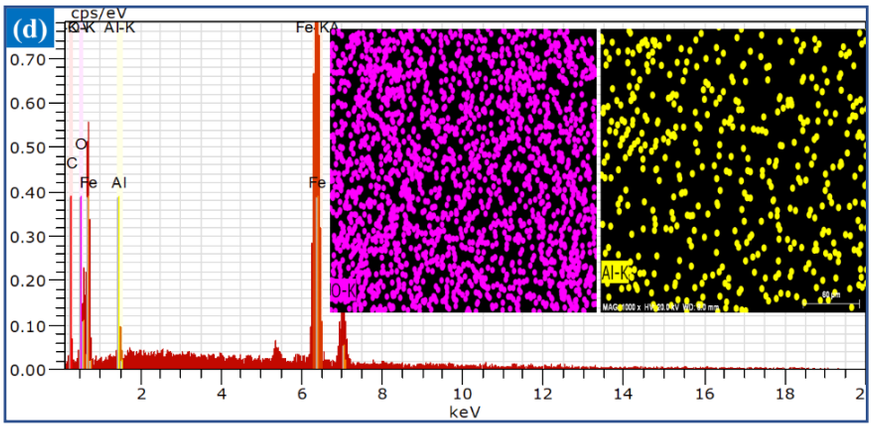

Figure 7.7 (a) EP (Extreme Pressure) performance (b) SEM micrograph of pre-weld ball lubricated with P_1 (c) Elemental mapping of pre-weld surface lubricated with P_1 (d) EDS analysis of pre-weld ball lubricated with P_1

Figure 7.7(b) shows the SEM micrograph of the pre-weld worn surface lubricated with P_1 nanolubricant. At extreme load, a significant proportion of lubricant is squeezed out of contact points and fails to form stable lubricant film resulting in relatively higher direct asperity contacts. This is obvious from the dominant adhesive wear of the pre-weld surface tested for extreme pressure properties. Figure 7.7(c) shows the elemental mapping of the active elements Al and O distributed on the worn surface. Figure 7.7(d) shows the complete EDS spectrum of the pre-weld surface.

7.3.5.Raman spectroscopy

EDS spectroscopy shows, the tribofilm formed on the worn surface is composed of a significant proportion of Al elements. To further investigate the nature of the Al elements of the tribofilm, i.e. whether it is in the Boehmite phase or dehydrated ($2AlOOH \Longrightarrow Al_2O_3+H_2O$) into Aluminium oxide ($Al_2O_3$) under tribostress, Raman spectroscopy was employed. Raman spectrum of the Boehmite nano-powder is shown in figure 7.8(b) giving active peaks at 363, 448, 494, 679, and 732 cm^{-1} in accordance with the earlier reported studies[158–160]. These peaks could be attributed to hydroxyl transmission mode and strong peak intensity at 363 cm^{-1} may be associated with Al ion coordinated by 6 O atoms. Raman spectrum of wear-tested and pre-weld worn surfaces are shown in figure 7.8(a). Pre-weld worn surface shows two Raman peaks at 360 and 496 cm^{-1} which could be attributed to the trapped boehmite NPs in the large pits/grooves due to severe adhesive wear (plastic deformation). In contrast, no distinguishable Boehmite peak was observed for the wear-tested surface. On the other hand, the wear-tested surface shows a large peak at 650-660 $cm^{-1,}$ which could be attributed to oxide film primarily composed of γ-FeOOH and α-Fe_2O_3 due to exposure to elevated temperature (>75^{O}C) for

longer test duration (3600 seconds) and relatively lower wear[161–163]. While the same peak was not visible for pre-weld surface plausibly due to shorter test duration (60 seconds) and progressive removal of the top layer due to severe adhesive wear. It was also interesting to note that, no distinguishable Aluminium oxide peaks (as per literature 375, 417, 432, 450, 578, 642, 751 cm^{-1}) were observed in the Raman spectrum of both the surfaces[164]. No distinguishable characteristic peaks of Boehmite and aluminium oxide could be due to various factors affecting peak intensities of the Raman spectrum such as low NPs concentration, strong fluorescent background, and detector noise.

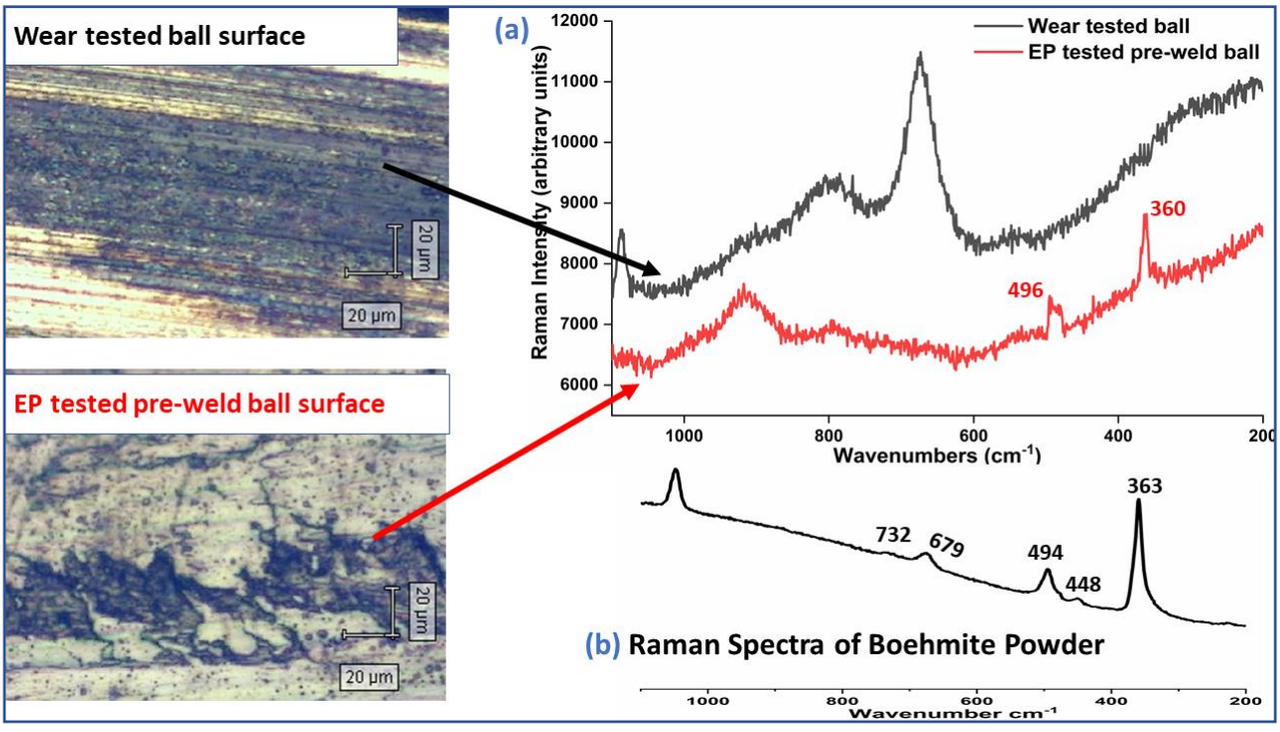

Figure 7.8 Raman spectrum of (a) Wear and EP tested ball (b) Boehmite nanoparticles

7.3.6. XPS analysis

X-ray photoelectron spectroscopy (XPS) was employed to further probe the triboactive elements i.e. Fe, O, Al to understand the chemical state and nature of the tribofilm. XPS scans a few atomic layer (1 to 5 nm) depths of the worn surface and may help in analyzing the chemical state of the elements[135]. Figure 7.9 shows the core level XPS spectrum of Fe 2p, O 1s, and Al 2p of the worn surface lubricated with $P_{0.5}$. XPS spectrum of Fe 2p shows two dominant peaks at binding energies of ≈710.8 eV and ≈724.5 eV which in association with O 1s peak of ≈530.1 eV could be attributed to Fe-O bonds i.e. Fe_2O_3 respectively[55, 133, 150]. Further XPS spectrum of Al 2p peak at ≈74.0 eV could most likely be attributed to Al_2O_3, but

a small chemical shift of binding energies among oxides (Al_2O_3), and oxyhydroxides (AlOOH) makes unambiguous distinction practically impossible[165–167]. A chemical shift occurs due to changes in the field of core electron's electrostatic potential and coordination (e.g. octahedra vs tetrahedral), Oxidation number, and ligand types[165]. Al 2p chemical shift binding energies are in the range of 0.2-0.5 eV among oxide, hydroxide, and oxyhydroxides which are nearly equal to that of XPS instruments precision, making accurate detection impossible[165, 167]. But O 1s peak inherits a larger chemical shift and could be used to identify the crystal structure of oxygen and hydroxyl groups[165]. The XPS spectrum of O 1s shows a peak at ≈530.9 eV, which could be attributed to the Oxygen of Al_2O_3 crystal while no distinct peak of Boehmite (OH bond, ≈532.2 eV) was observed, inferring elemental Al on the worn surface should be Al_2O_3[165]. Based on the surface characterization of worn surfaces lubricated with Boehmite NPs, we propose that just like Talc (dehydration temperature above 800°C) and Serpentine (dehydration temperature around 700°C), Boehmite mineral dehydrated under tribostress[91, 97, 99].

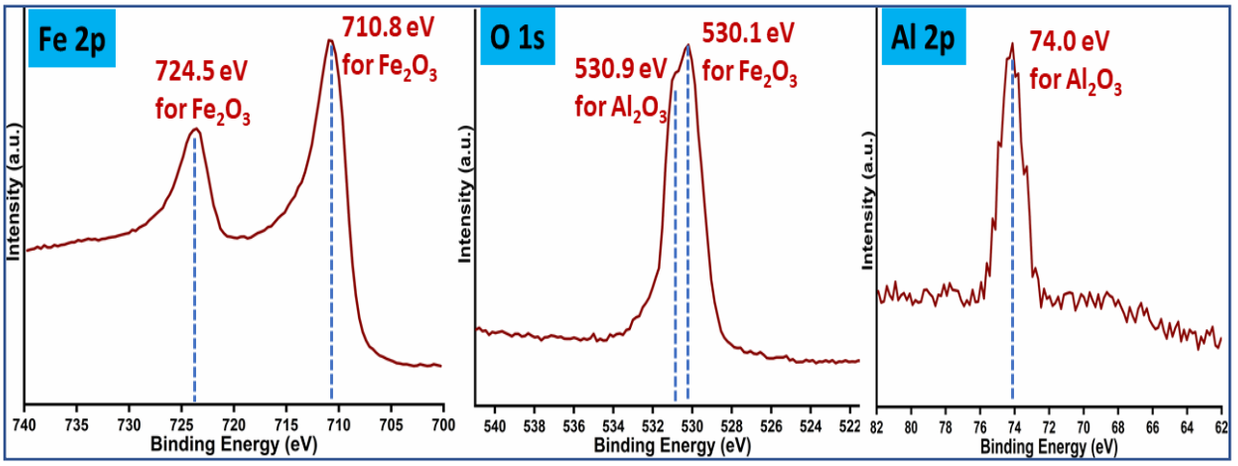

Figure 7.9 Core level XPS Spectra of Fe 2p, O 1s, Al 2p

7.4. Mechanism of tribofilm formation

Well dispersed NPs forms a thin, low shear film on the rubbing metallic surfaces due to two important factors. The first is undulation due to increased temperature at the rubbing junctions propagating NPs towards the rubbing surface. While the other is a stronger electric field due to the generation of exo-electron on the rubbing surface which may lead to migration of NPs[63]. Figure 7.10(a) shows the schematic diagram of the tetrahedral arrangement of four balls. During operation under tribostress, Boehmite NPs get dehydrated into aluminium oxide (Al_2O_3) and subsequently compacted and sintered on the rubbing surfaces as shown in figure

7.10(b). Simultaneously at higher load, nascent steel surfaces get oxidized and a few hundred nanometers thick self-repairing and porous tribofilm of iron oxides are formed[97, 168, 169]. Figure 7.10(c) depicts sacrificial, regenerative protective film formed on the rubbing surface composed of Ferrous oxides and tribosintered Al_2O_3.

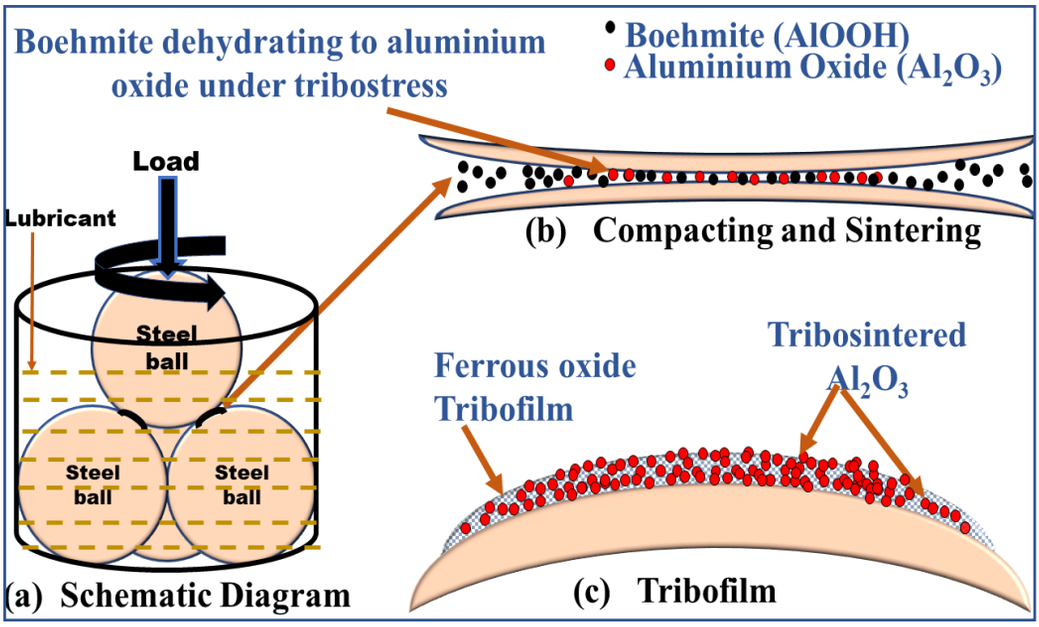

Figure 7.10 (a) Equilateral tetrahedral configuration of four-balls (b) Compacting and tribosintering of NPs under tribostress (c) Sacrificial protective film composed of Ferrous oxides and tribosintered Al_2O_3.

7.5.Important observations

This novel study explores Boehmite NPs as a lubricant additive in synthetic (PAO-6) base oil. The nanolubricants were prepared by varying NPs concentrations (0.25, 0.5, 0.75, 1wt%) and fixed concentration (1 wt%) of dispersant PIBSA. Based on the aim of this study, tribo-performances, and worn surface characterization, we would like to conclude that.

- Boehmite NPS showed excellent friction and wear reduction properties compared with the base oil. Following are the order of their performance and the highest improvement was observed with 0.5% concentration.

$P_{0.5}$ (24%) > $P_{0.25}$ (19%) > $P_{0.75}$ (16%) > P_1 (11%) $\Rightarrow$ Wear Reduction Performance

$P_{0.5}$ (15.36%) > $P_{0.25}$ (14.74%) > $P_{0.75}$ (11.61%) > P_1 (7.55%) $\Longrightarrow$ Friction Reduction Performance

- For the EP test, increased NPs concentration increased load-carrying capacity of the base oil. The performance order is listed below.

P_1 (40%) = $P_{0.75}$ (40%) > $P_{0.5}$ (25%) = $P_{0.25}$ (25%) $\Longrightarrow$ EP Performance

Based on the performance of formulated lubricants we recommend 0.5wt% as optimum concentration for excellent wear reduction. The improvement in tribological and EP performances could be attributed to the excellent dispersion stability and ability of NPs to form tribofilm composed of sintered NPs.

- The surface characterization techniques confirm dehydration of Boehmite into Aluminium oxide and tribofilm composed of tribosintered Aluminium oxides (Al_2O_3).
- Visual inspection and DLS analysis show excellent dispersion stability (negligible sedimentation for the first 30 days) of Boehmite NPs due to their ability to slow agglomeration.
- Relative viscosity increase due to the addition of NPs was higher at elevated temperature (100^OC) than at 40^OC and the highest viscosity index improvement of 4.35% was observed for P_1.

Part 2: Potential of Zinctitanate as lubricant additive

7.6.General

Lubricants are expected to provide not only mobility and durability but also energy efficiency, making them indispensable for modern civilization. The friction losses (engine, and transmission) can be reduced by advancement in additives with a potential for multifold benefits such as fuel economy, reduced cooling, and exhaust losses. Antiwear, antifriction and extreme pressure (EP) additives are generally added during lubricant formulation to impart desirable properties catering to specific service conditions[122, 170]. Antifriction additives generally form residual films on the rubbing surfaces having extremely low shear resistance resulting in friction reduction[89]. While antiwear additives generally disintegrate under tribostress and chemically react to the rubbing surfaces forming regenerative surface-bound protective tribofilm and reducing subsequent surface wear. Zinc-alkyldithiophosphates (ZDDPs) are the most popular antiwear additive class used in a wide range of lubricant formulations due to their excellent solubility, low cost, and ability to form tribofilm rich in S, P, and Zn on underline metallic surfaces [110, 143]. But ZDDP derived protective films on rubbing surfaces are system dependent and may form a very weak film at room temperature, while few studies have reported no ZDDP-induced tribofilm formation[171, 172]. Furthermore, it is observed that thiophosphate constituents of ZDDP after combustion poison the catalytic converter resulting in increased emission[121, 173]. Similarly, other antiwear, and EP additives such as organic phosphate and sulfide groups are primarily composed of Phosphorus, Sulphur, and various Chlorine compounds which are not eco-friendly and have been put under regulatory restriction for maximum permissible limits[147]. In addition, the automotive industry is aspiring for low viscosity grade oils for the potential of increased fuel economy due to reduced viscous/pumping losses[174, 175]. But due to lower viscosity, the lubrication regime may shift toward hydrodynamic, mixed, and boundary lubrication, resulting in increased asperity contacts and may need effective additive packages to reduce subsequent wear. While increasing the concentration of Phosphorus, Sulphur composition in low viscous oil may not be a viable option, due to the limit on maximum Phosphorus and Sulphur concentrations (maximum 800ppm) by International Lubricants Standardization and Approval Committee (ILSAC). This has prompted the relentless pursuit of alternative, eco-friendly, and effective lubricant additives such as nanoparticles and ionic liquids[7, 64, 82, 144].

In the last two decades nanoparticles (NPs) have shown promising potential in enhancing fuel economy and emission control as lubricant additives[65, 176, 177]. The detailed literature review of NPs in lubricants is discussed in chapter 2. Further, most of the NPs are eco-friendly and considered "green" and may decrease/replace harmful lubricant additives. These studies confirm that nanolubricants performance is influenced by various factors such as morphology, size, concentration, and chemical composition of NPs[64, 65]. Antiwear properties generally depend on the nature of the tribofilm formation on the counter surface under boundary lubrication which is highly influenced by the chemical composition of the NPs[65]. This has been a strong motivation for exploring various NPs groups (metal, metal oxide, composites, etc.) having different Physico-chemical properties for their antiwear, antifriction, and EP performances[65].

This novel study explores Zinctitanate ($ZnTiO_3$), a new type of metal-containing NPs as a potential additive for AW and EP properties. Zinctitanate has been investigated in various disciplines such as microwave dielectric, antibacterial, nanofiber, catalyst, gas sensor, white pigment, corrosion inhibitor, and luminescent material due to its outstanding properties, but its potential tribological properties have not been explored[108]. Further agglomeration of colloidal NPs in nonpolar base oil accelerates the sedimentation rate and is the single biggest hurdle for commercializing NPs in lubricants. This ternary oxide material inherits a larger specific surface area which could be instrumental in enhancing colloidal stability. The present study assesses the potential of Zinctitanate NPs for AW, AF, and EP performances along with dispersion stability and sacrificial film formation mechanism in a synthetic base oil.

7.7.Materials and Methodology

7.7.1.Materials and nano-lubricant formulation

Zinctitanate ($ZnTiO_3$) NPs used in this study were obtained from Sigma-Aldrich (CAS NO-12036-43-0, MW=161.26). As per the supplier, NPs have an average particle size (APS) <100 nm with a purity of 99%. PIBSA (Polyisobutylene Succinic Anhydride), kindly provided by Univenture Industries Pvt. Ltd (Product code: UNOL P1057) was used as a dispersant (1wt% fixed concentration) to enhance the dispersion stability of NPs. Synthetic base oil PAO6 used in this study was obtained from Synthomaxx India. It is an API group 4 base oil which is generally named with the abbreviation PAO (for Poly-alpha-olefin group) followed by its kinematic viscosity at $100^{O}C$. For lubricant formulation, firstly PIBSA dispersant of fixed

concentration (1 wt.%) was added in colourless base oil and stirred continuously till consistent light yellow colour (visual inspection) is obtained indicating homogeneous blending of dispersant at room temperature. Subsequently measured quantity of Zinctitanate nanoparticles was introduced into the oil and stirred for 10 minutes followed by a minimum of 30 minutes of sonicating (product of Dakshin Ultrasound operated in a pulsed mode of 2 seconds on 1 second off) to limit initial nanoparticles agglomeration. Different nanolubricants were prepared by varying nanoparticle concentrations in a succession of 0.25 wt.% up to 1 wt.% and were coded by PZT (abbreviation for PAO and ZincTitanate) followed by nanoparticles concentration.

7.7.2. Characterization of Zinctitanate ($ZnTiO_3$) nanoparticles

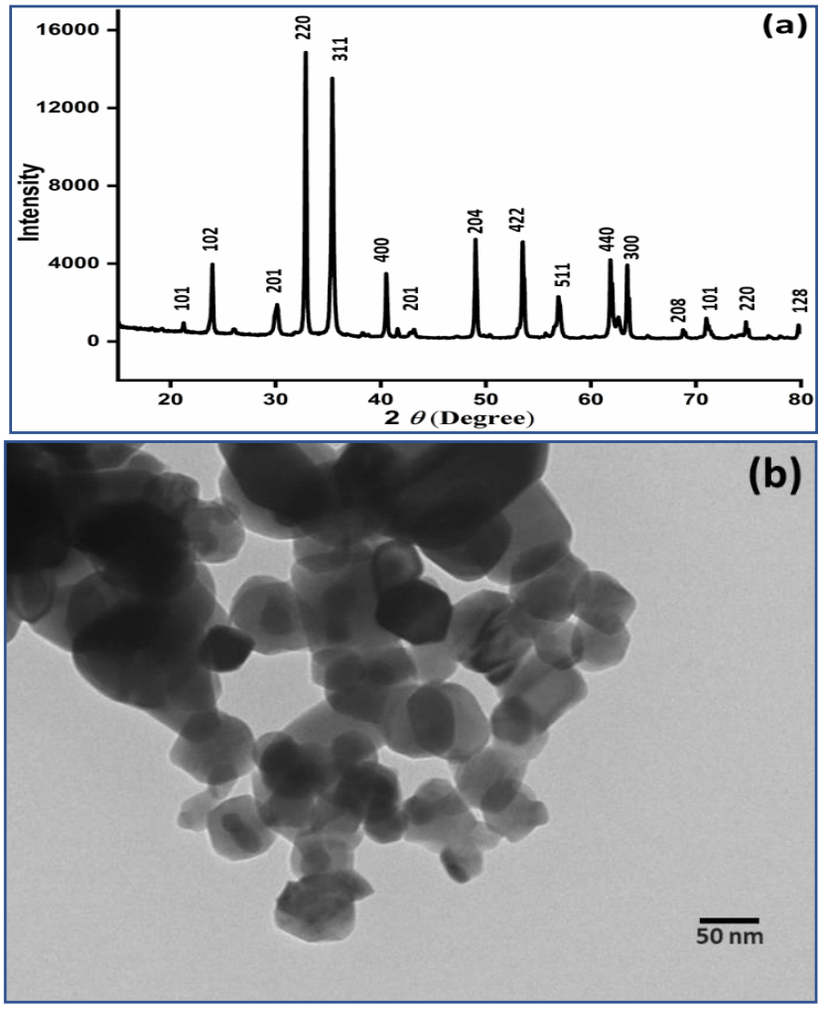

Figure 7.11 (a) XRD Spectrum (b) TEM micrograph of Zinctitanate nanoparticles. TEM micrograph reveals quasi spherical (pentagonal) morphology of nanoparticles.

XRD technique (make Bruker D8 Advance) with Cu Kα radiation was used to analyze the crystal size and phase structure of the NPs (figure 7.11(a)). The intense diffraction peak values (2θ) at 23.86, 30.16, 32.56, 35.33, 40.26, 49.20, 53.48, 56.89, 61.93, and 63.32 are in accordance with JPCDS card number 26-1500 confirming rhombohedral crystal structure[178, 179]. The nanocrystals have unit cell parameters a=b=5.082, c=13.84 A^o with the R3 space group. Average crystal size was calculated using Scherrer's equation (D β cosø=k λ, where D is crystalline size, k is Scherrer's constant, β is FWHM, λ is X-ray wavelength) and was observed to be in the range of 18-23 nm. Transmission electron microscope (TEM, make FEI Tecnai TF20) image of $ZnTiO_3$ NPs shows pentagonal (quasi-spherical) shaped morphology.

7.7.3.Tribological testing and worn surface characterization.

A Four-ball tribometer (make DuCom Instruments) mimicking boundary lubrication regime was employed to study AW, AF, and EP performance of Zinctitanate nano-oils. The detailed experimental setup is described in chapter 3. AW (antiwear) performance was assessed following industry standard (ASTM 4172B) which involves 1200 rpm of chuck rotation, 40kg applied load, at least 75^OC ball pot temperature, and tested for 60 minutes. For reliability and repeatability, the average value (friction coefficient and WSD) of three tests were considered for data representation. Extreme pressure performance was assessed following the Energy Institute's test standards (IP 239) which consist of 1450 rpm, 60 seconds of test duration, and progressive loading till lubricant film breakdown resulting in seizure (either WSD greater than 4mm or balls welded together).

7.7.4.Surface characterization

To remove any weakly absorbed contaminants (lubricant residues) tribo-tested balls were sonicated in Hexane for 5 minutes prior to any surface characterization. To explore morphology and elemental compositions of wear scars, a scanning electron microscope (SEM, brand: JEOL, model:780F, Japan) coupled with an energy dispersive X-ray spectroscope (EDS, make: Bruker crops) was employed. To further probe the chemical state of the tribofilm formed on the worn surface X-ray Photoelectron spectroscopy (XPS, brand: Thermo Fisher Scientific Instruments, model: K ALPHA+) with X-ray monochromatic source of Al Kα (1486.7 eV) focused on a spot of 300μm diameter was employed. C 1s with the binding energy of 284.8 eV was used for calibration of binding energies.

7.8.Results and Discussions

7.8.1.Colloidal stability of Zinctitanate nanolubricants

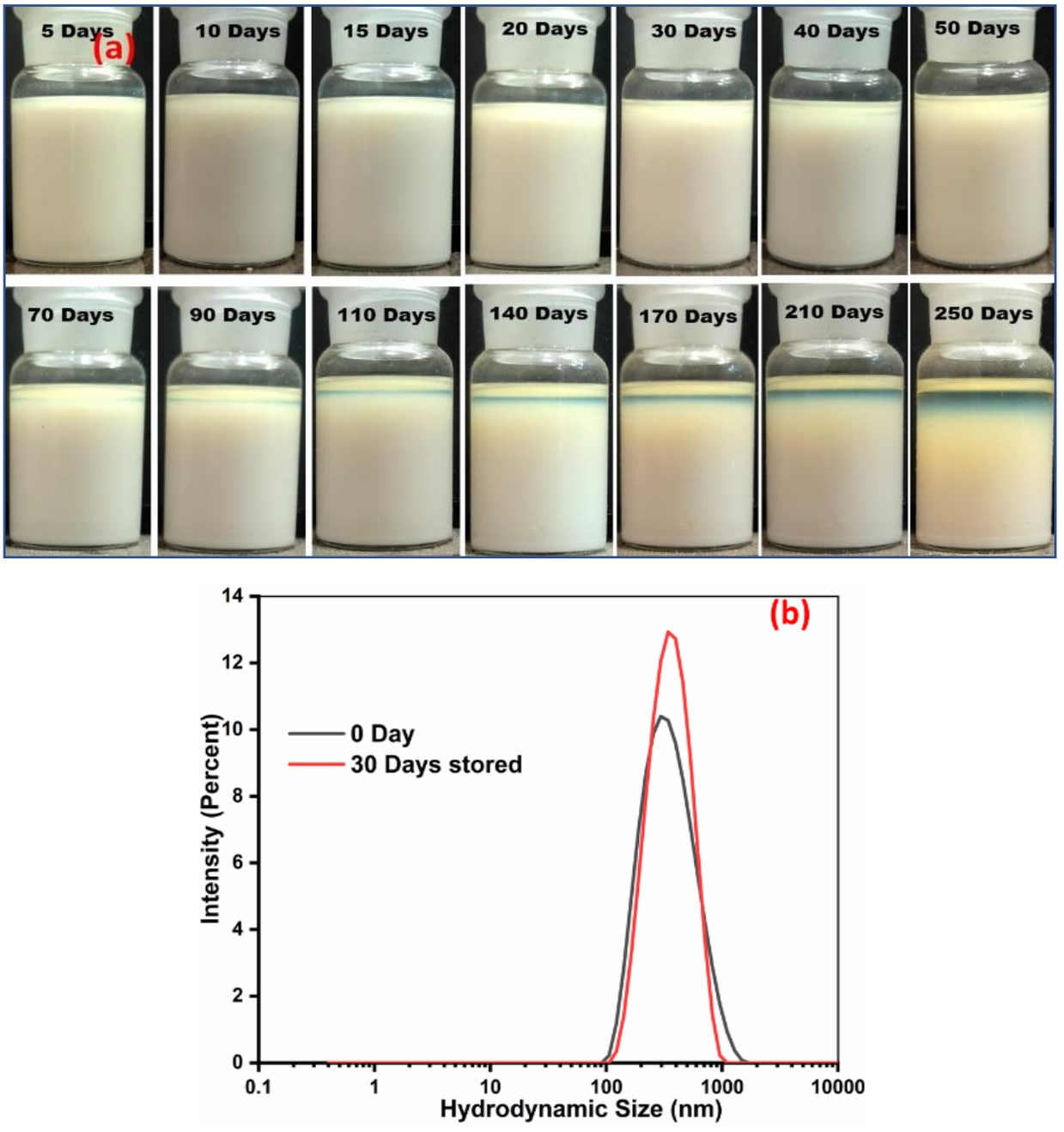

Figure 7.12 (a) Camera images of 1 wt% Zinctitanate nanoparticle dispersed in base oil over 250 days. (b) Dynamic light scattering (DLS) analysis of fresh and 30 days stored samples. Zinctitanate nanoparticles with dispersant PIBSA showed excellent dispersion stability in synthetic base oil.

Colloidal NPs tend to sediment over time predominantly due to agglomeration caused by Brownian motion and gravity (since NPs are denser than base oil)[66]. Visual inspection

and Dynamic Light Scattering (DLS) methods were used to study NPs stability in the base oil. DLS study was conducted once for a fresh sample (0 days) and another after 30 days of storage without any redispersion. For DLS (make: Zetasizer nano 590 Malvern Instruments UK) study sample was taken out carefully from the top of the container and diluted (0.1 mg/g) with neat PAO base oil[150]. The fresh sample of Zinctitanate nanolubricant gave hydrodynamic diameters (z-average) of 321nm (St Dev 248nm) and even after 30 days of storage, little agglomeration was observed with a hydrodynamic diameter of 346nm (St Dev 177nm) as shown in figure 7.12(b). Generally, a lower hydrodynamic diameter signifies better dispersion, and a small increase in hydrodynamic diameter over 30 days of storage infers the ability of Zinctitanate NPs to resist agglomeration resulting in excellent colloidal stability.

Further figure 7.12(a) (camera images) shows the visual observation of 1 wt. % NPs dispersed in the base oil enriched with 1 wt.% dispersant (PIBSA) over 250 days. Around 70 days of storage, some form of phase separation was visible near the top end of the sample but distinguishable phase separation was observed only around 110 days. The sedimentation has gradually increased over the next 100 days nevertheless a significant proportion of the NPs were still dispersed even after 250 days of storage. Thermal agitation pushes NPs in lubricants to move randomly resulting in Brownian motion, and if Brownian motion overcomes attractive forces among particles, stable dispersion is obtained. DLVO (Derjaguin and Landau, Verwey and Overbeek) and Steric stabilization are two widely accepted theories explaining the colloidal stability of particles[66]. According to DLVO theory particle polarization causes Van der Walls forces which attract nanoparticles towards each other while electrostatic forces among particles oppose it[66]. Though, in a nonpolar base oil, these forces are weak and believed to have limited or no role in colloidal stabilization[180]. While the steric stabilization theory proposes a balance between complex attractive Van der Walls forces and repulsive steric forces for stable dispersion. The steric repulsion comes into action when NPs adsorbed with surface layers approach each other, causing deformation of grafted/absorbed surface layer resulting in repulsive forces[66]. Physicochemical properties of Zinctitanate NPs and steric stabilization provided by dispersant may be a plausible explanation for the excellent colloidal stability of NPs in the synthetic nonpolar base oil.

7.8.2. Tribological performance

In absence of any additive, base oil registered the largest WSD as evident from figure 7.13(a) tested following ASTM 4172 standard. It was observed that successive increases in

nanoparticle concentration in base oil reduced average WSD respectively. A small concentration (0.25 wt%) of Zinctitanate nanoparticle in base oil reduced WSD by 9% and a maximum wear reduction of 26% was observed for 1wt% Zinctitanate concentration. AF behavior also gave a similar trend and a 14% friction coefficient reduction was observed for 0.75 wt% concentration while 1 wt% concentration registered a 12% improvement. Figure 7.13 (c) shows that base oil registered the highest μ fluctuation for the entire test duration. For the initial 500 seconds friction was relatively low but due to the inability of neat oil to form stable film and subsequent poor surface protection accelerated wear rate as evident from the increasing μ trend till the end of the test. Interestingly, the addition of a small concentration (0.25 wt%) of Zinctitanate nanoparticles gave very low initial friction, but the friction coefficient increased rapidly inferring weaker film formation, not sufficient to provide stable surface protection. Increasing NPs concentration reduced fluctuation of μ value and PZT-0.75 gave negligible fluctuation indicating thicker film coated on rubbing surfaces.

PZT-1(26%)> PZT-0.75(21%)> PZT-0.5(14%)> PZT-0.25(9%)>P AW performance @ ASTM 4172

PZT-0.75(14%)> PZT-1(12%)> PZT-0.5(9%)> PZT-0.25(6%)>P AF performance @ ASTM 4172

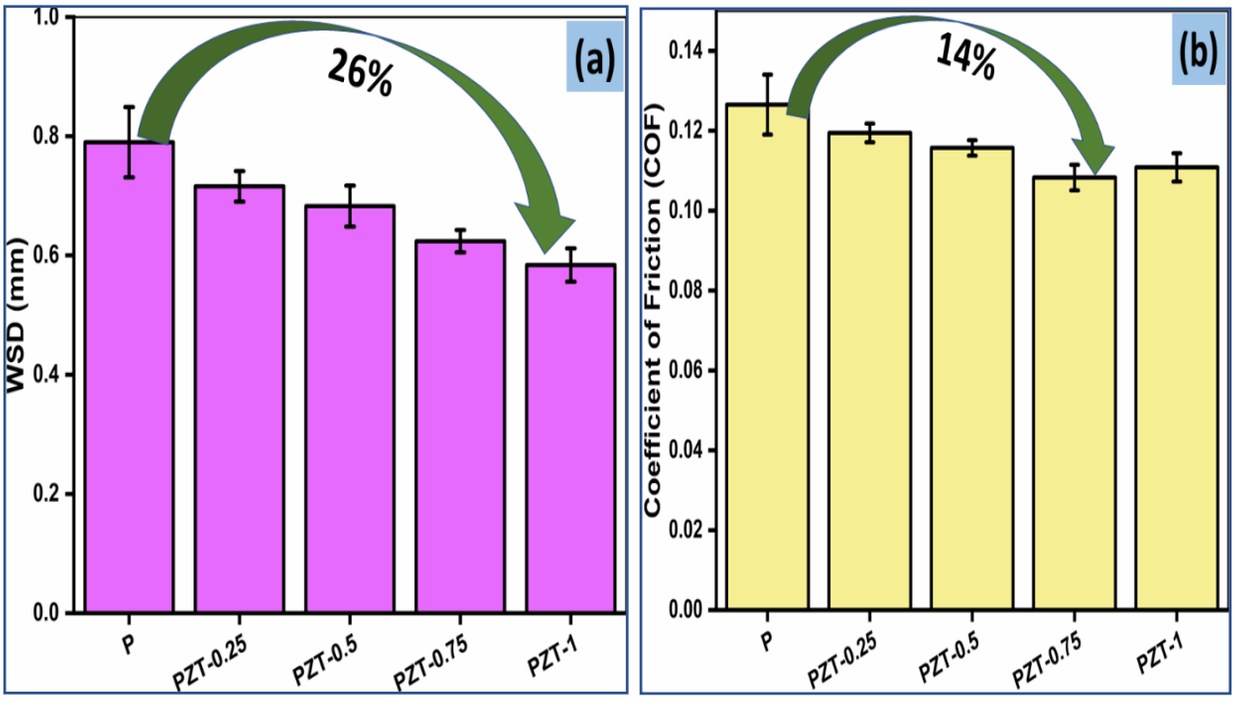

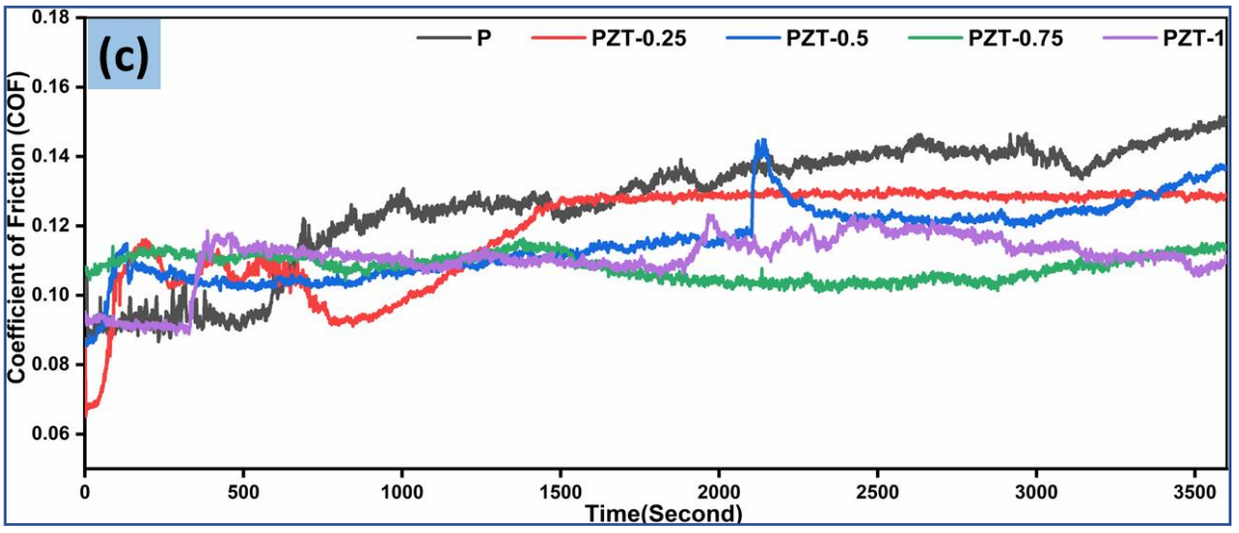

Figure 7.13 (a) Average Wear (b) Average Friction Coefficient (c) Friction Coefficient (μ) vs time performance throughout the test duration for formulated nanolubricants tested following ASTM 4172 standards i.e., 1200 rpm, 40kg applied load, 75^{O}C temperature, and 60 minutes of test duration. For the initial 500 seconds friction was relatively low but the inability of base oil to provide effective surface protection accelerated wear rate as evident from the increasing μ trend till the end of test duration. While nanoparticle concentration reduced fluctuation of μ and PZT-0.75 gave negligible fluctuation indicating thicker film coated on rubbing surfaces.

7.8.3.Topography analysis of the worn surface.

To explore the morphology of the wear scar and constituents of the plausible tribofilm, steel balls were thoroughly examined using SEM and EDS analysis. Figure 7.14 shows the SEM micrograph, elemental mapping (X 500), and chemical elements of respective wear scars. Counter surfaces in the boundary lubrication regime are generally separated by a very thin film (monolayer) of lubricant molecules adsorbed on rubbing pairs. The thin lubricant film under tribostress is unable to reduce direct asperity interaction which results in adhesive (plastic deformation) and/or abrasive wear [122]. The surface lubricated with the base oil (micrograph figure 7.14(a)) shows rough topography consisting of severe abrasion and plowing/micro-cutting. While the surface lubricated with Zinctitanate nanolubricants (micrograph figure 7.14 (b)) shows relatively shallower and narrower groves (minor abrasion marks) inferring protection provided by Zinctitanate nanoparticles. Other than abrasion marks, the micrograph of the worn surface with base oil lubrication shows micro pits throughout the worn surface that can be accredited to adhesive wear. Generally, asperity interaction under poor lubrication and

severe working condition may lead to localized bonding of asperities and subsequent sliding remove chunks of material (plastic deformation)[122]. In general, a good agreement between worn surface morphology and surface wear was observed in this study.

EDS elemental analysis of surfaces with base oil lubrication shows primarily O, Fe, Cr, and C as shown in figure 7.14. Interestingly, the Oxygen concentration was highest for surfaces undergone severe surface damage i.e. surfaces lubricated with neat base oil. Both signature elements of Zinctitanate (Ti, Zn) were detected for the surfaces lubricated with Zinctitanate nanolubricants.

Based on surface characterization reported in the literature there are four known mechanisms for increased wear protection provided by nanoparticles[64, 65]. Two of these mechanisms could be accredited to the direct action of NPs (film formation, and ball bearing) while others are due to secondary surface-enhancement (polishing and mending effects). Though, in various studies, the classification of active mechanisms is still a subject of discussion. The mending (self-repairing) effect occurs if nanoparticles occupy the scars and grooves of the counter surfaces, compensating for the loss of material, which may result in reduced wear[64]. While during the polishing effect, the average roughness of rubbing surfaces is minimized due to the abrasive action of the nanoparticles. Owing to lower surface roughness this polishing or "artificial smoothing" effect results in improved tribological performance[64]. The ball bearing effect is the result of a direct action of nanoparticles, which occurs when quasi-spherical or spherical nanoparticles roll between counter surfaces, converting sliding friction into a combination of rolling and sliding friction[64]. On the other hand, stronger film formation results in sacrificial film on top of the rubbing surface attributed to tribosintering/chemical reaction between substrate and nano-additives under tribostress. For effective protection of substrate, the tribofilm formation rate should be higher than the progressive material removal rate due to wear.

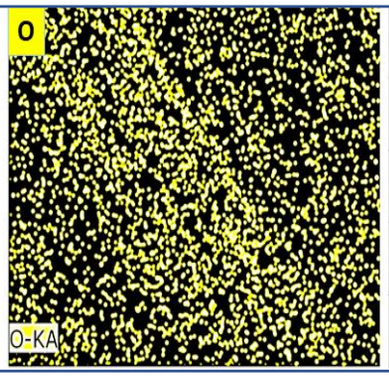

Elements	Atomic %
O	7.21
C	6.36
Fe	84.96
Cr	1.47

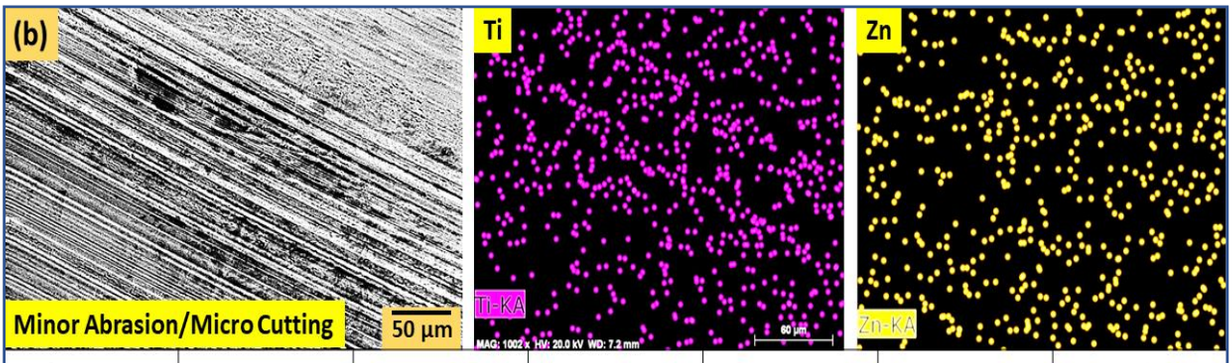

Elements	O	C	Fe	Cr	Zn	Ti
Atomic %	5.66	6.62	84.28	1.35	0.86	1.23

Figure 7.14 SEM-EDS characterization of worn surface lubricated with (a) PAO, (b) PZT-1 following ASTM 4172 test standards. SEM micrographs shows relatively smoother topography (less plowing/micro-cutting) of surfaces lubricated with nanolubricants than respective base oil.

7.8.4.Extreme Pressure performance

Based on the tribological performance and surface characterization results of this study, Zinctitanate NPs appear to be tribosintered/chemically reacted on the worn surface resulting in the formation of sacrificial, regenerative, and protective tribofilm. EDS analysis shows higher Zinctitanate NPs signature (Zn, Ti) on the worn surface tested following stipulated test condition (higher load) than ASTM 4172 standard. This could be due to relatively severe working conditions due to higher load-induced tribostress.

Generally, the EP performance of nanolubricants highly depends on the ability of nanoparticles to enter the contact zone and form a protective film on metallic rubbing surfaces. The film may form either due to tribochemical reaction or smeared nanoparticles or a combination of both[85, 99]. This film should not only be uniformly distributed, and coherent but also possess the ability to resist seizure by minimizing direct asperity contacts[99]. The EP performance test of Zinctitanate nanolubricants following IP 239 standard is shown in figure 7.15(a). Initially, a direct correlation between Zinctitanate concentration and EP performance (maximum non-seizure load / pre-weld load) was observed up to 0.75 wt.% with the highest enhancement of 65% beyond that (for 1wt %) no further enhancement was observed. During 60 seconds of the test, the top layer progressively gets removed several times due to tribostress,

and the presence of Zinctitanate nanoparticles between asperity contacts has certainly resisted seizure resulting in higher load-carrying capacity.

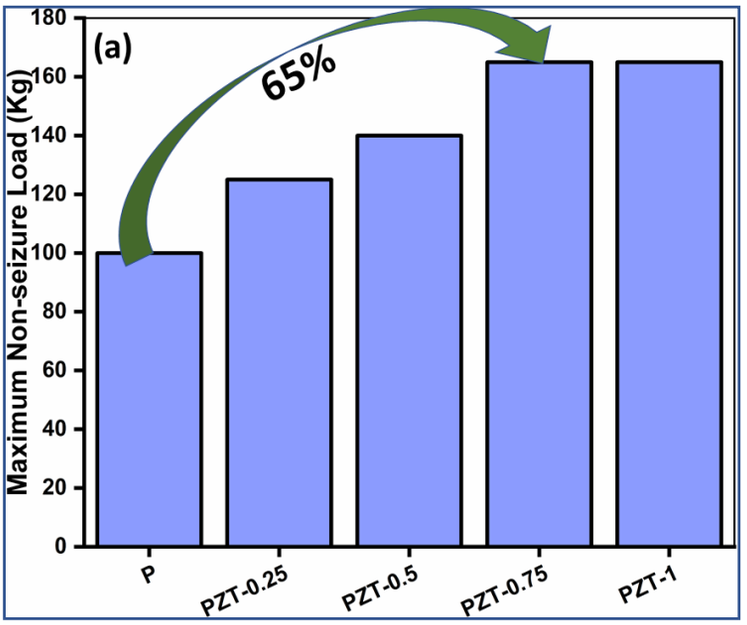

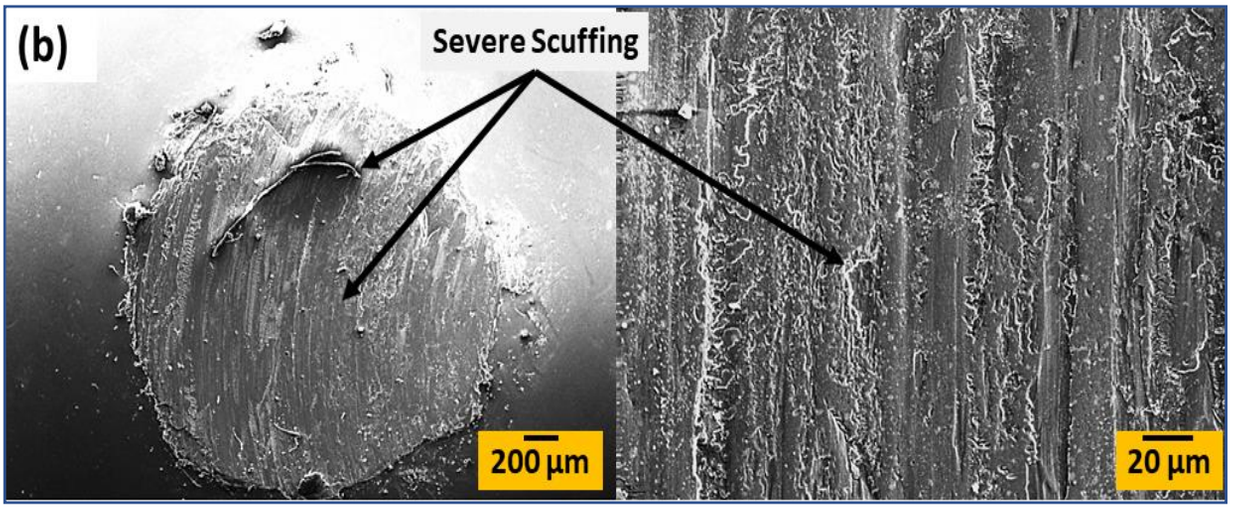

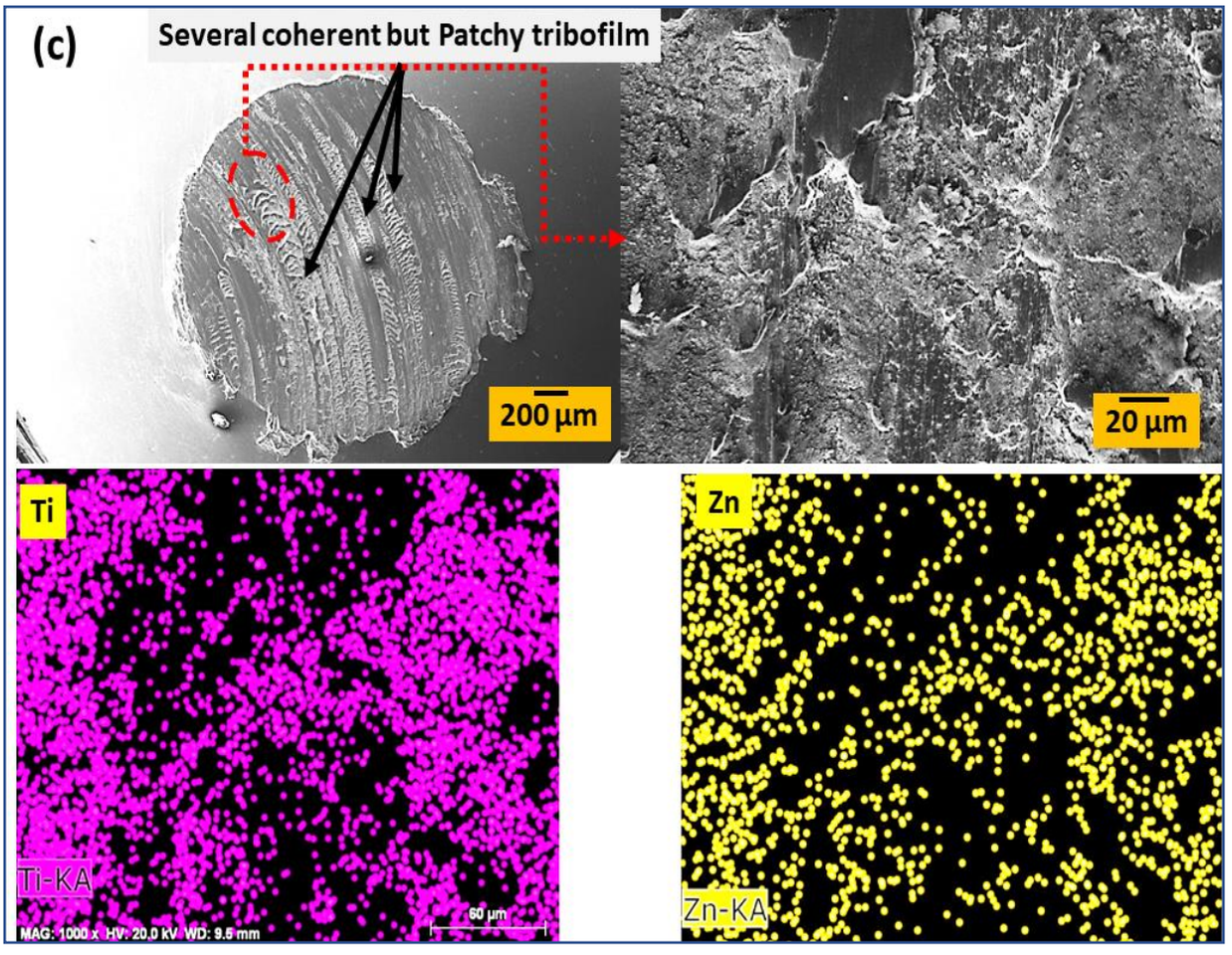

Figure 7.15 (a) EP performance of different nanolubricant concentration. (b) SEM micrographs of pre-weld worn surface under PAO base oil lubrication. (c) SEM micrographs and EDS dot map of pre-weld worn surface lubricated with nanolubricants. The SEM-EDS results indicated patchy, coherent tribofilm on worn surface composed of Zinctitanate nanoparticles attributed to excellent EP performance

To understand phenomenal EP performance enhancement and the presence of plausible transfer film, surface characterization (SEM-EDS) of respective pre-weld ball lubricated with PAO and 1 wt.% concentration is shown in figure 7.15. The worn surface of the pre-weld ball lubricated with the base oil (figure 7.15(b)) shows rough topography with severe scuffing marks in addition to deep continuous grooves along with sliding direction. Surface lubricated with nanolubricant shows tribofilm composed of Zinctitanate nanoparticles as evident from EDS elemental dot mapping as shown in figure 7.15(c). The tribofilm appears to be patchy strips and covers a large area of the worn surface as shown in respective SEM micrographs and EDS dot mapping.

7.8.5.XPS characterization of the tribofilm.

To further probe the chemical state of the tribofilm XPS spectrum of worn surface lubricated with 1 wt.% Zinctitanate nanolubricant was employed. The top of figure 7.16 (plotted with blue colour) shows core level XPS spectroscopy of near-surface zone while the bottom (plotted with red colour) shows core level spectroscopy of 100 nm deep surface obtained by ion sputtering. The core level Ti spectra show two main peaks of ≈458.8 and ≈464.5 eV binding energies that could be attributed to the formation of $FeTiO_3$[111, 183, 184]. Tribostress (compacting, sintering, and localized heating) may lead to the disintegration of Zinctitanate NPs and subsequent tribochemical reaction with Fe of exposed nascent steel surface resulting in the formation of $FeTiO_3$ film. This deposited film on the rubbing surface is sacrificial and may provide wear protection to interfacial surfaces. In addition to the above two peaks, Vinay Saini et.al has also reported a binding energy peak at ≈458.6 eV associated with TiO_2[111]. This peak in the near-surface zone is most likely to be buried inside the main peak of ≈458.8 eV and was not distinguishable[111]. The100 nm deep surface zone shows a distinguishable Ti peak with a binding energy of ≈458.6 eV that in association with the ≈530.0 eV peak of O1s can be accredited to TiO_2. The dominant O1s peak of ≈531.3 and ≈531.1 eV for near-surface and 100 nm deep zone respectively could be associated with ferrous oxide (Fe_xO_y) formed due to localized frictional heat[99, 133]. Both these surfaces also show Zn2p peaks around ≈1021 (Zn 2p3/2) and ≈1044 eV (Zn 2p1/2) which could be associated with ZnO. The Fe2p core level spectra show two dominant peaks with binding energies of ≈710.5 and ≈724.4 eV, which could be attributed to ferrous oxides (Fe_2O_3)[75, 133, 182].

Atomic composition of near-surface and 100 nm deep surface zone obtained from quantitative XPS analysis are tabulated in Table 7.4. The Ti and Zn composition obtained by XPS spectroscopy (3.74, 1.82 atomic%) were significantly higher than the respective EDS (1.23, 0.86 atomic%) compositions. This is due to dissimilar probing depths of XPS (few nanometers) and EDS (few micrometers). The 100 nm deep worn surface shows a significant presence of Zinctitanate constituents i.e., Ti (1.56 %) and Zn (0.97 %), inferring tribofilm thickness of over 100 nm.

Table 7.4 Atomic concentration of tribo-active elements obtained by XPS spectroscopy of worn surface lubricated with Zinctitanate nano-oil. The presence of a significant amount of Zn and Ti elements on the 100nm deep surface indicates the protective tribofilm to be at least 100nm deep.

Samples	Atomic %				
	O	C	Fe	Ti	Zn
Near surface zone	58.68	9.36	26.4	3.74	1.82
100 nm depth surface	25.37	4.12	67.98	1.56	0.97

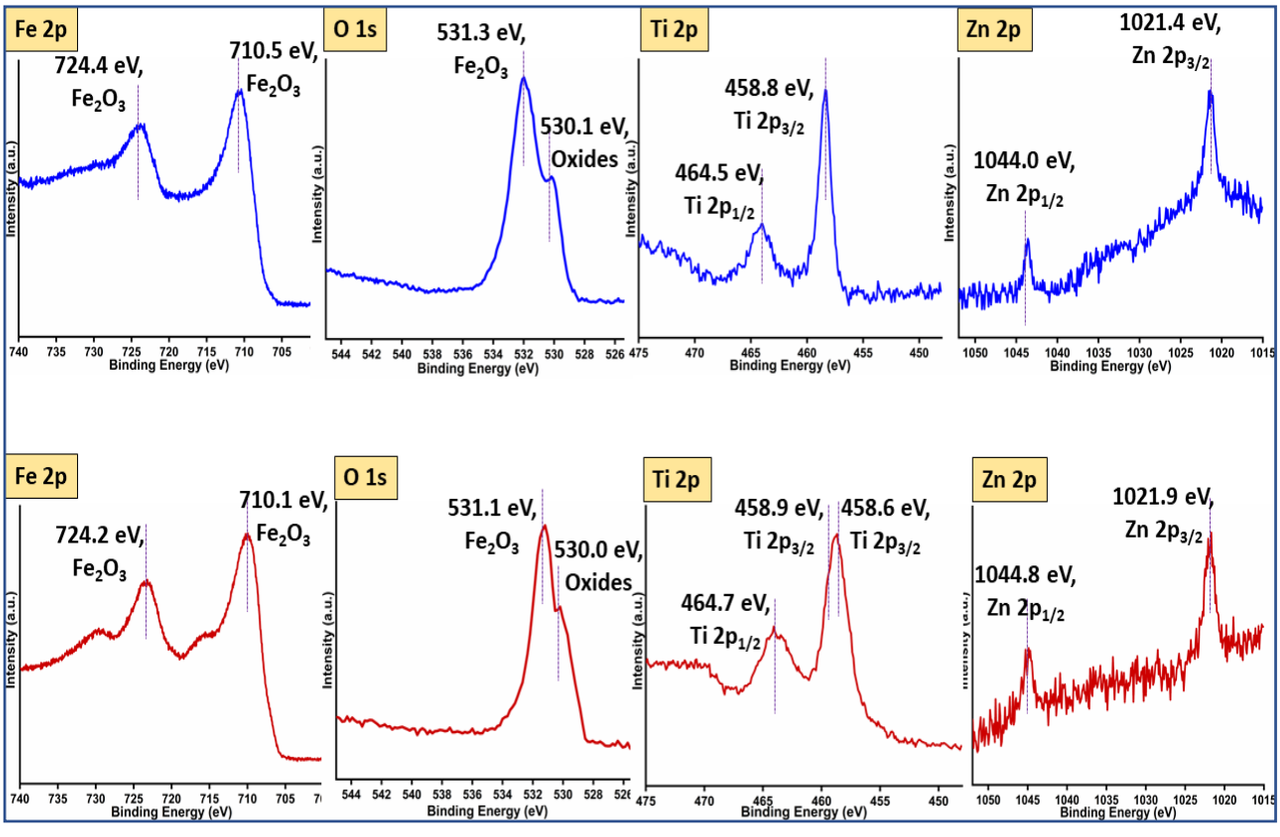

Figure 7.16 core level XPS spectra of Fe, O, Ti, Zn for worn surface lubricated with PZT-1. top spectra (plotted with blue colour) for near surface zone surface, bottom graph (plotted with red colour) 100 nm deep surface obtained by Ar-ion sputtering. Ti 2p core level spectra of both surfaces shows two binding energies at ≈458.8 and ≈464.5 eV which could be attributed to the formation of $FeTiO_3$ due to disintegration of Zinctitanate NPs and subsequent tribochemical reaction with nascent steel surface. While Zn2p peaks of transfer film around ≈1021 (Zn $2p_{3/2}$) and ≈1044 eV (Zn $2p_{1/2}$) could be associated with ZnO.

7.8.6.Synergistic effect of ionic liquid and nanoparticles.

The synergistic performance of both nanoparticles (Boehmite and Zinctitanate) with best performing phosphonium phosphate IL i.e. [P66614][DEHP] were assessed following ASTM 4172 standard and shown in figure 7.17. As single additive, optimum concentration (1 wt%) of Zinctitanate nano-oil registered slightly better wear reduction compared to Boehmite nanoparticles (0.5 wt%). While as hybrid nano-oil, Boehmite registered superior antiwear properties of 53% compared to 49% of Zinctitanate. Similarly, Boehmite hybrid nano-oil also gave 26 % friction reduction which was relatively higher than Zinctitanate hybrid nano-oil (24%). EP (extreme pressure) performance were assessed following IP 239 standard. Boehmite hybrid nano-oil showed 50% enhancement in load bearing capacity over base oil, which is higher than respective individual additive performance i.e. IL2 (40%), Boehmite (25%). It was interesting to note that Zinctitanate hybrid nano-oil gave 65 % enhancement in load bearing capacity which was similar to Zinctitanate as single additive. This could be attributed to severe operating condition and inability to provide continuous surface protection at extreme pressure.

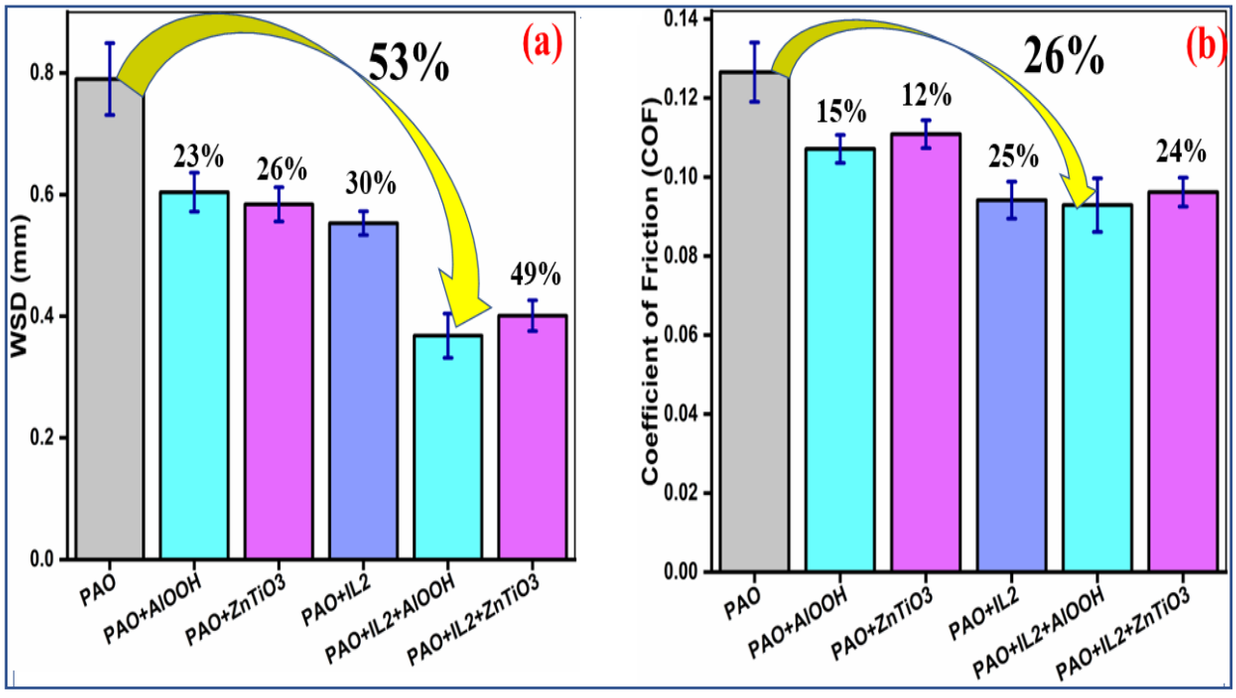

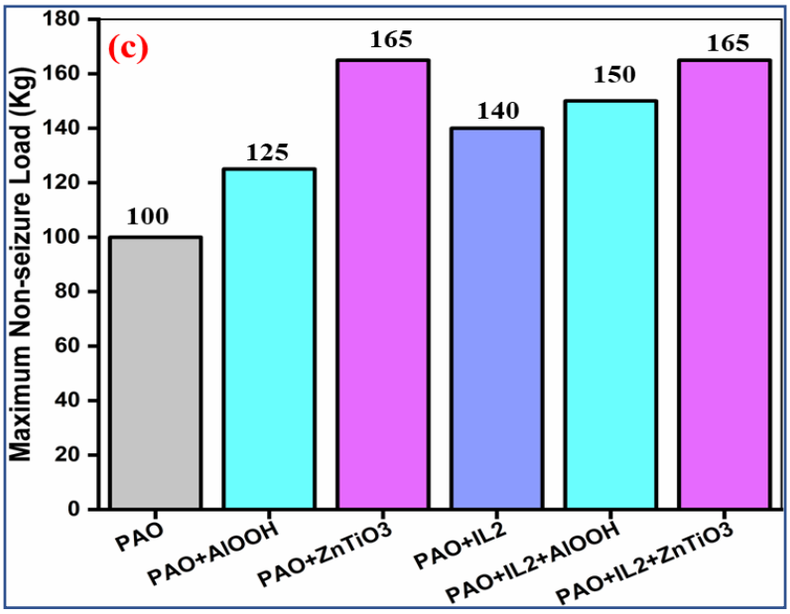

7.17 Tribological performance of Zinctitanate and Boehmite hybrid nano-oil. (a) antiwear, (b) antifriction performance tested according to ASTM 4172 standards i.e. 40kg load, 1200 rpm, 75°C temperature for 3600 seconds. (c) EP performance tested following IP 239 standards. Tribological performance of these hybrid nano-oil showed shows synergy with 53% wear and 26 % friction Coefficient reduction. Boehmite hybrid nano-oil slightly outperformed their Zinctitanate counterpart.

Table 7.5 gives the EDS analysis of the worn surfaces lubricated with boehmite and Zinctitanate hybrid nanolubricants. Presence of Phosphorus on the worn surface could be attributed to tribochemical reaction of phosphonium phosphate IL under tribostress and subsequent formation of iron-phosphate compounds ($FePO_4$) as observed in XPS analysis. While Al could be attributed to tribosintered nanoparticles in the form of Al_2O_3 due to dehydration of boehmite nanoparticles as observed in XPS analysis. On the other hand, presence of Ti on the worn surface lubricated with Zinctitanate may be associated with tribochemical reaction with substrate and subsequent formation of $FeTiO_3$, and TiO_2 as observed in XPS study. While Zn is present in the form of ZnO as given by XPS analysis.

Table 7.5 EDS analysis of worn surfaces

Lubricants	Atomic %							
	O	C	Fe	Cr	Zn	Ti	P	Al
PAO+IL2+Boehmite	5.87	6.72	84.06	1.23	-	-	1.47	0.65
PAO+IL2+Zinctitanate	5.36	6.89	83.25	1.31	0.73	1.12	1.34	-

7.9.Important Observations:

This novel study explores the potential of Zinctitanate nanoparticles as antiwear and extreme pressure additives along with synergy with best performing IL in API group four base oil mimicking boundary lubrication regime. Based on the colloidal stability, tribological behavior, and tribofilm characterization of worn surfaces, we conclude that.

1. Zinctitanate nanoparticles showed excellent dispersion stability (majority dispersed even after 225 days) in the synthetic base oil, and the DLS study confirms very limited agglomeration of colloidal nanoparticles over time. The excellent colloidal stability could be attributed to physicochemical properties of Zinctitanate nanoparticles along with steric repulsion provided by dispersant PIBSA.
2. Zinctitanate nanolubricant showed excellent antifriction (14%) and antiwear (26%) properties over PAO-6 synthetic base oil and based on the antiwear performance we recommend 1wt.% as optimum nanoparticle concentration.
3. An increase in nanoparticle concentration increased extreme pressure performance and a maximum improvement of 65% was observed at 1 wt. % concentration.
4. Morphology of worn surface lubricated with nanolubricants gave negligible adhesive wear and minor abrasive wear which may be accredited to the direct action of nanoparticles (bearing effect and tribosintering) in protective film formation.
5. Surface characterization techniques corroborate tribofilm (at least 100nm thick) composed of $FeTiO_3$ and ZnO attributed to tribosintering/tribochemical reaction under severe working conditions (compacting, sintering, and localized heating).
6. Boehmite hybrid nanolubricant marginally outperformed Zinctitanate counterpart with 53 and 49% wear reduction respectively but Zinctitanate gave superior dispersion stability compared to that to Boehmite.
7. Surface characterization confirm role of both additives (ILs and NPs) in tribofilm formation.

Chapter – 8

Conclusions and Scope for Future Work

8.1. General

In pursuit of efficient lubricant with potential to replace/minimize harmful SAPS compounds of commercial lubricants, 7 distinct NPs and 3 phosphonium phosphate ILs were studied. Other than tribological performances, the emphasis was given to long term stability of formulated hybrid nano-oil. This study explores tribological i.e. antiwear (AW), antifriction (AF) and extreme pressure (EP) performances along with physicochemical properties of formulated lubricants. Figure 8.1 gives the methodology employed for lubricant formulation and performance analysis.

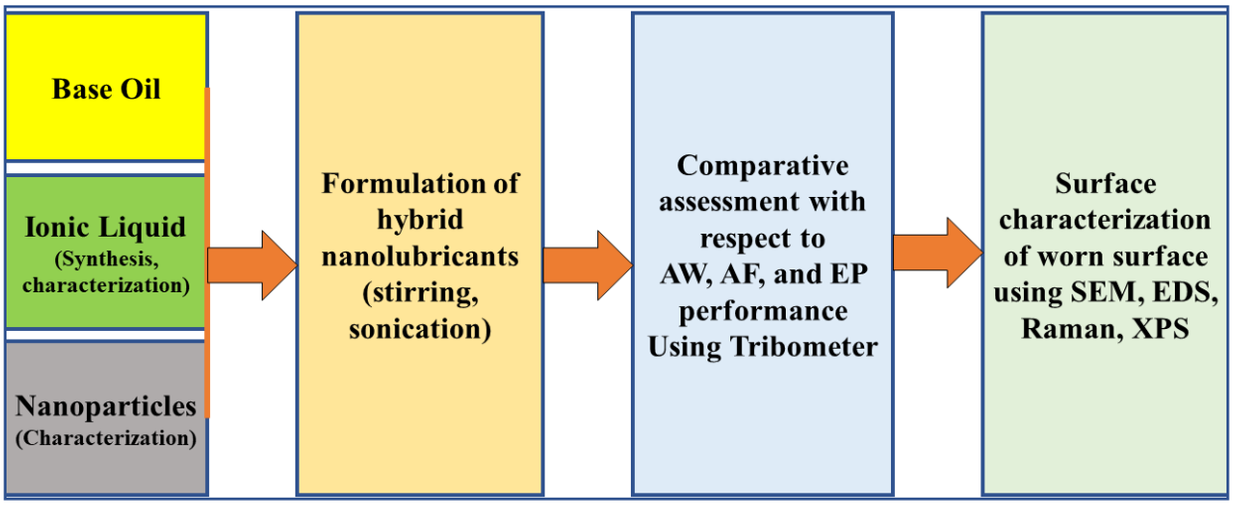

Figure 8.1 Methodology employed for lubrication formulation and performance analysis

8.2. Overall conclusions of the study.

- All three ILs showed excellent miscibility (at least 5 wt%) in PAO, strengthening the hypothesis that reducing the charge density of ions (due to longer alkyl chain length of both ions) would increase the IL's compatibility with neutral oil molecules.

- We are the first to explore IL3 i.e. [P66614][DBP] as a lubricant additive and observed very good tribological performance with 21 and 19% of wear and friction reduction, respectively.

- Based on AW, AF and EP performances these ILs can be ranked as
  IL2 (30%) > ZDDP (25%) > IL3 (21%) > IL1 (8%) AW performances

IL2 (25%) > ZDDP (20%) > IL3 (19%) > IL1 (10%) AF performances

IL2 (40%) = ZDDP (40%) > IL3 (25%) > IL1 (15%) EP performances

It was interesting to note that despite having same cation and similar phosphorus concentration, IL1 improved wear reduction marginally if compared with the other two ILs, inferring that tribochemistry of both cation and anion are equally important for the tribofilm formation.

- IL2 and IL3 showed excellent synergy with various nanoparticles and gave friction reduction in the range of 25 – 30%, while wear reduction was 41-57 %.

- IL2 and IL3 hybrid nanolubricants showed compatibility and enhanced extreme pressure (EP) performance of the base oil in the range of 65–75%.

- Ionic liquids (ILs) enhanced the dispersion stability of hBN and ZnO NPs by marginally. But it was observed that ILs on their own may not provide prolonged stability in lower viscosity oils and further dispersion stability enhancement methods for NPs should be explored.

- PIBSA dispersant did not negatively affect the performance of base oil or any additive combination. No precipitation or cloudiness was observed, inferring plausibly no chemical reaction among IL, NP, and dispersant PIBSA during sample preparation or storage. Which indicates that PIBSA dispersant can be employed along with phosphonium phosphate ILs to disperse non-miscible lubricant constituents (specially NPs)

- In search of better colloidal stability, we explored novel nanoparticles, i.e. Boehmite and Zinctitanate, which showed excellent friction (14-18%), wear (23-53%) reduction properties and enhanced EP performance (40-75%) compared with the base oil. Based on the wear performance of formulated lubricants we recommend 0.5 and 1 wt% as optimum concentration for Boehmite and Zinctitanate NPs respectively.

- The surface characterization techniques confirm dehydration of Boehmite into Aluminium oxide and tribofilm composed of tribosintered Aluminium oxides (Al_2O_3). While Zinctitanate formed tribofilm (at least 100nm thick) composed of $FeTiO_3$ and ZnO attributed to tribosintering/tribochemical reaction under severe working conditions (compacting, sintering, and localized heating).

- All the hybrid nanolubricants outperformed ZDDP indicating that compatibility between ILs and NPs can help in decreasing overdependence on ZDDP provided the long term dispersion stability of NPs is addressed.

Based on wear reduction results with best performing IL i.e. [P66614][DEHP], hybrid nano-oils can be ranked as:

hBN (57%) > AlOOH (53%) > ZnO (50%) > ZnTiO3(49%) > ZnDDP (25%)

- Visual inspection and DLS analysis show excellent dispersion stability of Boehmite (negligible sedimentation for the first 30 days) and Zinctitanate (110 Days for phase separation) NPs due to their ability to slow agglomeration over time. We recommend Zinctitanate hybrid nano-oils based on long term stability and tribological performance (49% wear reduction which is nearly double of ZDDP performance of 25%).

Table 8.1 dispersion stability of various nanoparticles in PAO non polar base oil enriched with dispersant PIBSA

Nanoparticles	Average Particle Sizes (nm)	Duration
CuO	40 nm	1 Week
Al_2O_3	30-50 nm	11 days
SiO_2	30-50 nm	10 Days
ZnO	30 nm	8 Days
hBN	70 nm	15 Days
Boehmite (AlOOH)	20 nm	45 Days
Zinctitanate ($ZnTiO_3$)	100 nm <	110 Days

`

- Surface characterization techniques confirmed synergy between ILs and NPs in the formation of regenerative sacrificial tribofilm on the counter surfaces composed of phosphates (Fe–P–O, plausibly $FePO_4$) and tribosintered/triboreacted NPs. Extensive characterization of worn surfaces lubricated with different lubricant formulations reveals primarily tribosintering for oxide nanoparticles (CuO, Al_2O_3, SiO_2, ZnO), while hBN and $ZnTiO_3$ appears to be disintegrated and chemically reacted with nascent steel surface. On the other hand, we observed just like Talc, and Serpentine, Boehmite mineral dehydrated in to Al_2O_3 and subsequently tribosintered on the worn surfaces.

8.3. Scope for future work

- Studies may focus on introduction of newer ionic liquids with tuning molecular structure.
- Studies can be extended to reused oils.
- The potential of nanolubricants can be further explored with different base oils, i.e. vegetable oils, synthetic oils, greases etc.
- The compatibility of ionic liquids and NPs can be explored in the presence of other essential additives (anti-oxidant, corrosion inhibitors, etc.)
- NPs can be functionalized to enhance the dispersibility in oils.

References

1. Stachowiak, G.W., Batchelor, A.W.: E N G I N E E R I N G T R I B O L O G Y.
2. Friction, Wear, Lubrication A Textbook in Tribology Second Edition.
3. Jost. H.P: Lubrication (tribology) : Education and research. A report on the present position and industry's needs. , London (1966)
4. Holmberg, K., Andersson, P., Erdemir, A.: Global energy consumption due to friction in passenger cars. Tribol Int. 47, 221–234 (2012). https://doi.org/10.1016/j.triboint.2011.11.022
5. Holmberg, K., Erdemir, A.: Influence of tribology on global energy consumption, costs and emissions, (2017)
6. Rizvi, S.Q.A.: A comprehensive review of lubricant chemistry, technology, selection, and design. ASTM International (2009)
7. Zhou, Y., Qu, J.: Ionic liquids as lubricant additives: A review. ACS Appl Mater Interfaces. 9, 3209–3222 (2017). https://doi.org/10.1021/acsami.6b12489
8. Spikes, H.A.: Additive-additive and additive-surface interactions in lubrication. Lubrication Science. 2, 3–23 (1989). https://doi.org/10.1002/ls.3010020102
9. Spikes, H.: Friction Modifier Additives. Tribol Lett. 60, (2015). https://doi.org/10.1007/s11249-015-0589-z
10. Hallett, J.P., Welton, T.: Room-temperature ionic liquids: Solvents for synthesis and catalysis. 2. Chem Rev. 111, 3508–3576 (2011). https://doi.org/10.1021/cr1003248
11. Welton, T.: Room-Temperature Ionic Liquids. Solvents for Synthesis and Catalysis. Chem Rev. 99, 2071–2084 (1999). https://doi.org/10.1021/cr980032t
12. Xiao, H.: Ionic Liquid Lubricants: Basics and Applications. Tribology Transactions. 60, 20–30 (2017). https://doi.org/10.1080/10402004.2016.1142629
13. Rogers, R.D., Seddon, K.R.: Ionic Liquids - Solvents of the Future? Science (1979). 302, 792–793 (2003). https://doi.org/10.1126/science.1090313
14. Welton, T.: Ionic liquids: a brief history. Biophys Rev. 10, 691–706 (2018). https://doi.org/10.1007/s12551-018-0419-2
15. P. Walden: Molecular weights and electrical conductivity of several fused salts. Bull. Acad. Imper. Sci. 8, (1914)
16. Wells, A.S., Coombe, V.T.: On the freshwater ecotoxicity and biodegradation properties of some common ionic liquids. Org Process Res Dev. 10, 794–798 (2006). https://doi.org/10.1021/op060048i

17. P.M., A., Rodriguez, O., A., E.: New Generations of Ionic Liquids Applied to Enzymatic Biocatalysis. Ionic Liquids - New Aspects for the Future. (2013). https://doi.org/10.5772/51897

18. Gorke, J., Srienc, F., Kazlauskas, R.: Toward advanced ionic liquids. Polar, enzyme-friendly solvents for biocatalysis. Biotechnology and Bioprocess Engineering. 15, 40–53 (2010). https://doi.org/10.1007/s12257-009-3079-z

19. Wilkes, J.S., Levisky, J.A., Wilson, R.A., Hussey, C.L.: Dialkylimidazolium. Encyclopedia of Lubricants and Lubrication. 237, 374–374 (2014). https://doi.org/10.1007/978-3-642-22647-2_100172

20. Dong, K., Liu, X., Dong, H., Zhang, X., Zhang, S.: Multiscale Studies on Ionic Liquids. Chem Rev. 117, 6636–6695 (2017). https://doi.org/10.1021/acs.chemrev.6b00776

21. Cai, M., Yu, Q., Liu, W., Zhou, F.: Ionic liquid lubricants: When chemistry meets tribology. Chem Soc Rev. 49, 7753–7818 (2020). https://doi.org/10.1039/d0cs00126k

22. Plechkova, N. v., Seddon, K.R.: Applications of ionic liquids in the chemical industry. Chem Soc Rev. 37, 123–150 (2008). https://doi.org/10.1039/b006677j

23. Somers, A.E., Biddulph, S.M., Howlett, P.C., Sun, J., MacFarlane, D.R., Forsyth, M.: A comparison of phosphorus and fluorine containing IL lubricants for steel on aluminium. Physical Chemistry Chemical Physics. 14, 8224–8231 (2012). https://doi.org/10.1039/c2cp40736a

24. Zhou, Y., Dyck, J., Graham, T.W., Luo, H., Leonard, D.N., Qu, J.: Ionic liquids composed of phosphonium cations and organophosphate, carboxylate, and sulfonate anions as lubricant antiwear additives. Langmuir. 30, 13301–13311 (2014). https://doi.org/10.1021/la5032366

25. Sharma, V., Doerr, N., Aswath, P.B.: Chemical-mechanical properties of tribofilms and their relationship to ionic liquid chemistry. RSC Adv. 6, 22341–22356 (2016). https://doi.org/10.1039/c6ra01915c

26. Gusain, R., Khatri, O.P.: Halogen-free ionic liquids: Effect of chelated orthoborate anion structure on their lubrication properties. RSC Adv. 5, 25287–25294 (2015). https://doi.org/10.1039/c5ra03092g

27. Holbrey, J.D., Seddon, K.R.: Tetrafluoroborates ; Ionic Liquids and Ionic Liquid Crystals. 2133–2139 (1999)

28. Ngo, H.L., LeCompte, K., Hargens, L., McEwen, A.B.: Thermal properties of imidazolium ionic liquids. Thermochim Acta. 357–358, 97–102 (2000). https://doi.org/10.1016/S0040-6031(00)00373-7

29. Gordon, C.M., Holbrey, J.D., Kennedy, A.R., Seddon, K.R.: Ionic liquid crystals: Hexafluorophosphate salts. J Mater Chem. 8, 2627–2636 (1998). https://doi.org/10.1039/a806169f

30. Zheng, W., Mohammed, A., Hines, L.G., Xiao, D., Martinez, O.J., Bartsch, R.A., Simon, S.L., Russina, O., Triolo, A., Quitevis, E.L.: Effect of cation symmetry on the morphology and physicochemical properties of imidazolium ionic liquids. Journal of Physical Chemistry B. 115, 6572–6584 (2011). https://doi.org/10.1021/jp1115614

31. Fredlake, C.P., Crosthwaite, J.M., Hert, D.G., Aki, S.N.V.K., Brennecke, J.F.: Thermophysical properties of imidazolium-based ionic liquids. J Chem Eng Data. 49, 954–964 (2004). https://doi.org/10.1021/je034261a

32. Xue, L., Gurung, E., Tamas, G., Koh, Y.P., Shadeck, M., Simon, S.L., Maroncelli, M., Quitevis, E.L.: Effect of Alkyl Chain Branching on Physicochemical Properties of Imidazolium-Based Ionic Liquids. J Chem Eng Data. 61, 1078–1091 (2016). https://doi.org/10.1021/acs.jced.5b00658

33. Zeng, Z., Phillips, B.S., Xiao, J.C., Shreeve, J.M.: Polyfluoroalkyl, polyethylene glycol, 1,4-bismethylenebenzene, or 1,4-bismethylene-2,3,5,6-tetrafluorobenzene bridged functionalized dicationic ionic liquids: Synthesis and properties as high temperature lubricants. Chemistry of Materials. 20, 2719–2726 (2008). https://doi.org/10.1021/cm703693r

34. Yao, M., Liang, Y., Xia, Y., Zhou, F., Liu, X.: Higherature tribological properties of 2-substituted imidazolium ionic liquids for si 3n 4-steel contacts. Tribol Lett. 32, 73–79 (2008). https://doi.org/10.1007/s11249-008-9364-8

35. Maton, C., de Vos, N., Stevens, C. v.: Ionic liquid thermal stabilities: Decomposition mechanisms and analysis tools. Chem Soc Rev. 42, 5963–5977 (2013). https://doi.org/10.1039/c3cs60071h

36. Sowmiah, S., Srinivasadesikan, V., Tseng, M.C., Chu, Y.H.: On the chemical stabilities of ionic liquids. (2009)

37. Tao, R., Tamas, G., Xue, L., Simon, S.L., Quitevis, E.L.: Thermophysical properties of imidazolium-based ionic liquids: The effect of aliphatic versus aromatic functionality. J Chem Eng Data. 59, 2717–2724 (2014). https://doi.org/10.1021/je500185r

38. Shirota, H., Mandai, T., Fukazawa, H., Kato, T.: Comparison between dicationic and monocationic ionic liquids: Liquid density, thermal properties, surface tension, and shear viscosity. J Chem Eng Data. 56, 2453–2459 (2011). https://doi.org/10.1021/je2000183

39. Wooster, T.J., Johanson, K.M., Fraser, K.J., MacFarlane, D.R., Scott, J.L.: Thermal degradation of cyano containing ionic liquids. Green Chemistry. 8, 691–69 (2006). https://doi.org/10.1039/b606395k

40. Salgado, J., Villanueva, M., Parajó, J.J., Fernández, J.: Long-term thermal stability of five imidazolium ionic liquids. Journal of Chemical Thermodynamics. 65, 184–190 (2013). https://doi.org/10.1016/j.jct.2013.05.049

41. Salgado, J., Parajó, J.J., Fernández, J., Villanueva, M.: Long-term thermal stability of some 1-butyl-1-methylpyrrolidinium ionic liquids. Journal of Chemical Thermodynamics. 74, 51–57 (2014). https://doi.org/10.1016/j.jct.2014.03.030

42. Minami, I., Kamimura, H., Mori, S.: Thermo-oxidative stability of ionic liquids as lubricating fluids. Society of Tribologists and Lubrication Engineers - 62nd Annual Meeting of the Society of Tribologists and Lubrication Engineers 2007. 2, 1038–1040 (2007). https://doi.org/10.1002/jsl

43. Ye, C., Liu, W., Chen, Y., Yu, L.: Room-temperature ionic liquids: A novel versatile lubricant. Chemical Communications. 21, 2244–2245 (2001). https://doi.org/10.1039/b106935g

44. Minami, I.: Ionic liquids in tribology. Molecules. 14, 2286–2305 (2009). https://doi.org/10.3390/molecules14062286

45. Zhou, F., Liang, Y., Liu, W.: Ionic liquid lubricants: Designed chemistry for engineering applications. Chem Soc Rev. 38, 2590–2599 (2009). https://doi.org/10.1039/b817899m

46. Minami, I., Inada, T., Sasaki, R., Nanao, H.: Tribo-chemistry of phosphonium-derived ionic liquids. Tribol Lett. 40, 225–235 (2010). https://doi.org/10.1007/s11249-010-9626-0

47. Perkin, S.: Ionic liquids in confined geometries. Physical Chemistry Chemical Physics. 14, 5052–5062 (2012). https://doi.org/10.1039/c2cp23814d

48. Iglesias, P., Bermúdez, M.D., Carrión, F.J., Martínez-Nicolás, G.: Friction and wear of aluminium-steel contacts lubricated with ordered fluids-neutral and ionic liquid crystals as oil additives. Wear. 256, 386–392 (2004). https://doi.org/10.1016/S0043-1648(03)00442-3

49. Palacio, M., Bhushan, B.: A review of ionic liquids for green molecular lubrication in nanotechnology. Tribol Lett. 40, 247–268 (2010). https://doi.org/10.1007/s11249-010-9671-8

50. Phillips, B.S., Zabinski, J.S.: Ionic liquid lubrication effects on ceramics in a water environment. Tribol Lett. 17, 533–541 (2004). https://doi.org/10.1023/B:TRIL.0000044501.64351.68

51. Blanco, D., Battez, A.H., Viesca, J.L., González, R., Fernández-González, A.: Lubrication of CrN coating with ethyl-dimethyl-2-methoxyethylammonium tris(pentafluoroethyl)trifluorophosphate ionic liquid as additive to PAO 6. Tribol Lett. 41, 295–302 (2011). https://doi.org/10.1007/s11249-010-9714-1

52. Qu, J., Bansal, D.G., Yu, B., Howe, J.Y., Luo, H., Dai, S., Li, H., Blau, P.J., Bunting, B.G., Mordukhovich, G., Smolenski, D.J.: Antiwear performance and mechanism of an oil-miscible ionic liquid as a lubricant additive. ACS Appl Mater Interfaces. 4, 997–1002 (2012). https://doi.org/10.1021/am201646k

53. Yu, B., Bansal, D.G., Qu, J., Sun, X., Luo, H., Dai, S., Blau, P.J., Bunting, B.G., Mordukhovich, G., Smolenski, D.J.: Oil-miscible and non-corrosive phosphonium-based ionic liquids as candidate lubricant additives. Wear. 289, 58–64 (2012). https://doi.org/10.1016/j.wear.2012.04.015

54. Qu, J., Bansal, D.G., Yu, B., Howe, J.Y., Luo, H., Dai, S., Li, H., Blau, P.J., Bunting, B.G., Mordukhovich, G., Smolenski, D.J.: Antiwear performance and mechanism of an oil-miscible ionic liquid as a lubricant additive. ACS Appl Mater Interfaces. 4, 997–1002 (2012). https://doi.org/10.1021/am201646k

55. Barnhill, W.C., Luo, H., Meyer, H.M., Ma, C., Chi, M., Papke, B.L., Qu, J.: Tertiary and Quaternary Ammonium-Phosphate Ionic Liquids as Lubricant Additives. Tribol Lett. 63, (2016). https://doi.org/10.1007/s11249-016-0707-6

56. Barnhill, W.C., Qu, J., Luo, H., Meyer, H.M., Ma, C., Chi, M., Papke, B.L.: Phosphonium-organophosphate ionic liquids as lubricant additives: Effects of cation structure on physicochemical and tribological characteristics. ACS Appl Mater Interfaces. 6, 22585–22593 (2014). https://doi.org/10.1021/am506702u

57. Otero, I., López, E.R., Reichelt, M., Villanueva, M., Salgado, J., Fernández, J.: Ionic liquids based on phosphonium cations As neat lubricants or lubricant additives for a steel/steel contact. ACS Appl Mater Interfaces. 6, 13115–13128 (2014). https://doi.org/10.1021/am502980m

58. González, R., Bartolomé, M., Blanco, D., Viesca, J.L., Fernández-González, A., Battez, A.H.: Effectiveness of phosphonium cation-based ionic liquids as lubricant additive. Tribol Int. 98, 82–93 (2016). https://doi.org/10.1016/j.triboint.2016.02.016

59. Somers, A.E., Khemchandani, B., Howlett, P.C., Sun, J., Macfarlane, D.R., Forsyth, M.: Ionic liquids as antiwear additives in base oils: Influence of structure on miscibility and antiwear performance for steel on aluminum. ACS Appl Mater Interfaces. 5, 11544–11553 (2013). https://doi.org/10.1021/am4037614

60. Fu, X., Sun, L., Zhou, X., Li, Z., Ren, T.: Tribological Study of Oil-Miscible Quaternary Ammonium Phosphites Ionic Liquids as Lubricant Additives in PAO. Tribol Lett. 60, 1–12 (2015). https://doi.org/10.1007/s11249-015-0596-0

61. S U S Chao, E.J.A.: Enhancing thermal conductivity of fluids with nanoparticles A metal-organic vapor phase epitaxy system for advanced in situ x-ray studies of III-nitride growth View project in situ oxide growth by radio frequency-magnetron sputtering View project.

62. Gulzar, M., Masjuki, H.H., Kalam, M.A., Varman, M., Zulkifli, N.W.M., Mufti, R.A., Zahid, R.: Tribological performance of nanoparticles as lubricating oil additives. Journal of Nanoparticle Research. 18, 1–25 (2016). https://doi.org/10.1007/s11051-016-3537-4

63. Kong, L., Sun, J., Bao, Y.: Preparation, characterization and tribological mechanism of nanofluids. RSC Adv. 7, 12599–12609 (2017). https://doi.org/10.1039/c6ra28243a

64. Uflyand, I.E., Zhinzhilo, V.A., Burlakova, V.E.: Metal-containing nanomaterials as lubricant additives: State-of-the-art and future development. Friction. 7, 93–116 (2019). https://doi.org/10.1007/s40544-019-0261-y

65. Dai, W., Kheireddin, B., Gao, H., Liang, H.: Roles of nanoparticles in oil lubrication. Tribol Int. 102, 88–98 (2016). https://doi.org/10.1016/j.triboint.2016.05.020

66. Chen, Y., Renner, P., Liang, H.: Dispersion of nanoparticles in lubricating oil: A critical review. Lubricants. 7, (2019). https://doi.org/10.3390/lubricants7010007

67. Zhou, Y., Qu, J.: Ionic liquids as lubricant additives: A review. ACS Appl Mater Interfaces. 9, 3209–3222 (2017). https://doi.org/10.1021/acsami.6b12489

68. Qu, J., Barnhill, W.C., Luo, H., Meyer, H.M., Leonard, D.N., Landauer, A.K., Kheireddin, B., Gao, H., Papke, B.L., Dai, S.: Synergistic Effects between Phosphonium-Alkylphosphate Ionic Liquids and Zinc Dialkyldithiophosphate (ZDDP) as Lubricant Additives. Advanced Materials. 27, 4767–4774 (2015). https://doi.org/10.1002/adma.201502037

69. Li, Y., Zhang, S., Ding, Q., Li, H., Qin, B., Hu, L.: Understanding the synergistic lubrication effect of 2-mercaptobenzothiazolate based ionic liquids and Mo nanoparticles as hybrid additives. Tribol Int. 125, 39–45 (2018). https://doi.org/10.1016/j.triboint.2018.04.019

70. Sanes, J., Avilés, M.D., Saurín, N., Espinosa, T., Carrión, F.J., Bermúdez, M.D.: Synergy between graphene and ionic liquid lubricant additives. Tribol Int. 116, 371–382 (2017). https://doi.org/10.1016/j.triboint.2017.07.030

71. Gusain, R., Mungse, H.P., Kumar, N., Ravindran, T.R., Pandian, R., Sugimura, H., Khatri, O.P.: Covalently attached graphene-ionic liquid hybrid nanomaterials: Synthesis, characterization and tribological application. J Mater Chem A Mater. 4, 926–937 (2016). https://doi.org/10.1039/c5ta08640j

72. Fan, X., Wang, L.: High-performance lubricant additives based on modified graphene oxide by ionic liquids. J Colloid Interface Sci. 452, 98–108 (2015). https://doi.org/10.1016/j.jcis.2015.04.025

73. Li, Z., Ren, T.: Synergistic effects between alkylphosphate-ammonium ionic liquid and alkylphenylborate as lubricant additives in rapeseed oil. Tribol Int. 109, 373–381 (2017). https://doi.org/10.1016/j.triboint.2016.11.032

74. Nasser, K.I., Liñeira del Río, J.M., López, E.R., Fernández, J.: Synergistic effects of hexagonal boron nitride nanoparticles and phosphonium ionic liquids as hybrid lubricant additives. J Mol Liq. 311, 113343 (2020). https://doi.org/10.1016/j.molliq.2020.113343

75. Seymour, B.T., Fu, W., Wright, R.A.E., Luo, H., Qu, J., Dai, S., Zhao, B.: Improved Lubricating Performance by Combining Oil-Soluble Hairy Silica Nanoparticles and an

Ionic Liquid as an Additive for a Synthetic Base Oil. ACS Appl Mater Interfaces. 10, 15129–15139 (2018). https://doi.org/10.1021/acsami.8b01579

76. Zhang, Y., Xu, Y., Yang, Y., Zhang, S., Zhang, P., Zhang, Z.: Synthesis and tribological properties of oil-soluble copper nanoparticles as environmentally friendly lubricating oil additives. Industrial Lubrication and Tribology. 67, 227–232 (2015). https://doi.org/10.1108/ILT-10-2012-0098

77. Dong, J., Chen, G.: Preparation of Ni nanoparticles and evaluation of their tribological performance as potential additives in oils. J Tribol. 123, 441–443 (2001). https://doi.org/10.1115/1.1286152

78. Xia, W., Zhao, J., Wu, H., Jiao, S., Zhao, X., Zhang, X., Xu, J., Jiang, Z.: Analysis of oil-in-water based nanolubricants with varying mass fractions of oil and TiO2 nanoparticles. Wear. 396–397, 162–171 (2018). https://doi.org/10.1016/j.wear.2017.02.031

79. Gulzar, M., Masjuki, H., Varman, M., Kalam, M., Mufti, R.A., Zulkifli, N., Yunus, R., Zahid, R.: Improving the AW/EP ability of chemically modified palm oil by adding CuO and MoS2 nanoparticles. Tribol Int. 88, 271–279 (2015). https://doi.org/10.1016/j.triboint.2015.03.035

80. Mousavi, S.B., Heris, S.Z., Estellé, P.: Experimental comparison between ZnO and MoS2 nanoparticles as additives on performance of diesel oil-based nano lubricant. Sci Rep. 10, 1–17 (2020). https://doi.org/10.1038/s41598-020-62830-1

81. Kotia, A., Borkakoti, S., Ghosh, S.K.: Wear and performance analysis of a 4-stroke diesel engine employing nanolubricants. Particuology. 37, 54–63 (2018). https://doi.org/10.1016/j.partic.2017.05.016

82. Upendra, M., Vasu, V.: Synergistic Effect Between Phosphonium-Based Ionic Liquid and Three Oxide Nanoparticles as Hybrid Lubricant Additives. J Tribol. (2020). https://doi.org/10.1115/1.4045769

83. Meng, Y., Su, F., Chen, Y.: Effective lubricant additive of nano-Ag/MWCNTs nanocomposite produced by supercritical CO2 synthesis. Tribol Int. 118, 180–188 (2018). https://doi.org/10.1016/j.triboint.2017.09.037

84. Gulzar, M., Masjuki, H.H., Kalam, M.A., Varman, M., Zulkifli, N.W.M., Mufti, R.A., Zahid, R., Yunus, R.: Dispersion Stability and Tribological Characteristics of TiO2/SiO2 Nanocomposite-Enriched Biobased Lubricant. Tribology Transactions. 60, 670–680 (2017). https://doi.org/10.1080/10402004.2016.1202366

85. Saini, V., Bijwe, J., Seth, S., Ramakumar, S.S.V.: Interfacial interaction of PTFE sub-micron particles in oil with steel surfaces as excellent extreme-pressure additive. J Mol Liq. 115238 (2020). https://doi.org/10.1016/j.molliq.2020.115238

86. Gong, K., Lou, W., Zhao, G., Wu, X., Wang, X.: Investigation on tribological behaviors of MoS2 and WS2 quantum dots as lubricant additives in ionic liquids under

severe conditions. Friction. 8, 674–683 (2020). https://doi.org/10.1007/s40544-019-0290-6

87. Rapoport, L., Leshchinsky, V., Lapsker, I., Volovik, Y., Nepomnyashchy, O., Lvovsky, M., Popovitz-Biro, R., Feldman, Y., Tenne, R.: Tribological properties of WS2 nanoparticles under mixed lubrication. Wear. 255, 785–793 (2003). https://doi.org/10.1016/S0043-1648(03)00044-9

88. Gupta, M.K., Bijwe, J., Kadiyala, A.K.: Tribo-Investigations on Oils with Dispersants and Hexagonal Boron Nitride Particles. J Tribol. 140, (2018). https://doi.org/10.1115/1.4038105

89. Saini, V., Seth, S., Ramakumar, S.S. v., Bijwe, J.: Carbon Nanoparticles of Varying Shapes as Additives in Mineral Oil Assessment of Comparative Performance Potential. ACS Appl Mater Interfaces. (2021). https://doi.org/10.1021/acsami.1c09478

90. Paul, G., Hirani, H., Kuila, T., Murmu, N.C.: Nanolubricants dispersed with graphene and its derivatives: An assessment and review of the tribological performance. Nanoscale. 11, 3458–3483 (2019). https://doi.org/10.1039/c8nr08240e

91. Chang, Q.Y., Wang, B., Gao, K.: Pressure-dependent anti-wear mechanisms of synthetic magnesium silicate hydroxide nanoparticles. Tribol Int. 135, 230–236 (2019). https://doi.org/10.1016/j.triboint.2019.03.016

92. Chang, Q., Rudenko, P., Miller, D.J., Wen, J., Berman, D., Zhang, Y., Arey, B., Zhu, Z., Erdemir, A.: Operando formation of an ultra-low friction boundary film from synthetic magnesium silicon hydroxide additive. Tribol Int. 110, 35–40 (2017). https://doi.org/10.1016/j.triboint.2017.02.003

93. Gao, R., Liu, W., Chang, Q., Zhang, H., Liu, Y.: Tribological property of biocarbon-based magnesium silicate hydroxide nanocomposite as lubricant additive at different concentrations of additive and dispersant, (2021)

94. Gao, K., Chang, Q., Wang, B., Zhou, N., Qing, T.: The tribological performances of modified magnesium silicate hydroxide as lubricant additive. Tribol Int. 121, 64–70 (2018). https://doi.org/10.1016/j.triboint.2018.01.022

95. Qi, X., Lu, L., Jia, Z., Yang, Y., Liu, H.: Comparative tribological properties of magnesium hexasilicate and serpentine powder as lubricating oil additives under High temperature. Tribol Int. 49, 53–57 (2012). https://doi.org/10.1016/j.triboint.2011.12.014

96. Zhang, B., Xu, Y., Gao, F., Shi, P., Xu, B., Wu, Y.: Sliding friction and wear behaviors of surface-coated natural serpentine mineral powders as lubricant additive. Appl Surf Sci. 257, 2540–2549 (2011). https://doi.org/10.1016/j.apsusc.2010.10.019

97. Yu, H., Xu, Y., Shi, P., Wang, H., Wei, M., Zhao, K., Xu, B.: Microstructure, mechanical properties and tribological behavior of tribofilm generated from natural

serpentine mineral powders as lubricant additive. Wear. 297, 802–810 (2013). https://doi.org/10.1016/j.wear.2012.10.013

98. Rudenko, P., Bandyopadhyay, A.: Talc as friction reducing additive to lubricating oil. Appl Surf Sci. 276, 383–389 (2013). https://doi.org/10.1016/j.apsusc.2013.03.102

99. Saini, V., Bijwe, J., Seth, S., Ramakumar, S.S.V.: Potential exploration of nano-talc particles for enhancing the anti-wear and extreme pressure performance of oil. Tribol Int. 151, 106452 (2020). https://doi.org/10.1016/j.triboint.2020.106452

100. Zanganeh, S., Kajbafvala, A., Zanganeh, N., Mohajerani, M.S., Lak, A., Bayati, M.R., Zargar, H.R., Sadrnezhaad, S.K.: Self-assembly of boehmite nanopetals to form 3D high surface area nanoarchitectures. Appl Phys A Mater Sci Process. 99, 317–321 (2010). https://doi.org/10.1007/s00339-009-5534-2

101. Laachachi, A., Ferriol, M., Cochez, M., Lopez Cuesta, J.M., Ruch, D.: A comparison of the role of boehmite (AlOOH) and alumina (Al2O3) in the thermal stability and flammability of poly(methyl methacrylate). Polym Degrad Stab. 94, 1373–1378 (2009). https://doi.org/10.1016/j.polymdegradstab.2009.05.014

102. Wilson, S.J.: The dehydration of boehmite, γ-AlOOH, to γ-Al2O3. J Solid State Chem. 30, 247–255 (1979). https://doi.org/10.1016/0022-4596(79)90106-3

103. Mohammad, A., Morteza, L., Mehdi, M., Kamazani, M., Zarghami, Z.: Rice-like Ag / Al 2 O 3 nanocomposites preparation from AlOOH nanostructures synthesized via a facile hydrothermal route for azo dyes photocatalytic degradation and Pb 2 + adsorption. Journal of Materials Science: Materials in Electronics. 29, 10234–10245 (2018). https://doi.org/10.1007/s10854-018-9074-4

104. Munusamy, G., Varadharajan, K., Narasimhan, S., Thangapandiyan, U.G.: Investigations on γ -AlOOH and NiWO4 coated boehmite micro / nanostructure under UV / visible light Photocatalysis. Research on Chemical Intermediates. (2018). https://doi.org/10.1007/s11164-018-3588-5

105. Huo, W., Li, L., Zhang, Y., Li, J., Xu, Q., Zhang, B., Zhang, L., Li, X.: Monodispersed hierarchical γ-ALOOH/Fe(OH)3 micro/nanoflowers for efficient oxygen evolution reaction. Front Mater. 6, 1–8 (2019). https://doi.org/10.3389/fmats.2019.00154

106. Forest, V., Pailleux, M., Pourchez, J., Boudard, D., Tomatis, M., Fubini, B., Sennour, M., Hochepied, J.F., Grosseau, P., Cottier, M.: Toxicity of boehmite nanoparticles: Impact of the ultrafine fraction and of the agglomerates size on cytotoxicity and pro-inflammatory response. Inhal Toxicol. 26, 545–553 (2014). https://doi.org/10.3109/08958378.2014.925993

107. Wu, L., Zhang, Y., Yang, G., Zhang, S., Yu, L., Zhang, P.: Tribological properties of oleic acid-modified zinc oxide nanoparticles as the lubricant additive in poly-alpha olefin and diisooctyl sebacate base oils. RSC Adv. 6, 69836–69844 (2016). https://doi.org/10.1039/c6ra10042b

108. Sarkar, M., Sarkar, S., Biswas, A., De, S., Kumar, P.R., Mothi, E.M., Kathiravan, A.: Zinc titanate nanomaterials—photocatalytic studies and sensitization of hydantoin derivatized porphyrin dye. Nano-Structures and Nano-Objects. 21, 100412 (2020). https://doi.org/10.1016/j.nanoso.2019.100412

109. Sanes, J., Avilés, M.D., Saurín, N., Espinosa, T., Carrión, F.J., Bermúdez, M.D.: Synergy between graphene and ionic liquid lubricant additives. Tribol Int. 116, 371–382 (2017). https://doi.org/10.1016/j.triboint.2017.07.030

110. Qu, J., Barnhill, W.C., Luo, H., Meyer, H.M., Leonard, D.N., Landauer, A.K., Kheireddin, B., Gao, H., Papke, B.L., Dai, S.: Synergistic Effects between Phosphonium-Alkylphosphate Ionic Liquids and Zinc Dialkyldithiophosphate (ZDDP) as Lubricant Additives. Advanced Materials. 27, 4767–4774 (2015). https://doi.org/10.1002/adma.201502037

111. Saini, V., Bijwe, J., Seth, S., Ramakumar, S.S.V.: Unexplored solid lubricity of Titanium nanoparticles in oil to modify the metallic interfaces. Appl Surf Sci. 580, 152127 (2022). https://doi.org/10.1016/J.APSUSC.2021.152127

112. Sun, J., Howlett, P.C., MacFarlane, D.R., Lin, J., Forsyth, M.: Synthesis and physical property characterisation of phosphonium ionic liquids based on P(O)2(OR)2- and P(O)2(R)2- anions with potential application for corrosion mitigation of magnesium alloys. Electrochim Acta. 54, 254–260 (2008). https://doi.org/10.1016/j.electacta.2008.08.020

113. Shahnazar, S., Bagheri, S., Abd Hamid, S.B.: Enhancing lubricant properties by nanoparticle additives. Int J Hydrogen Energy. 41, 3153–3170 (2016). https://doi.org/10.1016/j.ijhydene.2015.12.040

114. Kong, L., Sun, J., Bao, Y.: Preparation, characterization and tribological mechanism of nanofluids. RSC Adv. 7, 12599–12609 (2017). https://doi.org/10.1039/c6ra28243a

115. Rapoport, L., Leshchinsky, V., Lapsker, I., Volovik, Y., Nepomnyashchy, O., Lvovsky, M., Popovitz-Biro, R., Feldman, Y., Tenne, R.: Tribological properties of WS2 nanoparticles under mixed lubrication. Wear. 255, 785–793 (2003). https://doi.org/10.1016/S0043-1648(03)00044-9

116. Gulzar, M., Masjuki, H., Varman, M., Kalam, M., Mufti, R.A., Zulkifli, N., Yunus, R., Zahid, R.: Improving the AW/EP ability of chemically modified palm oil by adding CuO and MoS<inf>2</inf> nanoparticles. Tribol Int. 88, 271–279 (2015). https://doi.org/10.1016/j.triboint.2015.03.035

117. Kato, H., Komai, K.: Tribofilm formation and mild wear by tribo-sintering of nanometer-sized oxide particles on rubbing steel surfaces. Wear. 262, 36–41 (2007). https://doi.org/10.1016/j.wear.2006.03.046

118. Chen, Q., Zheng, S., Yang, S., Li, W., Song, X., Cao, B.: Enhanced tribology properties of ZnO/Al2O3 composite nanoparticles as liquid lubricating additives. J Solgel Sci Technol. 61, 501–508 (2012). https://doi.org/10.1007/s10971-011-2651-0

119. Xu, J.F., Ji, W., Shen, Z.X., Li, W.S., Tang, S.H., Ye, X.R., Jia, D.Z., Xin, X.Q.: Raman spectra of CuO nanocrystals. Journal of Raman Spectroscopy. 30, 413–415 (1999). https://doi.org/10.1002/(SICI)1097-4555(199905)30:5<413::AID-JRS387>3.0.CO;2-N

120. KRISHNAN, R.S.: Raman Spectrum of Alumina and the Luminescence and Absorption Spectra of Ruby. Nature. 160, 26–26 (1947). https://doi.org/10.1038/160026a0

121. Spikes, H.: Friction Modifier Additives. Tribol Lett. 60, (2015). https://doi.org/10.1007/s11249-015-0589-z

122. Rizvi, S.Q.A.: A Comprehensive Review of Lubricant Chemistry, Technology, Selection, and Design. (2009)

123. Qu, J., Bansal, D.G., Yu, B., Howe, J.Y., Luo, H., Dai, S., Li, H., Blau, P.J., Bunting, B.G., Mordukhovich, G., Smolenski, D.J.: Antiwear performance and mechanism of an oil-miscible ionic liquid as a lubricant additive. ACS Appl Mater Interfaces. 4, 997–1002 (2012). https://doi.org/10.1021/am201646k

124. Barnhill, W.C., Qu, J., Luo, H., Meyer, H.M., Ma, C., Chi, M., Papke, B.L.: Phosphonium-organophosphate ionic liquids as lubricant additives: Effects of cation structure on physicochemical and tribological characteristics. ACS Appl Mater Interfaces. 6, 22585–22593 (2014). https://doi.org/10.1021/am506702u

125. Zhou, Y., Qu, J.: Ionic liquids as lubricant additives: A review. ACS Appl Mater Interfaces. 9, 3209–3222 (2017). https://doi.org/10.1021/acsami.6b12489

126. Alves, S.M., Barros, B.S., Trajano, M.F., Ribeiro, K.S.B., Moura, E.: Tribological behavior of vegetable oil-based lubricants with nanoparticles of oxides in boundary lubrication conditions. Tribol Int. 65, 28–36 (2013). https://doi.org/10.1016/j.triboint.2013.03.027

127. Abdullah, M.I.H.C., Abdollah, M.F. Bin, Amiruddin, H., Tamaldin, N., Nuri, N.R.M., Hassan, M., Rafeq, S.A.: Improving engine oil properties by dispersion of hBN/Al2O3 nanoparticles. Applied Mechanics and Materials. 607, 70–73 (2014). https://doi.org/10.4028/www.scientific.net/AMM.607.70

128. Ramteke, S.M., Chelladurai, H.: Effects of hexagonal boron nitride based nanofluid on the tribological and performance, emission characteristics of a diesel engine: An experimental study. Engineering Reports. 2, 1–20 (2020). https://doi.org/10.1002/eng2.12216

129. Wan, Q., Jin, Y., Sun, P., Ding, Y.: Tribological behaviour of a lubricant oil containing boron nitride nanoparticles. Procedia Eng. 102, 1038–1045 (2015). https://doi.org/10.1016/j.proeng.2015.01.226

130. Kato, H., Komai, K.: Tribofilm formation and mild wear by tribo-sintering of nanometer-sized oxide particles on rubbing steel surfaces. Wear. 262, 36–41 (2007). https://doi.org/10.1016/j.wear.2006.03.046

131. Li, W., Kumara, C., Luo, H., Meyer, H.M., He, X., Ngo, D., Kim, S.H., Qu, J.: Ultralow Boundary Lubrication Friction by Three-Way Synergistic Interactions among Ionic Liquid, Friction Modifier, and Dispersant. ACS Appl Mater Interfaces. 12, 17077–17090 (2020). https://doi.org/10.1021/acsami.0c00980

132. Saini, V., Bijwe, J., Seth, S., Ramakumar, S.S.V.: Role of base oils in developing extreme pressure lubricants by exploring nano-PTFE particles. Tribol Int. 143, 106071 (2020). https://doi.org/10.1016/j.triboint.2019.106071

133. Li, Z., Ren, T.: Synergistic effects between alkylphosphate-ammonium ionic liquid and alkylphenylborate as lubricant additives in rapeseed oil. Tribol Int. 109, 373–381 (2017). https://doi.org/10.1016/j.triboint.2016.11.032

134. Zhang, J., Spikes, H.: On the Mechanism of ZDDP Antiwear Film Formation. Tribol Lett. 63, 1–15 (2016). https://doi.org/10.1007/s11249-016-0706-7

135. Anand, M., Hadfield, M., Viesca, J.L., Thomas, B., Hernández Battez, A., Austen, S.: Ionic liquids as tribological performance improving additive for in-service and used fully-formulated diesel engine lubricants. Wear. 334–335, 67–74 (2015). https://doi.org/10.1016/j.wear.2015.01.055

136. Zhou, Y., Dyck, J., Graham, T.W., Luo, H., Leonard, D.N., Qu, J.: Ionic liquids composed of phosphonium cations and organophosphate, carboxylate, and sulfonate anions as lubricant antiwear additives. Langmuir. 30, 13301–13311 (2014). https://doi.org/10.1021/la5032366

137. Westerholt, A., Weschta, M., Bösmann, A., Tremmel, S., Korth, Y., Wolf, M., Schlücker, E., Wehrum, N., Lennert, A., Uerdingen, M., Holweger, W., Wartzack, S., Wasserscheid, P.: Halide-Free Synthesis and Tribological Performance of Oil-Miscible Ammonium and Phosphonium-Based Ionic Liquids. ACS Sustain Chem Eng. 3, 797–808 (2015). https://doi.org/10.1021/sc500517n

138. Barnhill, W.C., Luo, H., Meyer, H.M., Ma, C., Chi, M., Papke, B.L., Qu, J.: Tertiary and Quaternary Ammonium-Phosphate Ionic Liquids as Lubricant Additives. Tribol Lett. 63, (2016). https://doi.org/10.1007/s11249-016-0707-6

139. Kimura, Y., Wakabayashi, T., Okada, K., Wada, T., Nishikawa, H.: Boron nitride as a lubricant additive. Wear. 232, 199–206 (1999). https://doi.org/10.1016/S0043-1648(99)00146-5

140. Rastogi, P.K., Sahoo, K.R., Thakur, P., Sharma, R., Bawari, S., Podila, R., Narayanan, T.N.: Graphene–hBN non-van der Waals vertical heterostructures for four-electron oxygen reduction reaction. (2019). https://doi.org/10.1039/C8CP06155F

141. Holmberg, K., Erdemir, A.: Influence of tribology on global energy consumption, costs and emissions. Friction. 5, 263–284 (2017). https://doi.org/10.1007/s40544-017-0183-5

142. Wells, S.: Transactions. Journal of the Society of Chemical Industry. 39, T51–T66 (1920). https://doi.org/10.1002/jctb.5000390517

143. Spikes, H.: The history and mechanisms of ZDDP. Tribol Lett. 17, 469–489 (2004). https://doi.org/10.1023/B:TRIL.0000044495.26882.b5

144. Maurya, U., Vasu, V., Kashinath, D.: Ionic Liquid-Nanoparticle-Based Hybrid-Nanolubricant Additives for Potential Enhancement of Tribological Properties of Lubricants and Their Comparative Study with ZDDP. Tribol Lett. 70, 11 (2022). https://doi.org/10.1007/s11249-021-01551-6

145. Gusain, R., Mungse, H.P., Kumar, N., Ravindran, T.R., Pandian, R., Sugimura, H., Khatri, O.P.: Covalently attached graphene-ionic liquid hybrid nanomaterials: Synthesis, characterization and tribological application. J Mater Chem A Mater. 4, 926–937 (2016). https://doi.org/10.1039/c5ta08640j

146. Fan, X., Wang, L.: High-performance lubricant additives based on modified graphene oxide by ionic liquids. J Colloid Interface Sci. 452, 98–108 (2015). https://doi.org/10.1016/j.jcis.2015.04.025

147. American Petroleum Institute: Engine Oil Licensing and Certification System Seventeenth Edition. API 1509 Appendix E (2021)

148. Qu, J., Luo, H., Chi, M., Ma, C., Blau, P.J., Dai, S., Viola, M.B.: Comparison of an oil-miscible ionic liquid and ZDDP as a lubricant anti-wear additive. Tribol Int. 71, 88–97 (2014). https://doi.org/10.1016/j.triboint.2013.11.010

149. Fan, X., Wang, L.: High-performance lubricant additives based on modified graphene oxide by ionic liquids. J Colloid Interface Sci. 452, 98–108 (2015). https://doi.org/10.1016/j.jcis.2015.04.025

150. Seymour, B.T., Fu, W., Wright, R.A.E., Luo, H., Qu, J., Dai, S., Zhao, B.: Improved Lubricating Performance by Combining Oil-Soluble Hairy Silica Nanoparticles and an Ionic Liquid as an Additive for a Synthetic Base Oil. ACS Appl Mater Interfaces. 10, 15129–15139 (2018). https://doi.org/10.1021/acsami.8b01579

151. Thrush, S.J., Comfort, A.S., Dusenbury, J.S., Xiong, Y., Qu, H., Han, X., Schall, J.D., Barber, G.C., Wang, X.: Stability, Thermal Conductivity, Viscosity, and Tribological Characterization of Zirconia Nanofluids as a Function of Nanoparticle Concentration. Tribology Transactions. 63, 68–76 (2020). https://doi.org/10.1080/10402004.2019.1660017

152. Wang, B., Chang, Q.Y., Gao, K., Fang, H.R., Qing, T., Zhou, N.N.: The synthesis of magnesium silicate hydroxide with different morphologies and the comparison of their

tribological properties. Tribol Int. 119, 672–679 (2018). https://doi.org/10.1016/j.triboint.2017.11.020

153. Qi, X., Jia, Z., Yang, Y., Fan, B.: Characterization and auto-restoration mechanism of nanoscale serpentine powder as lubricating oil additive under high temperature. Tribol Int. 44, 805–810 (2011). https://doi.org/10.1016/j.triboint.2011.02.001

154. Zhang, L., He, Y., Feng, S., Zheng, L., Jiao, Z., Zhan, Y., Wang, Y.: Preparation and tribological properties of novel boehmite/graphene oxide nano-hybrid. Ceram Int. 42, 6178–6186 (2016). https://doi.org/10.1016/j.ceramint.2015.12.178

155. Abdollahifar, M.: Synthesis and characterisation of γ-Al2O3 with porous structure and nanorod morphology. J Chem Res. 38, 154–158 (2014). https://doi.org/10.3184/174751914X13910938972748

156. Abdollahifar, M., Hidaryan, M., Jafari, P.: The role anions on the synthesis of AlOOH nanoparticles using simple solvothermal method. Boletin de la Sociedad Espanola de Ceramica y Vidrio. 57, 66–72 (2018). https://doi.org/10.1016/j.bsecv.2017.06.002

157. Abdollahifar, M., Zamani, M.R., Beiygie, E., Nekouei, H.: Synthesis of micro-mesopores flower-like γ-Al2O 3 nano-architectures. Journal of the Serbian Chemical Society. 79, 1007–1017 (2014). https://doi.org/10.2298/JSC130903007A

158. Yang, J., Frost, R.L.: Synthesis and Characterization of Boehmite Nanofibers. Research Letters in Inorganic Chemistry. 2008, 1–4 (2008). https://doi.org/10.1155/2008/602198

159. Doss, C.J., Zallen, R.: Raman studies of sol-gel alumina: Finite-size effects in nanocrystalline AlO(OH). Phys Rev B. 48, 15626–15637 (1993). https://doi.org/10.1103/PhysRevB.48.15626

160. Assih, T., Ayral, A., Abenoza, M., Phalippou, J.: Raman study of alumina gels. J Mater Sci. 23, 3326–3331 (1988). https://doi.org/10.1007/BF00551313

161. Wang, K., Wang, J., Hu, W.: Evaluation of temperature effect on the corrosion process of 304 stainless steel in high temperature water with electrochemical noise. Mater Des. 82, 155–163 (2015). https://doi.org/10.1016/j.matdes.2015.05.044

162. Lin, B., Zuo, Y.: Corrosion inhibition of carboxylate inhibitors with different alkylene chain lengths on carbon steel in an alkaline solution. RSC Adv. 9, 7065–7077 (2019). https://doi.org/10.1039/C8RA10083G

163. Gartner, N., Kosec, T., Legat, A.: The efficiency of a corrosion inhibitor on steel in a simulated concrete environment. Mater Chem Phys. 184, 31–40 (2016). https://doi.org/10.1016/j.matchemphys.2016.08.047

164. KRISHNAN, R.S.: Raman Spectrum of Alumina and the Luminescence and Absorption Spectra of Ruby. Nature. 160, 26–26 (1947). https://doi.org/10.1038/160026a0

165. Kloprogge, J.T., Duong, L. v., Wood, B.J., Frost, R.L.: XPS study of the major minerals in bauxite: Gibbsite, bayerite and (pseudo-)boehmite. J Colloid Interface Sci. 296, 572–576 (2006). https://doi.org/10.1016/j.jcis.2005.09.054

166. Nylund, A., Olefjord, I.: Surface analysis of oxidized aluminium. 1. Hydration of Al2O3 and decomposition of Al(OH)3 in a vacuum as studied by ESCA. Surface and Interface Analysis. 21, 283–289 (1994). https://doi.org/10.1002/sia.740210504

167. Strohmeier, B.R.: An ESCA method for determining the oxide thickness on aluminum alloys. Surface and Interface Analysis. 15, 51–56 (1990). https://doi.org/10.1002/sia.740150109

168. Barnhill, W.C., Gao, H., Kheireddin, B., Papke, B.L., Luo, H., West, B.H., Qu, J.: Tribological Bench and Engine Dynamometer Tests of a Low Viscosity SAE 0W-16 Engine Oil Using a Combination of Ionic Liquid and ZDDP as Anti-Wear Additives. Front Mech Eng. 1, 1–8 (2015). https://doi.org/10.3389/fmech.2015.00012

169. Mordukhovich, G., Qu, J., Howe, J.Y., Bair, S., Yu, B., Luo, H., Smolenski, D.J., Blau, P.J., Bunting, B.G., Dai, S.: A low-viscosity ionic liquid demonstrating superior lubricating performance from mixed to boundary lubrication. Wear. 301, 740–746 (2013). https://doi.org/10.1016/j.wear.2012.11.076

170. Huang, C., Lv, S., Gao, X., Wang, T., Chen, H., Wu, L.: Solvation CoMFA-QSTR and CoMSIA-QSTR models for predicting the anti-wear properties of lubricant additives. J Tribol. 1–55 (2022). https://doi.org/10.1115/1.4054669

171. Fujita, H., Spikes, H.A.: The formation of zinc dithiophosphate antiwear films. Proceedings of the Institution of Mechanical Engineers, Part J: Journal of Engineering Tribology. 218, 265–277 (2004). https://doi.org/10.1243/1350650041762677

172. Tse, J.S., Song, Y., Liu, Z.: Effects of temperature and pressure on ZDDP. Tribol Lett. 28, 45–49 (2007). https://doi.org/10.1007/s11249-007-9246-5

173. Khare, H.S., Lahouij, I., Jackson, A., Feng, G., Chen, Z., Cooper, G.D., Carpick, R.W.: Nanoscale Generation of Robust Solid Films from Liquid-Dispersed Nanoparticles via in Situ Atomic Force Microscopy: Growth Kinetics and Nanomechanical Properties. ACS Appl Mater Interfaces. 10, 40335–40347 (2018). https://doi.org/10.1021/acsami.8b16680

174. Holmberg, K., Andersson, P., Erdemir, A.: Tribology International Global energy consumption due to friction in passenger cars. Tribiology International. 47, 221–234 (2012). https://doi.org/10.1016/j.triboint.2011.11.022

175. Holmberg, K., Andersson, P., Nylund, N.O., Mäkelä, K., Erdemir, A.: Global energy consumption due to friction in trucks and buses. Tribol Int. 78, 94–114 (2014). https://doi.org/10.1016/j.triboint.2014.05.004

176. Li, S., Ma, Q., Tong, Z., Liu, Q., Dong, G.: Synergistic Lubricating Performance of h-BN/GF Nanoparticles as Oil Additives for Steel-Steel Contact. J Tribol. 144, (2022). https://doi.org/10.1115/1.4053033

177. Kumar, H., Harsha, A.P.: Augmentation in Tribological Performance of Polyalphaolefins by COOH-Functionalized Multiwalled Carbon Nanotubes as an Additive in Boundary Lubrication Conditions. J Tribol. 143, (2021). https://doi.org/10.1115/1.4051392

178. Santhosh Kumar, B., Manikandan, M., Mukilraj, T., Praveen Shankar, N., Venkateswaran, C.: Pentagonal shaped ZnTiO3 ceramics for microwave dielectric applications. Journal of Materials Science: Materials in Electronics. 30, 525–528 (2019). https://doi.org/10.1007/s10854-018-0318-0

179. Farahmand, T., Hashemian, S., Sheibani, A.: ZIF-based zinc titanate composite as sufficient sorbent for removal of Congo red from aqueous solutions. Journal of Asian Ceramic Societies. 8, 721–732 (2020). https://doi.org/10.1080/21870764.2020.1780718

180. Van Der Hoeven, P.C., Lyklema, J.: Electrostatic stabilization in non-aqueous media. Adv Colloid Interface Sci. 42, 205–277 (1992). https://doi.org/10.1016/0001-8686(92)80024-R

181. Gao, B., Yang, C., Chen, J., Ma, Y., Xie, J., Zhang, H., Wei, L., Li, Q., Du, J., Xu, Q.: Ferromagnetic photocatalysts of FeTiO3-Fe2O3 nanocomposites. RSC Adv. 7, 54594–54602 (2017). https://doi.org/10.1039/c7ra11007c

182. Guevremont, J.M., Guinther, G.H., Szemenyei, D., Devlin, M.T., Jao, T.C., Jaye, C., Woicik, J., Fischer, D.A.: Enhancement of engine oil wear and friction control performance through titanium additive chemistry. Tribology Transactions. 51, 324–331 (2008). https://doi.org/10.1080/10402000701772595

183. Li, Y., Zhang, S., Ding, Q., Li, H., Qin, B., Hu, L.: Understanding the synergistic lubrication effect of 2-mercaptobenzothiazolate based ionic liquids and Mo nanoparticles as hybrid additives. Tribol Int. 125, 39–45 (2018). https://doi.org/10.1016/j.triboint.2018.04.019

Publication on this Research

Journal paper:

1. Maurya, U., Vasu, V. Kashinath, D. "Ionic Liquid-Nanoparticle-Based Hybrid-Nanolubricant Additives for Potential Enhancement of Tribological Properties of Lubricants and Their Comparative Study with ZDDP". Tribol Lett 70, 11 (2022). **Tribology Letters (SCI IF 3.2)** https://doi.org/10.1007/s11249-021-01551-6
2. M. Upendra, V. Vasu, "Synergistic Effect Between Phosphonium-Based Ionic Liquid and Three Oxide Nanoparticles as Hybrid Lubricant Additives" J. Tribol. (2020). **Journal of Tribology ASME (SCI IF 1.9)** https://doi.org/10.1115/1.4045769
3. Maurya, U., Vasu, V.: "Boehmite nanoparticles for potential enhancement of tribological performance of lubricants. Wear." 498–499, 204311 (2022). **Journal of WEAR (SCI IF 4.7)** https://doi.org/10.1016/J.WEAR.2022.204311
4. Maurya, U., Vasu, V., Kashinath, D.: "Three-way compatibility study among Nanoparticles, Ionic Liquid, and Dispersant for potential in lubricant formulation." (2022) **Materials Today: Proceedings. (Scopus Index)**. https://doi.org/10.1016/J.MATPR.2022.03.329
5. M, Upendra and Vasu, V, "Ionic Liquids and its Potential in Lubricants: A Review" (December 13, 2018). **Proceedings of TRIBOINDIA-2018 An International Conference on Tribology, (Scopus)** http://dx.doi.org/10.2139/ssrn.3320367
6. Maurya, U, V. Vasu, "A novel study of Zinctitanate nano additives for potential enhancement of antiwear and EP performance of lubricants." **(Under Review Journal of Tribology , ASME)**

Book chapter:

1. Maurya, U., Vasu, V.: Ionic Liquids as a Potential Sustainable Green Lubricant for Machining in the Era of Industry 4.0. In: Advances in Sustainable Machining and Manufacturing Processes. pp. 135–155. **Book chapter CRC Press, Boca Raton (2022),** http://dx.doi.org/10.1201/9781003284574-9

Patent:

Patent filed with Indian patent office

Titled "Boehmite Nanolubricants"

Application number: 202141027846